# HIGH-EGR DILUTION ENABLED BY DUAL MODE, TURBULENT JET IGNITION (DM-TJI) FOR HIGH-EFFICIENCY INTERNAL COMBUSTION ENGINES

By

Cyrus Ashok Arupratan Atis

## A DISSERTATION

Submitted to
Michigan State University
in partial fulfillment of the requirements
for the degree of

Mechanical Engineering - Doctor of Philosophy

2021

#### ABSTRACT

# HIGH-EGR DILUTION ENABLED BY DUAL MODE, TURBULENT JET IGNITION (DM-TJI) FOR HIGH-EFFICIENCY INTERNAL COMBUSTION ENGINES

By

# Cyrus Ashok Arupratan Atis

To meet the increasingly stringent future fuel economy and CO<sub>2</sub> emission reduction targets for light-duty vehicles, fast and reliable solutions with broader market acceptance are required. It is not about predicting which powertrain technology would have market dominance in future, rather what combination of technologies provides a more accessible and sustainable way to meet those targets. Underlined by the current and future high market share of the internal combustion engines in vehicles with either stand alone or hybridized application, it is still of utmost importance (and will continue to be so) that substantial efforts are rendered towards increasing the efficiency and reducing the regulatory emissions from combustion engines used in light duty vehicles. Prechamber ignition enhanced by active air/fuel scavenging can serve as a key technology towards enabling several efficiency improvement techniques for combustion engines such as increased compression ratio or high rate of charge dilution. The Dual Mode, Turbulent Jet Ignition (DM-TJI)/ Jetfire® ignition system is a leading pre-chamber combustion technology which not only offers higher thermal efficiency due to its distinct capability to operate with very high level of external EGR dilution (up to ~50%) but at the same time ensures that compatibility with existing cost-effective aftertreatment systems such as three-way-catalyst (TWC) can be maintained. Dual Mode, Turbulent Jet Ignition (DM-TJI) incorporates an auxiliary air supply apart from the auxiliary fuel injection inside the pre-chamber of a divided chamber ignition concept. The supplementary air supply to the pre-chamber enables effective purging and ignitable mixture formation inside the pre-chamber even with very high EGR dilution. The current work focuses on

the testing and development of DM-TJI systems on single cylinder engine platforms. The first part of the study presents the experimental investigations carried out with an optical engine equipped with Prototype II DM-TJI system. This optical engine study reported the first published results with 40% external EGR dilution for a pre-chamber jet ignition engine. Both ultra-lean (up to  $\lambda \sim$ 2) and high EGR (up to ~40%) operation were demonstrated and a range of pre-chamber nozzle orifice diameters were tested. The relative timing between the auxiliary air and fuel inside the prechamber was found to be critical to maintaining successful operation at 40% EGR diluted condition. The latter part of the dissertation concerns experiments on Prototype III DM-TJI metal engine with 'Jetfire' cartridge design. A comparative analysis conducted on the relative effectiveness of excess air (lean) versus EGR dilution strategies indicated that compared to the lean burn operation, EGR dilution provided comparable thermal efficiency benefits with a marked improvement in NOx reduction, especially in a high compression, knock limited situation. This study showcased that high EGR dilution rates comparable to lean burn operation can be maintained with the DM-TJI system to achieve high thermal efficiency while still operating at stoichiometric air-fuel ratio. Finally, different pre-chamber scavenging/fueling strategies (active vs passive) were investigated in order to compare the EGR dilution tolerances between different scavenging strategies under identical pre-chamber design. The results were also compared with the conventional spark ignition (SI) configuration on the same engine. The analysis found that DM-TJI/Jetfire® ignition system becomes more advantageous in terms of thermal efficiency at higher loads and knock limited operation due to its considerably higher external EGR (up to ~50%) dilution tolerance. At 10 bar IMEPg and 1500 rpm with 13.3:1 compression ratio, DM-TJI/Jetfire delivered a maximum of 7 to 9% improvement in thermal efficiency compared to TJI mode of operation whereas the SI system failed to maintain stable operation at the same condition.

#### **ACKNOWLEDGEMENTS**

First and foremost, I would like to express my gratitude to my adviser Prof. Harold Schock for providing me the perfect opportunity to pursue my passion to work on engines in a hands-on manner. I would also like to thank my committee members, Prof. George Zhu, Prof. Giles Brereton, and Prof. Jason Nicholas for their guidance. I am grateful to Thomas Stuecken for his support and technical advice throughout every single research project I have been involved with. I would like to thank Kevin Moran for sharing his technical expertise. I would like to acknowledge Jennifer Higel, Brian Rowley, John Przybyl and Brian Deimling for their technical support at during different stages of my work. I would like to show my sincerest gratitude to Dr. Andrew Huisjen from FCA US LLC for his help and technical guidance with engine research. I would also like to thank Dr. Alexander Voice and Dr. Xin Yu for their technical advice. Special thanks to the current and former graduate students: Dr. Ravi Teja Vedula, Dr. Sedigheh Tolou, Shen Qu, Berk Duva, Chaitanya Wadkar, Jian Tang, Anuj Paul for sharing their knowledge. I would like to specially thank Yidnekachew Ayele for his constant support and assistance with my research work. My greatest gratitude goes to my family back in Bangladesh – my mother, my grandma, my dad, and my aunt for their unwavering support throughout this endeavor. I know that this is a proud moment for them too. Finally, I would like to thank my wife and colleague Sadiyah Sabah Chowdhury for her constant guidance and tireless support throughout my personal and professional life. Thank you for being there every step of the way.

# TABLE OF CONTENTS

LIST OF TABLES	vii
LIST OF FIGURES	viii
CHAPTER 1 INTRODUCTION  1.1 Background and Motivation  1.2 Structure of Dissertation.	1
CHAPTER 2 PRE-CHAMBER IGNITION SYSTEMS	6
2.1 Introduction	6
2.2 Divided chamber stratified charge systems	6
2.3 Pre-chamber Jet Ignition	
2.4 Turbulent Jet Ignition Pre-Chamber Combustion System	13
2.5 Dual-Mode Turbulent Jet Ignition or Jetfire® Ignition	
CHAPTER 3 ULTRA-LEAN AND HIGH-EGR OPERATION OF DM-OPTICAL ENGINE	_
3.1 Abstract	
3.2 Introduction	
3.3 Experimental Setup and Procedure	
3.4 Results and Discussion	
3.4.1 DM-TJI engine operating at lean conditions	
3.4.2 Effect of pre-chamber purge air	
3.4.3 DM-TJI engine operating at highly EGR (~40%) diluted condition	ıs 36
3.4.4 Effect of nozzle orifice diameter in DM-TJI engine operation	
3.4.5 Natural luminosity combustion imaging	
3.4.6 Parasitic Loss (to compress the purge air) and Thermal Efficience	y of Prototype II
DM-TJI engine	60
3.5 Summary and Conclusions	61
CHAPTER 4 COMPARISON OF EXCESS AIR (LEAN) VS EGR DILUTED (	ODED ATION AT
HIGH DILUTION RATE (~40%)	
4.1 Abstract	
4.2 Introduction	
4.3 Experimental Setup and Procedure	
4.4 Comparison of EGR vs excess air dilution effect on specific heat capacity	
heat ratio ( $\gamma$ ):	
4.5 Comparison of EGR vs excess air dilution effect on laminar flame speed:.	
4.6 EGR and excess air dilution rate determinations:	
4.7 Results and Discussion	
4.8 Summary and Conclusions	

CHAPTER	5 PERFORMANCE ASSESSMENT OF AIR/FUEL SCAVENGED	DM-TJI
SYSTEM A	GAINST TJI AND SI AT EGR DILUTED CONDITIONS	106
5.1 Abstra	ıct	106
	uction	
5.3 Experi	imental Setup and Procedure	111
5.4 Result	s and Discussion	
5.4.1	Jetfire: 6 bar IMEPg at 1500 rpm, different pre-chamber air pressure	115
5.4.2	TJI passive: 6 bar IMEPg at 1500 rpm	121
5.4.3	TJI active: 6 bar IMEPg at 1500 rpm	122
5.4.4	SI: 6 bar IMEPg at 1500 rpm	123
5.4.5	Comparison: Jetfire vs TJI active vs TJI passive vs SI at 6 bar IMEPg 150	0 rpm124
5.4.6	Jetfire: 10 bar IMEPg at 1500 rpm, different pre-chamber air pressure	136
5.4.7	TJI active: 10 bar IMEPg at 1500 rpm	141
5.4.8	TJI passive: 10 bar IMEPg at 1500 rpm	142
5.4.9	SI: 10 bar IMEPg at 1500 rpm	143
5.4.10	Comparison: Jetfire vs TJI active vs TJI passive vs SI at 10 bar IMEPg 15	00 rpm
5.4.11	Comparison: Jetfire vs SI at 8 bar IEMPg	152
5.4.12	Jetfire high EGR load sweep: 2 to 10 bar IMEPg at 1500 rpm	154
5.4.13	Jetfire: lower compression ratio 10 bar IMEPg at 1500 rpm	163
5.4.14	Jetfire: effect of compression ratio	
5.4.15	Jetfire: high loads at low compression ratio	166
5.4.16	Jetfire: effect of engine speed at high dilution	168
5.4.17	Jetfire: high loads (up to 21 bar IMEP) diluted operation at 2000 rpm	171
5.4.18	Comparison: Jetfire vs SI at low compression ratio	172
5.4.19	Jetfire: aluminum vs stainless steel cartridge design	178
5.5 Summ	ary and Conclusions	
CHAPTER (	6 CONCLUSIONS AND FUTURE WORK	187
6.1 Conclu	uding Remarks	187
6.2 Recon	nmendations for Future Work	188
RIBLIOGR	АРНУ	191

# LIST OF TABLES

Table 1.1 Prototype II DM-TJI optical engine engine specifications	27
Table 4.1 Prototype III DM-TJI engine specifications	74
Table 4.2 Variation of excess air dilution rate with $\lambda$	85

# LIST OF FIGURES

Figure 1.1	Transportation sector consumption by mode of transportation, quadrillion British thermal units[2]
Figure 1.2	Light-duty vehicle sales by fuel type – history and predictions, millions of vehicles[2]
Figure 2.1	Layout of Ricardo's 3-valve stratified charge engine[13]
Figure 2.2	2 Turbulent Jet Ignition pre-chamber and nozzle layout [3]
Figure 2.3	Prototype I DM-TJI engine design details
Figure 2.4	Prototype II DM-TJI engine design details
Figure 2.5	Prototype III DM-TJI engine design details
Figure 2.6	Jetfire cartridge design details
Figure 3.1	Prototype II DM-TJI engine design details
Figure 3.2	2 600 cycles IMEP and lambda traces of DM-TJI engine operating at lean conditions (λ 1.7~2.0), WOT, MAP 98 kPa, 7~8 bar IMEP @ 1500 rpm: (a) compression ratio 12:1, (b) compression ratio 10:1
Figure 3.3	Comparison of major combustion parameters between high and low compression ratios at lean conditions (λ 1.7~2.0), WOT, MAP 98 kPa, 7~8 bar IMEP @ 1500 rpm32
Figure 3.4	300 cycle IMEP traces with and without the purge air at throttled condition, 68 kPa manifold pressure, 6 bar IMEP @ 1500 rpm, λ~1, compression ratio 10:1
Figure 3.6	5 DM-TJI engine test results of 350 cycles of continuous operation at 40% EGR dilution, λ~0.96, 9.5 bar IMEP @ 1500 rpm, 1.25 mm nozzle orifice
Figure 3.8	3 DM-TJI engine test results of 300 cycles of continuous operation showing the effect of change in relative timing of the pre-chamber auxiliary air and fuel at 40% EGR dilution, $\lambda$ ~0.96, 9.5 bar IMEP @ 1500 rpm, 1.25 mm nozzle orifice
Figure 3.9	$0.800$ cycles IMEP trace for different pre-chamber nozzle orifice diameters at lean condition ( $\lambda$ ~ 1.75), 7.2 bar IMEP at 1500 rpm
Figure 3.1	0 300 cycle pressure trace analysis- average combustion parameters at six different nozzle orifice diameters, lean condition ( $\lambda \sim 1.75$ ), 7.2 bar IMEP at 1500 rpm 45
Figure 3.1	1 300 cycle average pre-chamber pressure trace for different nozzle orifice diameters

46
Figure 3.12 300 cycles IMEP trace for different pre-chamber nozzle orifice diameters at 40% EGR dilution (12.5% intake O <sub>2</sub> ), (λ~ 0.96), 9.5 bar IMEP @ 1500 rpm, WOT 47
Figure 3.13 300 cycle pressure trace analysis- average combustion parameters at four different nozzle orifice diameters
Figure 3.14 Pre-chamber purge air volumetric flow rate with different nozzle orifice diameters at 40% EGR diluted conditions
Figure 3.15 Effect of nozzle orifice diameters on pre-chamber pressure bump and their overlap with the pre-chamber fuel injection signal
Figure 3.16 Pre-chamber and main chamber pressure traces and phase- synchronized images of turbulent jet combustion events; lean ( $\lambda \sim 1.75$ ), 7.2 bar IMEP @ 1500 rpm, 1 mm nozzle orifice
Figure 3.17 Crank-angle-resolved binarized images of 200 cycle ensemble average jet structures for different nozzle orifice diameters; lean condition ( $\lambda$ ~1.75), 7. 2 bar IMEP @ 1500 rpm
Figure 3.18 Imaging view of the combustion chamber through the piston window
Figure 3.19 Normalized jet penetration vs orifice diameters, lean operation
Figure 3.20 Normalized jet enflamed area vs orifice diameters, lean operation
Figure 4.1 Prototype III DM-TJI engine with 'Jetfire cartridge' design. A cam actuated air valve was used to deliver purge air to the pre-chamber
Figure 4.2 Schematic of the experimental test bench
Figure 4.3 Specific heat capacity of species at different temperatures (adapted from [79,102]) . 79
Figure 4.4 Effect of dilution rate with different diluents on the laminar flame speed of iso-octane; 750 K; 30 bar
Figure 4.5 Comparison of IMEPg and PMEP between lean burn and EGR diluted operation at MBT/KLSA spark timing
Figure 4.6 Comparison of COV <sub>IMEP</sub> , MBT/KLSA spark timing and crank angle of 50% mass burned fraction between lean burn and EGR diluted operation
Figure 4.7 Main chamber pressure, pressure differential between pre-chamber and main chamber and main chamber apparent heat release rate with different EGR rates at MBT/KLSA spark timing
Figure 4.8 Main chamber pressure, pressure differential between pre-chamber and main chamber

	and main chamber apparent heat release rate with different excess air rate at MBT/KLSA spark timing
Figure 4.9	Comparison of main chamber apparent heat release rate between lean burn and EGR diluted operation at MBT/KLSA spark timing
Figure 4.1	10 Comparison of 10-90% mass fraction burn duration and 0-10% mass fraction burn duration between lean burn and EGR diluted operation at MBT/KLSA spark timing 94
Figure 4.1	1 Comparison of gross indicated thermal efficiency and combustion efficiency between lean burn and EGR diluted operation at MBT/KLSA spark timing
Figure 4.1	2 Comparison of exhaust gas temperature and manifold absolute pressure between lean burn and EGR diluted operation at MBT/KLSA spark timing
Figure 4.1	3 Comparison of NOx and hydrocarbon (THC) emissions between lean burn and EGR diluted operation at MBT/KLSA spark timing
Figure 4.1	4 Comparison of net indicated thermal efficiency with varying dilution rate between lean burn and EGR diluted operation at MBT/KLSA spark timing
Figure 5.1	Schematic of the experimental test bench (boost-cart active)
Figure 5.2	2 Prototype III DM-TJI engine at MSU EARL test cell
Figure 5.3	3 Jetfire cartridge design details
Figure 5.4	Finterchangeable Jetfire cartridges 114
Figure 5.5	5 Gross indicated efficiency and COV of IMEP versus CA50 with different EGR rate at 1500 rpm and 6 bar IMEPg obtained with 45 psig pre-chamber air pressure Jetfire configuration
Figure 5.6	6 Gross indicated efficiency and COV of IMEP versus CA50 with different EGR rate at 1500 rpm and 6 bar IMEPg obtained with 30 psig pre-chamber air pressure Jetfire configuration
Figure 5.7	7 Gross indicated efficiency and COV of IMEP versus CA50 with different EGR rate at 1500 rpm and 6 bar IMEPg obtained with 15 psig pre-chamber air pressure Jetfire configuration
Figure 5.8	Pre-chamber air flow rate measured by LFE for different compressed air pressures at 1500 rpm and 6 bar IMEPg
Figure 5.9	Split of losses with different purge air pressure for the Jetfire system operating at 30% EGR rate at 1500 rpm 6 bar IMEPg for CA50 of 7 °aTDC
Figure 5.1	10 Gross indicated efficiency and COV of IMEP versus CA50 with different EGR rate at 1500 rpm and 6 bar IMEPg obtained with TJI passive configuration

Figure 5.1	11 Gross indicated efficiency and COV of IMEP versus CA50 with different EGR rate at 1500 rpm and 6 bar IMEPg obtained with TJI active configuration
Figure 5.1	2 Gross indicated efficiency and COV of IMEP versus CA50 with different EGR rate at 1500 rpm and 6 bar IMEPg obtained with SI configuration
Figure 5.1	13 Comparison of gross indicated efficiency and COV of IMEP versus CA50 at 1500 rpm and 6 bar IMEPg with highest EGR rate between Jetfire, TJI active, TJI passive and SI
Figure 5.1	4 Comparison of net indicated efficiency and COV of IMEP versus CA50 at 1500 rpm and 6 bar IMEPg with highest stable EGR rate between Jetfire, TJI active, TJI passive and SI; Jetfire includes the work loss due to purge air supply
Figure 5.1	15 Comparison of net indicated efficiency and COV of IMEP versus CA50 at 1500 rpm and 6 bar IMEPg at approximately 20-22% EGR rate between Jetfire, TJI active, TJI passive and SI; Jetfire includes the work loss due to purge air supply
Figure 5.1	6 Comparison of split of losses between Jetfire, TJI passive, TJI active and SI operating at 1500 rpm and 6 bar IMEPg, at their maximum individual thermal efficiency points
Figure 5.1	17 Gross indicated efficiency, combustion efficiency, net indicated efficiency* and manifold absolute pressure at 1500 rpm and 6 bar IMEPg condition with varying EGR rate for Jetfire, TJI active, TJI passive and SI. The net indicated efficiency for Jetfire subtracts the work required to deliver the pre-chamber purge air (referred using an asterisk)
Figure 5.1	18 Split of losses for Jetfire at 1500 rpm and 6 bar IMEPg condition with varying EGR rate and 15 psig pre-chamber air. Numbers on the bar chart correspond to the percentages of total fuel energy
Figure 5.1	19 CA50, 0-10% burn duration, 10-90% burn duration and COV of IMEP at 1500 rpm and 6 bar IMEPg condition with varying EGR rate for Jetfire, TJI active, TJI passive and SI
Figure 5.2	20 Gross indicated efficiency and COV of IMEP versus CA50 with different EGR rate at 1500 rpm and 10 bar IMEPg with 75 psig pre-chamber air pressure; Jetfire 137
Figure 5.2	21 Gross indicated efficiency and COV of IMEP versus CA50 with different EGR rate at 1500 rpm and 10 bar IMEPg with 60 psig pre-chamber air pressure; Jetfire 138
Figure 5.2	22 Gross indicated efficiency and COV of IMEP versus CA50 with different EGR rate at 1500 rpm and 10 bar IMEPg with 45 psig pre-chamber air pressure; Jetfire 139
Figure 5.2	23 Pre-chamber air flow rate measured by LFE and the corresponding purge work requirement calculated using Womack fluid power design data sheet for varying compressed air pressure at 1500 rpm and 10 bar IMEPg

Figure 5.24 Gross indicated efficiency and COV of IMEP versus CA50 with different EGR rate at 1500 rpm and 10 bar IMEPg; TJI active
Figure 5.25 Gross indicated efficiency and COV of IMEP versus CA50 with different EGR rate at 1500 rpm and 10 bar IMEPg; TJI passive
Figure 5.26 Gross indicated efficiency and COV of IMEP versus CA50 with different EGR rate at 1500 rpm and 10 bar IMEPg; SI
Figure 5.27 Comparison of gross indicated efficiency and COV of IMEP versus CA50 at 1500 rpm and 10 bar IMEPg with highest EGR rate between Jetfire, TJI active, TJI passive and SI
Figure 5.28 Gross indicated efficiency, purge work subtracted gross indicated efficiency, combustion efficiency and manifold absolute pressure at 1500 rpm and 10 bar IMEPg condition with varying EGR rate for Jetfire, TJI active, TJI passive and SI
Figure 5.29 CA50, 0-10% burn duration, 10-90% burn duration and COV of IMEP at 1500 rpm and 10 bar IMEPg condition with varying EGR rate for Jetfire, TJI active, and TJI passive. SI inoperable without knock at high CR 10 bar load
Figure 5.30 Gross indicated efficiency and COV of IMEP versus CA50 with different EGR rate at 1500 rpm and 8 bar IMEPg; SI
Figure 5.31 Comparison of gross indicated efficiency and COV of IMEP versus CA50 between Jetfire and SI at 1500 rpm and 8 bar IMEPg with highest EGR rate within stable combustion limit, Jetfire pre-chamber air pressure 60 psig
Figure 5.32 Gross indicated efficiency, combustion efficiency and COV of IMEP at 1500 rpm and 4 bar IMEPg with different EGR rates close to dilution limit
Figure 5.33 Gross indicated efficiency, combustion efficiency and COV of IMEP at 1500 rpm and 7 bar IMEPg with different EGR rates close to dilution limit
Figure 5.34 Gross indicated efficiency, combustion efficiency and COV of IMEP at 1500 rpm and 8 bar IMEPg with different EGR rates close to dilution limit
Figure 5.35 Gross indicated efficiency, combustion efficiency and COV of IMEP at 1500 rpm and 9 bar IMEPg with different EGR rate close to dilution limit
Figure 5.36 Gross indicated efficiency, combustion efficiency and COV of IMEP at 1500 rpm and 10 bar IMEPg with different EGR rate close to dilution limit
Figure 5.37 Gross indicated efficiency, combustion efficiency, NOx emission and COV of IMEP at 1500 rpm and 2 bar to 10 bar IMEPg load sweep at maximum tolerable EGR limits
Figure 5.38 Comparison of gross indicated efficiency and COV of IMEP versus CA50 at 1500

rpm and 10 bar IMEPg with about 40% EGR rate at lower 8.9:1 compression ratio 163
Figure 5.39 Comparison of gross indicated efficiency and COV of IMEP between 13.3:1 and 8.9:1 compression ratio at 1500 rpm and 10 bar IMEPg with similar EGR dilution rate and 60 psig pre-chamber air pressure
Figure 5.40 Comparison of gross indicated efficiency and COV of IMEP at 10, 12 and 14 bar IMEPg and 1500 rpm at 8.9:1 compression ratio and pre-chamber air valve pressure of 75 psig
Figure 5.41 Comparison of gross indicated efficiency and COV of IMEP at 10, 12 and 14 bar IMEPg and 1500 rpm at 8.9:1 compression ratio and MBT/KLSA timing
Figure 5.42 Comparison of gross indicated efficiency and COV of IMEP at 12 and 14 bar IMEPs with different rpm
Figure 5.43 Split of losses at 12 and 14 bar IMEPg with different engine speed at MBT/KLSA timing
Figure 5.44 Gross indicated efficiency and COV of IMEP at 2000 rpm and different loads ranging from 7 to 21 bar IMEPg, 75 psig pre-chamber air pressure
Figure 5.45 Gross indicated efficiency and COV of IMEP with different EGR rate at 1500 rpm and 10 bar IMEPg at 8.9:1 compression ratio obtained with conventional SI system17
Figure 5.46 Comparison of (a) gross indicated efficiency, (b) COV of IMEP, (c) indicated specific hydrocarbon emission and (d) indicated specific NOx emission between the Jetfire and conventional SI systems at highest respective EGR dilution limit 174
Figure 5.47. Comparison of gross indicated efficiency and COV of IMEP between Jetfire and SI operating at 12 and 14 bar IMEPg and 1500 rpm at 8.9:1 compression ratio. For Jetfire the gross indicated efficiency includes the purge work loss
Figure 5.48 Gross indicated efficiency and COV of IMEP versus CA50 at varying EGR rate at 1500 rpm and 6 bar IMEPg with 25 psig pre-chamber air pressure; Jetfire with stainless steel cartridge
Figure 5.49 Net indicated efficiency and COV of IMEP versus CA50 at 1500 rpm and 6 bar IMEPg with the highest EGR rate at different pre-chamber air pressure; Jetfire aluminum versus stainless steel cartridge
Figure 5.50 Split of losses at 1500 rpm and 6 bar IMEPg condition between Jetfire, TJI active, TJI passive and SI with the highest dilution limits. Numbers on the bar chart correspond to the percentages of total fuel energy

### **CHAPTER 1**

#### INTRODUCTION

## 1.1 Background and Motivation

Transportation sector is one of the largest contributors to anthropogenic greenhouse gas (GHG) emissions in the United States. In 2018, the transportation sector accounted for the largest portion (28%) of the total U.S. GHG emissions [1]. Figure 1.1 presents the history and projection of energy consumption in transportation sector by different travel mode reported by the Energy Information Administration (EIA) in their Annual Energy Outlook (AEO) 2020 [2].). From figure 1.1, it is quite apparent that in U.S. light duty vehicles and medium and heavy-duty trucks dominate the transportation sector and the trend is not going to change significantly in upcoming years.

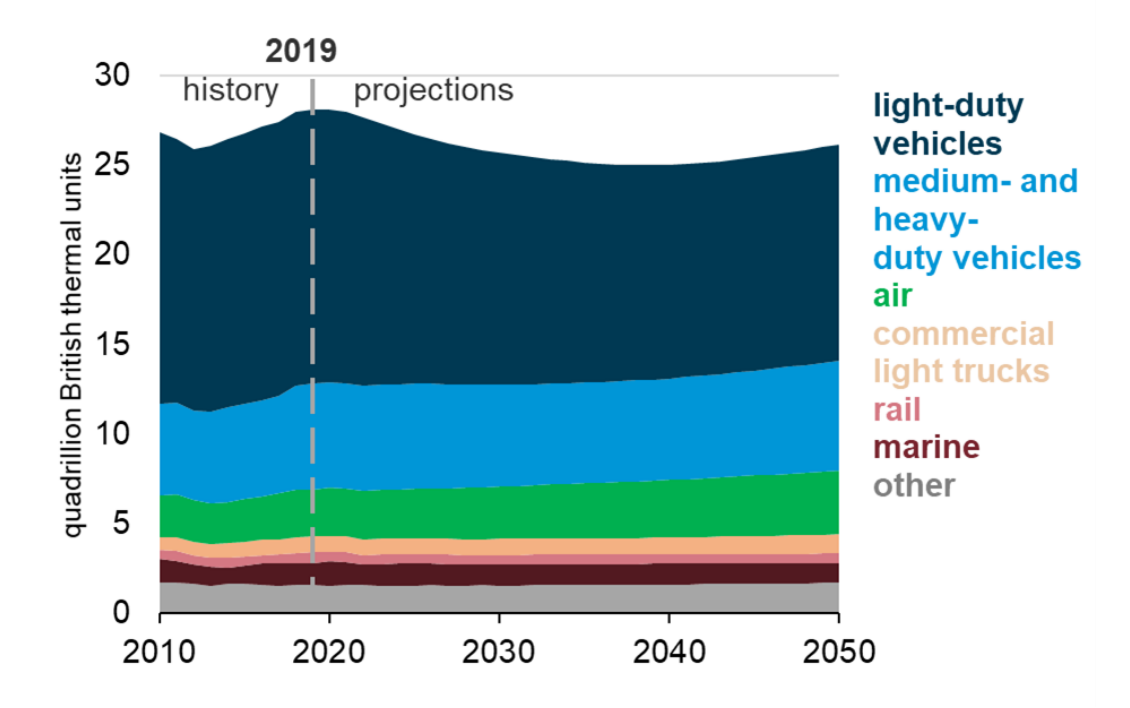


Figure 1.1 Transportation sector consumption by mode of transportation, quadrillion British thermal units[2]

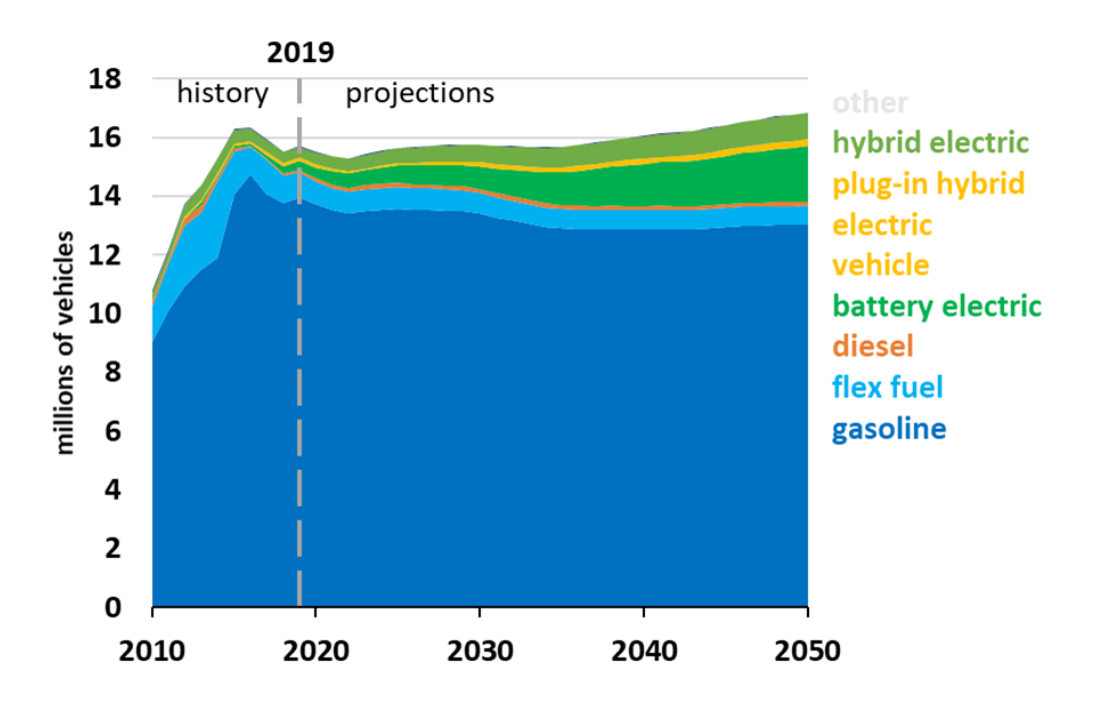


Figure 1.2 Light-duty vehicle sales by fuel type – history and predictions, millions of vehicles[2]

Additionally, the same report also presents the history and projections of light-duty vehicle sales by fuel type in United States (shown in figure 1.2) [2]. Gasoline and flex-fuel (gasoline blended with up to 85% ethanol) vehicles accounted for 94% of the light duty vehicle sales in 2019. Gasoline-driven vehicles have been the dominant vehicle type till now and based on the current predictions, will continue to do so in future as well. While the predictions show that the number of vehicles powered by sources of energy other than the traditional petroleum fuels will increase over time, it appears that vehicles that run on gasoline will still dominate the transportation sector in years to come. Thus, improving fuel economy of gasoline vehicles will play a critical role towards reducing the greenhouse gas (GHG) emissions (mainly CO<sub>2</sub>) from transportation sector.

While major electrification is predicted in automotive powertrain sector, it still remains difficult to foretell the state of the transportation sector in the future based on the current technological

advancements. Critical questions regarding topics such as battery energy density, charging cycle and infrastructure, long term reliability etc., are yet to be fully answered. While electric vehicles offer obvious advantages on emissions over internal combustion engine driven vehicles, the source of the electricity influences overall 'well-to-wheel' emissions. In regions that depend heavily on conventional fossil fuels for electricity generation, electric vehicles may not be as advantageous compared to regions that use relatively low-polluting energy sources for electricity generation. Thus, while all electric operation holds huge potential for emission reduction from transportation sector, the advantages are yet to be fully realized. In the meantime, hybrid vehicles might offer a practical solution. Thus, it will still be essential to continue developing highly efficient low emission internal combustion engines to meet the future efficiency and emission standards until the technology to move towards all electric architecture becomes mature enough for large scale implementation.

Lean burn or dilute gasoline combustion is one of the major combustion strategies to increase fuel economy for internal combustion engines. The Dual Mode, Turbulent jet Ignition (DM-TJI) system is a pre-chamber-initiated combustion technology that has already demonstrated the potential to offer very high thermal efficiency without requiring any additional aftertreatment costs by enabling ultra-lean and highly dilute operation.

While the potential of the DM-TJI system to offer high thermal efficiency was demonstrated before, actual engine test results were still very limited. Prior to the current work, only lean condition results have been experimentally reported for the DM-TJI engine which would still necessitate additional aftertreatment solutions. The focus of this work is the experimental investigations conducted on both DM-TJI optical and metal (with Jetfire cartridge design) engine platforms at high EGR (up to 50%) diluted stoichiometric operating conditions and provide a

preliminary assessment of the effectiveness of the high-EGR-dilution tolerant DM-TJI/Jetfire ignition system as a viable technology pathway to realize potential thermal efficiency benefits for future engines.

# **1.2 Structure of Dissertation**

The dissertation is organized as follows-

Chapter 1 provides a background and motivation behind the current work regarding the necessity of continued research on lean or diluted combustion to achieve higher thermal efficiency for the current and future generations of gasoline engines.

Chapter 2 includes a background and brief history of pre-chamber ignition systems. A brief history of the pre-chamber initiated stratified combustion systems is presented as well. This chapter also describes different stages of development of the DM-TJI or the Jetfire® ignition system.

In chapter 3 the operation of the DM-TJI optical engine at ultra-lean and at 40% EGR-diluted stoichiometric condition is presented. The importance of pre-chamber purge air to maintain stable combustion at high internal or external residual gas environment is also demonstrated. Experimentally the effect of different pre-chamber nozzle orifice diameters on engine performance at both ultra-lean and 40% EGR diluted conditions has been investigated. Results obtained from the optical investigation are presented to aid the in-cylinder pressure-based analysis.

In chapter 4 a comparative experimental investigation is provided on the relative effectiveness of EGR dilution versus excess air dilution (lean burn) strategies in a knock limited environment in terms of thermal efficiency and exhaust emissions.

Chapter 5 demonstrates the effectiveness of pre-chamber air supply in relation to high EGR tolerance. Jetfire ignition was compared to TJI active and passive configurations as well as the

conventional SI configuration at two different load conditions in order to assess the relative effectiveness of the pre-chamber systems with different pre-chamber scavenging strategy against the conventional SI configuration withing the same engine platform.

Chapter 6 provides the concluding remarks and suggestions for future works regarding the finding of the experimental investigations on the DM-TJI/Jetfire ignition system.

#### **CHAPTER 2**

#### PRE-CHAMBER IGNITION SYSTEMS

#### 2.1 Introduction

Dual Mode, Turbulent Jet Ignition (DM-TJI) technology is a variant of Turbulent Jet Ignition system and differs from its forerunner on how the pre-chamber is being scavenged. The turbulent jet ignition system is one of the most prominent pre-chamber-initiated combustion technologies that features a small pre-chamber volume (typically <3% of the clearance volume). Generally, the pre-chamber-initiated combustion is classified based on - pre-chamber volumes, pre-chamber fueling/dozing and orifice connections between pre-and main chamber [3]. Small pre-chamber volumes, compared to larger ones, offer benefits such as lower heat loss and hydrocarbon (HC) emissions, due to reduced crevice volume and combustion surface area [4]. Since DM-TJI is a variant of turbulent jet ignition (TJI) with small prechamber the current discussion will be focused on pre-chamber-initiated combustion technologies featuring small prechambers or jet ignition technologies only.

#### 2.2 Divided chamber stratified charge systems

A well-documented strategy to increase the thermal efficiency by extending the lean flammability limits of the four stroke spark ignition engines is the divided chamber stratified charge or 'prechamber' combustion initiation technique. The earliest concept on charge stratification through pre-chamber was proposed by H. R. Ricardo in 1918 [5,6]. The first report of the Ricardo 3-valve stratified charge 2-stroke engine was published in 1922 [7]. This 3-valve design incorporated two valves for intake and exhaust and a third auxiliary intake valve through which the rich fuel-air mixture was supplied to the pre-chamber. The pre-chamber was connected to a much larger-volume main chamber through a nozzle. A spark plug located in the pre-chamber ignited the rich

pre-chamber mixture which subsequently burned the leaner main chamber mixture. Figure 2.1 shows the main features of the Ricardo 3-valve engine design. This 3-valve engine design inspired several other charge stratification with pre-chamber concepts over the following decades after Ricardo's invention including but not limited to those proposed by Summers [8], Mallory [9], Bagnulo [10] and Heintz [11]. A historical comprehensive review on evolvement and progression of 3-valve stratified charge engines has been provided by Turkish [6,12].

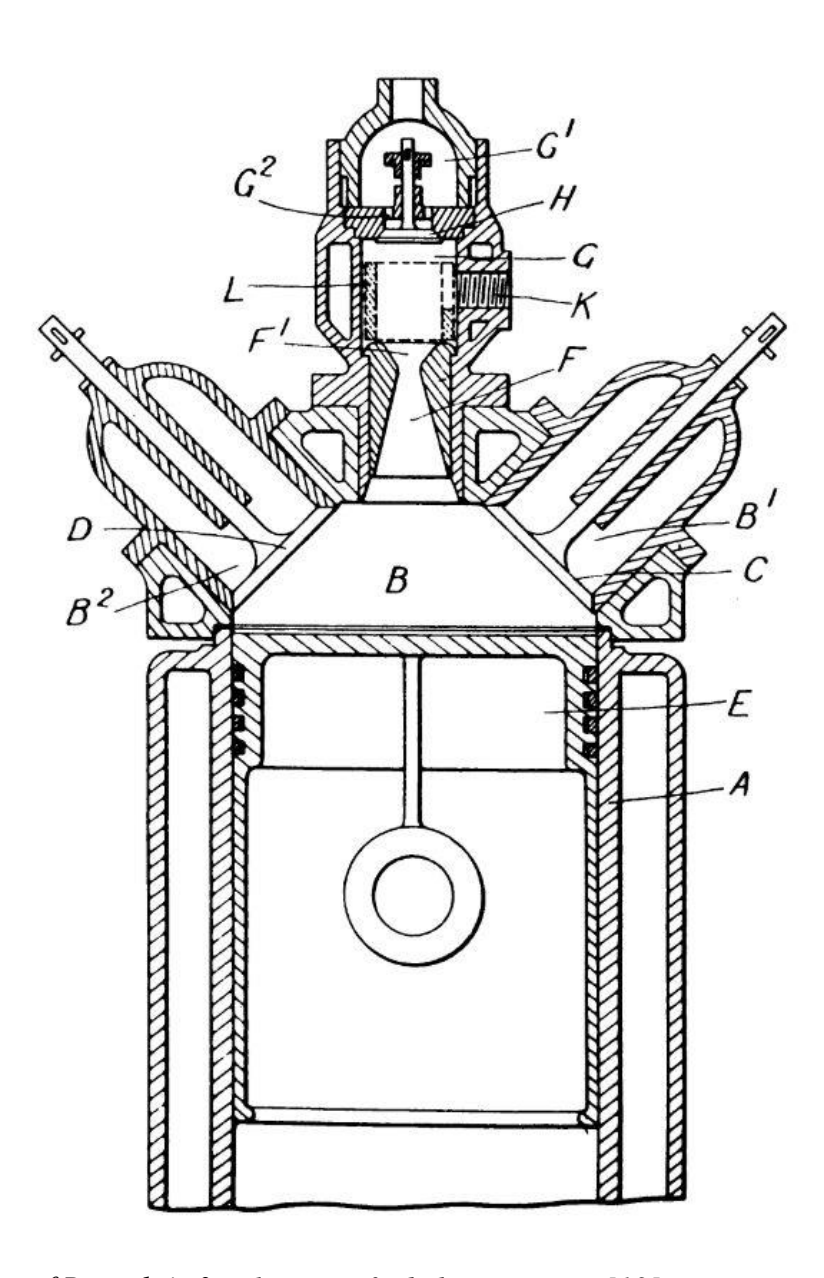


Figure 2.1 Layout of Ricardo's 3-valve stratified charge engine[13]

The torch ignition or torch cell engine designs developed by several OEMs (original equipment manufacturers) around 1980s [14–16] evolved from the 3-valve pre-chamber concepts and eliminated the need for pre-chamber fueling by containing only the spark plug inside the pre-chamber cavity. During compression, the pre-chamber is filled with main chamber charge and upon ignition a turbulent torch ignites the main chamber mixture. Contrary to the torch cells, in divided chamber stratified charge engines, additional fuel is supplied to the pre-chamber [4]. The divided chamber stratified charge systems were characterized by a large pre-chamber and large orifices with the regular flame front (instead of jets) exiting through the orifice into the main chamber. One of the most well-known examples of this technology is the mass-produced Compound Vortex Controlled Combustion (CVCC) engine developed by Honda [17] to comply with the 1975 US emission standards without a catalytic converter [18].

Jet igniters are a variation of the divided chamber stratified charge concepts that are characterized by much smaller orifice(s) connecting the pre-chamber and main chamber cavities [19]. The smaller orifices cause the initial flame kernel inside the pre-chamber to get transformed into multiple pressure driven flame jets passing into the main chamber. Depending on orifice configuration the jets can contain either partially combusted products or actual flames [20,21]. These jets have substantial surface area that can successfully ignite extremely lean or dilute mixtures in the main chamber.

#### 2.3 Pre-chamber Jet Ignition

The concept of Jet ignition was first theorized by Nikolai Nikolaievich Semenov, 1956 Nobel prize winner in chemistry for developing the chain reaction theory [4,22]. This concept saw further development through the experimental work of L. A. Gussak who developed the first jet ignition/pre-chamber torch ignition engine in Soviet Union [13,23–25]. Gussak named the

combustion process as 'LAG-process' (Lavinia Aktivatisia Gorenia) or 'avalanche activated combustion' process [13,23]. Gussak discussed that the incomplete combustion of rich mixture inside the pre-chamber results in chemically active reacting jets containing radical species that cause the main chamber combustion to be fast, stable and complete. The orifice connecting the pre- to the main combustion chamber acts as an extinguisher (quencher) to the flame initiated inside the pre-chamber leading to radical species downstream of the main chamber [3,23]. As the pre-chamber flame breaks into chemically active radicals, a number of vortices are created. These vortices carry the active radicals further down into the main chamber resulting in a complete and stable combustion in the main chamber [23]. Gussak reported 'a pre-chamber volume of 2-3% of the clearance volume, an orifice area 0.03-0.04 cm2 per 1 cm3 of pre-chamber volume with an orifice length to diameter ratio of 0.5' as the optimized condition for engines equipped with LAG process [13]. The LAG process was implemented into the powertrain of the Volga passenger vehicle [13,26]. It was Gussak's work that demonstrated the importance of radical species in this type of combustion technology.

LAG ignition was also studied by Yamaguchi et al. [20] in a divided chamber bomb. Four different ignition patters were identified on a LAG system: well-dispersed burning, composite ignition, flame kernel torch ignition, and flame front torch ignition. They concluded that composite ignition was the best for lean burn conditions due to the contribution of both active radicals and thermal effects [20].

Attard and colleagues [3] performed a comprehensive literature study regarding past jet ignition technologies from 1950s to 2007. Several variants of pre-chamber jet ignition have been investigated in the last few decades. Pulsed jet combustion (PJC) or flame jet researched by Oppenheim and his associates [26,27] at UC Berkeley for over a decade is one of them. Lezanski

et al. [28] performed engine studies with pulsed jet combustion (PJC) and found that richer prechamber performed better than a pre-chamber mixture close to stoichiometry.

Oppenheim and colleagues later introduced jet plume injection and combustion (JPIC) [29], a modified version of PJC. While PJC used high pressure generated inside the pre-chamber due to combustion to initiate the radical jet igniters, JPIC on the other hand utilized its high-pressure injection system to produce the jets. The fuel injector in the JPIC system could inject either fuel or air/fuel mixture into the cavity at the bottom of its combustor [29]. The self-purging capability of JPIC was an advantage over its predecessor, the PJC system. The high-pressure injector of JPIC systems forced the flow out of the pre-chamber into the main chamber. Thus, JPIC eliminated the problem caused by trapped residuals in the cavity of PJC systems.

The swirl chamber spark plug was first introduced by Reinhard Latsch at Bosch Stuttgart in early 1980s [30], as an attempt toward simplification of the LAG process. The LAG system included an auxiliary fuel-air supply to the pre-chamber, which was removed in swirl chamber spark plugs. Further studies on the same concept as the swirl chamber spark plug were published by Latsch and colleagues under bowl pre-chamber ignition (BPI) systems [31]. The swirl chamber spark plug and BPI solely depended on the piston motion during the compression stroke to direct the main air/fuel mixture into the small pre-chamber cavity, housed inside the spark plug. There were two fuel injection events for the swirl chamber spark plug and BPI systems. The first occurred during the intake stroke to maintain a lean air/fuel mixture inside the main chamber. The second fuel injection event contained only a small amount of fuel (~3% of total fuel mass) and happened during the compression stroke toward the piston bowl. The piston motion would push the additional fuel toward the cavity of the spark plug, causing a rich mixture inside the pre-chamber at the time of ignition.

The hydrogen-assisted jet ignition system (HAJI) was introduced by Watson et al. [32–34] where a small amount of hydrogen (~2% of the main fuel) was injected next to the spark plug inside the pre-chamber to create a rich air/fuel mixture at the time of ignition. The rich mixture inside the pre-chamber would ignite and form chemically active radical jets which penetrated into the main chamber. Chemically active turbulent jets caused by the HAJI system were estimated to provide an ignition source of energy more than two orders of magnitude higher than that of spark plugs [4]. The lean flammability limit could be extended to lambda of 5 at wide-open throttle, with gasoline as the main chamber fuel and a small amount of hydrogen in the pre-chamber [33]. The hydrogen flame jet ignition (HFJI) system developed by Gifu University and Toyota College of Technology in Japan [35,36], was similar to HAJI system. The authors of these papers conducted a thorough analysis to understand the influence of radical species formed by rich hydrogen combustion compared to jet turbulence concerning the extension of lean limit of stable ignition. They found that the turbulence caused by the jets played a larger role in combustion stability at lean limits [36].

Self-ignition triggered by radical injection (APIR) [37,38] was a similar technology to the PCJ developed at UC, Berkeley. The APIR system, like PCJ technology, utilized smaller-hole orifices which were used to quench flame propagation and simultaneously to prevent combustion from reappearing in the vortex of jets going from pre-chamber to the main chamber. The main difference lay in the number of orifices connecting the pre-chamber to the main chamber. The APIR system increased the number of orifices for radial seeding of the chemically active turbulent jets inside the main chamber [4].

Paul Najt et al. at General Motors patented a dual -mode combustion process [39]. At light loads and speeds, the premixed charge forced auto ignition (PCFA) would be used as its first mode of

combustion and for higher loads and speeds, a second mode of combustion utilizing either spark ignition and/or pulse jet ignition (PJI) would be used. The dual-mode combustion process aimed to overcome the known limitations of homogenous charge compression ignition (HCCI) systems, such as unpredictability of charge ignition timing (combustion phasing) and technology limitations at higher loads and speeds. The PCFA mode of combustion employed pulse jet ignition to ignite an ultra-dilute premixed charge in the main combustion chamber. The PJI system would work similar to a pre-chamber-initiated combustion by forcing a spark-ignited jet of hot reacting fuel mixture from a pre-chamber into the ultra-dilute charge of the main chamber [4].

Homogeneous combustion jet ignition (HCJI) [40], introduced by Kojic et al. of Robert Bosch GmbH, was another innovation in the jet ignition technologies. Like the dual-mode combustion of Paul Najt and colleagues, HCJI was an attempt to control the combustion phasing of HCCI engines. The HCJI system contained two small pre-chambers which were coupled to the main chamber. Each pre-chamber had its own 'pre-chamber piston'. As there was no spark plug into the pre-chamber, small and precisely-controlled pistons of the two pre-chambers managed the start of combustion inside the pre-chamber through auto-ignition. The connection between pre-and main combustion chambers was maintained using two microvalves which were closed till early compression inside the main chamber. The valves had been opened by the time the pre-chamber combustion was started, so hot gas jets initiated by auto-ignition of the pre-chamber could induce a second auto-ignition inside the main combustion chamber.

At the end of combustion cycle, a large quantity of residual gas could remain in the pre-chamber due to improperly scavenged combustion products [41]. The pre-chamber spark plug with pilot injection [41] was an attempt to avoid the problems caused by improperly scavenged pre-chamber of the jet ignition technologies. The pilot fuel was injected during the intake stroke with an aim of

purging the pre-chamber. The amount of pilot fuel injected would vary based on injection pressure and the operating conditions. An air/fuel mixture was then formed inside the pre-chamber during the compression stroke as the air/fuel mixture from the main chamber was pushed into the pre-chamber. The initiation of combustion inside the pre-chamber occurred by a spark event and the jets generated would pass through the holes connecting the pre-to main chamber. Combustion inside the main chamber occurred as a result of hot, chemically active turbulent jets from the pre-to main chamber. Getzlaff and colleagues studied several gaseous fuels [41] to purge the pre-chamber, including methane and hydrogen. The most promising results were obtained using hydrogen as the pilot fuel for the pre-chamber.

### 2.4 Turbulent Jet Ignition Pre-Chamber Combustion System

In 2010, William Attard and colleagues of MAHLE Powertrain introduced the MAHLE 'Turbulent Jet Ignition' system in a series of publications [3,42–44]. MAHLE TJI was originally conceived as a non-hydrogen fueled variant of the hydrogen-assisted jet ignition (HAJI) concept researched by Harry Watson at the University of Melbourne [32,33,45–51]. The main objective of TJI was to make the technology more feasible than other laboratory-based jet ignition systems as well as to develop a system that can operate on readily available commercial fuel such as gasoline, propane and natural gas. In these studies, a peak net thermal efficiency of 42% was reported for TJI equipped 0.6L single cylinder research engine derived from a production level I4 Ecotec LE5 GM engine with 4-valves pent roof combustion chamber design [44]. This 42% peak efficiency was obtained with 10.4:1 compression ratio at about 6 bar IMEPn and 1500 rpm operating at lambda ~1.6 with near zero engine out NOx emission. Additionally, it was demonstrated that the TJI prechamber combustion system was capable of tolerating up to 54% mass fraction diluent (excess air) at 3.3 bar IMEPn and 1500 rpm with a 18% improvement in fuel economy compared to

conventional spark ignition engine operating at the same load and speed [3]. Figure 2.2 demonstrates the pre-chamber and nozzle layout of the Turbulent Jet Ignition system presented by Attard et al. [3]. Some of the defining features of the MAHLE TJI system are [3,4,42–44]:

- Very small pre-chamber (~2% of the clearance volume)
- Pre-chamber connected to main chamber by one or more small orifices (~1.25 mm in diameter)
- Separate auxiliary pre-chamber direct fuel injector
- Main chamber fuel injector (port fuel injector (PFI) or direct injector (DI))
- Spark discharge initiated pre-chamber combustion
- Use of readily available commercial fuels for both main and pre-chambers

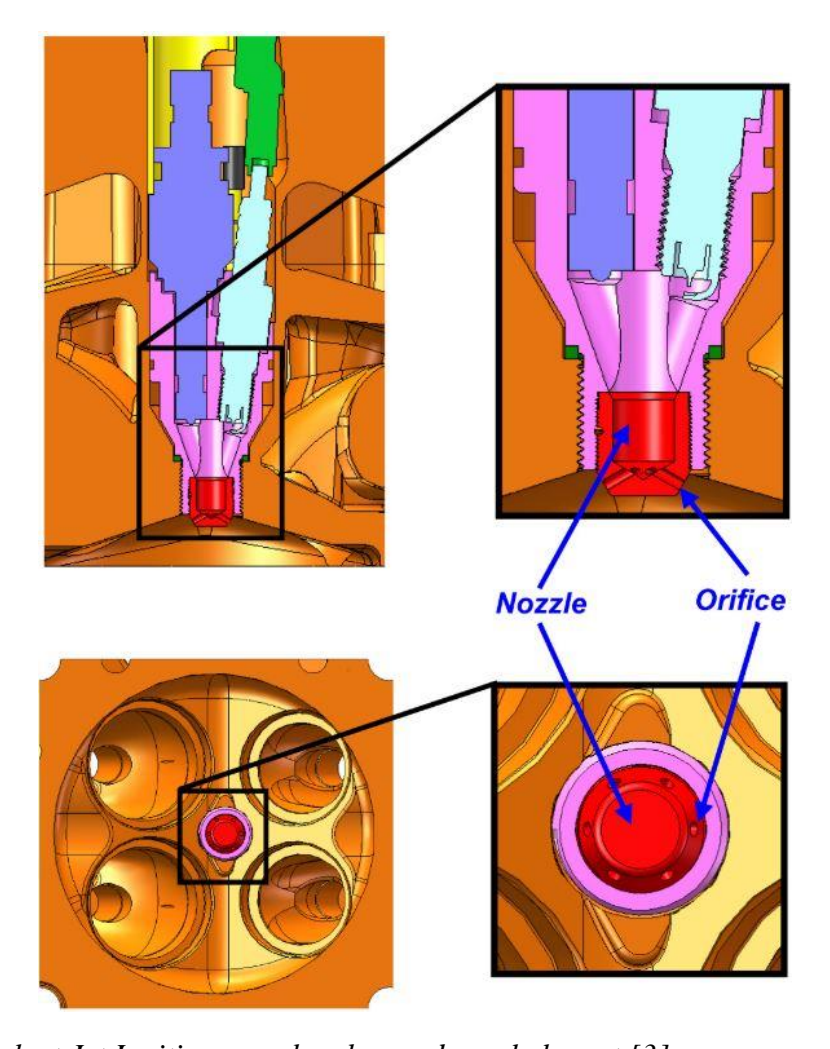


Figure 2.2 Turbulent Jet Ignition pre-chamber and nozzle layout [3]

In 2012, William Attard of MAHLE Powertrain patented "turbulent jet ignition pre-chamber

combustion system for spark ignition engines" [52,53]. Following its introduction in 2010, Attard et al. [54–58] and later his colleagues Bunce et al. [59–61] at MAHLE Powertrain published several studies regarding the development of MAHLE Turbulent Jet Ignition system which was later trade marked as MAHLE Jet Ignition or MJI®. A recent study by Peters et al. [62] from MAHLE Powertrain reported a peak brake thermal efficiency greater than 42% from a 1.5L 3-cylinder gasoline fueled Jet Ignition engine. The same authors reported several research works on MAHLE Jet Ignition equipped single cylinder engines fueled with natural gas [63–65]. In terms of number of published studies conducted on development of modern pre-chamber ignition technologies MAHLE TJI and its' variants are perhaps one of the most well-known and well-developed in terms of technology readiness level.

## 2.5 Dual-Mode Turbulent Jet Ignition or Jetfire® Ignition

While Turbulent Jet Ignition (TJI) system developed by MAHLE offers a huge potential in improving the thermal efficiency compared to conventional spark ignition system by extending the lean operation capability considerably, one of the persisting challenges with lean combustion is the NOx conversion efficiency of the three-way-catalytic (TWC) converter at lean conditions. The NOx conversion efficiency of the TWC decreases sharply if the air/fuel ratio becomes even slightly leaner. This makes the TJI systems operating lean (excess air as diluent) nearly incompatible with the widely used TWC emission reduction system or requires rather complex and expensive additional deNOx systems such as the selective catalytic reduction (SCR) or lean NOx traps. Thus, making the TJI system rather expensive in terms of aftertreatment system requirements. EGR diluted stoichiometric operation could be a viable solution to this problem. Utilizing EGR as diluent instead of excess air permits the use of TWC while offering similar level of advantages to improve thermal efficiency. However, one problem with EGR dilution relating to

the pre-chamber ignition system is the mixture combustibility or stoichiometry inside the pre-chamber at high dilution rate. TJI systems with only auxiliary fuel injection inside the pre-chamber operates poorly with high level (40% and above) of EGR dilution due to the lack of control to maintain the pre-chamber mixture stoichiometry within a combustible limit. High level of diluents containing either trapped residuals or the EGR coming from the main chamber during compression stroke compromises the pre-chamber ignitability. With lean combustion pre-chamber ignitability is not compromised due to the availability of excess air. With additional fuel injection inside the pre-chamber, the pre-chamber ignitability can be maintained over a broader dilution rate. Using EGR as diluent on the other hand does not have this availability of additional air inside the pre-chamber and makes the pre-chamber mixture much harder to ignite especially at high dilution rate. The concept of Dual Mode, Turbulent Jet Ignition introduced by Schock et al. [66] of Michigan State University addresses this problem.

The Dual Mode, Turbulent Jet Ignition (DM-TJI) system is an engine combustion technology wherein an auxiliary air supply apart from an auxiliary fuel injection is provided into the prechamber. Thus, the DM-TJI adds an additional auxiliary air supply to the pre-chamber of the existing TJI concepts. The supplementary air supply and its method of delivery to the pre-chamber of a DM-TJI system are the main modifications to the technology's predecessor, the Turbulent Jet Ignition (TJI) system. This enables enhanced control of the mixture stoichiometry in the pre-chamber and delivers stable combustion even with high level of EGR dilution.

Although DM-TJI technology is in early stages of development, a number of studies have been conducted to investigate its potential. Atis et al. [67] showed that the Prototype II DM-TJI system equipped gasoline fueled optical engine with a cooled EGR system could maintain stable operation (COV<sub>IMEP</sub><2%) with 40% external EGR at stochiometric ( $\lambda$ ~1) operating conditions. In that study,

effect of pre-chamber air/fuel timing relative to EGR tolerance was investigated. Ultra-lean operation (up to  $\lambda$ ~2) was also demonstrated while a correlation between the nozzle orifice diameters and overall burn duration was suggested. Tolou et al. [68] developed a physics-based GT-POWER model of the Prototype II DM-TJI system and predicted the ancillary work requirement to operate the additional components of the DM-TJI system. Vedula et al. [69] reported the net indicated thermal efficiency of the Prototype I DM-TJI engine for both lean and 30% nitrogen diluted, near stochiometric operation. Vedula et al. [70] also studied the effect of pre-chamber fuel injection timing including pre-chamber air injection and different injection pressures on iso-octane/air combustion in a DM-TJI system equipped rapid compression machine for a global lambda of 3.0. Song et al. [71] studied control-oriented combustion and state-space models based on the Prototype I DM-TJI engine.

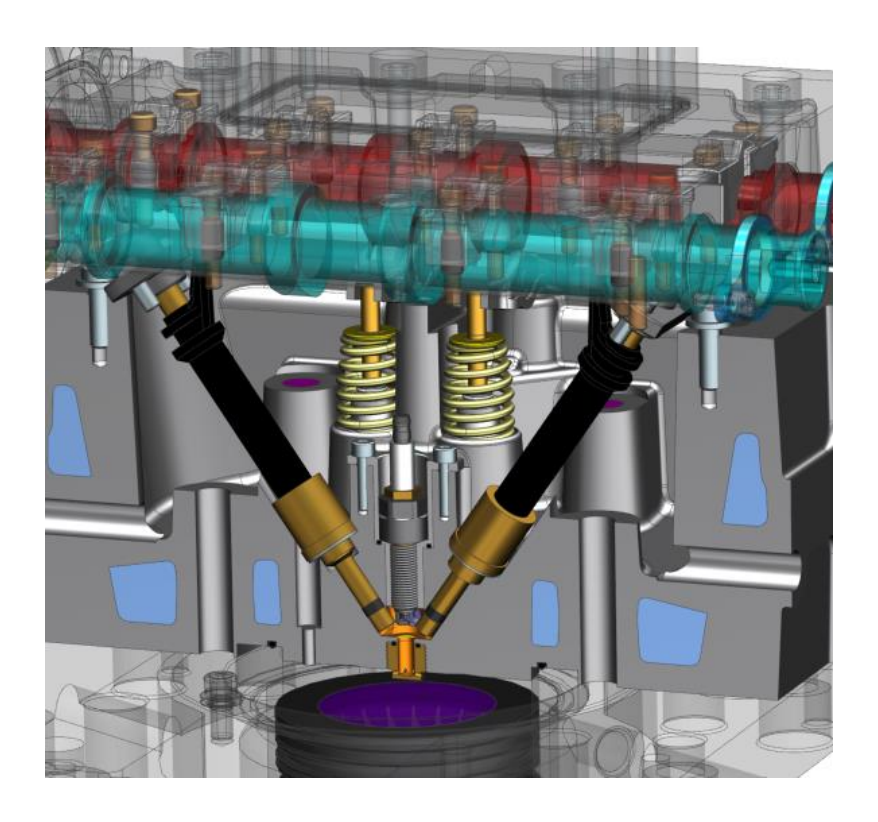


Figure 2.3 Prototype I DM-TJI engine design details

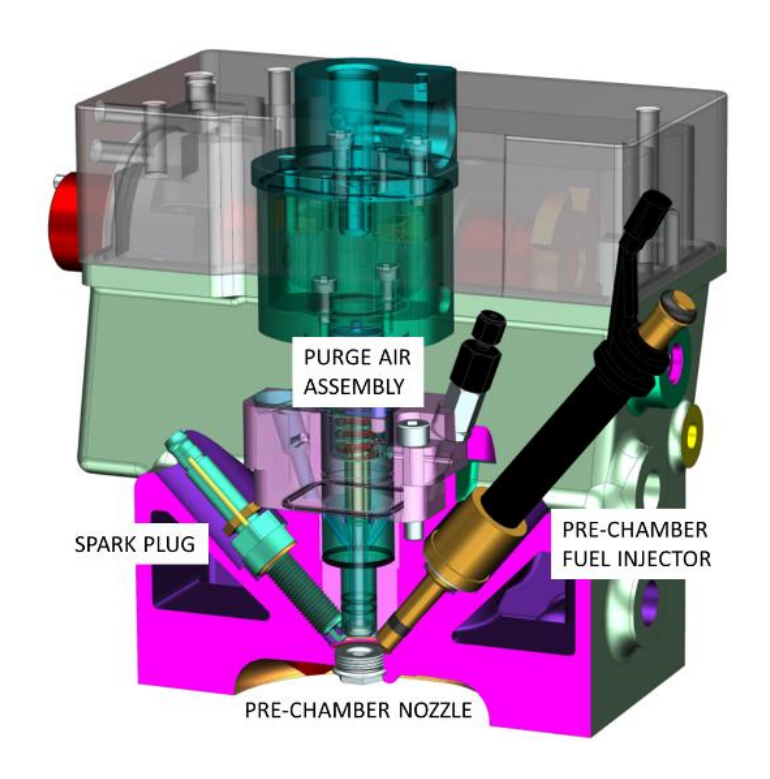


Figure 2.4 Prototype II DM-TJI engine design details

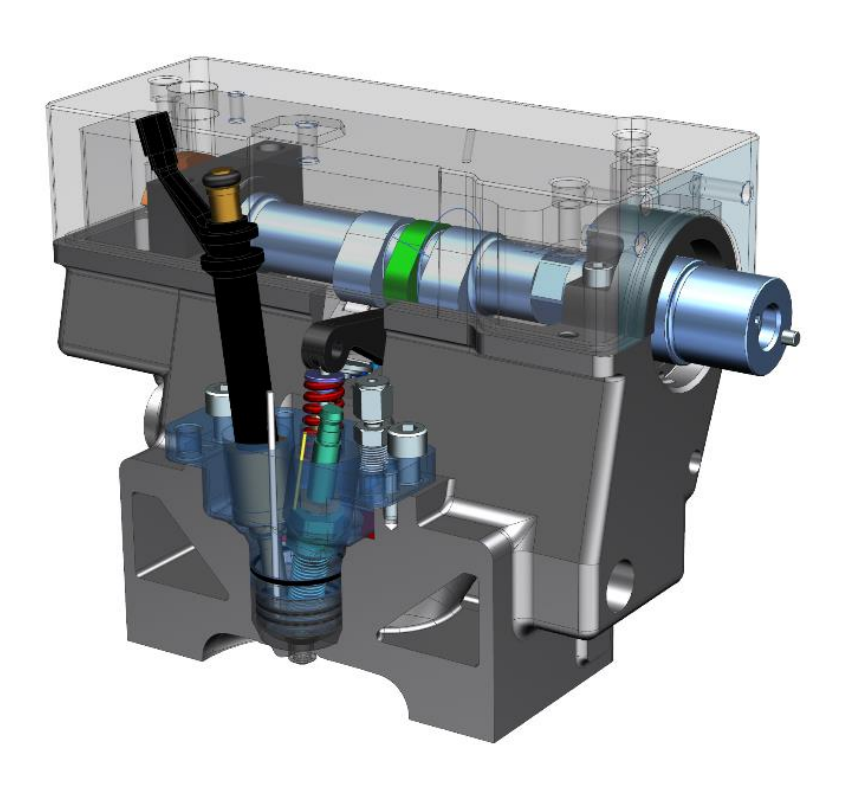


Figure 2.5 Prototype III DM-TJI engine design details

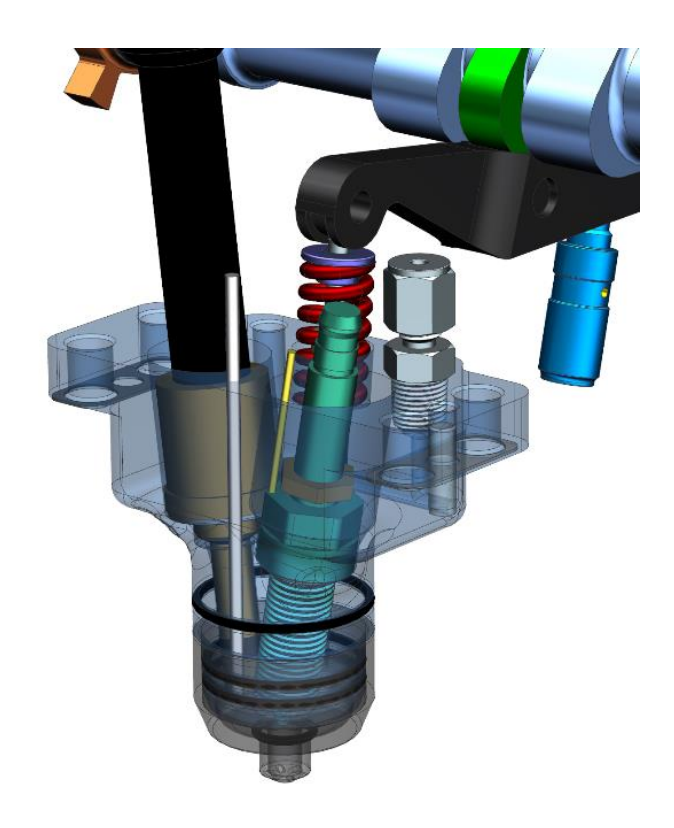


Figure 2.6 Jetfire cartridge design details

Prototype I of the DM-TJI engine was tested in both optical and metal variants with Bowditch piston arrangement whereas prototype II was configured as an optical engine only. Prototype I utilized an air injector (fuel injector that delivers air) inside the pre-chamber to deliver the auxiliary air whereas prototype II replaced the pre-chamber air injector with a hydraulically controlled poppet valve for pre-chamber air delivery. Figure 2.3 shows the Prototype I DM-TJI engine layout and figure 2.4 shows the Prototype II DM-TJI design details. The latest Prototype III metal engine replaces the hydraulically controlled pre-chamber air valve with a more production viable intake camshaft driven air valve and packages the pre-chamber components (fuel injector, spark plug and air valve) inside a more compact 'Jetfire' cartridge design. The DM-TJI system was later trademarked as Jetfire® ignition system. Figure 2.5 and 2.6 show the Prototype III DM-TJI engine and the Jetfire cartridge design details, respectively. This dissertation will focus on the work conducted with Prototype II optical and Prototype III metal engines.

#### **CHAPTER 3**

# ULTRA-LEAN AND HIGH-EGR OPERATION OF DM-TJI EQUIPPED OPTICAL ENGINE

### 3.1 Abstract

Continuous efforts to improve thermal efficiency and reduce exhaust emissions of internal combustion engines have resulted in development of various solutions toward improved lean burn ignition systems in spark ignition engines. The Dual Mode, Turbulent Jet Ignition (DM-TJI) system is one of the leading technologies in that regard which offers higher thermal efficiency and reduced NOx emissions due to its ability to operate with very lean or highly dilute mixtures. Compared to other pre-chamber ignition technologies, the DM-TJI system has the distinct capability to work with a very high level of EGR dilution (up to ~40%). Thus, this system enables the use of a three-way catalyst (TWC). Auxiliary air supply for pre-chamber purge allows this system to work with such high EGR dilution rate. This work presents the results of experimental investigation carried out with a Dual Mode, Turbulent Jet Ignition (DM-TJI) optical engine equipped with a cooled EGR system. The results show that the DM-TJI engine could maintain stable operation (COV<sub>IMEP</sub><2%) with 40% external EGR at stoichiometric ( $\lambda \sim 1$ ) operating conditions. The relative timing between the auxiliary air and fuel inside the pre-chamber was found to be critical to maintaining successful operation at 40% EGR diluted condition. Ultra-lean (up to  $\lambda \sim 2$ ) operation was also demonstrated at two different compression ratios with good combustion stability. A range of pre-chamber nozzle orifice diameters were tested with both lean and EGR diluted conditions. In general, smaller orifice diameters resulted in shorter overall burn duration due to more favorable distribution in ignition sites.

#### 3.2 Introduction

Light-duty vehicle fuel economy improvement and tailpipe CO<sub>2</sub> emission reduction targets are becoming increasingly stringent. In Europe, by 2030 a 37.5% reduction in average CO<sub>2</sub> emission is targeted for the light-duty applications relative to the 2021 baseline[72]. Similar trends have been observed in CO<sub>2</sub> reduction targets for light-duty vehicles in all major markets, and they will require 3-6% improvement in fuel economy per year[73]. While such ambitious targets will have a major impact on changing the structure of the global automotive market with an emphasis to move towards more electrified powertrain architectures, it will still be essential to continue developing highly efficient, low-emission internal combustion engines to compensate for the limitations of electrical components such as battery energy density or the charging schedule. Even with major hybridization, in situations such as highway driving conditions, highly efficient internal combustion engines provide a major advantage to maximize overall efficiency of the vehicle. Thus, even with predicted electrification in the future, the focus on improving thermal efficiency of the internal combustion engine has never been greater. This accelerated drive to improve thermal efficiency and reduce exhaust emission from internal combustion engines has resulted in several advanced engine technologies, especially in the SI (spark ignition) engine sector[73]. One of the promising approaches towards high thermal efficiency and reduced regulated emission from SI engines is to operate with an increased level of air-fuel mixture dilution, by means of either excess air or EGR (exhaust gas recirculation).

Lean burn engines operating with excess air dilution improve the thermal efficiency of the spark ignition engines through higher mixture-specific heat ratio ( $\gamma$ ) and reduced heat loss due to lower in-cylinder temperature, as well as reduced pumping loss during part load operation. While lean combustion in modern SI engines has been shown to provide improved thermal efficiency, it also

produces higher NOx emission compared to operation at stoichiometric conditions, necessitating additional aftertreatment systems such as a lean NOx trap or SCR (selective catalytic reduction) catalysts. Significant improvements in NOx emissions from such lean burn combustion systems could only be observed during ultra-lean operation ( $\lambda$ >1.6). However, a major limitation of such lean and ultra- lean operation is the compromised combustion stability due to less favorable ignition quality of the mixture as well as the slow flame propagation speed through the lower temperature lean mixture. Poor combustion stability leads to increased HC emissions and decreased thermal efficiency due to misfires and partial burns. To overcome these challenges, a higher-energy distributed ignition source is required. This need for higher-energy ignition sources, to achieve stable combustion with lean and ultra-lean air-fuel mixture, led to the development of modern pre-chamber-based jet ignition systems.

The turbulent jet ignition (TJI) system is a modern pre-chamber-based jet ignition system characterized by small pre-chamber volume (<3% of the clearance volume), auxiliary pre-chamber fueling, and multiple small orifices connecting the main and the pre-chamber[3]. The TJI concept presented by Attard et al.[3] is one of the many jet ignition technologies based on the "LAG-Avalanche Activated Combustion" works by Gussak et al.[4, 5]. An exhaustive review of pre-chamber initiated jet ignition combustion systems is presented by Toulson et al.[4] and discusses various stages of progress in pre-chamber-initiated combustion systems. In a TJI system, the initial flame around the spark plug inside the pre-chamber is transformed through the nozzle orifices into multiple pressure-driven, chemically active, high-temperature turbulent jets distributed around the main combustion chamber with substantial surface areas. These multiple distributed high-energy ignition sites enable very fast burn rates with minimal combustion variability. TJI systems have been extensively studied[59,60,74,75] and have been shown to extend the lean limit considerably

with reduced NOx emission at higher dilution [3,43,44,56,63,76,77].

While stable lean operation with TJI systems offers a high level of improvement in thermal efficiency compared to conventional spark ignition engines[55,56,61], a major challenge with such lean operation is the conversion efficiency of the three-way catalyst (TWC) for NOx. The NOx conversion efficiency of the TWC degrades rapidly if the air-fuel ratio (AFR) varies even slightly toward the lean conditions[78]. The TJI system operating on excess air dilution  $(1 < \lambda < 2)$  makes the use of TWC extremely inefficient and requires additional rather complex and expensive deNOx aftertreatment systems, such as a lean NOx trap or SCR catalyst. A solution to this major problem with TJI is to operate the engine at stoichiometric conditions ( $\lambda$ =1) with EGR as the diluent instead of excess air.

Using EGR as the diluent instead of excess air makes the use of TWC possible, while still offering the similar advantages of excess air dilution[79]. Thus, high thermal efficiency can still be maintained at low-/medium load conditions with effective emission reduction through TWC. Using EGR as the diluent instead of excess air requires the engine to operate with very high level of EGR (up to 40%), and that is where the TJI systems become ineffective. TJI systems cannot operate effectively under dilute conditions with very high levels of EGR (~40%) due to their difficulty in reliably igniting the high EGR fraction mixture in the pre-chamber. With such a high level of EGR mixed with the intake air-fuel reactants along with the trapped residuals, it becomes very difficult to control mixture stoichiometry in the pre-chamber using the auxiliary pre- chamber fuel injection only. With excess air dilution, this is not a major problem since there is a high percentage of excess air available in the pre-chamber air-fuel and residual gas mixture, so that a small additional amount of fuel injection still enables the formation of an ignitable mixture in the pre-chamber. With EGR instead of excess air used as the diluent, this availability of excess air to

maintain an ignitable mixture inside the pre-chamber decreases and consequently the pre-chamber misfires leading to main chamber misfiring which renders the TJI systems unusable with high level (~40%) of EGR dilution. The DM-TJI system addresses this problem.

The Dual Mode, Turbulent Jet Ignition (DM-TJI) system is an engine combustion technology wherein an auxiliary air supply apart from an auxiliary fuel injection is provided into the prechamber [12,13,14]. The supplementary air supply and its method of delivery to the pre-chamber of a DM-TJI system are the main modifications to the technology's predecessor, the Turbulent Jet Ignition (TJI) system [3,44,52,55–57].

The DM-TJI system enhances stoichiometry control in the pre-chamber, independently of the main chamber, by adding in supplementary auxiliary air as well as auxiliary fuel to maintain pre-chamber mixture ignitability, thus resulting in better combustion stability in the pre-chamber and subsequently in the main chamber. Lean and/or highly dilute mixtures generally require high ignition energy, long duration of ignition and wide dispersion of ignition sources in order to achieve fast burn rates[4] and maintain acceptable combustion stability. Initiating combustion at multiple sites distributed around the combustion chamber is of particular importance to achieve the fast burn rates due to the low flame velocities inherent in a highly lean/dilute air-fuel mixture. The DM-TJI ignition strategy extends the mixture flammability limits by enabling faster burn rates of lean and/or highly dilute mixtures through multiple pressure-driven, chemically active reacting turbulent jets distributed around the combustion chamber to initiate combustion parallelly from multiple sites. The DM-TJI system's unique capability to work alongside the conventional TWC by permitting stoichiometric operation with high level of EGR dilution (up to 40%) through enhanced pre-chamber scavenging makes it a very promising combustion technology.

Several studies have been conducted on the DM-TJI system. Vedula et al.[69] reported a net

indicated thermal efficiency of  $45.5\% \pm 0.5\%$  for both lean ( $\lambda \sim 1.85$ ) and 30% nitrogen-diluted, near-stoichiometric operations of a DM-TJI engine running on gasoline. The experiments were conducted on a Prototype I DM-TJI engine at Michigan State University (MSU). Engine specifications can be found at [69]. This work was preceded by the DM-TJI based optically accessible rapid compression machine[70]. Song et al.[19, 20] presented control-oriented combustion and state-space models based on the Prototype I DM-TJI engine. Prototype I, while successfully demonstrating the combustion concept, was not a production-viable system; and Prototype II with a pre-chamber purge air valve arrangement was built. Tolou et al.[68] developed a novel, reduced order and physics-based model of the Prototype II DM-TJI engine with pre-chamber air valve assembly and for the first time, predicted the ancillary work requirement to operate the DM-TJI system. Previous studies on DM-TJI systems[21,22] had predicted high (~40%) EGR-diluted engine operation with the DM-TJI strategy. However, the actual experimental validations were absent.

In the present paper, results are reported from the experimental investigation using the Prototype II DM-TJI single-cylinder optical engine equipped with a cooled EGR system at MSU. For the first time, experimental results are demonstrated for the DM-TJI engine running with 40% external EGR at stoichiometric ( $\lambda \sim 1$ ) conditions. In the latter section of this study, several pre-chamber nozzle orifice diameters were tested in both very lean and high EGR diluted conditions to investigate the role of nozzle orifice diameter on the performance of DM-TJI system.

# 3.3 Experimental Setup and Procedure

Tests were carried out on a single-cylinder Prototype II DM-TJI engine. The first prototype engine [21] had an air injector (fuel injector that delivers air) inside the pre-chamber to deliver auxiliary

air to the pre-chamber whereas the current Prototype II replaces the pre-chamber air injector with a hydraulically controlled poppet valve. This arrangement also decreases the pre-chamber purge work input considerably[68]. Figure 3.1 shows the layout of different components of the Prototype II DM-TJI single-cylinder engine.

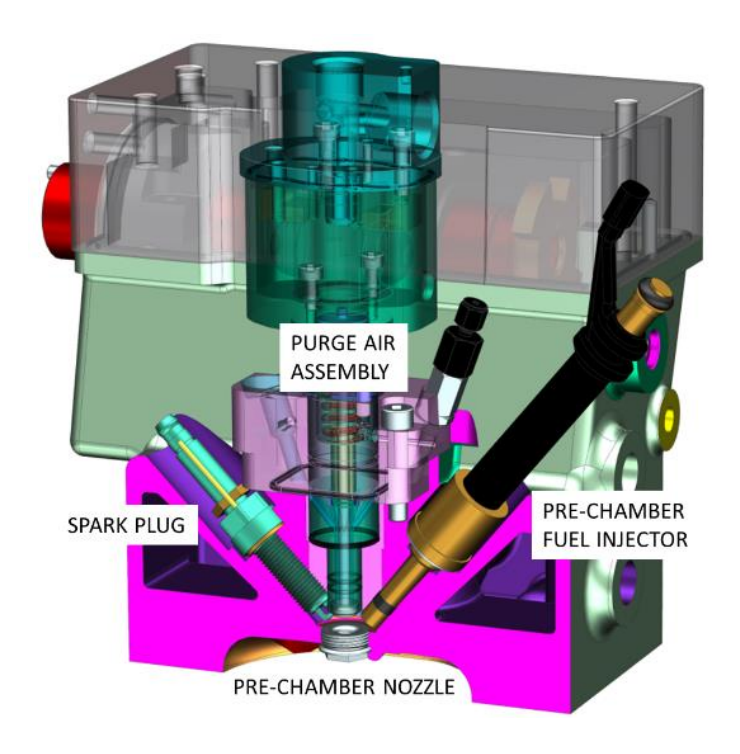


Figure 3.1 Prototype II DM-TJI engine design details

The Prototype II DM-TJI engine has a pent roof head modified to incorporate the pre-chamber design. It is an optically accessible engine, utilizing a sapphire window mounted in a Bowditch piston assembly. The piston utilized standard production piston rings that ride on a lubricated cast iron bore. A circulated 50:50 ethylene glycol-water mixture was used to maintain the head and cylinder temperature at 90°C.

A variable-speed centrifugal pump was used to draw a fraction of the engine exhaust through an EGR cooler and introduce it upstream of the induction throttle. Further specifications of the engine are listed in Table 1.1.

Table 1.1 Prototype II DM-TJI optical engine engine specifications

Bore	86 mm
Stroke	95 mm
Connecting rod length	170 mm
Compression ratio	12:1
Pre-chamber volume	2532 mm3 (~5% of clearance volume)
Main chamber swept volume	0.552L
Fuel injection	High-pressure injectors
Number of orifices in nozzle	6

Pre-chamber fuel was supplied in DI configuration, whereas the main chamber fuel was supplied in PFI configuration but with a higher flow rate DI injector. Both the pre-chamber and main chamber fuel injection pressures were set at 1450 psi (~100 bar). Pre-chamber pressure data was collected using a spark plug with an integrated piezoelectric pressure transducer (Kistler 6115CF-8CQ01-4-1). Pre-chamber combustion was initiated by this 'hot' type of spark plug and a conventional automotive inductive ignition system with 30 mJ of ignition energy. A second piezoelectric pressure transducer (Kistler 6052A) installed in the engine head captured the main chamber combustion pressure. An OEM MAP sensor was used to measure intake manifold pressure. The exhaust runner pressure was measured by a Kistler 4045A5 piezo-resistive pressure transducer mounted in a water-cooled jacket.

Pre-chamber purge air was supplied using the shop compressed air supply line. The compressed air pressure was regulated via a pressure regulator. The compressed air was introduced into the pre-chamber through a hydraulically controlled poppet valve. Air flow rate was monitored with a Meriam laminar flow element (LFE), Z50MJ10-11, which was installed in the pressurized air line. A second LFE was installed upstream from the intake manifold to measure main chamber air flow rate. The engine was equipped with k-type thermocouples to monitor intake runner, exhaust

runner, coolant and pre-chamber air temperatures.

To measure the EGR percentage and lambda, pressure-compensated O<sub>2</sub> sensors (ECM Lambda-5200) were installed on the intake and exhaust runners respectively. An in-house control system managed within an NI Veristand environment was used to control the main engine parameters such as spark timing, fuel injection timing and duration for pre- and main chamber, air valve open-close timing, and the number of firing cycles. High-speed crank resolved in-cylinder pressure data was recorded using a A&D Technologies' Phoenix AM high-speed combustion analysis system (CAS) with a sampling resolution of 1 crank angle degree. Low-speed data was captured using NI DAQ modules connected to the Veristand program. Exhaust emissions were sampled using a Horiba MEXA-7200 DEGR automotive emission analyzer, capable of measuring CO, HC and NOx emissions.

Before each experiment, apart from preheating the head and cylinder assemblies to 90° C, the engine was run through 200 consecutive warm-up cycles and then EGR was introduced until the required amount of EGR was achieved. Being an optical engine with a sapphire window on the piston, the engine was run around 800-1000 cycles at a time to avoid potential damage to the piston window and keep the piston surface temperature at a normal operating temperature. Typically, for lean conditions, data processing was carried out for the last 600 cycles after the engine warmed up; whereas with 40% EGR test runs, data were processed for the last 300-400 cycles where a stable EGR rate was achieved. For all these tests, the engine was operated at wide open throttle (WOT) condition, with the inlet air pressure being close to 1 bar. To maintain the WOT operation with 40% EGR at around lambda 1, IMEP was higher compared to the WOT lean conditions tested. At lean conditions two different compression ratios were tested. At a lower 10:1 compression ratio, the engine was throttled to trap more residual gases inside the combustion chamber and show

the effectiveness of auxiliary purge air inside the pre-chamber at high residual scenarios and lambda 1. During all the tests the engine speed was kept at 1500 rpm using a DC dynamometer.

#### 3.4 Results and Discussion

## 3.4.1 DM-TJI engine operating at lean conditions

The Prototype II DM-TJI engine maintained a very good combustion stability (COV<sub>IMEP</sub><2) during lean operation up to lambda ( $\lambda$ ) 2. Contiguous IMEP plots can be useful to detect misfires or partial burns and represent combustion stability for a series of firing cycles. Figure 2 shows the results of the experiments performed with the DM-TJI engine at lean conditions at 12:1 and 10:1 compression ratios, in terms of 600- cycle IMEP and corresponding lambda traces. During these experiments the throttle position was kept fully open with a manifold absolute pressure of 98 kPa. Main chamber fuel was injected at 360 CAD bTDC using three split injection pulses at a rate of 19.8 mg/cycle. Pre-chamber fuel was injected at 120 CAD bTDC using a single pulse at a rate of 0.8 mg/cycle. The pre-chamber purge air upstream pressure was set at 1 bar (gauge), and the air valve was opened for 15 CAD starting at 160 CAD bTDC. With the 12:1 compression ratio the spark timing was fixed at 29 CAD bTDC throughout the 600-cycle test period. On the other hand, at 10:1 compression ratio the spark timing was set at 29 CAD bTDC during the first 200 cycles and then advanced by 5 CAD steps during the next two 200 cycles steps. Since these experiments did not involve any external EGR and the settling time required to get the required amount of the EGR, the last 600 cycles after the warm-up were used to lean out the mixture in three consecutive steps where each step was comprised of 200 cycles at a specific lambda. With each step fuel injection pulse duration was decreased to lean out the air-fuel mixture and achieve a higher lambda.

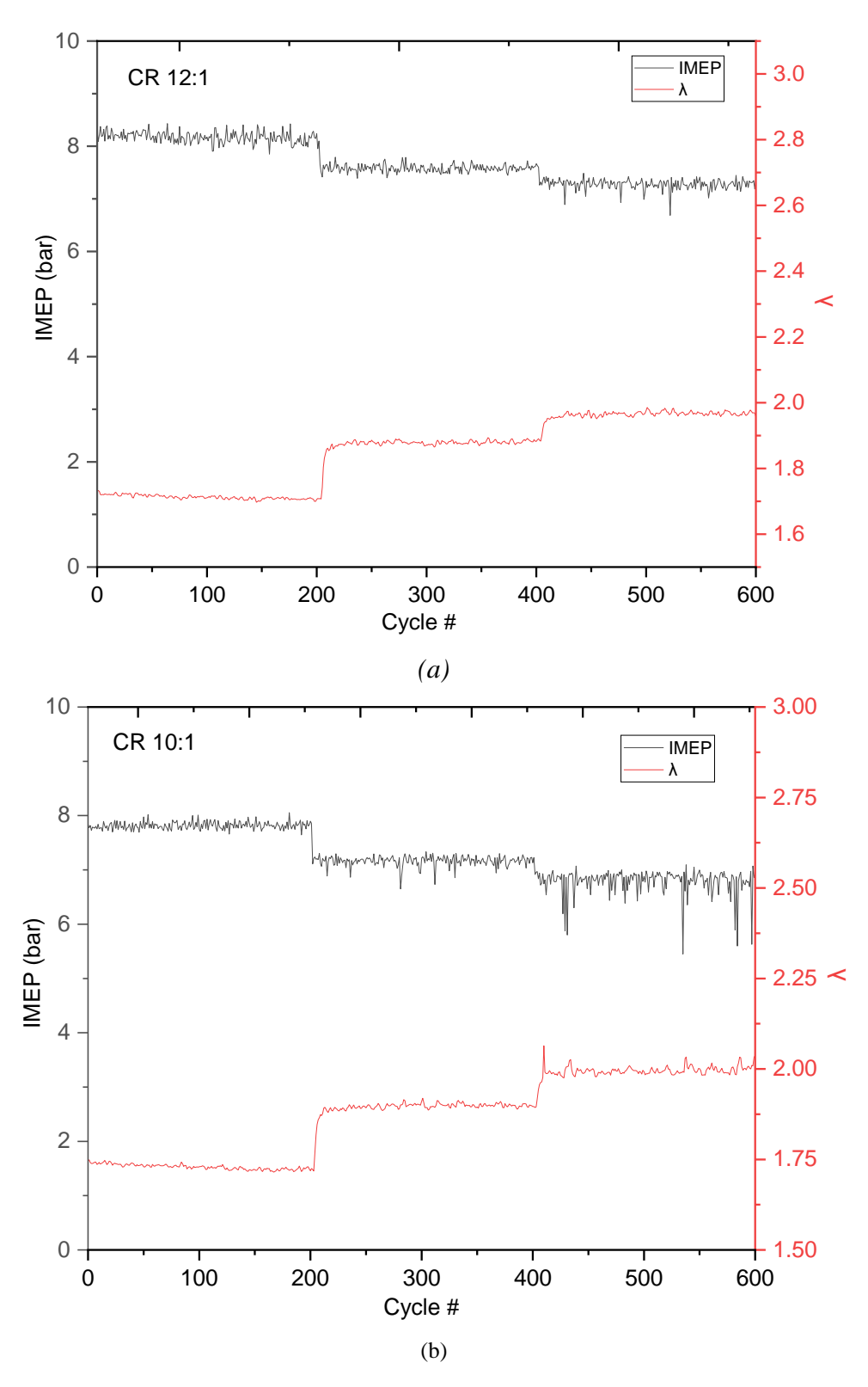


Figure 3.2 600 cycles IMEP and lambda traces of DM-TJI engine operating at lean conditions ( $\lambda$  1.7~2.0), WOT, MAP 98 kPa, 7~8 bar IMEP @ 1500 rpm: (a) compression ratio 12:1, (b) compression ratio 10:1

In Figure 3.2(a), 12:1 compression ratio, lean condition test results are plotted. With each 200 cycles section, due to decreased main fuel injection pulse duration the IMEP dropped and the corresponding lambda increased. The lambda was around 1.7 in the first 200 cycles step and then it increased to around 1.9 in the next step and finally to lambda around 2 during the last 200 cycles. The COV<sub>IMEP</sub> of the last 200 cycles with lambda close to 2 was still less than 2%, which demonstrated the ability of the DM-TJI system to operate on a very lean mixture. At this condition the volumetric flow rate of the purge air measured by the pre-chamber LFE was around 0.15 SCFM.

The next set of experiments was carried out with the same dialed conditions of the air, fuel and spark as mentioned above but at a lower compression ratio of 10:1. The same technique of leaning out the mixture in three steps of 200 cycles each was followed. During the last two steps, with lambda around 1.9 and 2 respectively, the combustion stability suffered slightly. Therefore, for the next set of runs, the spark was advanced by a step of 5 CAD during the last two steps. The results of this modified set of experiments with the same air-fuel timing and advanced spark during the last two steps at a lower 10:1 compression ratio are shown in Figure 3.2(b). As can be seen from Figure 3.2(b), even with total spark advance of 10 CAD compared to the first 200 cycles step, for the last 200 cycles combustion stability was worse than for the 12:1 compression ratio results at similar conditions.

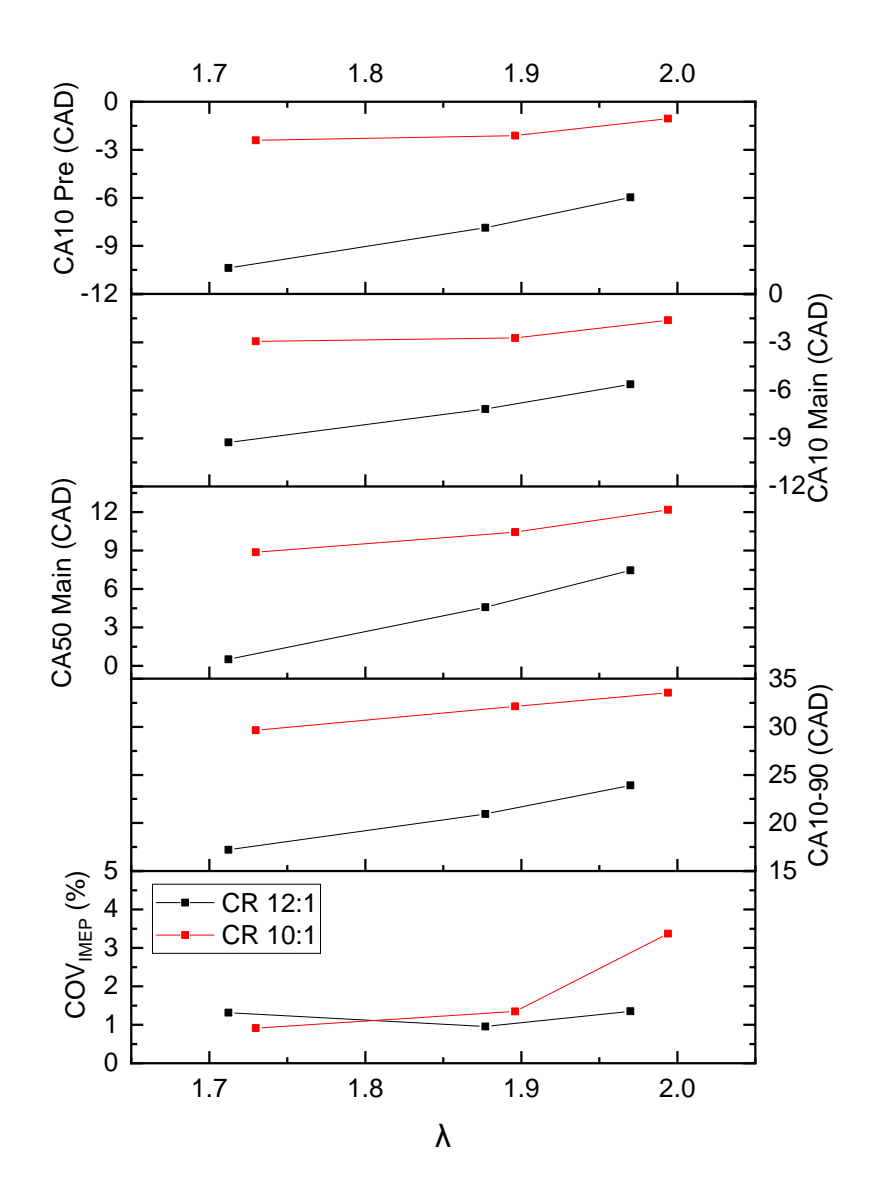


Figure 3.3 Comparison of major combustion parameters between high and low compression ratios at lean conditions ( $\lambda$  1.7~2.0), WOT, MAP 98 kPa, 7~8 bar IMEP @ 1500 rpm

Figure 3.3 compares the major combustion parameters from the two sets of experiments presented in 3.2(a) and 3.2(b). In Figure 3.3, the first plot shows the pre-chamber CA10 value. Its increasing trend with higher lambda suggests longer ignition delays in the pre-chamber due to the increased probability of leaner air-fuel mixture inside the pre-chamber, as the main chamber mixture becomes leaner. The second and the third plot from the top in Figure 3.3 show the main chamber CA10 and CA50 values respectively. Both show the same increasing trend with lambda; this is a

direct consequence of earlier pre-chamber CA10 values. The fourth plot from the top in Figure 3.3 shows the main chamber 10-90 mass fraction burn duration. A similar increasing trend with lambda was seen here as well, because flame propagation becomes increasingly slower as the airfuel mixture becomes leaner and thus overall burn duration increases. The pre-chamber CA10, main chamber CA10, main chamber CA50 and main chamber 10-90 burn durations all show an increasing trend with increase in lambda in both the 12:1 and 10:1 compression ratio cases.

This increasing trend in burn parameters with increase in lambda was expected, since with leaner air-fuel mixture it becomes increasingly difficult for the pre-chamber mixture to ignite and then the flame propagation through the main chamber mixture also becomes slower which consequently increases the overall 10-90 burn durations. In the bottom plot of the Figure 3.3, combustion stability in terms of COV<sub>IMEP</sub> is given for each of the 200 cycles steps during the two set of test runs. While at 12:1 compression ratio the combustion stability does not vary significantly up to lambda 2, the same lambda 2 operation at 10:1 compression ratio has a higher COV value of 3.4% compared to lower than 1.5% values for the rest of the cases. This decrease in combustion stability with lower compression ratio during lean operation is due to the increased amount of trapped residual gases at lower compression. With lower compression ratio the trapped residual percentage increases[79] and with this increased amount of residual gases the already lean air-fuel mixture becomes even more diluted. The effect of increased residuals is more apparent at lambda 2 compared to lambda 1.72 and 1.87. Since the air-fuel mixture is already very lean and close to the lean limit, any further increase in dilution due to higher percentage of residuals makes the combustion unstable.

Moreover, higher compression had the added benefit of higher peak pressure and temperature which aids mixture formation, decreases ignition delay in the pre-chamber and increases flame speed. From Figure 3.3 it is apparent that 12:1 compression ratio had earlier pre-chamber ignition (earlier CA10 for the pre-chamber) with earlier combustion phasing (CA50 of the main chamber) as well as shorter burn duration (CA10-90) compared to 10:1 compression ratio setup. The slight increase in global lambda values also suggest reduced combustion efficiency for the 10:1 compression ratio as well. Moreover, for the same fueling rate the higher compression ratio yielded better IMEP values.

## 3.4.2 Effect of pre-chamber purge air

The previous tests at lean conditions showed that lowering the compression ratio increases the trapped residuals inside the cylinder due to which the combustion stability suffers especially close to the lean limit. Those tests were performed at WOT conditions with manifold absolute pressure of 98 kPa. The next set of experiments were performed with the same low 10:1 compression ratio but at a throttled condition with a manifold absolute pressure of 68 kPa. The load was also decreased to 6 bar IMEP and air-fuel ratio was kept stoichiometric ( $\lambda$ ~1). Figure 3.4 shows the 300 cycle IMEP traces of the experiment conducted at this throttled stoichiometric condition with the first 150 cycles without the purge air and the last 150 cycles with the purge air. It is clear from the IMEP traces that the engine could not maintain stable operation without the pre-chamber purge air at this throttled low compression stoichiometric condition. With lower manifold pressure the trapped amount of residual gases inside the cylinder increases even further and due to the prechamber design with small orifices this increased amount of residual gases have a higher probability to get trapped inside the pre-chamber. Without the pre-chamber purge air, the air-fuel mixture inside the pre-chamber necessarily contained a very high percentage of residual gases and consequently the mixture inside the pre-chamber was not able to ignite and initiate jets to burn the main chamber mixture. Without the pre-chamber purge air, the engine showed continuous misfires.

In contrast, during the last 150 cycles in Figure 3.4, the pre-chamber air valve was turned on and the engine maintained stable combustion with no misfires. This demonstrates the importance of pre-chamber purge air in maintaining stable operation with high amounts of residual gases at stoichiometric conditions. In previous tests, it was seen that at WOT lean operating conditions, the DM-TJI engine could maintain stable operation even without the pre-chamber purge air. The other auxiliary fueled pre-chamber designs show similar results[57]. However, when the amount of internal residue increases (as shown by the throttled test result mentioned above), the pre-chamber purge air becomes critical for maintaining stable operation. This especially applies close to stoichiometry, where the residual gases do not contain any unburnt air from the previous cycle. This result, showing the effectiveness of the DM-TJI system in dealing with mixtures containing high percentages of internal residuals at stoichiometric condition, encouraged the high-external-EGR experiments which are discussed in the following sections.

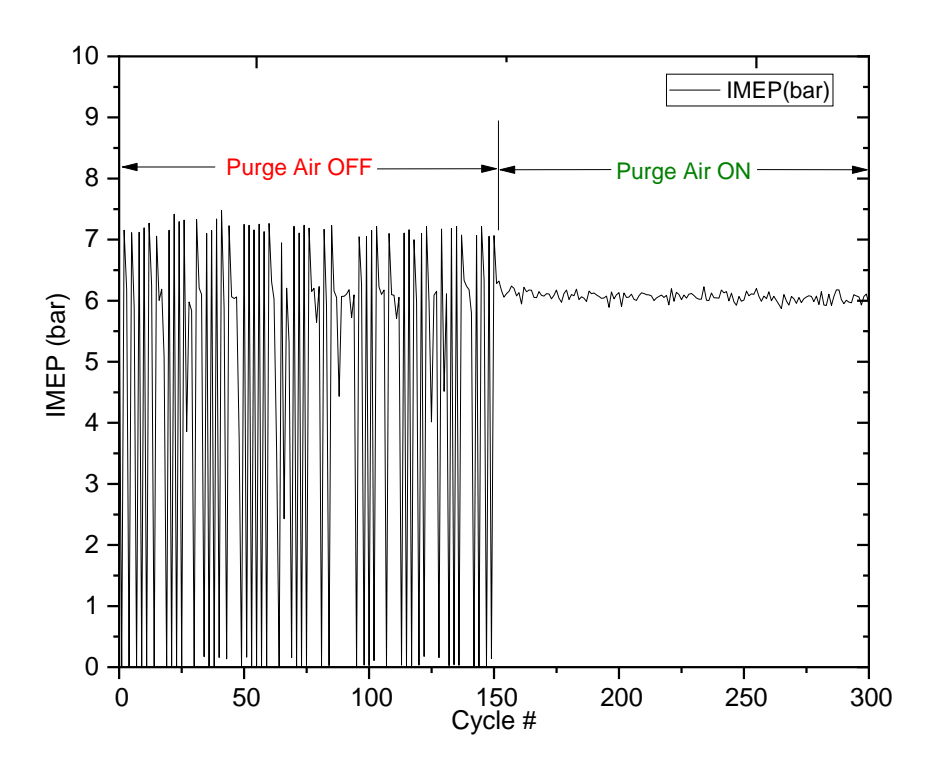


Figure 3.4 300 cycle IMEP traces with and without the purge air at throttled condition, 68 kPa manifold pressure, 6 bar IMEP @ 1500 rpm,  $\lambda \sim 1$ , compression ratio 10:1

### 3.4.3 DM-TJI engine operating at highly EGR (~40%) diluted conditions

Experiments with external EGR were performed at 12:1 compression ratio. All the tests with external EGR were performed at WOT conditions with manifold absolute pressure around 98 kPa. The same fueling strategy as before was followed: a three-pulse split injection in the main chamber and a single injection in the pre-chamber. The fuel injection rate was increased to 26.8 mg/cycle to ensure lambda 1 operation at WOT with external EGR. Fuel timing in the main chamber was kept at 360 CAD bTDC. The pre-chamber auxiliary fueling rate was maintained at 0.8 mg/cycle, but the timing was changed to 90 CAD bTDC. The pre-chamber purge air upstream pressure was set at 4 bar (gauge). The air valve was opened at 145 CAD bTDC, with an opening duration of 30 CAD. These operating parameters were found to be adequate to maintain stable operation at 40% EGR diluted condition and were chosen based on previous experiments with a 1.25 mm nozzle orifice setup.

At the start of each 800 cycles test run, the engine was run without EGR for about 100 cycles to warm up; then the EGR control valve was opened to introduce EGR to the intake. The EGR line was connected upstream from the main throttle valve. The large intake plenum ensured that enough space was provided for EGR to mix properly before entering the combustion chamber.

The Prototype II DM-TJI engine operated successfully at 40% external EGR dilution at stoichiometric conditions ( $\lambda\sim1$ ), with a COV<sub>IMEP</sub> < 1.5%. Figure 3.5 shows the results of 200 cycles of engine operation at 12.5% intake O<sub>2</sub> or 40% EGR. It can be observed that the net IMEP at this condition was around 9.2 bar and no misfires or partial burns were detected during 40% EGR diluted operation with the DM-TJI engine. The exhaust lambda during the test stayed at 1 while the real-time COV<sub>IMEP</sub> trace remained less than 1.5% for the 200 cycles.

As illustrated in Figure 3.5, during the 200 cycles of engine operation the intake  $O_2$  measured at the intake manifold stayed around 12.5%, which translates to ~40% EGR. It should be noted that this intake  $O_2$  measurement does not account for the auxiliary purge air introduced through the air valve in the pre-chamber.

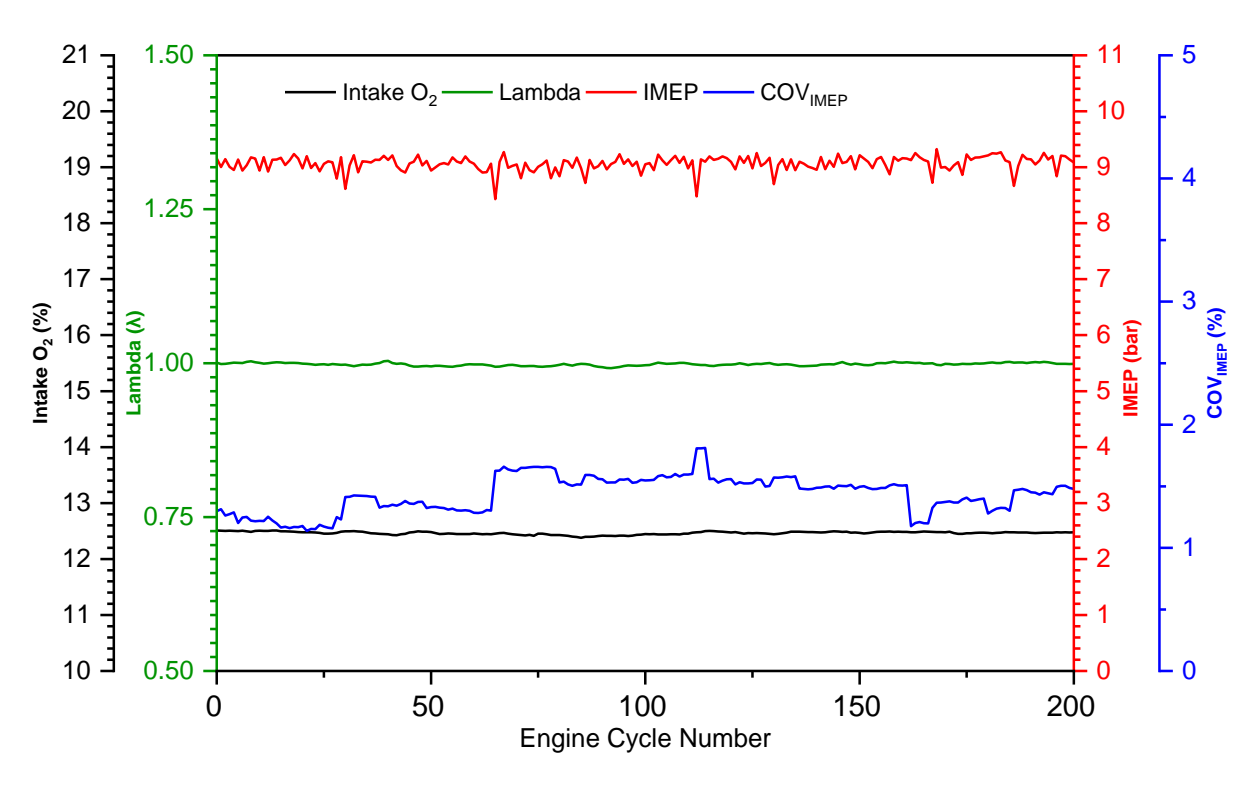


Figure 3.5 DM-TJI engine test results of 200 cycles of continuous operation at 40% EGR dilution,  $\lambda \sim 1$ , 9.2 bar IMEP @ 1500 rpm, 1.25 mm nozzle orifice

With a slightly rich mixture, combustion stability of the DM-TJI engine running with 40% EGR dilution was found to be even higher. Figure 3.6 shows 350 cycles of DM-TJI engine operation with 40% EGR at approximately lambda 0.96. Main chamber fuel injection was increased to attain a slightly fuel-rich condition. In Figure 3.6, 350 cycles of IMEP traces show no misfires or partial burns, and the corresponding COV<sub>IMEP</sub> for these 350 cycles was less than 1%. The fluctuating COV<sub>IMEP</sub> trace shows the real-time values using 10 adjacent cycle IMEP values to get a good response on the COV<sub>IMEP</sub> while the engine was running. The lambda trace shows that during these

350 cycles the exhaust lambda was around 0.96.

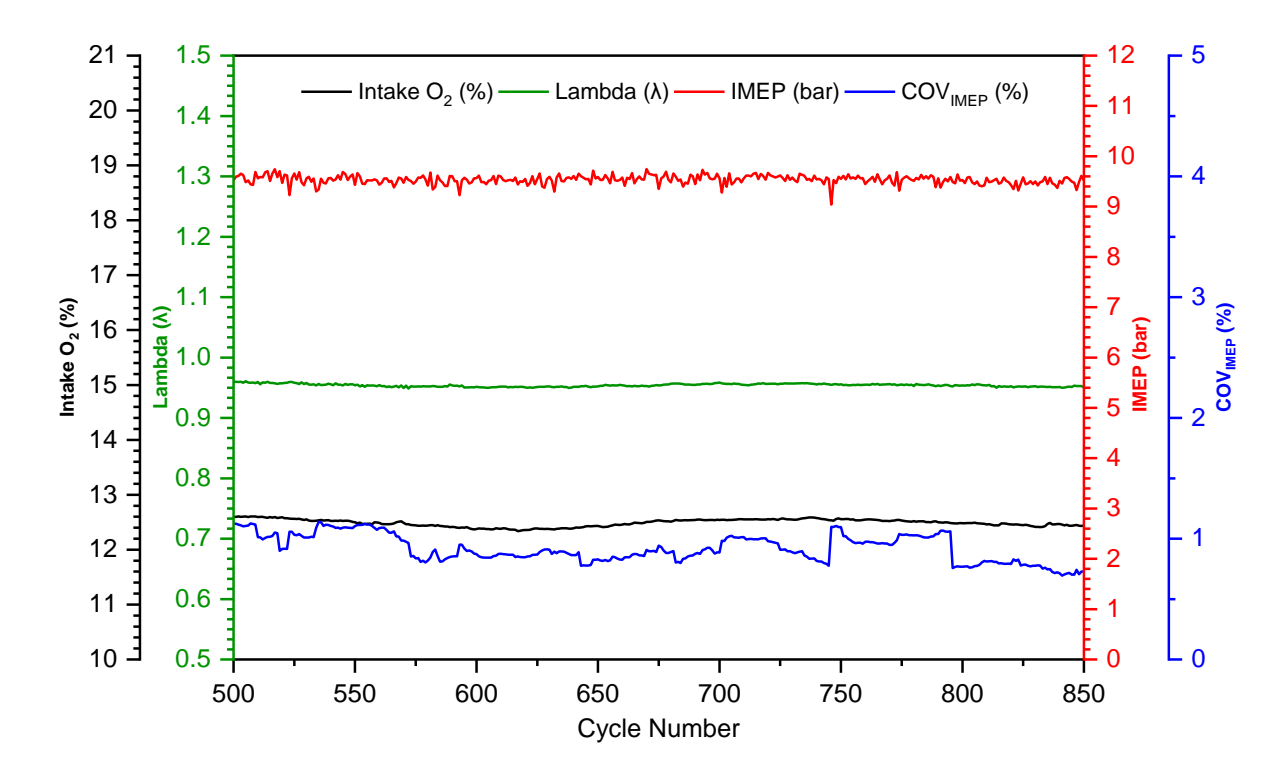


Figure 3.6 DM-TJI engine test results of 350 cycles of continuous operation at 40% EGR dilution,  $\lambda$ ~0.96, 9.5 bar IMEP @ 1500 rpm, 1.25 mm nozzle orifice

This slightly rich condition was chosen to achieve a very robust combustion stability ( $COV_{IMEP}$ <1%) to be reused during the nozzle orifice diameter tests that will be described in later sections. At this 40% EGR diluted condition, the spark timing was set at 29 degrees BTDC and the resulting average CA50 was found to be ~7 CAD aTDC with a 10 to 90 burn duration of ~17 CAD.

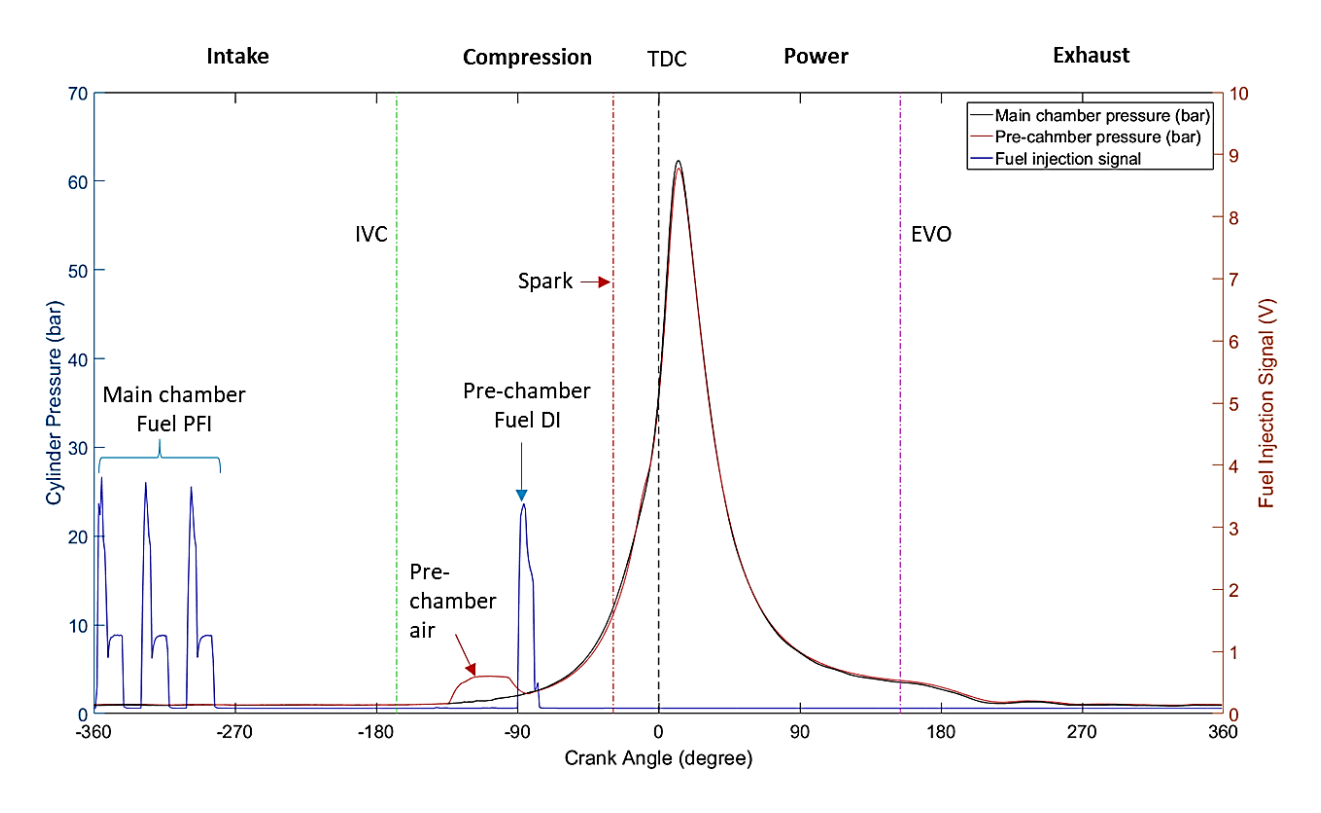


Figure 3.7 DM-TJI engine sequence of events at 40% EGR diluted condition

Figure 3.7 shows the DM-TJI engine sequence of events at a 40% EGR diluted condition. During previous experiments, the relative timing of the pre-chamber auxiliary air and auxiliary fuel was found to be critical. In Figure 3.7, the bump shown in the pre-chamber pressure trace during the compression stroke was due to the introduction of compressed purge air inside the pre-chamber, which resulted in a net flow from the pre-chamber to the main chamber. Auxiliary fuel injection inside the pre-chamber was started close to the pressure equalization point between pre-chamber and main chamber. The relative timing between these two events was found to be of paramount importance to maintain successful operation at such high-EGR diluted conditions. If the pre-chamber fuel were injected earlier while there was still considerable pressure differential between the pre-chamber and the main chamber, a considerable portion of the injected fuel would blow out of the pre-chamber, causing pre-chamber misfire.

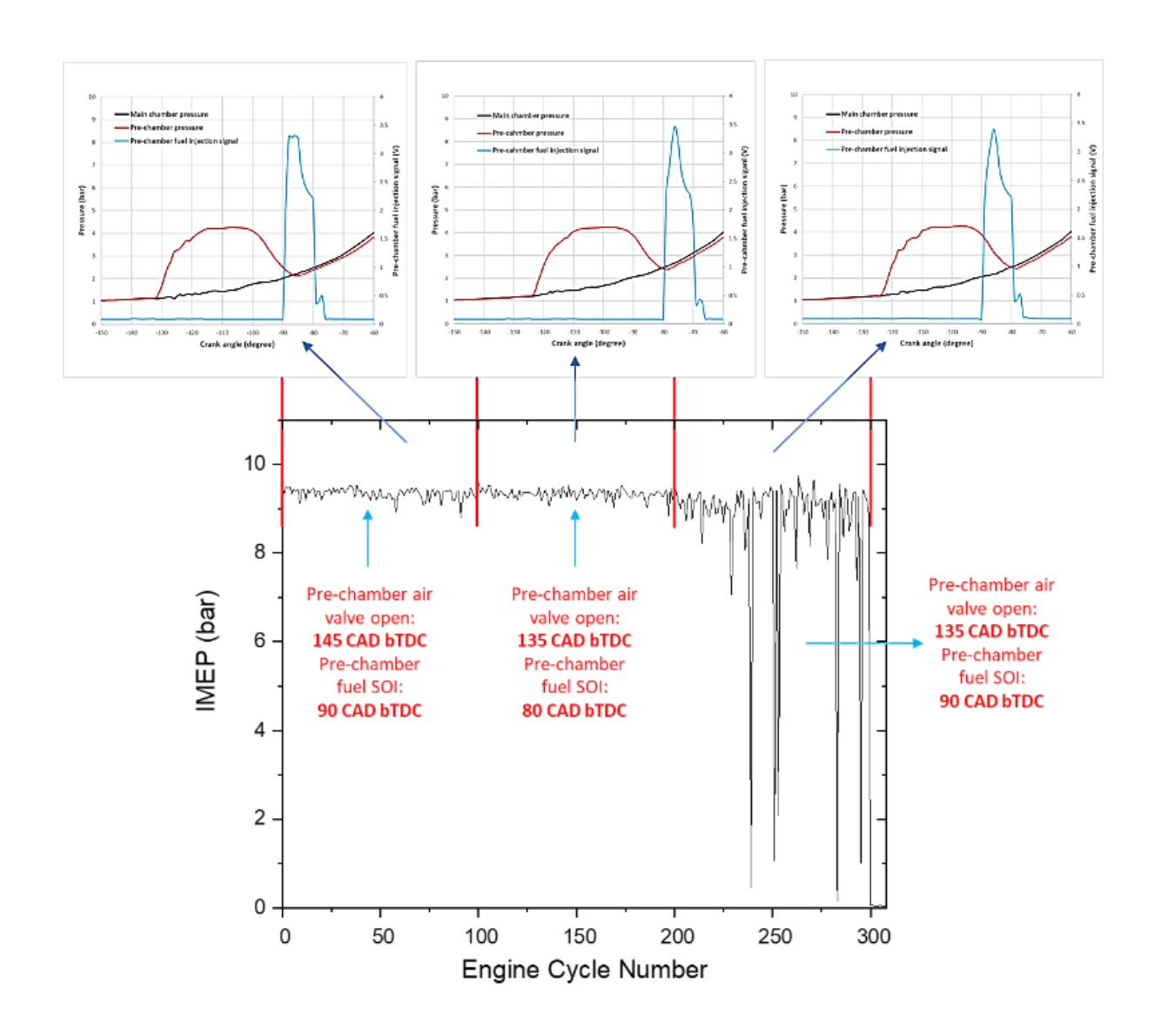


Figure 3.8 DM-TJI engine test results of 300 cycles of continuous operation showing the effect of change in relative timing of the pre-chamber auxiliary air and fuel at 40% EGR dilution,  $\lambda$ ~0.96, 9.5 bar IMEP @ 1500 rpm, 1.25 mm nozzle orifice

In Figure 3.8, the effect of change in relative timing of the pre-chamber auxiliary air and fuel has been demonstrated using IMEP traces for 300 cycles of continuous engine operation at 40% EGR diluted condition. In the first 100 cycles, the pre-chamber air valve opening timing was set at 145 CAD bTDC and the start of fuel injection timing was set at 90 CAD bTDC. With these timings, no misfire was detected. During the next 100 cycles, both the air valve timing and start of fuel injection were retarded by 10 CAD at 135 CAD bTDC and 80 CAD bTDC respectively. The

engine still operated without misfires. Then, in the last 100 cycles, the air valve timing was kept at 135 CAD bTDC but the start of fuel injection was moved back to 90 CAD bTDC. This meant the pre-chamber fuel was injected while there was a net flow out of the pre-chamber to the main chamber, causing the fuel to blow out of the pre-chamber and subsequently causing misfires. In the IMEP trace it is clearly visible that during this last 100 cycles of overlapped air-fuel timing, many misfires and partial burns were detected. Thus, maintaining the relative timing between the pre-chamber auxiliary air and auxiliary fuel within an operable range is very important, especially with high EGR dilution.

The air valve pressure setting and the duration were determined through a series of tests leading to acceptable combustion stability at 40% EGR condition. It should be noted that the pressure settings for the purge air, the air valve open duration and method of air delivery inside the prechamber mentioned during the 40% EGR operation are not optimized and are used to demonstrate the proof of concept. Work is already underway with the Prototype III DM-TJI metal engine to optimize the pre-chamber scavenging setup.

While these test results have shown that at loads of 9.2 to 9.5 bar IMEP, the DM-TJI engine could successfully tolerate up to 40% external EGR dilution, it should be noted that these loads are fairly high and typically at higher loads the dilution tolerance is better. These load points were chosen based on wide open throttle (WOT) operation with 40% EGR diluted stoichiometric condition ( $\lambda$ ~1). Lower load was not attempted in order to maintain the WOT operation with 40% EGR dilution. At lower loads dilution tolerance may be lower and this will be investigated in future.

However, the results found in this current study clearly demonstrate that even at the high-EGR diluted condition, the DM-TJI engine was able to maintain very stable operation with fast burn rates. The auxiliary purge air inside the pre-chamber ensures that the residual gases are purged out

after every cycle so that ignitable air-fuel mixture can be maintained inside the pre-chamber even with very high external EGR. Once the pre-chamber mixture ignites, the initial flame around the pre-chamber spark plug is transformed into multiple pressure-driven turbulent flame jets penetrating the main chamber through the pre-chamber nozzle orifices. The multiple turbulent jets, with substantial surface area and high ignition energy, form multiple ignition sites distributed around the combustion chamber. These multiple distributed ignition sites work in parallel and ensure that the traveling distance of the flames are short, resulting in such fast burn rates even with very high EGR. The DM-TJI system solves the scavenging problem of the pre-chamber initiated turbulent jet ignition systems by introducing auxiliary purge air to the pre-chamber and maintains stable operation with very high EGR (up to  $\sim$ 40%) at stoichiometric ( $\lambda\sim$ 1) condition. This enables the DM-TJI system to attain high thermal efficiency without sacrificing the effective usage of TWC.

#### 3.4.4 Effect of nozzle orifice diameter in DM-TJI engine operation

Experiments were conducted with six different pre-chamber nozzle orifice sizes. While the layout of the orifices was kept the same, the orifice diameters were varied. The pre-chamber nozzle orifice diameters used for the six configurations were 0.9 mm, 1.0 mm, 1.25 mm, 1.5 mm, 1.75mm, and 2.0 mm. The influence of nozzle orifice diameter was studied to determine how the orifice diameter affected engine operation with respect to running stability and major combustion parameters.

### 3.4.4.1 Lean operating condition

First, the six different nozzle orifice diameters were tested at lean operating conditions ( $\lambda \sim 1.75$ ) with excess air dilution. The DM-TJI optical engine was operated for 800 cycles at WOT with a load of approximately 7.2 bar at 1500 rpm. Figure 3.9 shows the captured 800 cycles IMEP traces

for the six orifice diameters tested. As depicted in Figure 3.9, all six orifice diameters for the prechamber nozzle performed in a stable manner at lean conditions after engine warm-up. Even though combustion stability was high for all of them (COV<sub>IMEP</sub><1.5%), during the warm-up cycles some differences could be seen from these traces. The larger-diameter orifices showed fewer partial burns during the warm-up. The 0.9 mm nozzle setup experienced misfires during the start of 800 cycles and required the highest number of cycles for complete warm-up and operation without misfires or partial burns.

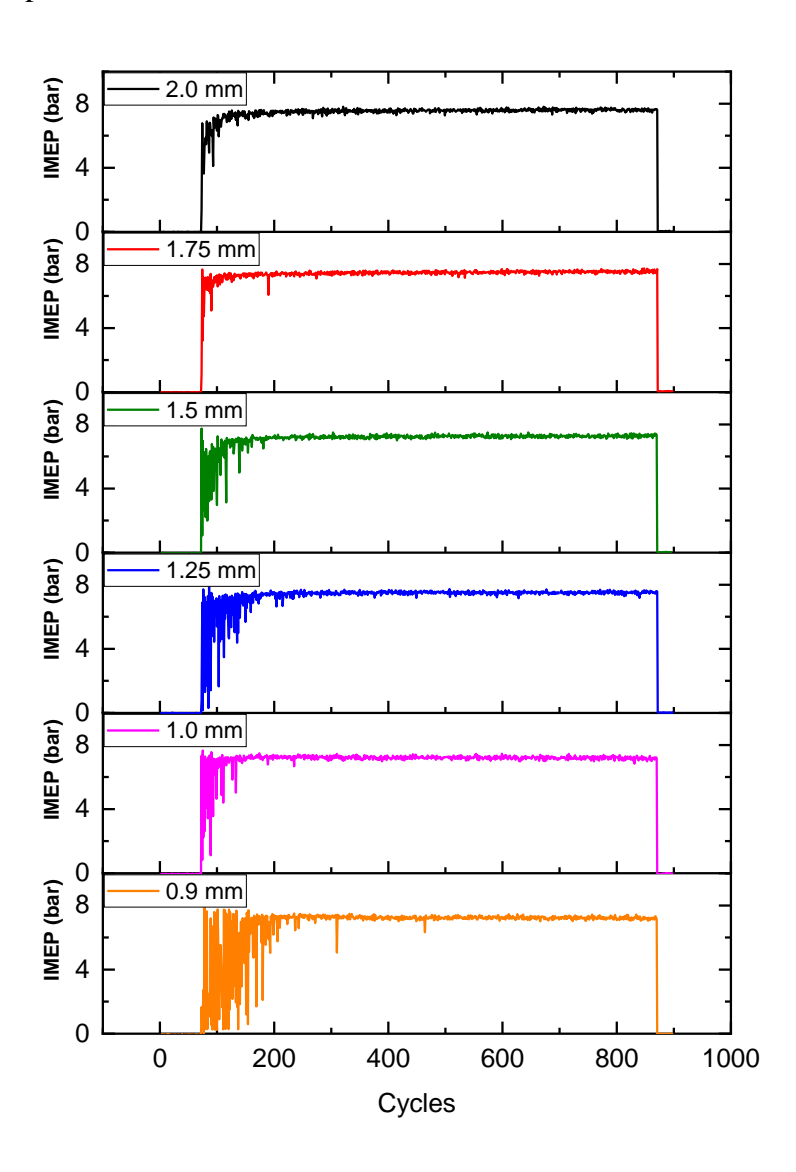


Figure 3.9 800 cycles IMEP trace for different pre-chamber nozzle orifice diameters at lean condition ( $\lambda \sim 1.75$ ), 7.2 bar IMEP at 1500 rpm

These tests suggested that the smaller-diameter orifices contribute towards additional quenching of the turbulent jets leaving the pre-chamber nozzle; however, once the combustion chamber heated up, the quenching effect did not contribute to jet/flame extinction. This was expected since flame quenching distance typically decreases with increase in wall temperature [84].

Since all six orifice diameters maintained stable combustion at the lean condition of lambda ~1.75, further cylinder pressure-trace-based analysis was carried out using the last 300 cycles of each test run at different orifice diameters to investigate their effect on major combustion parameters. Figure 3.10, from top to bottom, plots average values of pre-chamber CA10, main chamber CA10, main chamber CA50, main chamber 10-90 burn duration and COV<sub>IMEP</sub> for 300 cycles for different orifice diameters respectively.

As shown in Figure 3.10, the pre-chamber CA10 values for the 0.9 mm and 1.0 mm nozzle were almost 10 CAD earlier compared to the rest of the configurations tested. This 10 CAD advance in pre-chamber CA10 did not necessarily translate to the same amount of CAD shift in the main chamber CA10 or the CA50 phasing (given by their similar but somewhat flatter distribution over a smaller range). However, in the case of 10-90 burn duration, the 0.9 mm and 1.0 mm diameter nozzle exhibited shorter overall burn duration compared to the rest of the diameters tested. These earlier pre-chamber CA10 and shorter main chamber 10-90 burn durations could be the result of increased restriction to flow with decreasing orifice diameters. As depicted in Figure 3.11, only the 0.9 mm and 1.0 mm configuration showed distinct pressure rise inside the pre-chamber after the ignition. Once the contents of the pre-chamber ignited, the pressure started rising in the pre-chamber due to increased resistance to flow through smaller orifices. In contrast, pressure did not rise considerably with larger-diameter orifices once the pre-chamber combustion started, due to less flow restriction in the pre-chamber. The combustion parameters are calculated using the well-

known Rassweiler and Withrow method [85]. With the distinct pressure rise inside the prechamber, the pre-chamber CA10 values for the 0.9 mm and 1.0 mm nozzle were identified to be much earlier than the rest.

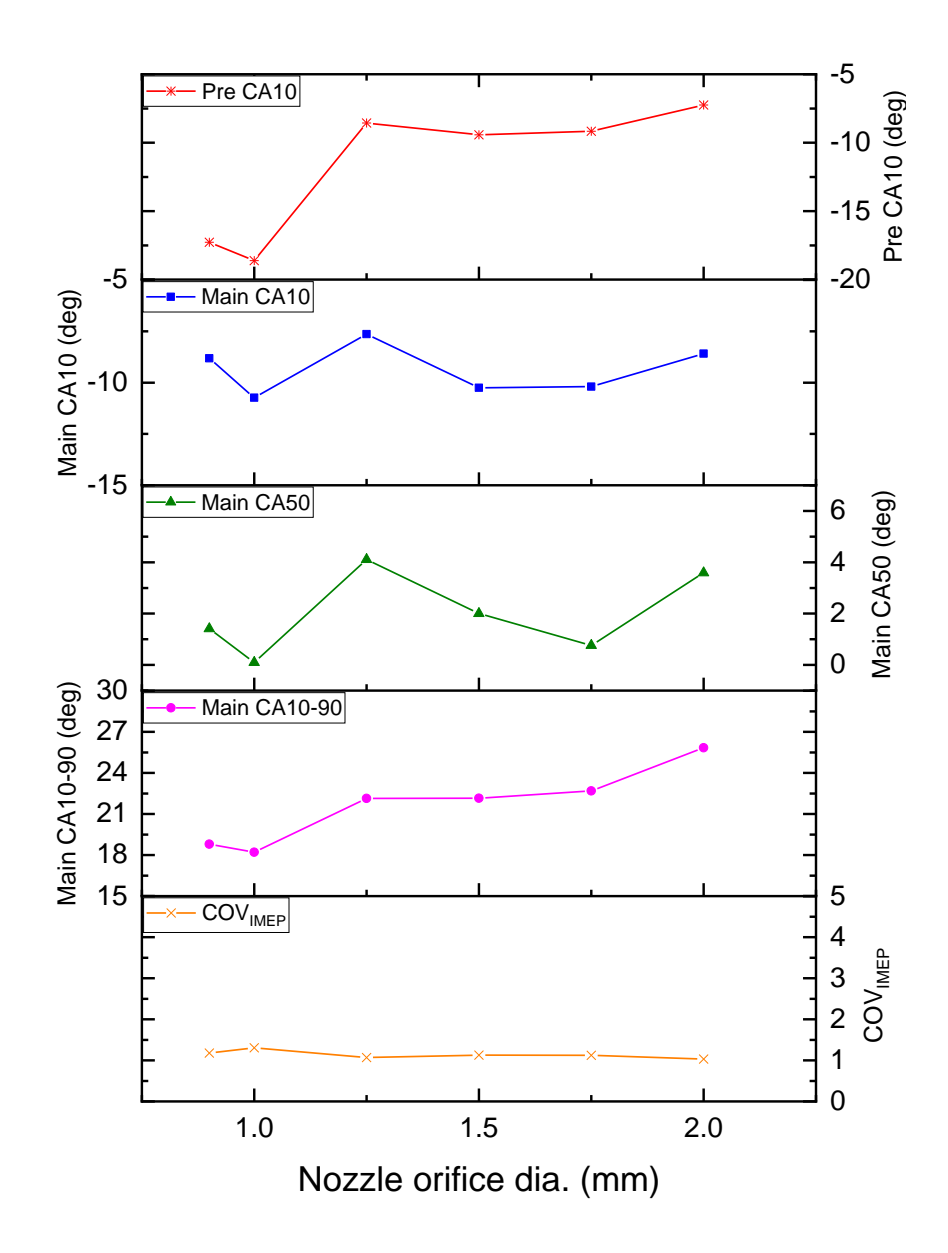


Figure 3.10 300 cycle pressure trace analysis- average combustion parameters at six different nozzle orifice diameters, lean condition ( $\lambda \sim 1.75$ ), 7.2 bar IMEP at 1500 rpm

The CA10-90 plot in Figure 3.10 shows that the 10-90 burn duration increases with increasing orifice diameter. With smaller-diameter orifices, the increased flow restriction resulted in deeper

jet penetration into the main chamber, yielding a better spatial distribution of ignition sites. This shortened flame travel paths and consequently reduced the overall burn duration. Combustion stability for all the orifice diameters tested were found to be very good ( $COV_{IMEP} < 1.5$ ), as shown in the bottom plot of Figure 3.10.

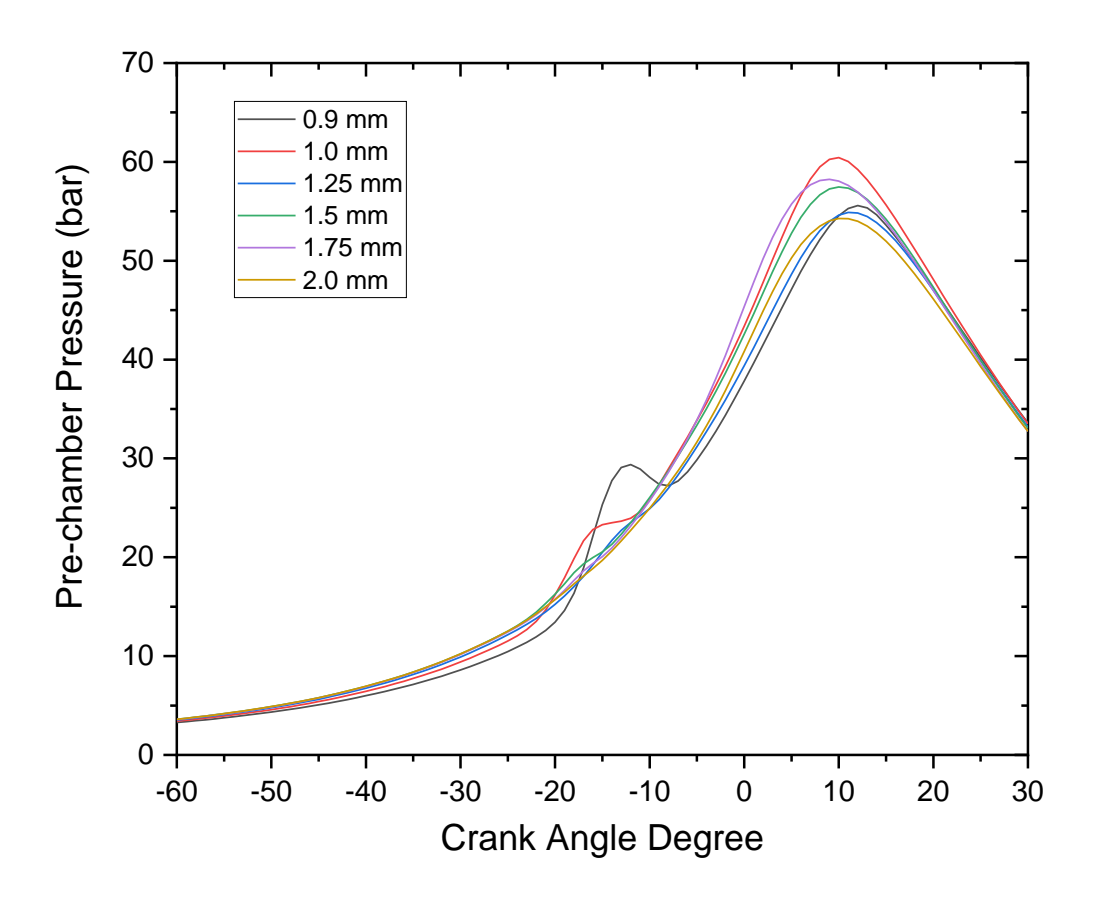


Figure 3.11 300 cycle average pre-chamber pressure trace for different nozzle orifice diameters

#### 3.4.4.2 40% EGR diluted condition

The same six orifice diameters were tested with 40% EGR diluted condition. A slightly rich ( $\lambda \sim 0.96$ ) air-fuel mixture was used during this set of experiments to ensure better combustion stability. Figure 3.12 presents 300 continuous cycles of IMEP traces obtained with different nozzle orifice sizes at 40% EGR dilution. Figure 3.12 shows that the nozzles with 1.25 mm diameter and greater performed consistently at 40% EGR, with no misfires or partial burns detected during the 300

cycles of continuous engine operation. With the 1.0 mm nozzle orifice, partial burns were detected (shown by the drop in IMEP values) and combustion stability was low. The nozzle with 0.9 mm orifice exhibited the worst performance with lots of misfires (IMEP dropping to zero) and partial burns. Stable operation at 40% EGR was not achieved with the 0.9 mm nozzle orifices.

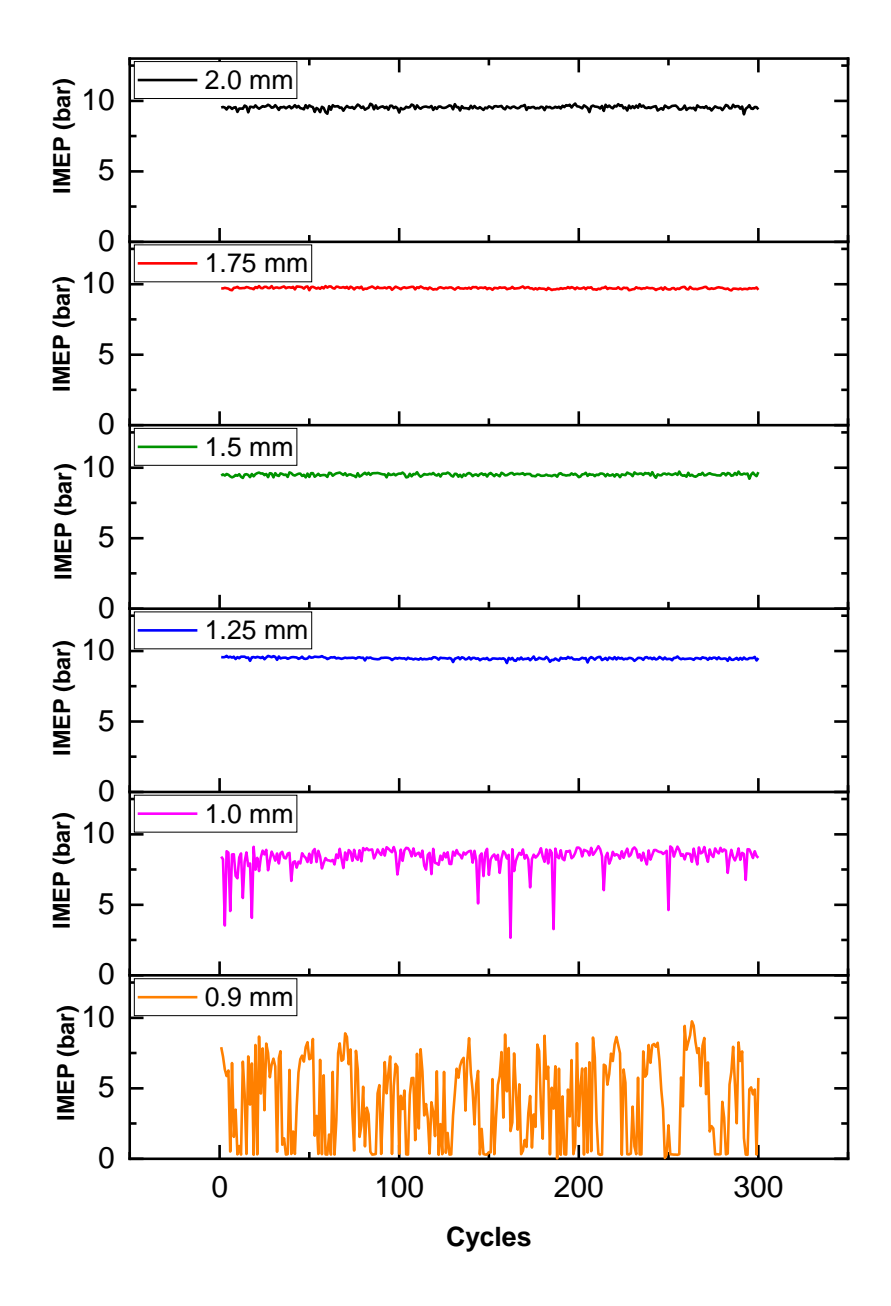


Figure 3.12 300 cycles IMEP trace for different pre-chamber nozzle orifice diameters at 40% EGR dilution (12.5% intake  $O_2$ ), ( $\lambda \sim 0.96$ ), 9.5 bar IMEP @ 1500 rpm, WOT

Since the nozzles with orifice diameters of 1.25 mm, 1.5 mm, 1.75 mm and 2.0 mm all showed good combustion stability at 40% EGR operating conditions, further analysis was carried out based on 300 cycle pressure data to identify how the major combustion parameters were affected by different nozzle sizes. Results of this analysis are depicted in Figure 3.13.

During all these 40% EGR tests with varied nozzle sizes, the spark timing, the amount of main chamber fuel, the amount of pre-chamber fuel and the respective injection timings were kept the same as mentioned in the previous section. The pre-chamber purge air pressure and the air valve open-close duration were also unchanged. Thus, changes in combustion parameters would be primarily due to nozzle geometry. At this high EGR level the 1.25 mm, 1.5 mm, 1.75 mm and 2.0 mm configurations maintained very high combustion stability (COV<sub>IMEP</sub><1.5). While all the four larger-diameter configurations showed stable combustion, with fixed spark dial their combustion behaviors were slightly different. The CA10-90 plot shows that the 10-90 burn duration increased with increasing nozzle orifice diameters. This increase could be attributed to the unfavorable distribution of ignition sites due to decreased jet penetration, as was discussed above. Even though the 1.25 mm nozzle provided the fastest 10 to 90 burn duration among all the configurations, the 1.5 mm nozzle provided the earliest start of combustion, with the CA10 and CA50 values being the earliest. The 2.0 mm nozzle configuration exhibited the slowest combustion, with the largest 10 to 90 burn duration of almost 26 CAD and the CA50 shifted around 11 CAD. Even though the 2.0 mm nozzle had CA10 values comparable to those of the 1.25 mm nozzle, the CA90 values shifted by almost 6 CAD, manifesting a slower burn rate due to increase in flame travel distance from the ignition initiation sites (discussed in later sections).

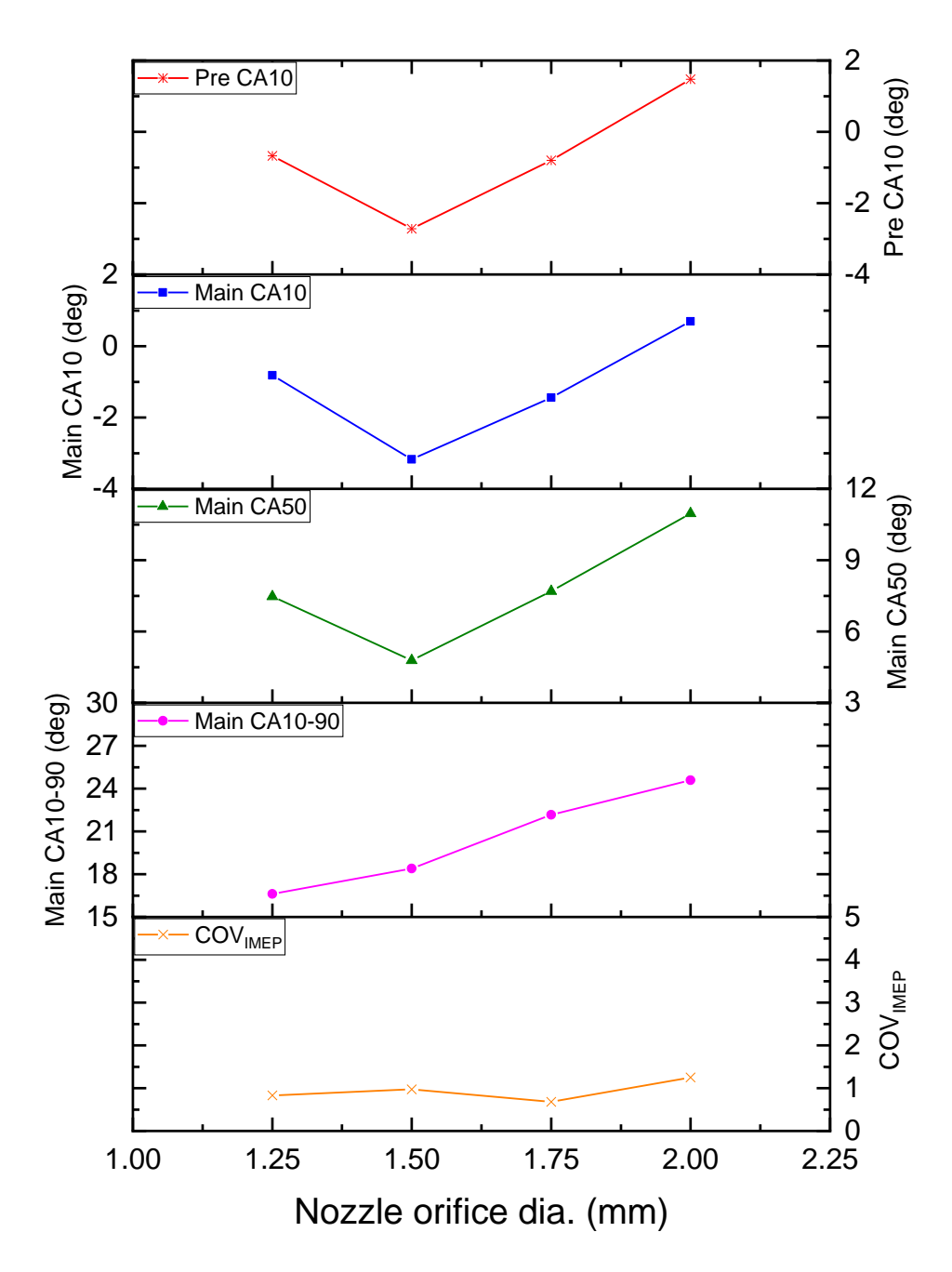


Figure 3.13 300 cycle pressure trace analysis- average combustion parameters at four different nozzle orifice diameters

Thus, at 40% EGR condition with fixed auxiliary air and fuel timings, the orifice diameter of the pre-chamber nozzle had a significant effect on the operation of the DM-TJI engine. The 0.9 mm orifice did not maintain stable operations and showed a series of misfires. Likewise, the 1.0 mm orifice had many partial burns with very high  $COV_{IMEP}$ . On the other hand, the nozzle orifices with

greater diameters (1.25 mm, 1.5mm, 1.75mm and 2.0mm) all maintained stable operation.

This result is opposite to those obtained at lean operation. At lean operating conditions, both the 0.9 mm and 1.0 mm diameter nozzle performed favorably whereas at 40% EGR they could not maintain stable operation at all. Since 0.9 mm and 1.0 mm orifices performed well with excess air dilution, quenching of the jets with smaller orifices might not have been the issue. Instead, the inability of the smaller orifices to maintain stable combustion at 40% EGR diluted condition could be attributed to the lack of formation of combustible mixture inside the pre-chamber due to the unavailability of either the purge air or the fuel.

With smaller orifice diameter of the pre-chamber nozzle, the resistance to air flow through the prechamber air valve increases and consequently the amount of purge air introduced through the air valve at fixed upstream air pressure and same open duration decreases. The volume flow rates of the air introduced through the air valve inside the pre-chamber for different orifice diameters of the nozzle have been plotted in Figure 3.14. Figure 3.14 demonstrates that with the largest orifice diameter of 2.0 mm, the flow rate was around 1.15 SCFM. With the smallest 0.9 mm diameter orifice, the volume flow rate dropped by almost half to approximately 0.53 SCFM. It is clear that the volume flow rate decreases with decrease in orifice diameter of the pre-chamber nozzle due to increased flow resistance. At 40% EGR dilution, the purge air is critical. With smaller-diameter nozzle orifice setups, this lack of purge air could have been unfavorable. However, as mentioned previously, the purge air pressure settings and the air valve open duration are not optimized at all and the resulting purge air volume flow rate is estimated to be much higher than the amount needed to purge the pre-chamber optimally, Also, if the volume flow rates of purge air for 1.0 mm and 1.25mm nozzle orifices are compared, they are within 10% of each other. It is unusual that such a small change in purge air volume flow rate would cause a drastic change in combustion stability,

especially when the volume flow rate is considerably higher than the actual scavenging requirement. To ensure the fact that it was not the lack of scavenging air that caused the misfires, subsequent tests were carried out with 1.0 mm nozzle setup and upstream pressure of the air valve set at 5 bar (gauge). The resulting volume flow rate was around 0.92 SCFM, which is higher than the volume flow rate of the 1.25 mm diameter orifices and close to that for 1.5 mm diameter orifices. Thus, the fact that the 1.0 mm configuration did not perform as well as the 1.25mm or the 1.5 mm nozzles with similar volume flow rate of the purge air indicates that it was not the lack of scavenging air that caused the smaller-diameter orifices to behave adversely.

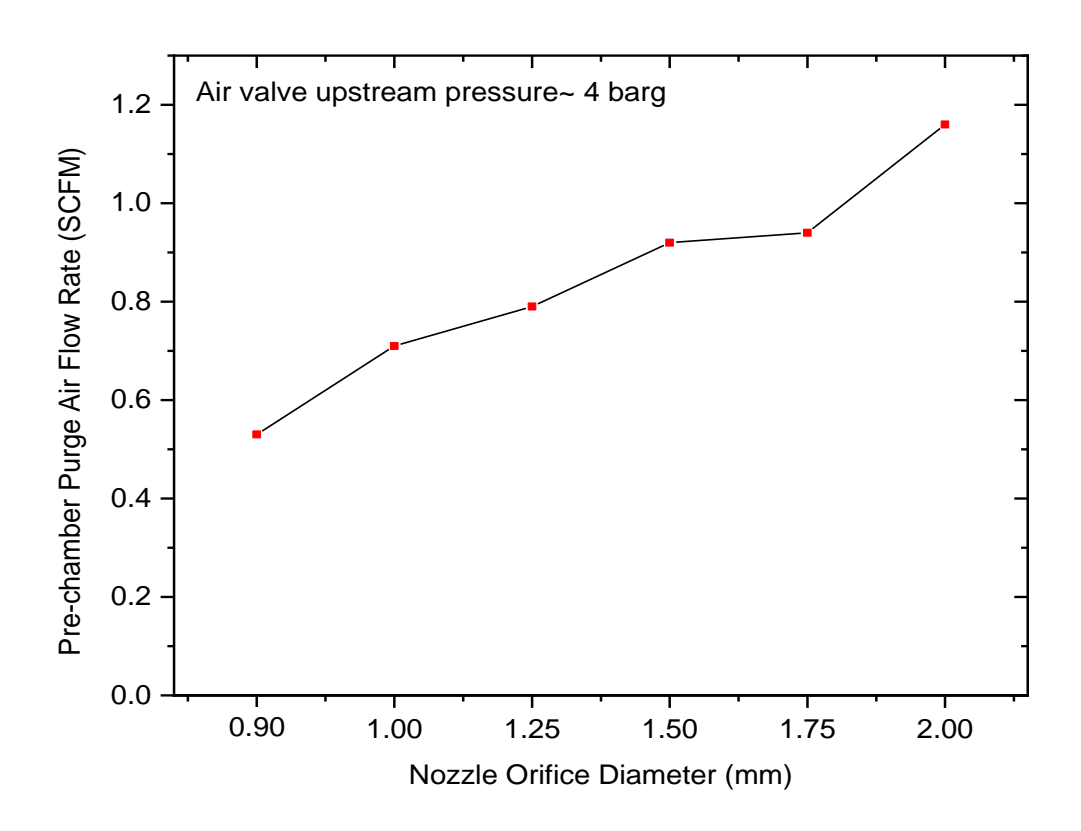


Figure 3.14 Pre-chamber purge air volumetric flow rate with different nozzle orifice diameters at 40% EGR diluted conditions

Upon further investigation with the pre-chamber pressure traces for different orifice diameters, an interesting trend with the pre-chamber air bump in the pressure trace was discovered. Figure 3.15

shows the relevant section of the pre-chamber pressure traces with the bump (caused by introduction of pre-chamber auxiliary air) for the tested nozzle orifice diameters along with the main chamber pressure and pre-chamber fuel injection signal. As demonstrated in Figure 3.15, with smaller orifice diameter the bump in the pre-chamber pressure trace increases with higher pressure and extended pressure equalization duration (with the main chamber pressure). The increased restriction to flow due to smaller-diameter orifices caused this to happen. As mentioned previously, a difference in pre-chamber and main chamber pressure would result in a net flow out of the pre-chamber to the main chamber. The air valve timing and pre-chamber fuel start of injection timing was set based on the 1.25 mm nozzle orifice setup and was kept the same with all orifice diameters tested. In Figure 3.15, the blue trace shows the pre-chamber fuel injection signal that was kept unchanged throughout all the tests with different orifice diameters. It is clear from this figure that due to extension of the air bump with the 0.9 mm and 1.0 mm orifices, there is a considerable overlap between the air bump in the pre-chamber pressure trace and the fuel injection signal. Physically, this means that a considerable amount of the injected fuel inside the prechamber was blowing out of the pre-chamber along with the flow resulting from the pressure difference between the pre- and the main chamber. This unavailability of fuel inside the prechamber is attributed to the lack of formation of combustible mixture inside the pre-chamber and hence the misfires and partial burns. As seen from Figure 3.15, the overlap was greater with the 0.9 mm compared to the 1.0 mm orifices, which means that more fuel would be blown out of the pre-chamber with the 0.9 mm nozzle; causing more misfires. The IMEP traces shown in Figure 3.12 verify that. This also strengthens the finding discussed previously: for stable operation at 40% EGR diluted condition, the relative timing between the pre-chamber auxiliary air and fuel is critical. Pre-chamber design and operating conditions will dictate the optimum timings.

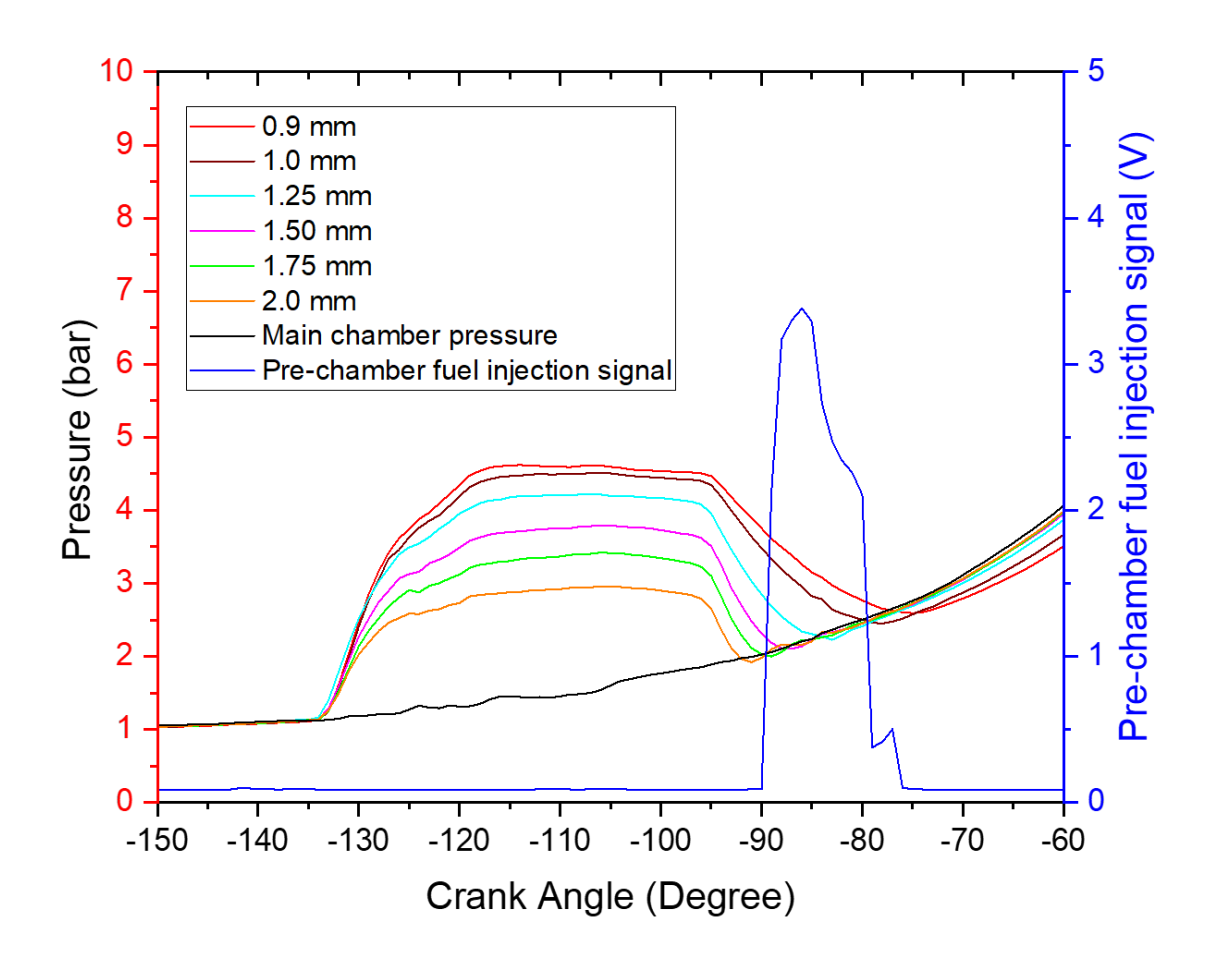


Figure 3.15 Effect of nozzle orifice diameters on pre-chamber pressure bump and their overlap with the pre-chamber fuel injection signal

It was found that the 0.9 mm and 1.0 mm orifice diameters performed very well during the lean operation tests. The reason behind their poor performance during 40% EGR diluted condition was found to be the blowing out of fuel from the pre-chamber due to extended duration of net outflow from the pre-chamber during air introduction. Thus, it can be predicted that with some adjustment of the air valve timing and the start of pre-chamber fuel injection timing, the smaller- diameter 0.9 mm and 1.0 mm orifices would have also performed well with the 40% EGR tests. Further tests need to be carried out to verify this conjecture. Nonetheless, this analysis demonstrates that the nozzle orifice diameter has a substantial effect on the overall 10-90 burn duration. Generally, it was observed that with decrease in the pre-chamber nozzle orifice diameters, the overall 10-90

burn duration also decreased. In other words, for the range of orifice diameters tested, it was found that the smaller orifice diameters provided faster combustion for both ultra-lean and high EGR diluted conditions.

### 3.4.5 Natural luminosity combustion imaging

Optical access to the main combustion chamber was attained through the 66 mm diameter sapphire window inserted on top of the Bowditch piston extension. The natural luminosity combustion images in the main chamber were captured with a non-intensified high-speed PHOTRON APX-RS visible spectrum video camera coupled with a Schneider-Kreuznach Xenon f/0.95 25 mm lens. Combustion events of the last 200 cycles were captured at an imaging frame rate of 5000 frames/sec with a resolution of 512x512 pixels. At 1500 rpm this frame rate corresponds to a temporal resolution or the imaging interval of 1.8 CAD between consecutive images. The start of imaging at each cycle was triggered by the spark ignition signal.

Figure 3.16 shows the crank-angle-resolved natural luminosity images at 1500 rpm and 7.2 bar lean ( $\lambda$ ~ 1.75) operating condition, along with the main chamber and pre-chamber pressure trace for a section of a single cycle. The label under each circular image corresponds to the crank angle degree at which the images were captured (negative value means crank angle degree before TDC). In the DM-TJI system, combustion starts inside the pre-chamber which is hidden from the planar view at the center of the images. The discharged jets from the pre-chamber to the main combustion chamber begin to appear at ~11 CAD after ignition and then consume the main charge rapidly. The first appearance of the visible jet discharge had very low luminosity, and the next recorded images had considerably higher luminosity. As the jet plumes grew bigger, they entrained and consumed more charge; and their luminosity increased. The imaging method here is 'line of sight' imaging, and thus a two-dimensional representation of the three-dimensional jets have been

captured. The luminosity signal from each jet was essentially an integration of all the signals throughout the line of sight. For this reason, the central regions of the jets were comparably more luminous. The main chamber pressure started to rise at ~13 CAD, which is around one CAD before the pre-chamber pressure peaked. By this time, almost all the jets have reached the outer edge of the circular sapphire window. Pre-chamber pressure then starts to drop, indicating the end of the jet discharge event. The jets are seen to spread out in a lateral direction through flame propagation. At around 6 CAD before TDC, jets started to merge together and individual jet plumes became harder to identify.

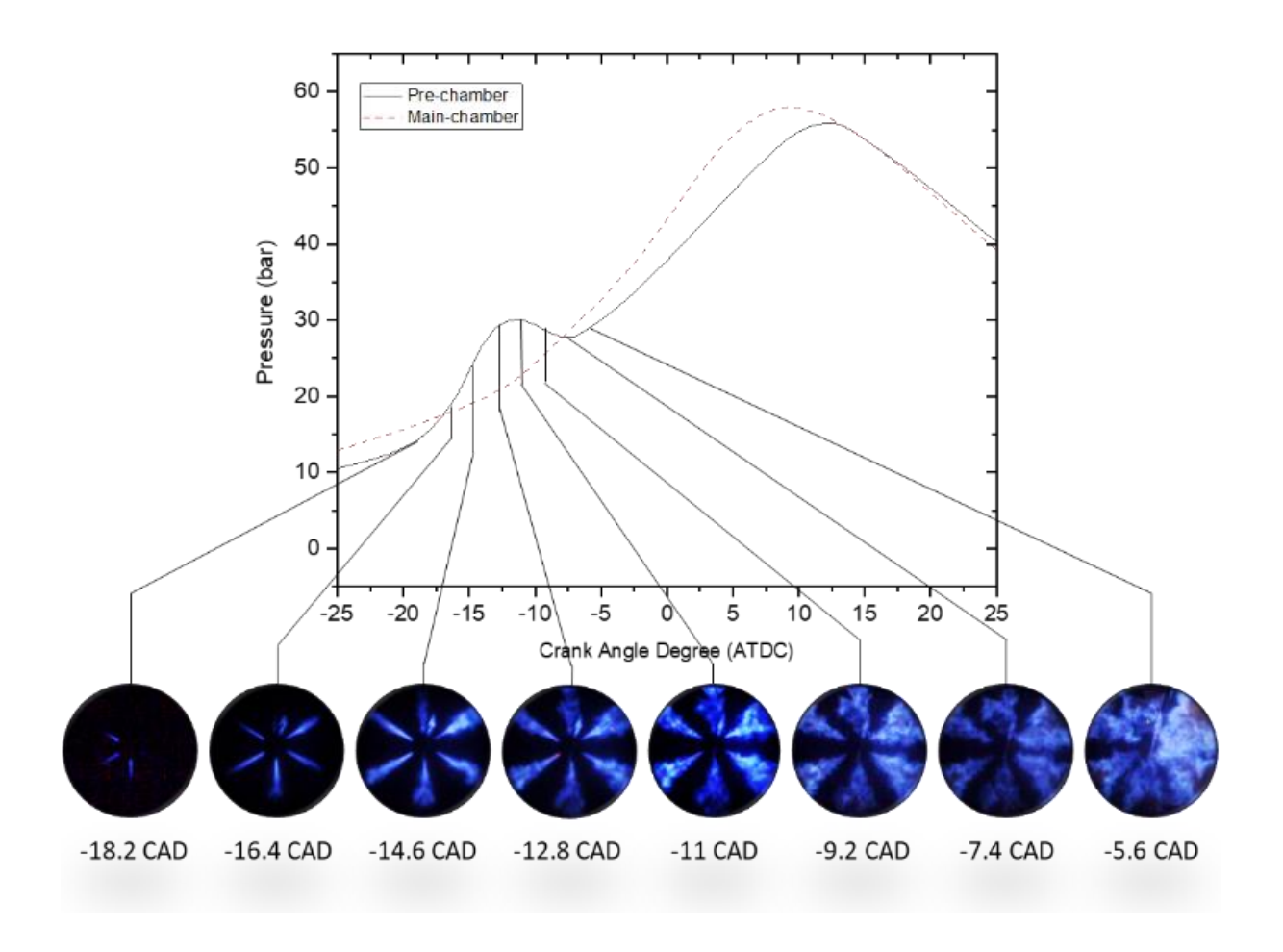


Figure 3.16 Pre-chamber and main chamber pressure traces and phase-synchronized images of turbulent jet combustion events; lean ( $\lambda \sim 1.75$ ), 7.2 bar IMEP @ 1500 rpm, 1 mm nozzle orifice

The sequence of events (visual identification of initial jet, jet penetration, propagation through the main chamber and finally dispersion of the jets in a contiguous flame structure) takes about  $12\sim14$  crank angle degrees. For most of the lean running conditions ( $\lambda\sim1.75$ ), this whole sequence of events finishes around the same time when 10% of the main chamber mass fraction gets burned (i.e., around the CA10 timing). While the jet formation and propagation events only last for a small duration and the line of sight imaging technique has some inherent limitations, optical access to the combustion event can still provide valuable insights about jet penetration, ignition site distribution and rate of air-fuel charge consumption.

Figure 3.17 shows the crank-angle-resolved binarized images of 200 cycle ensemble average jet structures for different nozzle orifice diameters tested at lean ( $\lambda$ ~1.75) operating conditions of 7.2 bar at 1500 rpm. Only the lean operating condition images are used for this comparative analysis, since at 40% EGR the 0.9 mm and 1.0 mm diameter nozzles had difficulty maintaining stable combustion.

Since the jets are turbulent in nature and their formation, penetration and development vary depending on pre-chamber and main chamber mixture distribution, especially at lean/dilute conditions, analyzing a single cycle crank-angle-resolved image to get quantitative or qualitative information is difficult. Therefore, in Figure 3.17, 200 cycle ensemble-averaged images are used to compare how nozzle orifice diameters affect the jet structures and consequently combustion. An in-house MATLAB code was used for this purpose. The images were binarized for better visualization of the average jet structures and quantification of average jet penetration and enflamed area for different nozzle orifice diameters.

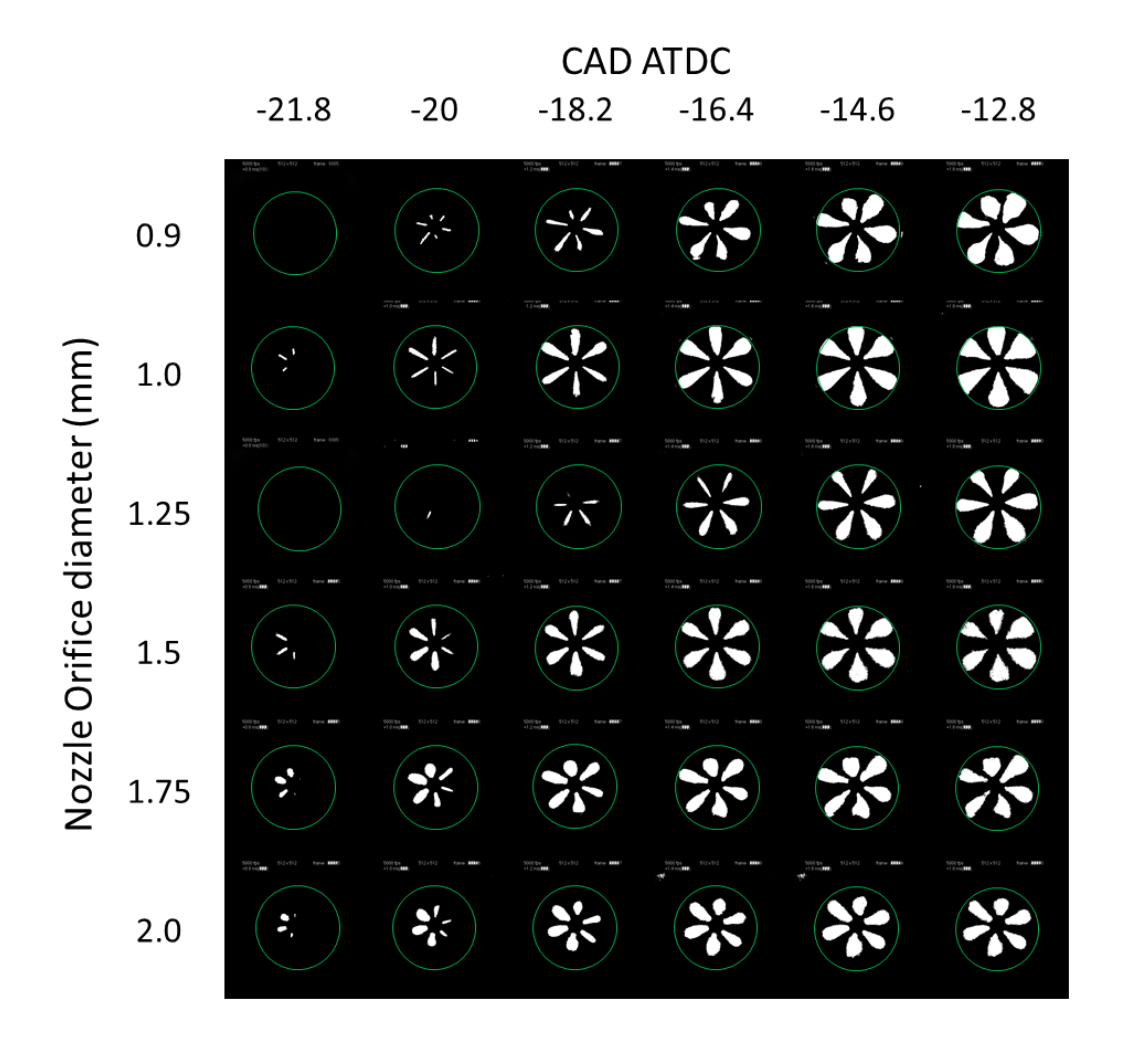


Figure 3.17 Crank-angle-resolved binarized images of 200 cycle ensemble average jet structures for different nozzle orifice diameters; lean condition ( $\lambda \sim 1.75$ ), 7. 2 bar IMEP @ 1500 rpm

In Figure 3.17, consecutive crank-angle-resolved images have been shown starting from -21.8 CAD aTDC to -12.8 CAD aTDC. From these images it is apparent that for all the orifice configurations, the jets started to appear first from the left side of the nozzle and were typically more prominent there. A possible explanation for this behavior could be the arrangement of spark plug location inside the pre-chamber. Figure 3.18 shows a schematic diagram of the relative arrangement of the components seen from the imaging view. As represented in Figure 18, the spark plug tip is located at an angle on the left inside the pre-chamber nozzle. The injector is located on

the right (also inclined) and injects fuel toward the direction of spark plug. The air valve is located centrally inside the pre-chamber. This arrangement results in combustion initiating in the left side of the pre-chamber nozzle, and thus the jets are typically seen to show up first from the left side of the pre-chamber nozzle.

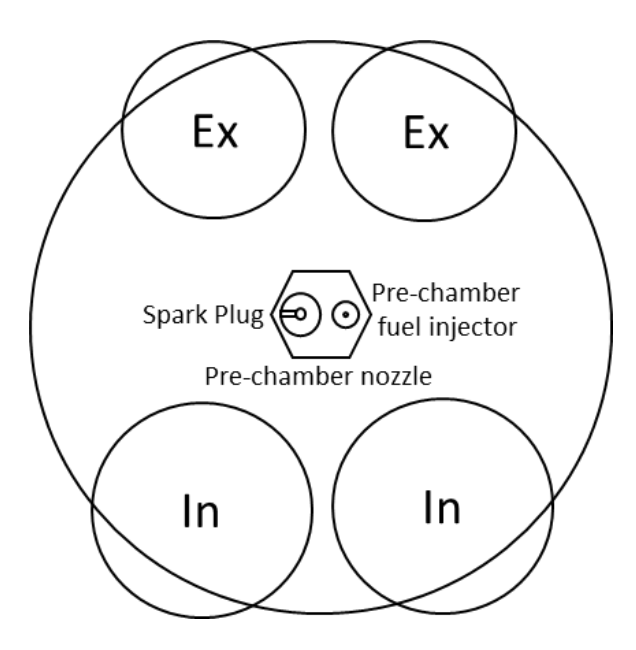


Figure 3.18 Imaging view of the combustion chamber through the piston window

In Figure 3.17, for each orifice configuration, after the initial jet discharge event the jet plumes grew bigger in both radial and lateral directions with each consecutive frame. While this trend was the same for all the orifice diameters, the actual structure of the jets and their degree of penetration into the main chamber as well as the growth rate were seen to vary between different nozzle orifice diameters. As depicted in Figure 3.17, the aspect ratio of the initial jets coming out of the nozzle differs with orifice size. With smaller-diameter orifices, the initial jets are longer with smaller width; whereas with larger-orifice designs, the initial jet plumes are shorter in length with larger width. As the orifice diameter increases, the jet plumes become shorter and wider. Thus, with larger pre-chamber nozzle orifice diameters, the jets are more concentrated toward the central

region of the combustion chamber; whereas with smaller-diameter nozzles, the jets penetrate more toward the peripheral regions of the combustion chamber and create comparatively wider distribution of the ignition sites. This results in shorter overall burn duration. This conclusion is supported by average pressure trace analysis done in previous sections (ref. Figure 3.10).

Figure 3.19 plots the average jet penetration for varying nozzle orifice diameters. This is based on the 200 cycle average frames taken 7.2 CAD after the jets were first seen in order to include all six jets leaving the pre-chamber nozzle in the analysis. From this plot it is apparent that with increase in nozzle orifice diameter, the jet penetration distance decreases. In other words, smaller orifice diameter resulted in longer jet penetration. However, note that continuing to decrease the orifice diameter will eventually result in a choke flow condition and aggressive quenching, rather than an increase in jet penetration.

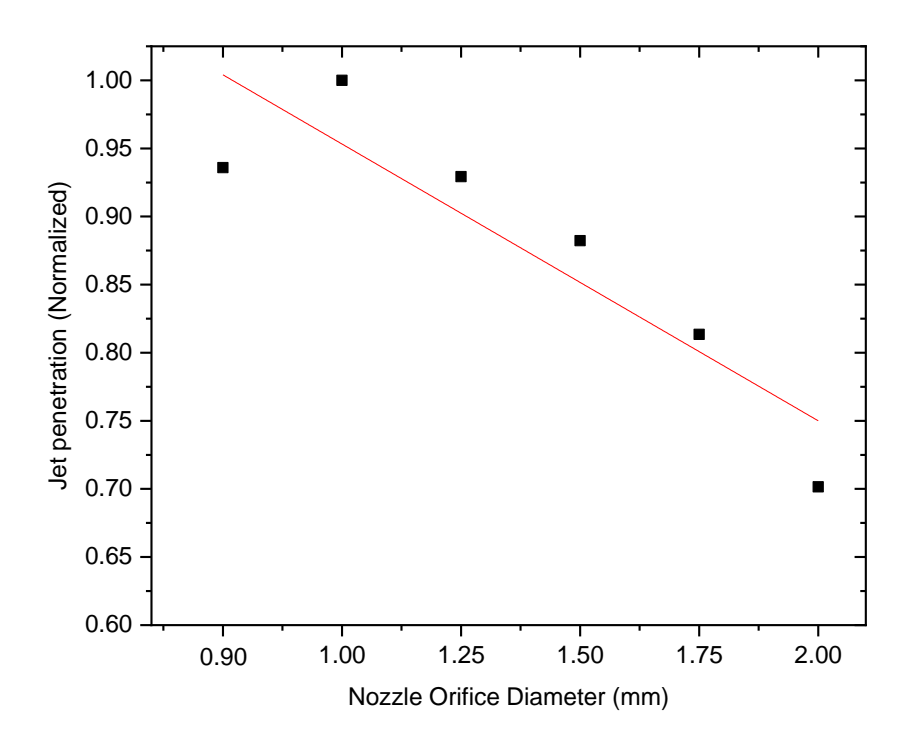


Figure 3.19 Normalized jet penetration vs orifice diameters, lean operation

In Figure 3.20, the enflamed two-dimensional projected area from the binarized average images is

plotted for all nozzle orifice diameters. A similar decreasing trend with increasing orifice diameter is seen here as well, which strengthens the argument that smaller-diameter orifices provide better spatial distribution of the jets and cover a higher portion of the main combustion chamber. This decreases the flame travel distance and results in fast burn rates.

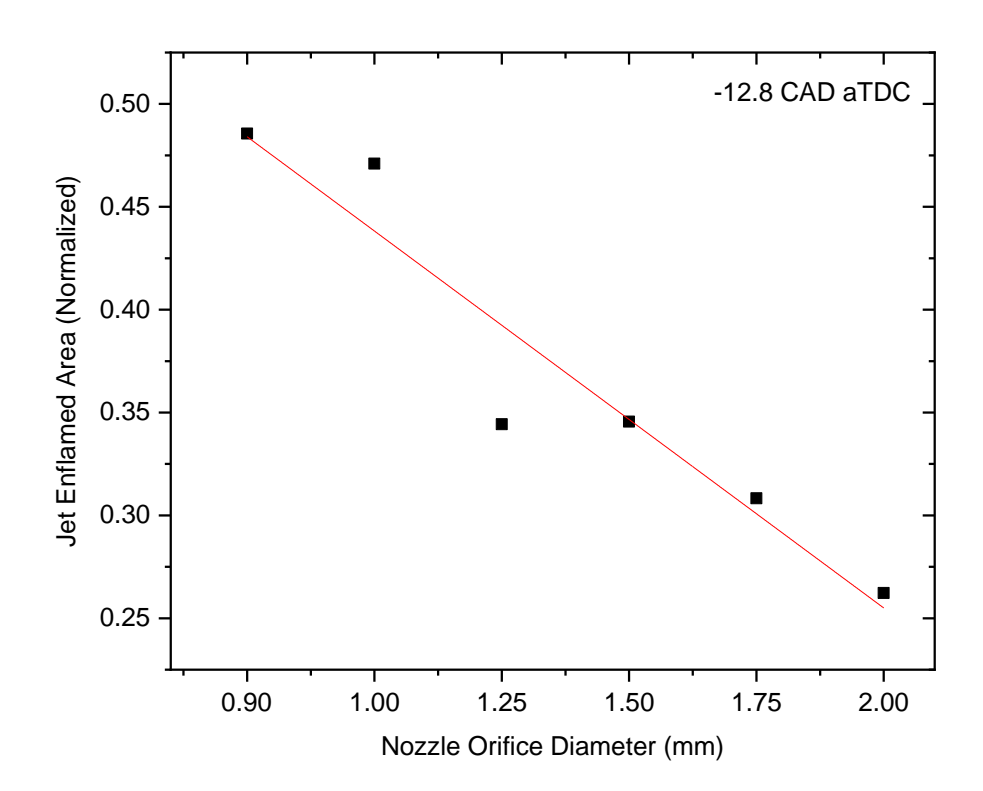


Figure 3.20 Normalized jet enflamed area vs orifice diameters, lean operation

# 3.4.6 Parasitic Loss (to compress the purge air) and Thermal Efficiency of Prototype II DM-TJI engine

During lean operation the upstream pressure for purge air was set at 1 bar (gauge), and the average volume flow rate of compressed air was measured by the LFE to be approximately 0.12 SCFM (for 1.25 mm nozzle setup). For the same nozzle configuration, in the case of 40% EGR diluted condition, the upstream pressure was set at 4 bar (gauge). The resulting average volume flow rate of the compressed air for pre-chamber scavenging was determined to be approximately 0.8 SCFM.

Using the Womack fluid power design data sheet [86], at these upstream pressure conditions the power required to compress the purge air for the lean and EGR diluted conditions was estimated. The resulting decrease in indicated thermal efficiency was well below 1%. Based on the current test results, after subtracting the work required to compress the purge air, the resulting indicated thermal efficiency of the DM-TJI engine at 1500 rpm, 7.3 bar IMEP, WOT, ultra-lean ( $\lambda \sim 2$ ) operating conditions was around 45.2 %. As for the 40% EGR diluted operation at 1500 rpm, 9.2 bar IMEP, stoichiometric ( $\lambda \sim 1$ ) condition, the purge work subtracted indicated thermal efficiency was found to be 41.8%. The corresponding indicated specific fuel consumption (ISFC) at these ultra-lean and EGR diluted conditions were 184.3 and 196.7 gm/kW-hr, respectively. The increase in specific heat ratio ( $\gamma$ ) is greater with excess air dilution compared to EGR dilution [87], and thus typically ultra-lean operating conditions result in greater thermal efficiency benefits compared to EGR diluted operation. In practice, the more effective emission reduction with a three-way catalyst makes the EGR diluted operation more viable.

# 3.5 Summary and Conclusions

In this study, the DM-TJI Prototype II optical engine installed at Michigan State University's Energy and Automotive Research Laboratory has been used to demonstrate ultra-lean and highly EGR diluted operation capability of the auxiliary air- and fuel-enabled DM-TJI pre-chamber ignition system for the SI engine. Different pre-chamber nozzle orifice diameters were examined at both lean and EGR diluted conditions. The following conclusions are drawn from the experiments performed.

• The DM-TJI engine was able to maintain very stable operation (COV<sub>IMEP</sub><2) with 40% external EGR dilution at stoichiometric condition ( $\lambda$ ~1). Auxiliary pre-chamber purge air allows this system to work with such a high dilution rate (~40%). While pre-chamber fuel

- supply was necessary, without the pre-chamber air supply high-EGR-diluted operation could not be maintained.
- At 40% EGR diluted condition, the relative timing between the auxiliary air and fuel inside
  the pre-chamber was critical to maintain successful operation with such high level of EGR
  dilution.
- Ultra-lean operation (up to λ~2) with the DM-TJI system at two different compression ratios (12:1 and 10:1) was also demonstrated with good combustion stability (COV<sub>IMEP</sub><3). At wide open throttle λ~2 condition, a lower compression ratio (10:1) yielded worse combustion stability compared to a higher compression ratio (12:1); this was probably due to the increased quantity of trapped residuals and lower in-cylinder pressure and temperature. Also, compared to the 12:1 compression ratio, combustion at the lower 10:1 compression ratio was found to be considerably slower with more prechamber ignition delay and longer overall 10-90 burn duration.
- During the 10:1 compression ratio with throttled operation at stoichiometric condition, the auxiliary air supply to the pre-chamber was essential in order to maintain stable combustion. Thus, in cases where a high amount of external or internal EGR was involved, auxiliary air supply to the pre-chamber was extremely important.
- Six different nozzle orifice diameters were tested at both lean ( $\lambda$ ~1.75) and 40% EGR diluted stoichiometric operating conditions. Generally, it was found that for the range of orifice diameters tested, smaller-diameter orifices provided faster combustion (shorter overall 10-90 burn duration).
- During lean operation, smaller-diameter nozzle orifices exhibited more partial burns during warm-up cycles due to the more pronounced jet/flame quenching effect of the

smaller orifices compared to the larger ones. Once the engine warmed up, the quenching effect became nonexistent. Orifices of 1.0 mm and 0.9 mm diameter exhibited shorter overall 10-90 burn duration compared to the other diameters tested.

- At 40% EGR diluted condition with upstream air pressure, air valve open duration and fuel injection timing inside the pre-chamber being the same for all tested orifice diameters, 0.9 mm and 1.0 mm nozzle orifice diameters did not perform well. They had many misfires and partial burns. It was found that with 0.9 mm and 1.0 mm orifices, a considerable amount of injected pre-chamber fuel was blown out of the pre-chamber due to extended duration of net outflow from the pre-chamber during scavenging with compressed air. This lack of auxiliary fuel inside the pre-chamber caused the engine to experience misfires and partial burns for these orifices. With appropriate adjustment in pre-chamber purge air and fuel injection timing, 0.9 mm and 1.0 mm orifices are expected to perform in a similar manner to the rest of the orifice diameters tested. This showed that at high EGR diluted condition, successful operation depends on appropriate pre-chamber design and effective scavenging and fueling strategies.
- Analysis of 200 cycle ensemble-averaged, crank-resolved combustion images acquired during lean operating condition (λ~1.75) showed that with decrease in nozzle orifice diameter, both the average jet penetration and enflamed jet area increased. This resulted in shorter flame travel distance from individual ignition sites and consequently shorter 10-90 burn duration for smaller-diameter nozzle orifices. Similar trend in shortening of the 10-90 burn duration with smaller-diameter orifices was observed in case of 40% EGR diluted operation as well for the range of diameters that maintained stable operation.
- After subtracting the work required to supply the compressed air for the pre-chamber

purging, the resulting indicated thermal efficiency of the Prototype II DM-TJI engine at ultra-lean ( $\lambda$ ~2) operating condition was found to be 45.2% and for 40% EGR diluted stochiometric ( $\lambda$ ~1) operation it was 41.8%.

- The limitations of conducting these high EGR diluted tests in an optical engine prevented optimization of the auxiliary pre-chamber purge air or the auxiliary fuel in terms of quantity and timing. These experiments, however, demonstrated the potential of the DM-TJI system to work with very high EGR dilution at conditions where a three-way catalytic converter can still be used efficiently.
- While 40% EGR dilution tolerance has been demonstrated at fairly high load conditions
  (around 9 bar IMEP), at lower loads dilution tolerance may be lower and that will be
  investigated in future.

While this study has effectively demonstrated the capability of the DM-TJI system to work with high level of EGR dilution (up to 40%), limitations of the optical engine restricted more involved investigation on the dilution rate or thermal efficiency. For this reason, the Prototype III DM-TJI metal engine employing a cam-driven air-valve arrangement was built and tested. Those results will be discussed in the next chapters.

### **CHAPTER 4**

# COMPARISON OF EXCESS AIR (LEAN) VS EGR DILUTED OPERATION AT HIGH DILUTION RATE (~40%)

### 4.1 Abstract

Charge dilution is widely considered as one of the leading strategies to realize further improvement in thermal efficiency from current generation spark ignition engines. While dilution with excess air (lean burn operation) provides substantial thermal efficiency benefits, drastically diminished NOx conversion efficiency of the widely used three-way-catalyst (TWC) during offstoichiometric/lean burn operation makes the lean combustion rather impractical, especially for automotive applications. A more viable alternative to lean operation is the dilution with EGR. The problem with EGR dilution has been the substantially lower dilution tolerance limit with EGR and a consequent drop in thermal efficiency compared to excess air/lean operation. This is particularly applicable to the pre-chamber jet ignition technologies with considerably higher lean burn capabilities but much lower EGR tolerance due to the presence of a high fraction of residuals inside the pre-chamber. The Dual Mode, Turbulent Jet Ignition (DM-TJI) technology with its unique ability to work with high external EGR dilution (up to 40% wet/mass basis) due to its additional air delivery to the prechamber offers a viable alternative to the lean burn strategy. DM-TJI could be the technology pathway to realize high EGR diluted combustion with comparable dilution limits to those of the lean burn strategy while still enabling effective use of TWC technology. Present study compares the excess air versus EGR dilution strategy under identical level of dilution (up to 40 %) in a DM-TJI equipped single cylinder engine operating on a high (13.3:1) compression ratio. The results show that compared to the lean burn operation, EGR dilution provides marginally lower but still comparable thermal efficiency benefits with a marked improvement in NOx reduction, especially in a high compression, knock limited situation. This study showcases that high EGR dilution rates comparable to lean burn operation can be maintained with the DM-TJI system to achieve high thermal efficiency while still operating at stoichiometric air-fuel ratio.

### 4.2 Introduction

Inlet charge dilution is one of the most promising approaches to achieve high thermal efficiency and regulated emission reduction from spark ignition (SI) engines under the newer, increasingly stricter emission regulations for light-duty vehicles. With the added impetus on SI engines fueled by natural gas and its alternatives to become more competitive with diesel engines, research activities on lean and diluted combustion to increase thermal efficiency and lower NOx emissions have seen a substantial increase in recent years. Charge dilution improves the thermal efficiency and emission behavior by decreasing the peak combustion temperature, leading to reduced heat loss and also reducing the formation of nitrous oxides (NOx). At the same time, at low and medium loads reduced throttling results in lower pumping work, leading to further improvement of brake thermal efficiency. The lower combustion temperature leads to reduced knock tendency, enabling higher compression ratio and more aggressive spark advance for increased thermal efficiency. The mixture specific heat ratio ( $\gamma$ ) improvement also aids in increasing the thermal efficiency.

Typically, two different strategies are employed to achieve charge dilution: 'excess air' dilution (also referred as lean burn strategy) and 'exhaust gas recirculation (EGR)' dilution. While both approaches essentially offer similar benefits in achieving low temperature combustion (LTC) to realize thermal efficiency benefits and emission improvements, there is a substantial difference in additional aftertreatment requirements between the two approaches. While lean burn operation with excess air dilution in SI engines has been shown to offer substantial improvement in thermal efficiency [76,88,89], it is still difficult to meet the legal NOx emission requirement in the lean burn mode without employing expensive and rather complex additional exhaust gas aftertreatment

systems such as lean NOx trap or selective catalytic reduction (SCR) catalysts. With lean burn strategy a major challenge has always been the reduced NOx conversion efficiency of the widely used three-way catalyst (TWC). In gasoline fueled SI engines the three-way catalyst (TWC) has proved to be very efficient at reducing the engine out HC, CO and NOx emissions. The limitation is that the engine needs to operate very close to stoichiometric conditions in order to make the catalytic conversion efficient. The NOx conversion efficiency of the TWC goes down rapidly if the air-fuel ratio (AFR) varies even slightly toward lean operation [78]. To overcome this issue, an alternative strategy can be exhaust gas recirculation (EGR). If the inlet charge is diluted by recirculated exhaust gas (EGR), similar advantages to the excess air dilution/lean operation can be attained while still maintaining the stoichiometric air/fuel ratio ( $\lambda$ ~1) that permits the effective usage of TWC.

The recirculated exhaust gas affects the in-cylinder combustion in several ways. Due to increased charge gas quantity and higher specific heat capacity, the inlet thermal capacity increases. The oxygen concentration of the inlet charge mixture decreases as well. During combustion endothermic dissociation reactions of CO<sub>2</sub> and /or water vapor (H<sub>2</sub>O) are induced which also lower the combustion temperature [90]. All these thermal, dilution and chemical effects [91–94] result in lowering of the flame temperature and O<sub>2</sub> partial pressure, and subsequently to reduced NOx formation [95]. This effectively allows the utilization of turbocharging, higher compression ratio and advanced spark timing, which all leads to thermal efficiency benefits while maintaining the effective usage of TWC, a more economically viable alternative to the expensive additional lean burn emission reduction systems such as SCR or NOx traps.

While benefits of charge dilution strategies are well documented, a major limitation of charge dilution strategy (both lean and EGR) is the compromised combustion stability due to less

favorable ignition quality of the diluted mixture as well as slow flame propagation speed due to addition of diluents. Reduction in combustion stability leads to increased hydrocarbon (HC) emissions and decreased thermal efficiency due to misfires and partial burns. Historically, this has limited the use of diluents in higher percentages to realize the potential thermal efficiency benefits of charge dilution in conventional spark ignition engines. To overcome the inherent challenges that come with the usage of diluted combustion in spark ignition engines, a higher-energy distributed ignition source is required [4]. This led to the development of modern pre-chamber-based jet ignition systems.

Divided chamber stratified charge or 'pre-chamber' combustion initiation technique is not new, and the earliest concept can be traced back to Ricardo's 3-valve stratified charge engine work published in 1922 [7]. Jet igniters are a variation of the divided chamber stratified charge concepts that are characterized by much smaller orifice(s) connecting the pre-chamber and main chamber cavities. First major development of the jet ignition/pre-chamber torch ignition engine was reported by Gussak et al. [13,23,24] in the 1970s. The turbulent jet ignition (TJI) concept presented by Attard et al. [76] is one of the many variants of the technologies based on the works of Gussak. In pre-chamber turbulent jet ignition (TJI) systems, a small pre-chamber (typically <3% of the clearance volume) accompanies the main chamber and is connected through multiple small nozzle orifices [4,76,77]. In a pre-chamber-initiated jet ignition system, the initial flame kernel around the spark plug inside the pre-chamber is transformed through nozzle orifices into multiple pressure-driven, chemically active, high-temperature turbulent jets with substantially greater surface areas distributed around the main combustion chamber. These multiple high energy distributed ignition sites enable very fast burn rate with minimal combustion variability even with high rate of dilution.

While TJI and similar systems with auxiliary pre-chamber fueling strategy have been shown to work effectively with high rate of excess air dilution/lean combustion [55,77], on similar level of EGR dilution the TJI and similar systems become highly ineffective due to their difficulty in reliably igniting the pre-chamber mixture containing high EGR (and residual) fraction. The 'auxiliary pre-chamber fuel injection only' strategy employed by those technologies makes it extremely difficult to control mixture stoichiometry inside the pre-chamber that essentially contains a very high level of EGR mixed with the air-fuel reactants along with the residual gases. With the excess air dilution strategy, because of the high percentage of excess air availability in the pre-chamber mixture, ignition does not become an issue since a small amount of additional pre-chamber fuel injection still enables the formation of ignitable mixture inside the pre-chamber. But with the EGR dilution, that availability of excess air inside the pre-chamber diminishes since the additional air is replaced by products of combustion instead. This leads to pre-chamber misfires which lead to misfires in the main chamber. Consequently, the combustion stability suffers, rendering the TJI and similar fuel scavenged pre-chamber systems unusable with high level of EGR dilution. The DM-TJI system resolves these issues inherent to the utilization of higher level of EGR dilution.

The Dual Mode, Turbulent Jet Ignition (DM-TJI) system is an engine combustion technology in which the pre-chamber is equipped with an auxiliary air supply along with the auxiliary fuel injection [67–69]. In a DM-TJI system the additional air supply and its method of delivery to the pre-chamber are the main modifications from the technology's forerunner the Turbulent Jet Ignition (TJI) system [3,42–44,57,58]. The DM-TJI system provides enhanced control of stoichiometry inside the pre-chamber by adding supplementary air to the auxiliary fuel injection. This additional air supply to the pre-chamber solves two issues- first, it provides effective purging

of the pre-chamber residuals and second, it helps maintain pre-chamber mixture ignitability even under high EGR dilution. This makes the DM-TJI system a unique pre-chamber combustion technology that offers stable operation at very high level of EGR dilution while still permitting the use of conventional TWC through stochiometric operation.

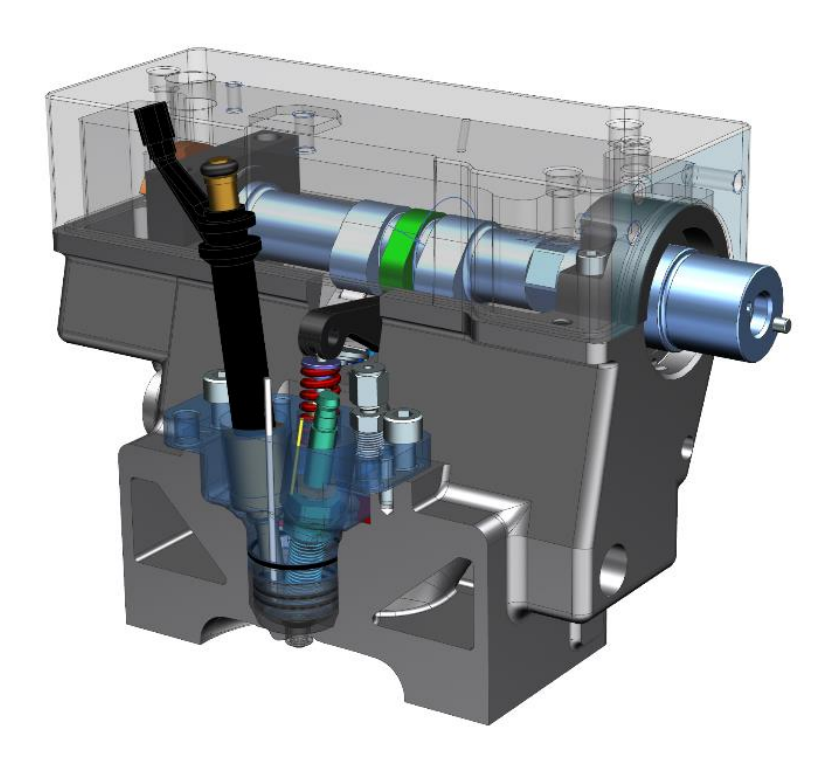


Figure 4.1 Prototype III DM-TJI engine with 'Jetfire cartridge' design. A cam actuated air valve was used to deliver purge air to the pre-chamber

Atis et al. [67] showed that the prototype II DM-TJI system equipped gasoline fueled optical engine with a cooled EGR system could maintain stable operation (COV<sub>IMEP</sub><2%) with 40% external EGR at stochiometric ( $\lambda$ ~1) operating conditions. In that study, effect of pre-chamber air/fuel timing relative to EGR tolerance was investigated. Ultra-lean operation (up to  $\lambda$ ~2) was also demonstrated while a correlation between the nozzle orifice diameters and overall burn duration was suggested. Tolou et al. [68] developed a physics-based GT-POWER model of the prototype II DM-TJI system and predicted the ancillary work requirement to operate the additional

components of the DM-TJI system. Vedula et al. [69] reported the net indicated thermal efficiency of the prototype I DM-TJI engine for both lean and 30% nitrogen diluted near stochiometric operation. Vedula et al. [70] also studied the effect of pre-chamber fuel injection timing including pre-chamber air injection and different injection pressures on iso-octane/air combustion in a DM-TJI system equipped rapid compression machine for a global lambda of 3.0. Song et al. [71] worked on control oriented combustion and state-space models based on the prototype I DM-TJI engine.

Previous study by the author conducted on the DM-TJI system have successfully demonstrated the effectiveness of the DM-TJI system to operate with high EGR dilution tolerance (up to ~40%) [67]. This unique ability to work with very high level of EGR dilution permits the opportunity to compare the relative effectiveness of the excess air versus the EGR dilution strategy at a significantly high dilution rate on an actual engine platform. While there have been several studies that either used engine simulations [87,96] or actual SI engine experiments [89,97] to compare the two dilution strategies, they were either limited by maximum EGR tolerance [97] or the requirement of rather impractical hydrogen enhancement [89]. Ibrahim et al. [98] numerically studied the effect of both EGR and lean-burn on a natural gas SI engine and compared the performance and NO emission at similar operating conditions. A two-zone combustion model was developed, and it was found that EGR dilution offered significantly decreased NO emission at the cost of increased fuel consumption. Caton [96] used a thermodynamic engine cycle simulation to better understand the fundamental thermodynamic aspects of both the lean and EGR dilution approaches and found that in both cases the thermal efficiency increases due to decreasing temperatures, lower heat transfer, reduced pumping loss, and increase in specific heat ratio. According to that study, lean operation provides a higher ratio of specific heats compared to EGR dilution due to the composition changes. This was reflected in efficiency gains as well.

Similar findings were shown in a study conducted by Lavoie et al. [87] that employed a GT-POWER model to perform an extensive parametric study. They concluded that dilution with either air or EGR provided a benefit to gross efficiency due to improved thermodynamic properties (in terms of both composition changes and reduced temperatures) and EGR dilution provided almost as much improvement as air dilution. Saanum et al. [99] also studied lean burn versus stoichiometric operation with EGR on a natural gas fueled engine and found that compared to lean burn operation EGR operation offered lower NOx emission but the maximum brake thermal efficiency was lower as well. Although in this study the authors did not use similar level of dilution to compare the two conditions. Lee et al. [97] performed a comparative study on EGR and lean burn strategies using an SI engine fueled by low calorific gas. They could test only up to 15% EGR dilution until the combustion stability limit was reached and concluded that EGR operation was a superior strategy in reducing NOx emission compared to the lean burn operation but had a negative impact on thermal efficiency and HC emissions. More interestingly the dilution window for EGR was found to be almost half of that of lean burn condition (15% for EGR versus about 30% for lean burn).

Thus, most of the experimental studies that involved comparative analysis between the excess air and EGR dilution strategies could not investigate high level of EGR dilution. Generally, one of the major reasons that EGR dilution offered less thermal efficiency benefits compared to excess air/lean operation was the substantially lower EGR tolerance versus excess air tolerance. While lean operation involves marginally better thermodynamic benefits compared to EGR operation there exists no study at all that experimentally investigates and compares the two methods under similar level of dilution especially with pre-chamber jet ignition systems. The DM-TJI system

offers a platform where high levels of both excess air and EGR dilution can be employed and stable operation for both strategies can be achieved to compare their relative effectiveness on performance and emission parameters. While other comparable pre-chamber ignition systems could achieve a similar level of excess air dilution, their inherent shortcoming with EGR tolerance [100] makes them ineffective to conduct such a comparative analysis. The purpose of this study is to examine and compare the 'excess air' dilution to 'EGR' dilution strategy at high dilution level (up to ~40%), to determine their relative effectiveness from performance and emission point of view for a gasoline-fueled SI engine employing a high compression ratio.

# 4.3 Experimental Setup and Procedure

Engine tests were performed on a single-cylinder Prototype III DM-TJI metal engine. The first two prototypes [67,69] were optical variants of the engine with the first prototype having an air injector (fuel injector that delivers air) inside the pre-chamber to deliver auxiliary air whereas prototype II replaced the pre-chamber air injector with a hydraulically controlled poppet valve for pre-chamber air delivery. The current Prototype III replaces the hydraulically controlled pre-chamber air valve with a more production-viable, intake camshaft-driven air valve and packages the pre-chamber components (fuel injector, spark plug and air valve) inside a more compact 'Jetfire' cartridge design. The Prototype III DM-TJI engine has a pent roof head modified to incorporate the pre-chamber 'Jetfire' cartridge and air-valve driving assembly. Figure 4.1 shows the isometric view of the Prototype III DM-TJI single-cylinder engine head. Major specifications of the Prototype III DM-TJI metal engine are listed in Table 4.1.

Table 4.1 Prototype III DM-TJI engine specifications

Bore	86 mm
Stroke	95 mm
Connecting rod length	170 mm
Compression ratio	13.3:1
Pre-chamber volume	2900 mm <sup>3</sup> (~6 % of clearance volume)
Main chamber swept volume	0.55 L
Fuel injection	Main chamber – High pressure DI (used in PFI
	configuration)
	Pre-chamber – High pressure DI
Fuel injection pressure	100 bar
Pre-chamber air valve assembly	Intake cam actuated
Pre-chamber compressed air supply	15-90 psi
pressure	
Nozzle orifice configuration	6*1.25 mm, Symmetric
Valve timing (max lift)	Intake timing - 90 CAD aTDCGE,
	Exhaust timing - 90 CAD bTDCGE
	Air valve timing - 120 CAD bTDCF

As mentioned in Table 4.1 pre-chamber fuel was supplied with a custom developed two hole low flow DI injector, whereas the main chamber fuel was supplied in PFI configuration but with a higher flow rate six hole DI injector. A fuel cart containing a fuel tank, Coriolis fuel flow meter, and high-pressure fuel pump was used to deliver fuel to the high-pressure DI injectors. Both the pre-chamber and main chamber fuel injection pressures were set at 1450 psi (~100 bar). All tests were performed with Tier III regular certification gasoline fuel. The combined (main chamber + pre-chamber) fuel flow rate was measured using a Micro Motion CMFS007M Coriolis flow meter.

The test bench incorporated a boost-cart assembly with a single stage EATON TVS R410 supercharger along with a charge air cooler (CAC), upstream throttle and a blow-off valve to control intake conditions for boosted operation. An EGR line from the exhaust system on the engine was connected to the EGR valve mounted on the boost-cart. An EGR cooler was used to

cool down the exhaust before it reached the EGR valve assembly. A pressure delta across the EGR system was maintained using the upstream throttle and the EGR valve. The current set of tests was conducted at naturally aspirated (NA) condition without running the supercharger, but the CAC temperatures were controlled to a specific level to avoid any condensation due to high EGR rate and maintain constant temperature of the intake charge throughout the tests. The outlet of the boost-cart was attached to the intake plenum mounted to the engine head through the intake runner. The test rig was equipped with k-type thermocouples to monitor and log various system temperatures. A cooling system having a separate controller and coolant pump was used to circulate 50:50 ethylene glycol-water mixture through the engine to maintain the head and cylinder temperature at 95°C.

Pre-chamber pressure data was collected using a spark plug with an integrated piezoelectric pressure transducer (Kistler 6115CF-8CQ01-4-1). Pre-chamber combustion was initiated by this 'hot' type spark plug and a conventional automotive inductive ignition system with 60 mJ of ignition energy. A second piezoelectric pressure transducer (Kistler 6052A) installed in the engine head captured the main chamber combustion pressure. Piezoresistive pressure transducers (Kistler 4045A and Kulite EWCTV-312) were installed on the intake and exhaust system to measure the port pressures, respectively. These were used to log high-speed, crank angle resolved pressure data at all four locations using an A&D Technologies' Combustion Analysis System (CAS). Sampling resolution of the pre-chamber and main chamber pressure was set to 0.1 crank angle degree (CAD) and for the port pressure at 0.5 CAD. Low speed steady state data were logged using NI DAQ modules connected to a custom-developed LabVIEW control and data acquisition program.

An in-house control system containing NI-PXI chassis and Mototron ECM-5554 controllers managed within an NI Veristand environment was used to control the main engine control

parameters such as pre-chamber spark timing, pre- and main chamber fuel injection timings and durations, throttle and EGR valve positions, etc.

Pre-chamber purge air was supplied using the shop compressed air supply line. The compressed air pressure was regulated via a pressure regulator. The compressed air was introduced into the pre-chamber through the pre-chamber air valve actuated by the intake camshaft containing a separate air-valve cam lobe. Air flow rate was monitored with a Meriam laminar flow element (LFE), Z50MJ10-11, which was installed in the pressurized air-line upstream of a compressed air plenum (to minimize fluctuation).

Exhaust emissions were sampled using a Horiba MEXA-7100 DEGR automotive emission analyzer, capable of measuring CO<sub>2</sub>, CO, HC and NOx emissions in exhaust gas. The analyzer also has a dedicated separate intake CO<sub>2</sub> sampling line connected to the intake manifold to measure the volumetric EGR rate. The volumetric EGR rate was also cross-checked with pressure compensated O<sub>2</sub> sensors (ECM Lambda-5200) installed in the intake manifold. The exhaust lambda was measured both by the emission bench and and a separate lambda sensor (ECM Lambda-5200) installed at the exhaust system. Figure 4.2 shows a schematic diagram of the experimental test bench.

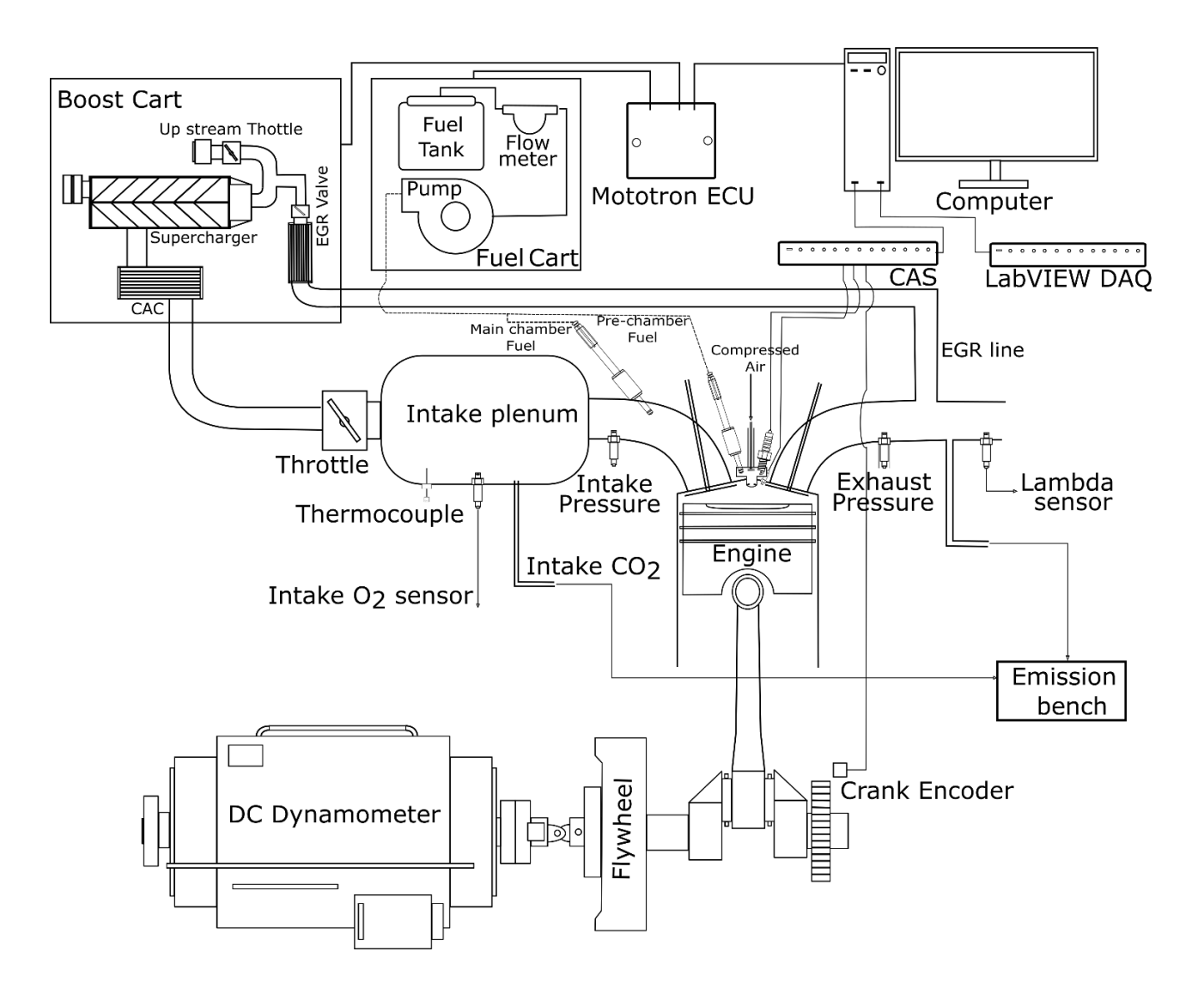


Figure 4.2 Schematic of the experimental test bench

All engine tests were performed at nominal gross IMEP value of 6 bar and at 1500 rpm. The load - speed condition of 6 bar IMEPg @ 1500 rpm was selected based on the highest achievable IMEPg at naturally aspirated (NA) condition without requiring any boost while maintaining 40% external EGR rate at stochiometric condition ( $\lambda$ ~1). A large intake plenum was utilized to ensure proper mixing of EGR before entering the combustion chamber. EGR sweep was performed from 40% external EGR rate to 0% external EGR rate and excess air dilution sweep was performed from lambda 1.8 to lambda 1.0. The same fuel flow rate was maintained throughout the entire test

matrix. For lower EGR rates, the upstream throttle and EGR valve settings were controlled to maintain lambda 1 operation. The intake air/air-EGR mixture temperature was maintained to 45°C for all the tests. Fuel injection strategy (amount and timing) for both the pre-chamber and main chamber were kept the same throughout the entire EGR and lambda sweep. The main chamber fuel was injected at 360 CAD bTDCF using three split injection pulses. The pre-chamber fuel was injected at 70 CAD bTDCF using a two split injection strategy. The air valve upstream pressure was set at 30 psig for all the tests (both lean and EGR diluted). For each operating point 200 consecutive cycles of crank resolved pressure data were recorded. Additionally, time-averaged data of temperatures, pressures, fuel flow rates and emissions were obtained. DC dynamometer was used to control the engine speed.

Automotive SI engines having higher geometric compression ratio similar to the current test engine (13:1) typically employ LIVC (Late Intake Valve Closing) strategy to limit the maximum effective compression ratio to around 11:1 or lower in order to avoid knock while runnning on regular gasoline fuel [101]. In the current study, no EIVC (Early Intake Valve Closing) or LIVC strategy has been utilized to lower the effective compression ratio to limit the knocking tendency. Due to such high compression ratio (13.3:1) the current engine has been found to exhibit considerable knock even while running at a moderate load of 6 bar IMEPg. No EIVC or LIVC techniques were employed in this study in order to exhibit the impressive knock reduction potential and accompanying thermal efficiency benefits of high rate of EGR dilution at high compression ratio, compared to rather typical lean/excess air operation pursued in most pre-chamber jet ignition systems.

# 4.4 Comparison of EGR vs excess air dilution effect on specific heat capacity $(C_p)$ and specific heat ratio $(\gamma)$ :

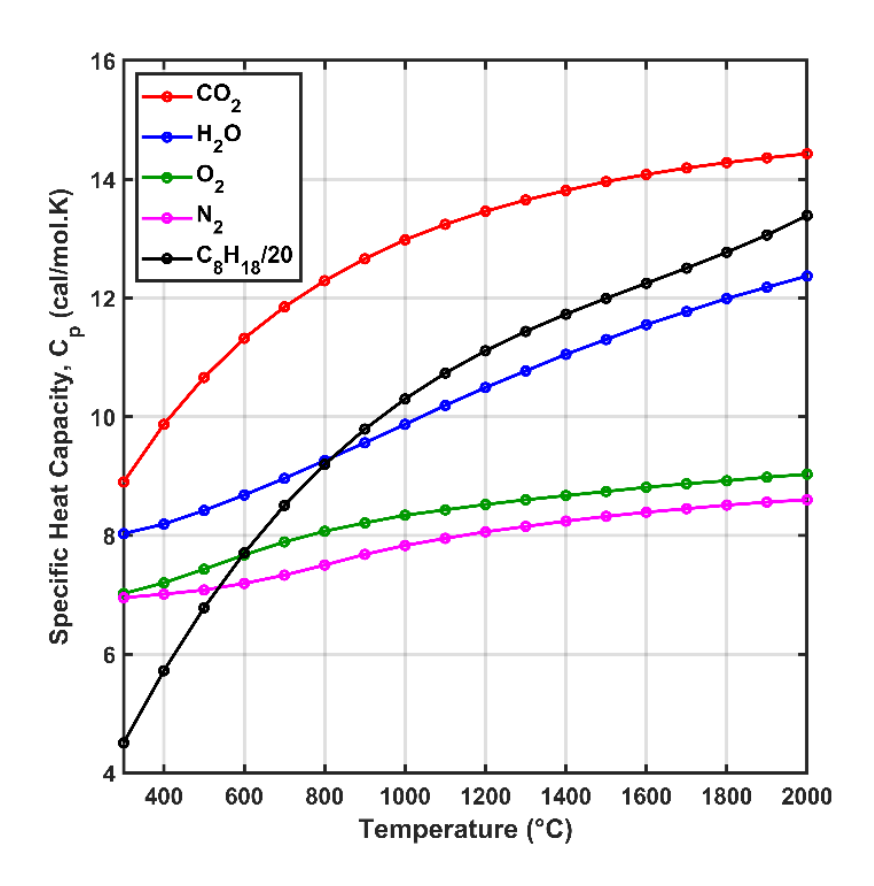


Figure 4.3 Specific heat capacity of species at different temperatures (adapted from [79,102])

Fuel typically has a higher specific heat capacity compared to the the rest of the species present inside the cylinder and it substantially contributes to the specific heat capacity of the air-fuel charge. Figure 4.3 shows the specific heat capacities of iso-octane and different constituents of EGR and air at different temperatures. As seen from figure 4.3,  $C_8H_{18}$  has a substantially higher specific heat capacity compared to other species (reduced by a factor of 20 to show in the same graph). Also, the EGR constituents such as  $CO_2$  and  $H_2O$  have much higher  $C_p$  values compared to the constituents of air ( $N_2$  and  $O_2$ ). Thus, dilution with EGR would result into slightly higher mixture specific heat capacity compared to dilution with excess air.

The specific heat ratio ( $\gamma$ ) has an inverse relation with the specific heat capacity ( $C_P$ ) [equation (1)]. Adding diluents to the inlet charge decreases the fraction of high  $C_P$  fuel in the mixture which leads to a decrease in  $C_P$  and subsequently an increase in  $\gamma$  [87,103].

$$\gamma = \frac{1}{1 - \frac{R}{C_P}} \tag{1}$$

Dilution is advantageous to thermal efficiency partly due to change in composition and partly from the decrease in burned gas temperature [87]. Dilution increases the specific heat ratio ( $\gamma$ ) of both the unburned and burned mixtures, which enables the charge to expand through a higher temperature ratio during expansion, thus enabling more work output [79]. The effect of increasing burned and unburned gas ( $\gamma$ ) values with increased dilution has been reported to be greater for (by about 2%) excess air dilution compared to EGR dilution [87]. Thus, it is expected to have a slight fall-off in gross efficiency with EGR dilution compared to identical level of excess air dilution.

# 4.5 Comparison of EGR vs excess air dilution effect on laminar flame speed:

A numerical simulation was performed using a freely propagating flame configuration in CHEMKIN software to investigate the effect of different diluents on the combustion of iso-octane. The high temperature kinetic scheme developed by Chaos et al. [104] was chosen as the input combustion mechanism. This mechanism was chosen over the more frequently used Lawrence Livermore comprehensive mechanism [105] based on the reports of superior laminar flame speed predictions [106] and the quickness of solution enabled by a reduced mechanism. The temperature and pressure for the inlet condition for the simulation were approximated through an isentropic compression of intake air (45 ° C and 1 atm) and the engine geometry. All simulations were performed at 750 K and 30 bar. Figure 4.4 shows the results of estimated laminar flame speed of

iso-octane at different dilution rate (v/v) with different diluents. From figure 4.4 it is apparent that other than  $O_2$ , rest of the diluents decrease the laminar flame speed monotonically. With  $O_2$ , the laminar flame speed first increases due to higher availability of oxidant and then starts decreasing due to the dilution effect becoming stronger at higher dilution rate.

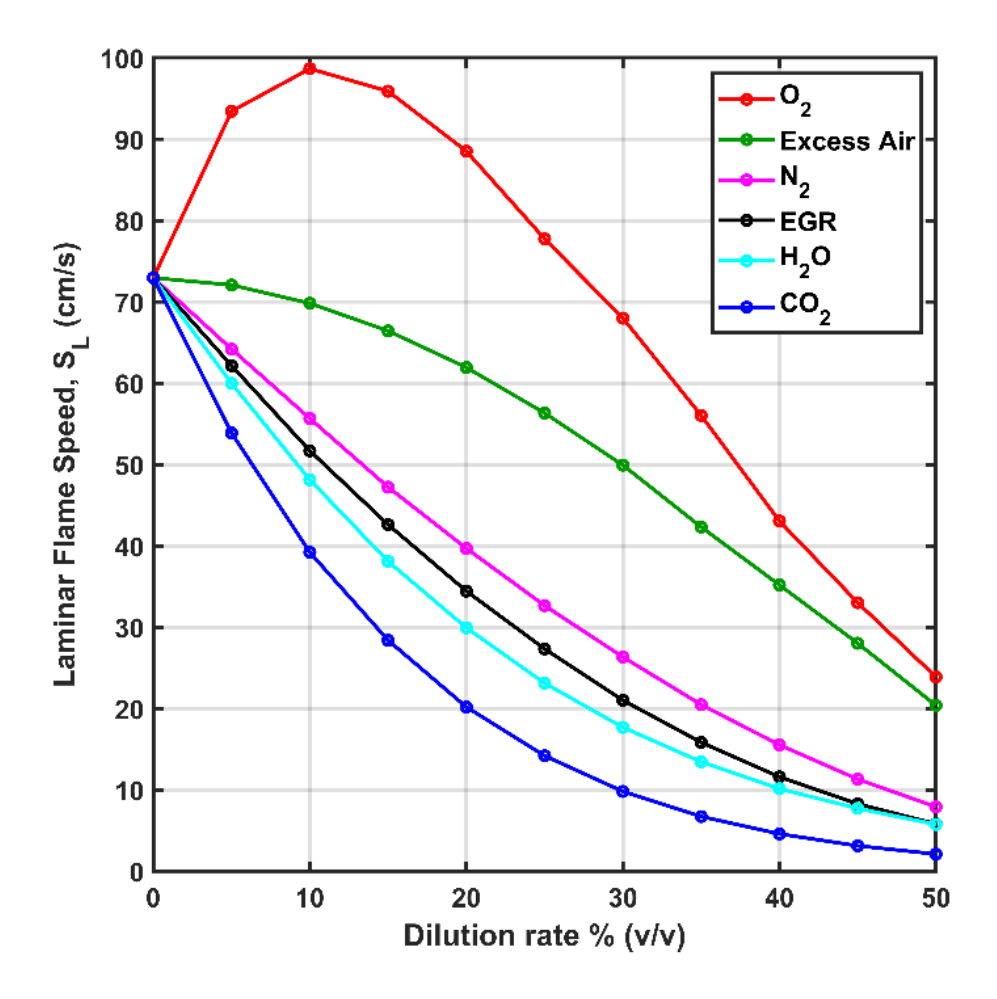


Figure 4.4 Effect of dilution rate with different diluents on the laminar flame speed of iso-octane; 750 K; 30 bar

Charge dilution changes the combustion characteristics through a combination of chemical, thermal and dilution effect [90,93]. It is apparent that EGR has a much greater effect on decreasing the laminar flame speed compared to excess air dilution. This happens partly due to the presence of high  $C_p$  components like  $CO_2$  and  $H_2O$  in EGR decreasing the peak combustion temperature,

the dissociation of CO<sub>2</sub> and H<sub>2</sub>O causing further decrease in combustion temperature, and lowering of oxidant concentration due to lower oxygen availability. On the other hand, in case of excess air dilution, the oxygen concentration does not drop, and the C<sub>p</sub> values remain lower. Additional results showing N2, O2, CO2 and H2O show how individual components affect the laminar flame speed. It is clear that CO<sub>2</sub> has a much larger effect in lowering the laminar flame speed compared to the other species. N2, while still providing the dilution effect of lowering the reactant concentration, mostly does not take effect in chemical reactions due to its inert nature. Combined with its lower C<sub>p</sub>, N<sub>2</sub> does not reduce the flame speed as aggressively as H<sub>2</sub>O or CO<sub>2</sub>. The effect of EGR falls between those of its constituents (N<sub>2</sub>, H<sub>2</sub>O an CO<sub>2</sub>); and the effect of excess air also falls between those of its constituents (N<sub>2</sub> and O<sub>2</sub>). In general, it is observed that at high dilution rate (beyond 25%) the laminar flame speed of iso-octane obtained with EGR dilution drops to more than half the value obtained with identical level of excess air dilution. This explains why it is generally harder to achieve comparable level of high dilution rate between EGR and excess air/lean burn operation in SI engines. The DM-TJI system provides a practical solution toward achieving a similar level of dilution tolerance between EGR diluted and lean burn strategy.

### 4.6 EGR and excess air dilution rate determinations:

During the experiments EGR percentage (v/v) was determined using the following equation [99,107]-

$$EGR_{volume} = \frac{(CO_2)_{intake}}{(CO_2)_{exhaust}}$$
 (2)

where,  $EGR_{volume}$  is the EGR rate determined in volume basis, and  $(CO_2)_{intake}$  and  $(CO_2)_{exhaust}$  are concentrations of  $CO_2$  sampled from engine intake (mixture of fresh air + EGR) and exhaust, respectively. Both are measured on a 'dry' basis. Since the intake and exhaust contain different

concentration of water (%), the 'dry' to 'wet' conversion factor is not the same between the two. Thus, the EGR rate based on 'dry' measurements would be different from the 'wet' measurements. Typically, it is recommended that all constituent concentrations be reported on a wet basis. The following equations [108,109] were used to convert the 'dry' concentration of CO<sub>2</sub> (measured by the emission bench) to 'wet' concentration of CO<sub>2</sub>.

$$(H_2O)_{dry} = y * \frac{[(CO) + (CO_2)]}{2*[\frac{(CO)}{3.8*(CO_2)} + 1]}$$
(3)

$$(CO_2)_{wet} = \frac{(CO_2)_{dry}}{\left(1 + \frac{(H_2O)_{dry}}{100}\right)} \tag{4}$$

where (CO) and  $(CO_2)$  are concentrations of CO and CO<sub>2</sub> in percentages in the exhaust gas measured on the 'dry' basis by the emission analyzer, y is the H:C ratio of the fuel used,  $(H_2O)_{dry}$  is the theoretical concentration of water (%) in the exhaust gas,  $(CO_2)_{dry}$  and  $(CO_2)_{wet}$  are the concentrations of CO<sub>2</sub> determined on dry and wet basis, respectively.

Additionally, the volumetric EGR rate was cross-verified with the intake O<sub>2</sub> percentage measured by the pressure compensated wideband O<sub>2</sub> sensors using the following relation (similar approach used in [110])-

$$EGR_{volume} = \left[\frac{(O_2)_{ambient} - (O_2)_{intake}}{(O_2)_{ambient} - (O_2)_{exhaust}}\right] * 100 \%$$
 (5)

where  $(O_2)_{ambient}$ ,  $(O_2)_{intake}$  and  $(O_2)_{exhaust}$  are the volumetric  $O_2$  concentration in the ambient air, intake charge and exhaust gas, respectively. A Previous publication by the author has already shown verification of the EGR rate determined from intake  $O_2$  measurement and the EGR rate based on volume flow rate measured by LFE. A similar approach of using flow measurements to

determine EGR rate has been used in [101].

A more conventional mass based EGR dilution rate definition used in several sources [79] is as follows

% 
$$EGR_{mass} = \frac{m_{EGR}}{m_{air} + m_{fuel} + m_{EGR}} * 100 \%$$
 (6)

where  $m_{air}$ ,  $m_{fuel}$  and  $m_{EGR}$  are the mass flow rates of intake air, fuel, and recycled exhaust gas, respectively. A similar relation can be used to define a universal dilution rate equation irrespective of whether the diluent is EGR or excess air. This would provide a metric to compare the effects of EGR and excess air on engine performance parameters under identical level of charge dilution irrespective of the diluents [97,98].

% Dilution rate = 
$$\frac{m_{diluent}}{m_{air,stoich} + m_{fuel} + m_{diluent}} * 100 \% (7)$$

where  $m_{air,stoich}$ ,  $m_{fuel}$  and  $m_{diluent}$  are the mass flow rates of air for stoichiometric combustion, fuel, and the diluent, respectively. For EGR dilution the  $m_{diluent}$  is replaced by  $m_{EGR}$  and for excess air dilution the  $m_{diluent}$  is replaced by  $m_{excess\;air}$  air in the above equation. Now, typically in engine research air-fuel equivalence ratio lambda ( $\lambda$ ) is used for determining how lean or rich the air fuel mixture is.

$$\lambda = \frac{(AFR)_{actual}}{(AFR)_{stoich}} \tag{8}$$

where  $(AFR)_{actual}$  and  $(AFR)_{stoich}$  are the mass based actual and stochiometric air fuel ratio, respectively. Since, lambda ( $\lambda$ ) already provides a metric for how much air is present in the mixture compared to the stoichiometric mixture, after some rearranging the excess air dilution rate can be

expressed in terms of lambda ( $\lambda$ ) [97,98].

% Excess air dilution rate = 
$$\frac{m_{excess air}}{m_{air,stoich} + m_{fuel} + m_{excess air}} * 100$$

$$= \frac{m_{air,actual} - m_{air,stoich}}{m_{air,actual} + m_{fuel}} * 100\%$$

$$= \frac{(AFR)_{actual} - (AFR)_{stoich}}{(AFR)_{actual} + 1} * 100\%$$

$$= \frac{\lambda - 1}{\lambda + (FAR)_{stoich}} * 100\%$$
(9)

where  $m_{air,actual}$ , (FAR)<sub>stoich</sub> are the mass flow rate of actual air in inlet charge and fuel-air stoichiometric ratio, respectively. Since the stoichiometric fuel-air ratio for the fuel used is typically a known quantity (1/14.16 for the current fuel), the excess air dilution rate can be expressed in terms of a function of lambda ( $\lambda$ ) only. The variation of excess air dilution rate with  $\lambda$  is given in table 4.2.

Table 4.2 Variation of excess air dilution rate with  $\lambda$ 

Lambda (λ)	Excess air dilution rate (%)
1	0
1.1	8.56
1.2	15.77
1.3	21.92
1.4	27.25
1.5	31.89
1.6	35.97
1.7	39.59
1.8	42.86

While volumetric EGR rate provides a straightforward approach in determining EGR dilution, to

compare EGR dilution percentage to an identical level of excess air dilution percentage (a mass-based quantity); the volumetric EGR fraction is converted to mass based EGR fraction according to the following rearranged relation-

$$EGR_{mass} = \frac{1}{1 + \frac{MW_{air}}{MW_{EGR}} \left(\frac{1 - EGR_{volume}}{EGR_{volume}}\right) (1 + FAR_{stoich})}$$
(10)

where  $EGR_{mass}$  is the the mass-based EGR rate,  $EGR_{volume}$  is the volume-based EGR rate, and  $MW_{air}$  and  $MW_{EGR}$  are molecular weight of air and recycled exhaust gas, respectively. In this current study, the EGR rates reported in subsequent sections are all based on 'wet' and 'mass' basis.

### 4.7 Results and Discussion

Figure 4.5 shows the IMEPg and PMEP values obtained during the EGR and excess air dilution sweeps performed at a nominal IMEPg of 6 bar and at either MBT or KLSA timing. As shown in the bottom graph in figure 5, running at lean condition the engine was always knock limited; but at EGR diluted condition with more than 30% EGR MBT (Maximum Brake Torque) operation was possible. Both excess air and EGR diluted operation showed increasing trend of IMEPg with increasing dilution rate. This is due to a combined effect of better combustion phasing permitted by lower knocking tendency with higher rate of dilution and decreased heat loss as a result of reduced combustion temperature with higher dilution. As for the PMEP values shown in the upper graph in figure 4.5 it is seen that both lean and EGR operation significantly reduce the pumping loss, with the lean operation providing slightly more benefit. Typically, lean or excess air diluted operation would provide slightly better thermal efficiency compared to EGR diluted operation due to improvement in specific heat ratio and combustion efficiency. However, as shown in the IMEPg traces, at knock limited conditions EGR dilution could provide comparable work output to the lean

operation (as long as good combustion stability can be maintained).

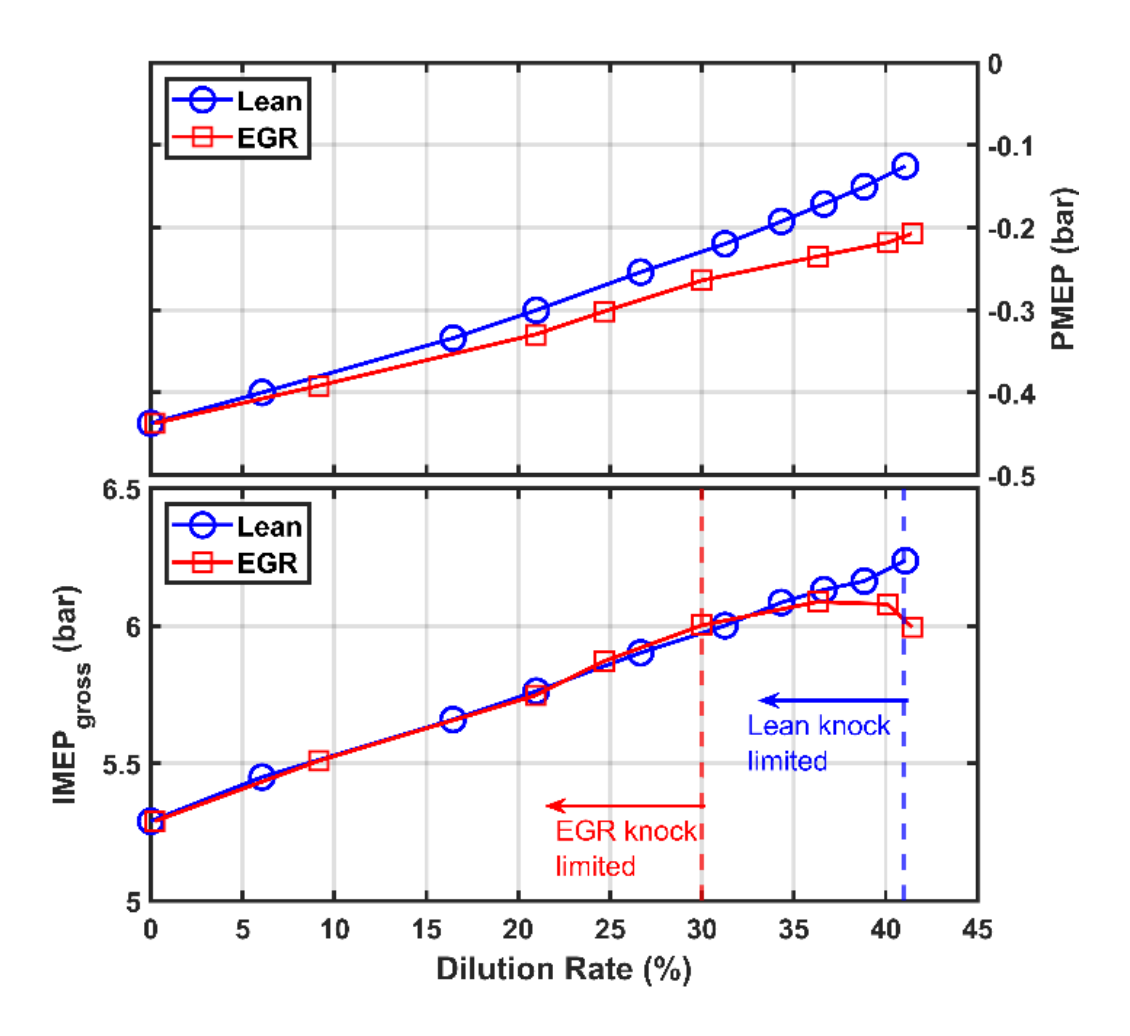


Figure 4.5 Comparison of IMEPg and PMEP between lean burn and EGR diluted operation at MBT/KLSA spark timing

Figure 4.6 shows the comparison of COV<sub>IMEP</sub>, spark timing and the resulting CA50 values between the lean and EGR diluted operation at different dilution rates. COV<sub>IMEP</sub> of 5% has been used here as the combustion stability limit. As shown in the COV<sub>IMEP</sub> versus dilution rate graph in figure 4.6, the DM-TJI system exhibits similar combustion stability between EGR-diluted and lean opeartion (less than 2% COV<sub>IMEP</sub>) up to about 37% dilution rate and still shows less than 5% COV<sub>IMEP</sub> at 40% external EGR dilution. Additional air delivery to the pre-chamber allows this

system to maintain good combustion stability with high EGR rate (up to 40%). At approximately 42% EGR dilution rate, the COV<sub>IMEP</sub> increases beyond the 5% stability limit. However, with a similar dilution rate excess air dilution provided better combustion stability (2% COV<sub>IMEP</sub>). This is due to the fact that lean operation still permitted formation of ignitable mixture inside the prechamber, even at more than 40% dilution rate. The considerably lower percentage of residual gas fraction inside the pre-chamber during lean operation enables such behavior. With high EGR dilution rate, even with auxiliary pre-chamber air purging, there will still be a considerably higher presence of EGR fraction inside the pre-chamber, thus compromising the pre-chamber ignitability and flame propagation. This explanation is supported by the results shown in the middle graph in figure 4.6 where it is clear that with both EGR and lean operation greater spark advance was required to yield good combustion stability as the dilution rate became higher. With EGR dilution this spark advance requirement was higher and the difference between the advancing requirement between the EGR and lean operation became broader with higher dilution. At around 40% EGR rate, the spark is so advanced that it might actually cause several problems for the pre-chamber ignitability. First, the spark timing becomes so close to the pre-chamber fuel injection timing that it does not permit enough time for the pre-chamber fuel to mix properly and second, the prechamber temperature would be lower at the time of ignition with such advanced spark timing. Both of these factors will cause problems in pre-chamber ignitability and subsequent combustion stability. The EGR dilution limit of about 40% is probably more a result of pre-chamber ignitability than the main chamber ignition and burn characteristics.

The CA50 results shown in the top graph in figure 4.6 show the combustion phasing benefit provided by the EGR dilution compared to the lean operation, especially at high dilution rate. As demonstrated in this graph, the lean operation was always knock limited and did not permit CA50

phasing of 7-8 CAD bTDC. On the other hand with EGR diluted operation with more than 30% EGR rate, preferable CA50 phasing was obtained. While poor ignitability can be an issue with higher EGR rate, due to the same reason the end gas autoignition potential is reduced and consequently EGR dilution strategy provides better combustion phasing benefits compared to lean operation, especially in knock limited situations such as this one.

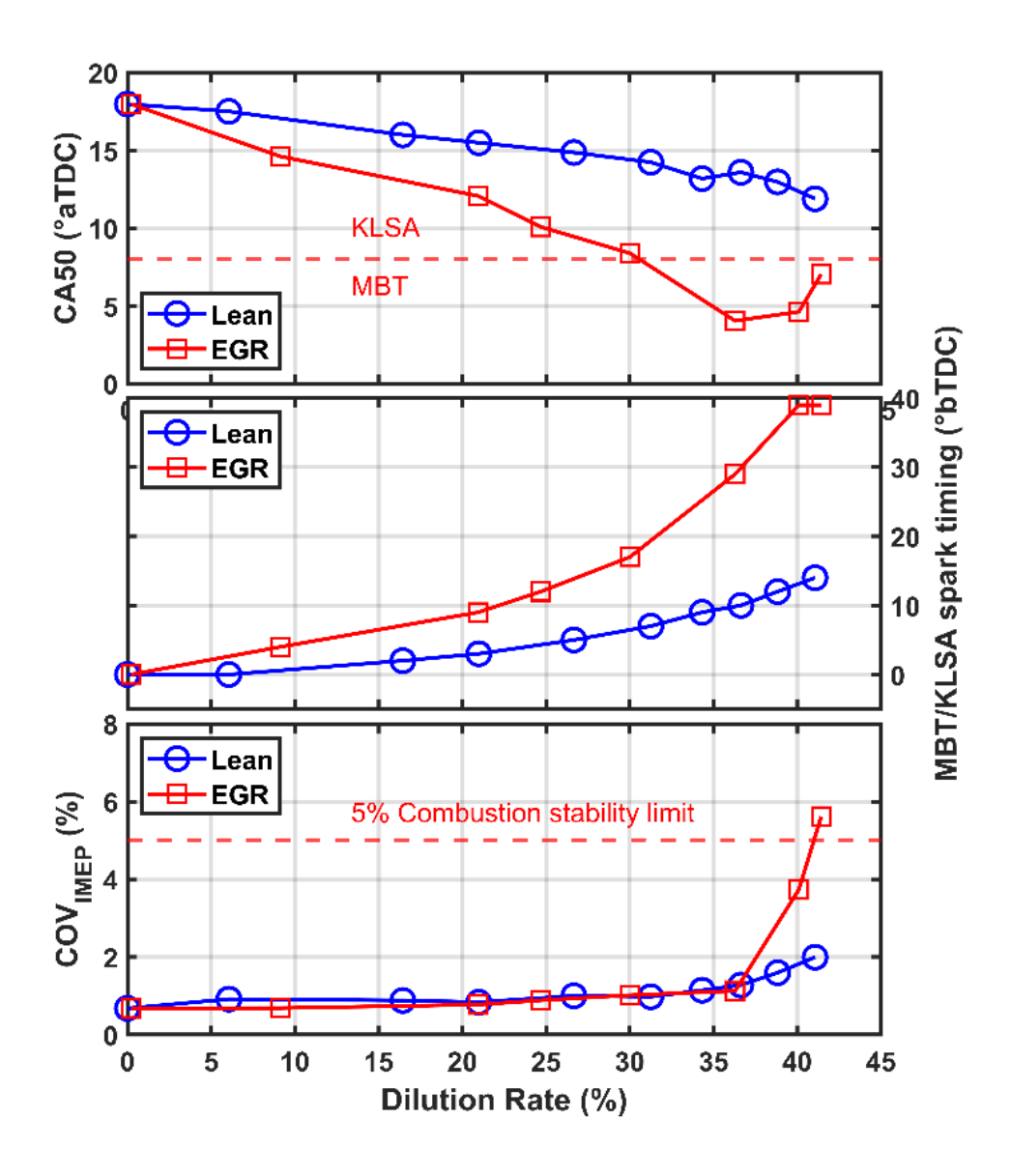


Figure 4.6 Comparison of  $COV_{IMEP}$ , MBT/KLSA spark timing and crank angle of 50% mass burned fraction between lean burn and EGR diluted operation

Dilution decreases the laminar flame speed and consequently leads to slower combustion. Thus, dilution has a similar effect of retarding the combustion phasing. Also, dilution changes the ignition chemistry through increase of quenching reactions due to diluents and leads to increased ignition delay which is reported to be the dominant mechanism behind high effectiveness of EGR for knock reduction [103]. The combustion phasing benefit and better knock relief provided by the high EGR dilution rate along with the pre-chamber ignitability are better visualized in the form of the results shown in figure 4.7.

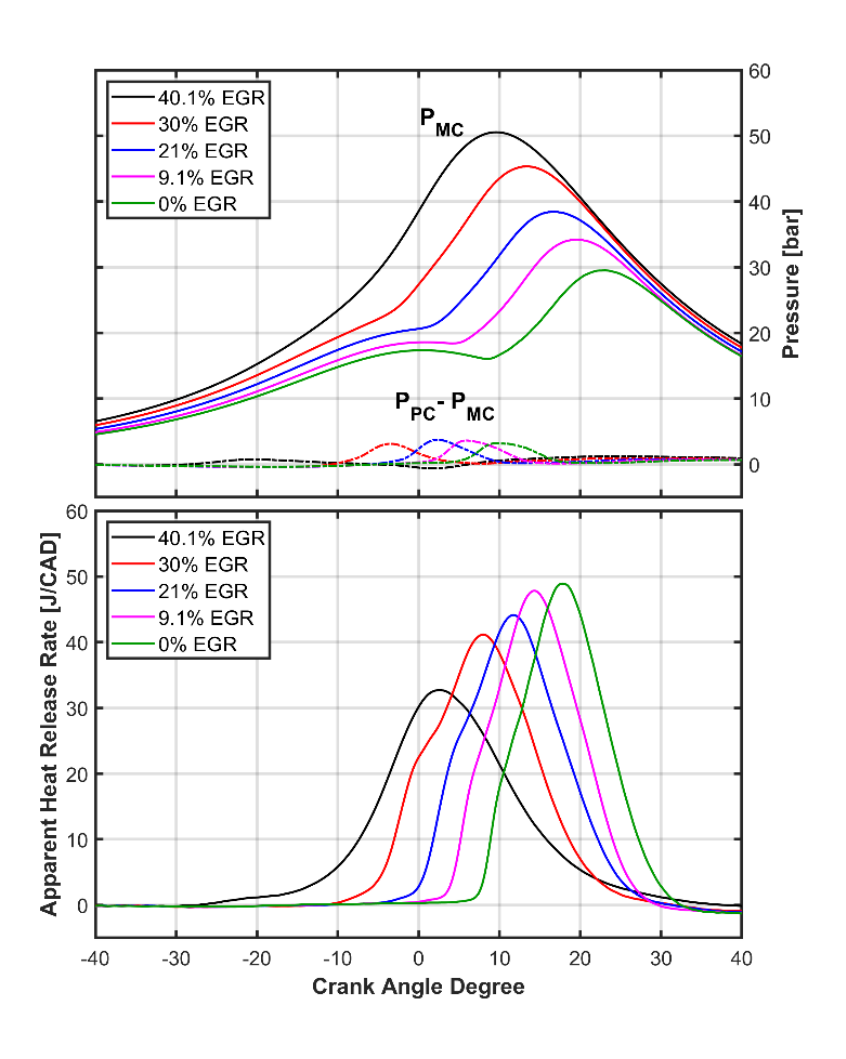


Figure 4.7 Main chamber pressure, pressure differential between pre-chamber and main chamber and main chamber apparent heat release rate with different EGR rates at MBT/KLSA spark timing

Figure 4.7 includes the main chamber pressure, the pressure differential between the chambers and the main chamber apparent heat release rate at different EGR dilution rates. As shown by the top graph, increasing amount of EGR permits better combustion phasing and higher cylinder pressure. On the other hand, the bottom graph shows that increasing the EGR dilution rate up to 40% decreases the heat release rate considerably which provides more knock relief while still maintaining good combustion stability. Knock typically exhibits itself with high heat release rate. If the pressure differential between the pre-chamber and main chamber in the top graph in figure 4.7 is considered, it is apparent that at 40% EGR the pre-chamber ignitability is poor, and the pressure rise in the pre-chamber is compromised. This pressure differential is the driving force which initiates the jets that start main chamber combustion. If the pre-chamber faces difficulty igniting, the main chamber follows.

In contrast, the same set of results shown in figure 4.8 for lean operation under similar dilution level show that even at 41% dilution, very good pre-chamber to main chamber pressure differential is maintained. Hence better combustion stability could be maintained with excess air compared to EGR (figure 4.6). While pre-chamber ignitability is better at high dilution rate for lean operation, the increased knocking potential limits the actual benefits. As it appears in figure 8 top graph, the peak pressures are lower in case of lean operation compared to the EGR diluted operation due to the constraints of the increased knock tendency. Similar to the EGR diluted cases, excess air dilution also shows decrease in apparent heat release rate with increase in dilution rate (figure 4.8, bottom graph).

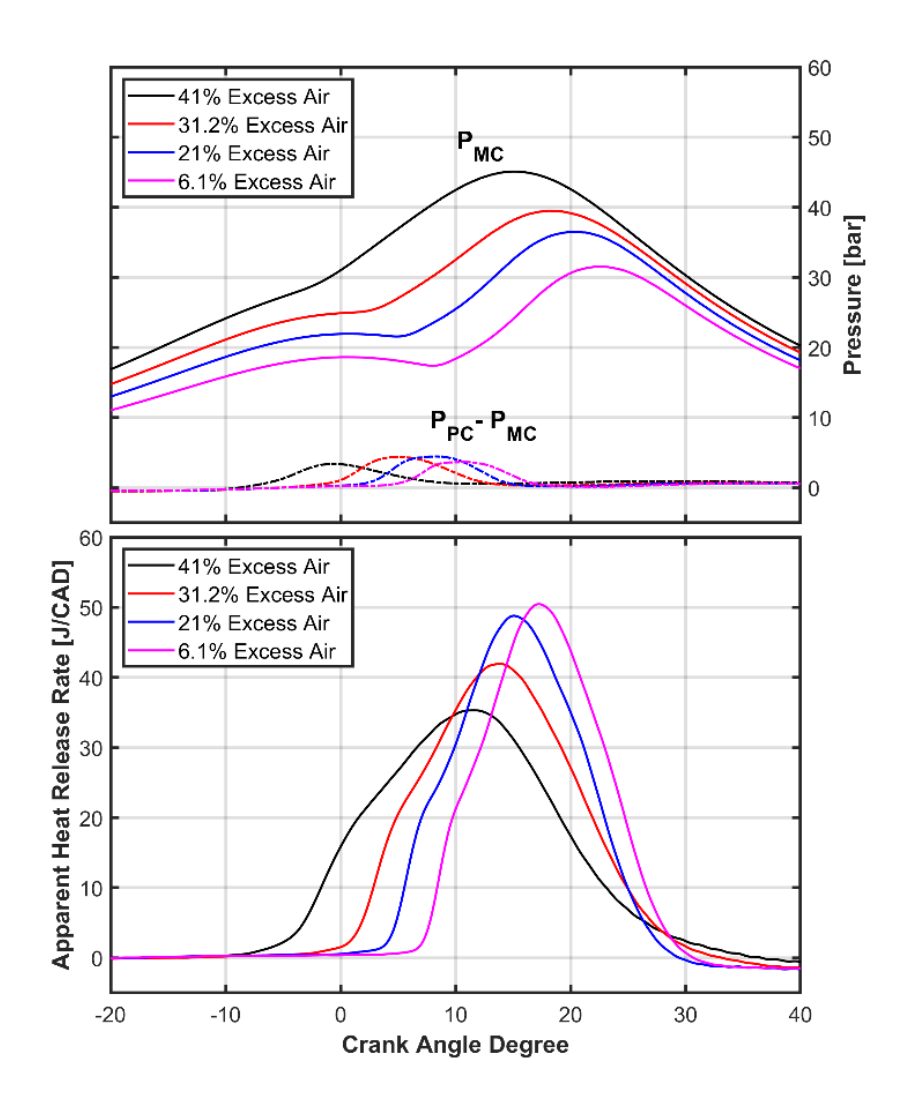


Figure 4.8 Main chamber pressure, pressure differential between pre-chamber and main chamber and main chamber apparent heat release rate with different excess air rate at MBT/KLSA spark timing

Figure 4.9 provides a comparison of the apparent heat release rate at different dilution rates between EGR and excess air dilution strategies. At similar dilution level lean/excess air dilution yields higher heat release rate compared to the EGR diluted operation. Consequently, in a knocking environment lean operation would exhibit more knocking tendency compared to that at a similar level of EGR dilution.

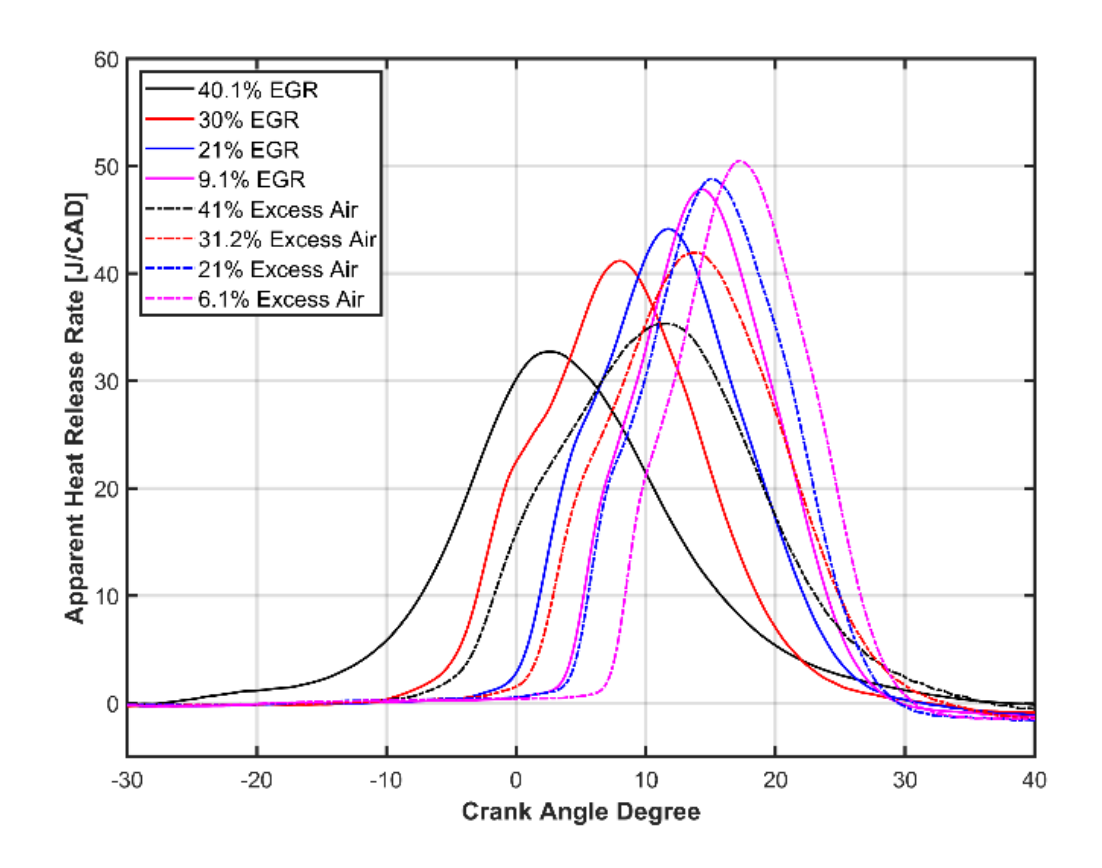


Figure 4.9 Comparison of main chamber apparent heat release rate between lean burn and EGR diluted operation at MBT/KLSA spark timing

Figure 4.10 compares the 10-90% mass fraction burn duration and 0-10% mass fraction burn duration (based on main chamber pressure) at different dilution rates between the EGR and lean operation strategies. In both the lean and EGR cases, 10-90% burn duration increases with increase in dilution rate which is as expected since with the addition of diluents the flame speed decreases, and the resulting burn rate becomes slower. The 0-10% burn duration shows increasing trend with dilution rate as well but not until around 25 to 30% dilution rate. While beyond 30% dilution rate the 0-10% burn duration increases with increasing dilution, up to about 30% dilution the 0-10% mass fraction burn duration essentially stays the same. This is in contrary to other studies involving diluted combustion in spark ignition engines that did not involve pre-chamber ignition technology

[89,111]. This shows the effectiveness of pre-chamber-initiated jet ignition systems to deal with the issues of diluted combustion. From the 0-10% burn duration graph it is apparent that beyond 30% dilution rate, EGR has a more substantial effect on the 0-10% burn duration compared to excess air dilution cases (which show smoother and more moderate increase). This again demonstrates the poor ignitability and flame propagation behavior inside the pre-chamber due to unfavorable presence of EGR diluents. This results in weaker jets with reduced potential to ignite the main chamber mixture successfully.

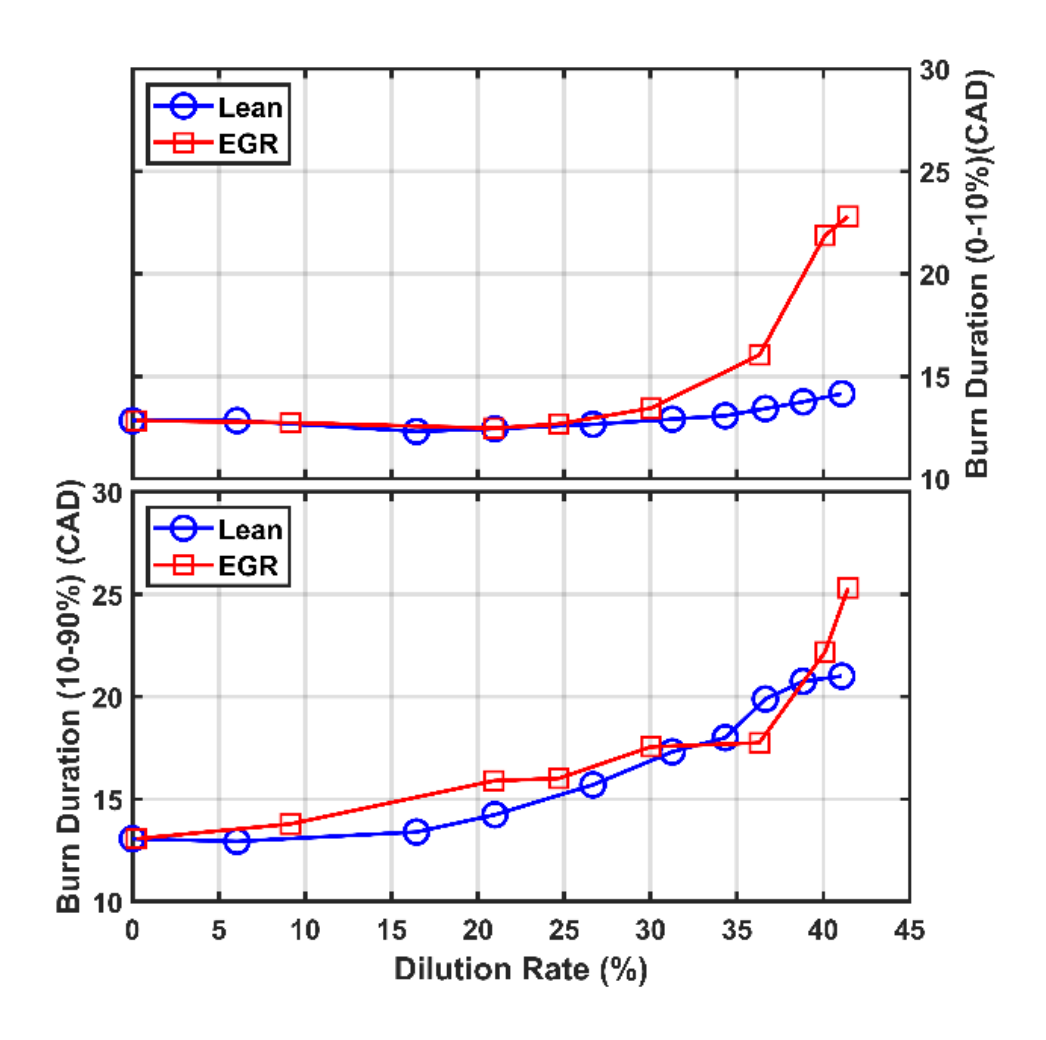


Figure 4.10 Comparison of 10-90% mass fraction burn duration and 0-10% mass fraction burn duration between lean burn and EGR diluted operation at MBT/KLSA spark timing

Another interesting observation from figure 4.10 is that at 40% EGR and 40% excess air dilution rate both the 0-10% burn duration and 10-90% burn duration are well below the limiting values of total burn durations (70~80 CAD) reported by other researchers for lean/diluted operations of SI engines [89,111,112]. The excess air dilution rate in this study was limited by the maximum lambda operation that could be achieved at naturally aspirated (NA) condition under 6 bar IMEPg load. However, based on the burn duration values reported in figure 4.10 it is clear that higher excess air dilution can be easily achievable under the same load with boosting. On the other hand, at high dilution rate with EGR diluted operation, combustion stability suffers beyond 40% EGR rate (figure 4.6). However, the main chamber burn characteristics (presented in figure 4.10) suggest that better pre-chamber purging and fueling strategy could provide better pre-chamber ignition and consequently higher EGR dilution tolerance. At present, the pre-chamber ignitability seems to be the limiting factor for lower dilution tolerance with EGR operation compared to lean/excess air operation. Pre-chamber ignitability, especially with high residual gas fraction (RGF) or recirculated exhaust gas (EGR), has always been an issue with pre-chamber jet ignition systems. The DM-TJI system provides a viable technology path to resolve that and provide higher EGR dilution tolerance (and possibly better thermal efficiency) for SI engine platform.

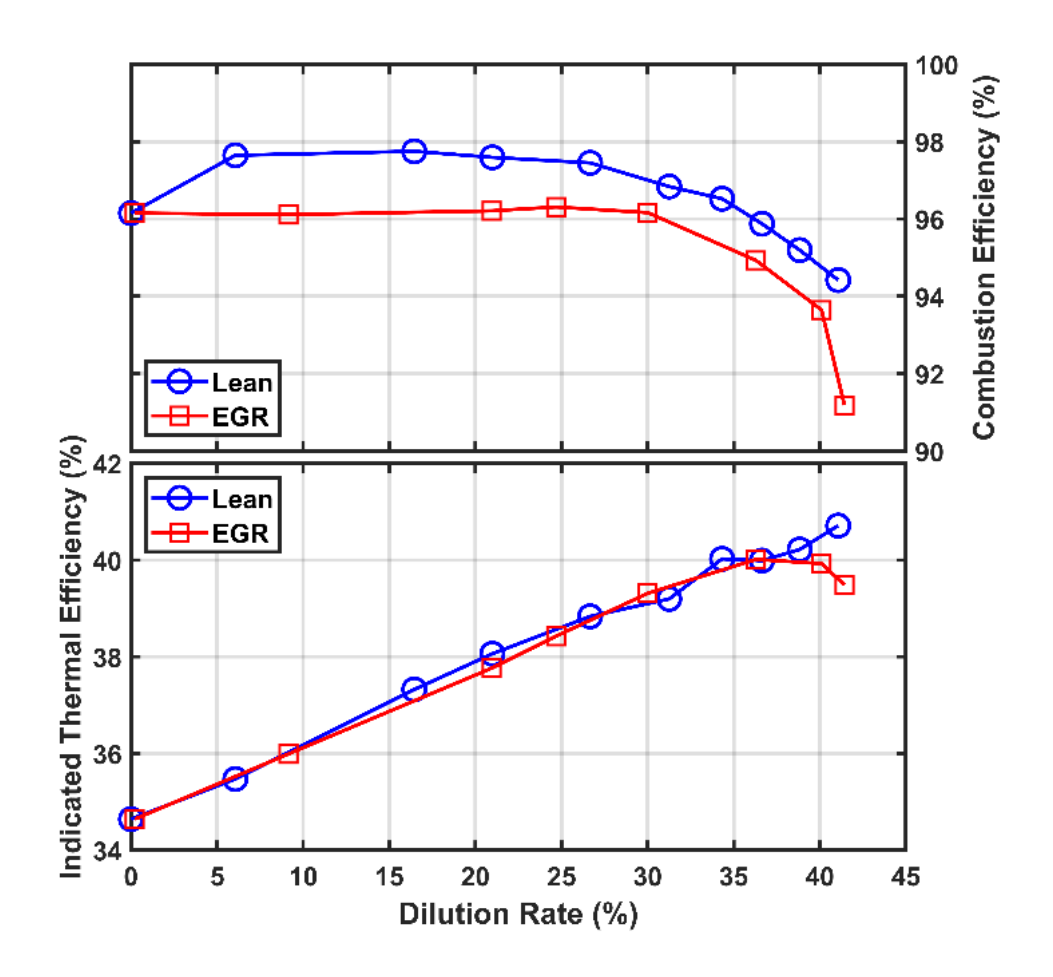


Figure 4.11 Comparison of gross indicated thermal efficiency and combustion efficiency between lean burn and EGR diluted operation at MBT/KLSA spark timing

Figure 4.11 compares the indicated thermal efficiency (gross) and combustion efficiency between lean/excess air and EGR diluted operation. The top graph in figure 4.11 shows that for lean burn strategy, combustion efficiency first increases compared to stoichiometric operation and then after around 25% dilution (or  $\lambda \sim 1.3$  to 1.4), combustion efficiency starts decreasing. This initial increase in combustion efficiency is due to the oxidation of unburned hydrocarbon in the hot exhaust stream due to the presence of excess air [79]. EGR dilution strategy does not have this excess air in the hot exhaust to oxidize the unburnt hydrocarbon and hence remains comparable to 0 to 30% dilution rate. At higher dilution (beyond 30%) both lean and EGR diluted operation show

a decreasing trend in combustion efficiency. In general, the lean burn strategy has 1.5 to 2 percentage point benefit in terms of combustion efficiency which is expected because of the presence of excess air inside the cylinder to burn the fuel in a more complete manner and in the exhaust stream as well to further oxidize the unburnt hydrocarbons. However, in the current study, despite higher combustion efficiency shown by the lean operation the resulting indicated efficiency is comparable between the excess air and the EGR dilution strategy. This could be due to the better knock relief provided by the EGR compared to excess air and the subsequent phasing benefits offsetting the combustion efficiency disadvantage. Alternatively, the combustion efficiency in excess air dilution might not represent an actual higher percentage of fuel being consumed inside the cylinder due to the post combustion oxidation taking place in the exhaust stream which does not necessarily add to the work output of the engine.

The drastic reduction of combustion efficiency in case of 42% EGR rate is due to high combustion variability induced by poor reliability of pre-chamber ignition. This consequently resulted in a decrease in thermal efficiency as well (bottom graph figure 4.11). In fact, beyond 36% EGR the indicated efficiency starts to taper off even with increasing level of dilution. This is a direct consequence of decrease in combustion efficiency at these higher dilution points where reduction in heat loss cannot offset the loss incurred by reduced burnt fuel quantity. The excess air dilution results do not show the same trend though. The indicated efficiency keeps on increasing with higher dilution even though the combustion efficiency decreases. This is due to the reduced heat loss benefit of higher dilution as well as better knock relief (and consequently better combustion phasing) benefit obtained at high dilution rate. Under non knocking conditions, the excess air dilution strategy should generally provide slightly higher (1~2 percentage point) indicated efficiency compared to EGR diluted operation at a similar dilution level [87].

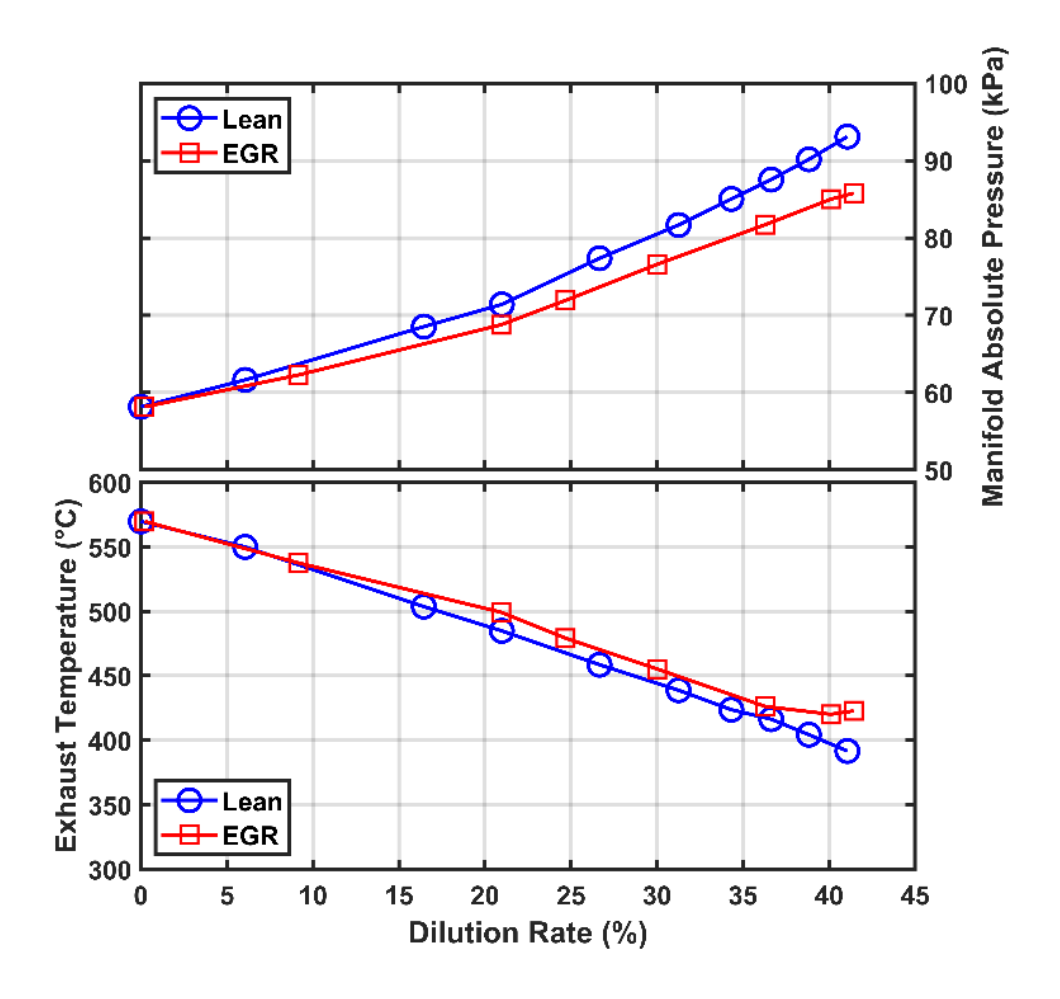


Figure 4.12 Comparison of exhaust gas temperature and manifold absolute pressure between lean burn and EGR diluted operation at MBT/KLSA spark timing

Figure 4.12 compares the exhaust gas temperature and the manifold absolute pressure between lean burn and EGR diluted operation. Both exhaust temperature and manifold pressure demonstrate how higher dilution improves the efficiency. In the bottom graph in Figure 4.12, a decrease in exhaust temperature is seen with increase in dilution rate for both lean and EGR diluted condition. This is due to the fact that higher dilution rate increases the mixture specific heat ratio and this consequently increases the expansion work by allowing the burned gases to expand through a larger temperature ratio before the exhaust [89]. As seen from this graph, lean/excess air dilution provides slightly more decrease in exhaust temperature compared to EGR dilution. This

is due to the larger value of specific heat ratio obtained through excess air dilution compared to EGR dilution under identical level of dilution rate [87].

The top graph shown in figure 4.12 demonstrates that with increasing dilution rate the manifold absolute pressure increases considerably since the engine has to operate less throttled to allow more diluent flow to the cylinder. This again greatly reduces the pumping losses and consequently increases the engine efficiency. Excess air dilution provides a slightly higher manifold pressure (and hence lower pumping losses reported in figure 4.5) compared to the EGR dilution case. With EGR dilution, manifold pressure suffers slightly due to the requirement of maintaining a positive pressure differential to induce higher EGR flow from the exhaust to the intake system. Excess air dilution does not require this since all the flow is coming through the intake air duct. Both exhaust gas temperature and manifold absolute pressure results again indicate that excess air dilution should yield slightly better thermal efficiency compared to EGR dilution. However, under knock limited conditions such as those investigated in this study, EGR dilution provides very comparable results to the excess air dilution and the efficiency disadvantage becomes negligible.

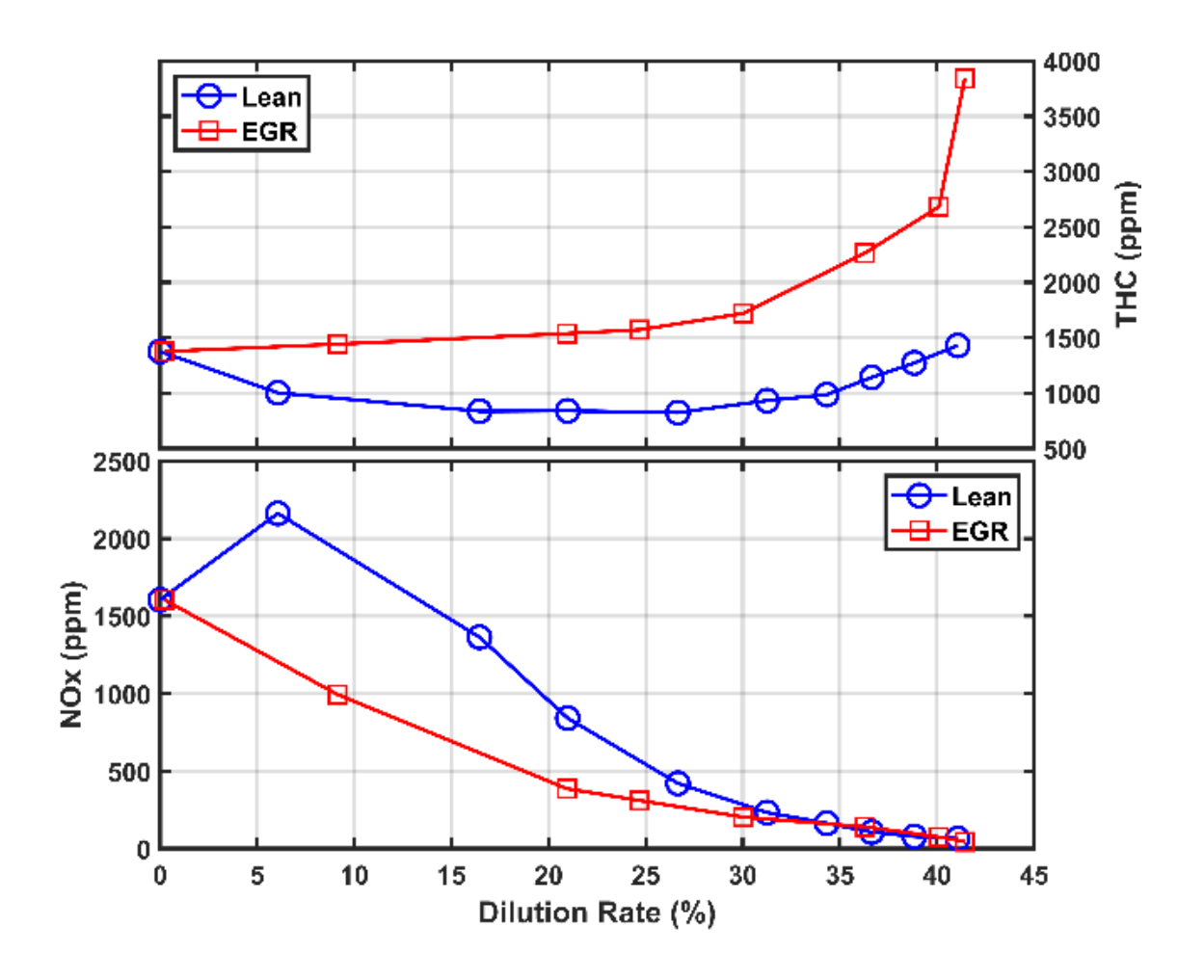


Figure 4.13 Comparison of NOx and hydrocarbon (THC) emissions between lean burn and EGR diluted operation at MBT/KLSA spark timing

Figure 4.13 compares the NOx and THC emission results between the lean-burn and EGR-diluted operations. From the bottom graph in figure 4.13 it is seen that in both the EGR diluted and excess air diluted cases, increasing dilution rate significantly reduces the NOx emission due to reduction of peak combustion temperature. Excess air dilution causes the NOx levels to peak near 6% dilution rate (or  $\lambda$  around 1.05 to 1.1) and then decrease gradually, whereas for the EGR dilution case, increasing dilution rate always leads to decreasing NOx emissions. It is also clear that under identical dilution rates, EGR dilution offers greater NOx reduction than excess air dilution. This

is similar to the findings reported by other researchers [89,99]. In the current study, NOx emissions become comparable at high dilution rates due to the difference in combustion phasing between the two dilution strategies. However, in general, under identical dilution rate and combustion phasing EGR (due to slightly higher specific heat capacity of the mixture and a greater decrease in combustion temperature) should yield greater reduction in NOx emissions. While EGR provides a significant advantage over lean burn when it comes to NOx emission, an opposite trend is seen in unburnt hydrocarbon emission.

The top graph in Figure 4.13 shows the THC emission at different dilution rates between the leanburn and EGR-diluted operation. With lean burn/excess air dilution the hydrocarbon first decreases with increase of dilution rate, then levels off and finally at around 30% dilution rate starts increasing again. This initial reduction in HC emission is due to higher combustion efficiency provided by slightly leaner operation compared to stoichiometric combustion. In case of EGR diluted operation, an always increasing trend of HC emission is observed with increasing dilution rate. HC emission shows a significant increase beyond 30% EGR rate. All these THC emission results are directly linked to the combustion efficiency (reported in figure 4.11). As expected, reduction in combustion efficiency causes a proportional increase in unburnt hydrocarbon emissions. In general, HC emission increases (and combustion efficiency decreases) with increasing dilution rate (for both EGR and excess air dilution) due to increased flame quenching effect at higher dilution [79]. Even though HC emission increases with EGR dilution compared to excess air dilution, the fact that a significant improvement in NOx emission can be realized with EGR with no substantial losses in indicated efficiency, while ensuring that the TWC can be utilized efficiently to reduce the tailpipe emission, makes EGR dilution far more advantageous over lean burn/excess air dilution.

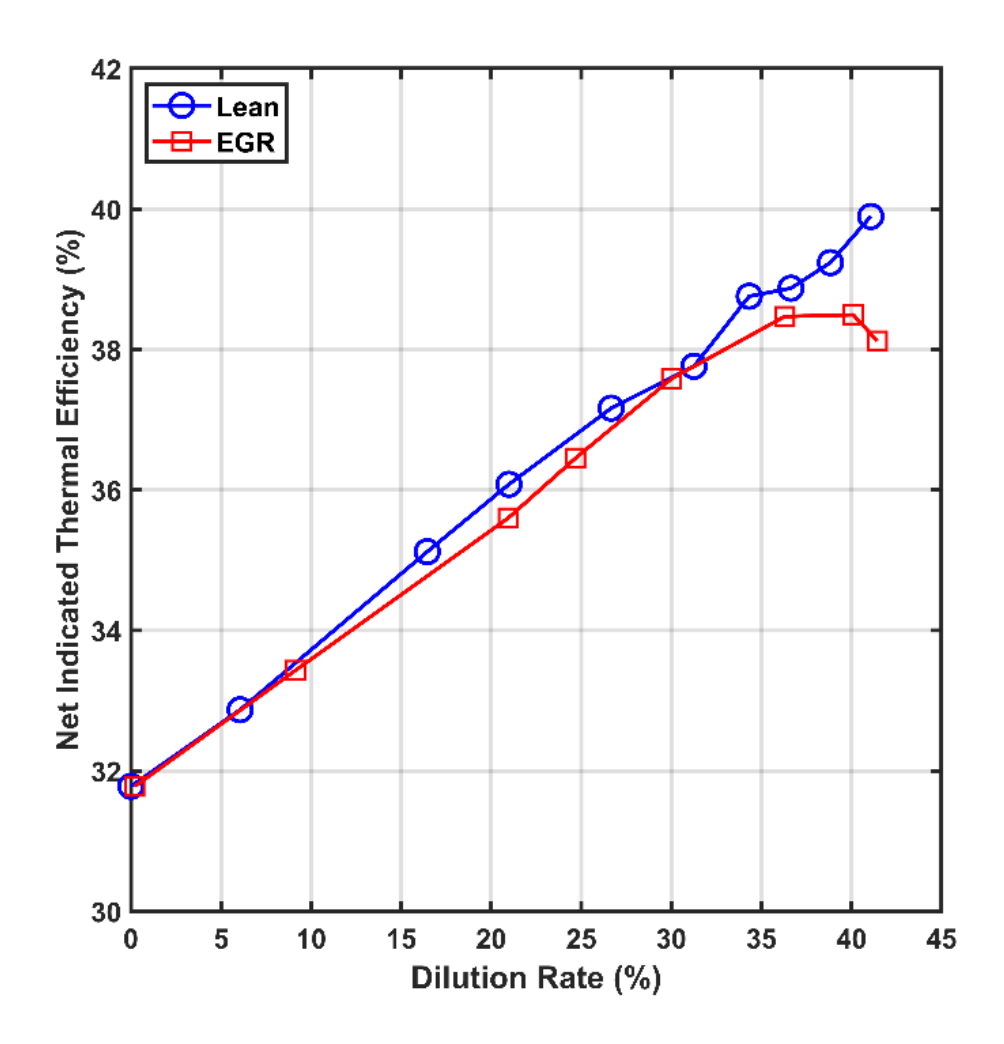


Figure 4.14 Comparison of net indicated thermal efficiency with varying dilution rate between lean burn and EGR diluted operation at MBT/KLSA spark timing

Figure 4.14 compares the net indicated thermal efficiency between the lean burn and EGR diluted strategy. With both dilution strategies, higher dilution rate leads to higher thermal efficiency. For EGR diluted operation beyond 40% dilution rate the thermal efficiency starts to drop due to loss of combustion efficiency and increased COV<sub>IMEP</sub>. It is observed that excess air dilution strategy generally provides slightly better net indicated thermal efficiency (about 1 to 1.5 percentage point) under identical dilution rate compared to EGR dilution strategy. This is due to a combination of marginally better specific heat ratio, better combustion efficiency and small improvement in

pumping loss. Even with such advantages the excess air dilution strategy was greatly limited by high knock propensity to realize any further thermal efficiency improvement. At higher loads with greater knocking tendency this thermal efficiency advantage would be even more diminished. This is particularly applicable to engines operating at high compression ratios.

It should be noted that Dual Mode, Turbulent Jet Ignition technology is still in its infancy. Many critical parameters in TJI-specific application have not gone through any rigorous optimization process and are designed largely based on prior experiences. These parameters include prechamber shape and volume, nozzle diameter, nozzle orifice 1/d ratio, orifice orientation and distribution, pre-chamber fueling strategy, pre-chamber air delivery strategy, air valve timing and phasing, and intake and exhaust valve timings. Further studies are required to achieve optimal engine performance using the DM-TJI system. Nonetheless, the current study does showcase the potential of the DM-TJI system to operate with high level of EGR dilution rate (up to 40%). This study also identifies the benefits and disadvantages to expect while operating at high EGR dilution rate compared to operating lean at an identical level of dilution.

## 4.8 Summary and Conclusions

A comparative experimental study of lean burn and EGR diluted operation has been carried out in a pre-chamber air/fuel scavenged dual mode, turbulent jet ignition (DM-TJI) system in a high compression ratio, single cylinder engine fueled with gasoline. The results of the experimental investigation can be summarized as follows-

- EGR dilution strategy provides slightly lower but still comparable thermal efficiency benefits compared to an identical level of excess air dilution rate.
- EGR dilution provides substantially better knock mitigation compared to excess air

dilution/lean burn strategy. At high compression ratio (13.3:1) operation, even with more than 40% excess air dilution rate (or  $\lambda$  around 1.8) the combustion was knock limited and MBT phasing was not possible. On the other hand, EGR dilution rate of 30% and above provided substantial knock relief and enabled MBT combustion phasing.

- EGR dilution was more effective in NOx emission reduction than excess air dilution. On
  the other hand, THC emission was greater with EGR dilution compared to excess air
  dilution due to lower combustion efficiency.
- Under identical pre-chamber air delivery and fuel injection strategies, a maximum 40%
   EGR dilution rate was achievable with COV<sub>IMEP</sub> less than 4%. Identical excess air dilution rate exhibited more stable 2% COV<sub>IMEP</sub>. The excess air dilution rate could be extended with either added boost or a decreased fueling strategy.
- Investigation on main chamber burn parameters (0-10% burn duration and 10-90% burn duration) suggests that the maximum EGR tolerance of 40% is probably limited by the poor pre-chamber ignitability. Improvements in purging strategy and pre-chamber design should provide an even better EGR dilution rate.
- A maximum of 38.5% net indicated thermal efficiency was achieved with 40% EGR dilution rate running at a load of 6 bar IMEPg at 1500 rpm. At a similar dilution level, excess air dilution provided 39.9% net indicated efficiency.
- While excess air dilution provided slightly better thermal efficiency compared to EGR dilution, the diminished usefulness of the widely used TWC converter makes the lean burn strategy rather impractical, especially for automotive applications.

• The Dual mode, Turbulent Jet Ignition technology provides a viable alternative to lean burn TJI technologies. The DM-TJI system realizes a similar level of dilution tolerance and comparable thermal efficiency benefits to those achieved through the lean-burn strategy but with the use of EGR instead. Usage of EGR as the diluent instead of excess air ensures that well-established and inexpensive emission reduction technologies such as three-way-catalyst can still be utilized effectively.

In future work, higher engine loads with a lower effective compression ratio will be investigated to determine relative effectiveness of lean burn versus EGR dilution under a higher and broader speed-load range.

While dilution with either air or EGR has considerable benefits in terms of thermal efficiency it should be noted that high rate of dilution has significant impact on the brake torque capability of the engine or the engine power density. Moreover, high EGR boosted application poses additional challenges such as boost device sizing, EGR handling and availability, etc. While DM-TJI successfully solves the primary obstacle of igniting high EGR diluted mixture, further developmental works are necessary for complete assessment of its practical viability.

#### **CHAPTER 5**

# PERFORMANCE ASSESSMENT OF AIR/FUEL SCAVENGED DM-TJI SYSTEM AGAINST TJI AND SI AT EGR DILUTED CONDITIONS

#### 5.1 Abstract

Dual Mode, Turbulent Jet Ignition (DM-TJI) is an engine combustion technology that incorporates an auxiliary air supply apart from the auxiliary fuel injection inside the pre-chamber of a divided chamber ignition concept. Compared to other active (auxiliary fueled) and passive pre-chamber ignition technologies, the DM-TJI system has the distinct capability to operate with very high level of external EGR dilution (up to ~50%). Thus, unlike typical lean (excess air dilution) operated prechamber ignition technologies, the DM-TJI system enables the use of widely accepted, lower cost three-way-catalyst (TWC) while still running at high level of dilution (with EGR). The supplementary air supply to the pre-chamber enables effective purging and ignitable mixture formation inside the pre-chamber even with very high EGR dilution. The current work presents the results of experimental investigations conducted on a Prototype III Dual Mode, Turbulent Jet Ignition (DM-TJI) metal engine. Different pre-chamber scavenging/fueling strategies (active vs passive) are investigated in order to compare the EGR dilution tolerances between different scavenging configurations under the same pre-chamber design parameters (pre-chamber volume and nozzle configuration). The EGR dilution tolerance was investigated at two regularly encountered operating conditions (6 bar and 10 bar IMEPg at 1500 rpm) in typical drive cycles. The results are also compared with an open chamber SI design in the same engine to quantify the percentage difference in thermal efficiency with different scavenging configurations. The results indicate that to maintain very high EGR diluted (up to ~50%) operation the auxiliary air supply to the pre-chamber is of paramount importance. The analysis found that DM-TJI/Jetfire ignition system is more effective in terms of thermal efficiency at high-load, knock-limited situation due to its considerably higher external EGR dilution tolerance. Higher EGR rate offers better combustion phasing and improves thermal efficiency considerably. It was found that with the elevated 13.3:1 compression ratio and 10 bar load, SI could not maintain knock free stable operation; and DM-TJI/Jetfire delivered 7 to 9% improvement in thermal efficiency compared to TJI mode of operation with no air delivery to the pre-chamber.

### **5.2 Introduction**

To meet the future CO<sub>2</sub> neutrality targets the transportation sector must make a major contribution. To reduce the real-world CO<sub>2</sub> emissions, fast and dependable solutions with broader market acceptance are required. Instead of trying to reinvent the transportation sector based on the prediction of which powertrain technology will have what percentage of market share in future, a more sustainable approach will be to adapt the powertrain technologies to specific requirements demanded by the type of application. Underlined by the current and future high market share of the internal combustion engines in vehicles with either stand alone or hybridized application, it is still of utmost importance (and will continue to be so) that substantial efforts are rendered towards increasing the efficiency of combustion engines used in light duty vehicles. One of the downsides of using the IC engine as the standalone power source is the inherent efficiency drop due to a broad range of speed-load requirements to meet the driver's demands. With a limited operating range on the speed-load map and lower dynamic requirements (as provided by series or parallel hybridization), efficiency enhancement technologies such as higher compression, Miller cycle timing and higher EGR dilution can be applied to achieve even greater overall fuel efficiency benefits. While none of these concepts are new or not that they have not been implemented before, in conventional SI configuration it becomes increasingly difficult to apply such technologies beyond certain limits due to higher knock susceptibility and poor mixture ignitability. Pre-chamber

ignition with active air/fuel scavenging can serve as a key technology to extend the EGR dilution tolerance considerably and enable higher compression operation beyond the typical limits of conventional SI engines.

In conventional SI there is typically a spherical flame propagation from a central ignition location to the peripheral region. In pre-chamber ignition the mixture in consumed from the peripheral to the central region. Thus, the areas that are critical in terms of 'end gas autoignition' – such as the piston top land – are reached by the flame much earlier during the combustion event to prevent knocking. Together with the shorter burn duration, combustion phasing can be advance by several crank angle degrees (CAD). This essentially allows a higher compression ratio to be used compared to the conventional SI. This knock mitigation advantage is extended even further by 50-100% increase in EGR dilution tolerance to utilize even higher compression ratio.

Pre-chamber scavenging is critical to enhancing the lean operation limit for pre-chamber-based ignitions systems. This becomes even more important with EGR dilution because of the unavailability of excess air inside the pre-chamber. With lean operation the availability of excess air inside the main chamber ensures that during compression the pre-chamber is scavenged with a mixture where excess air is available. Thus, additional fuel injection inside the pre-chamber enables control of pre-chamber stoichiometry to be maintained within a combustible zone. Now, with EGR dilution this excess air is not available anymore; instead, pre-chamber is scavenged with a mixture of air, fuel and high percentage of recirculated exhaust gas. Combined with the existing residuals inside the pre-chamber, this EGR diluted mixture makes it difficult to form a combustible mixture inside the pre-chamber. And that is where the pre-chamber air delivery becomes beneficial. Additional air delivery to the pre-chamber not only ensures that the pre-chamber is purged properly to drive out any residuals; at the same time, it delivers enough air around the

vicinity of pre-chamber to help ensure that a higher percentage of fresh air is available inside the pre-chamber during the compression scavenging as well. Then, with additional fuel injection a combustible pre-chamber stoichiometry can be maintained even with very high EGR dilution rate.

The Dual Mode, Turbulent Jet Ignition (DM-TJI) system is an engine combustion technology in which the pre-chamber is equipped with an auxiliary air supply along with the auxiliary fuel injection [67–69]. In a DM-TJI system the additional air supply and its method of delivery to the pre-chamber are the main modifications from the technology's forerunner the Turbulent Jet Ignition (TJI) system [3,42–44,57,58]. The DM-TJI system provides enhanced control of stoichiometry inside the pre-chamber by adding supplementary air to the auxiliary fuel injection. This additional air supply to the pre-chamber solves two issues- first, it provides effective purging of the pre-chamber residuals and second, it helps maintain pre-chamber mixture ignitability even under high EGR dilution. This makes the DM-TJI system a unique pre-chamber combustion technology that offers stable operation at very high level of EGR dilution while still permitting the use of conventional TWC through stochiometric operation.

There have been several studies on DM-TJI systems. Atis et al. [67] showed that the Prototype II DM-TJI system equipped gasoline-fueled single-cylinder optical engine with a cooled EGR system could maintain stable operation (COV<sub>IMEP</sub><2%) with 40% external EGR at stochiometric ( $\lambda$ ~1) operating conditions. In that study, effect of pre-chamber air/fuel timing relative to EGR tolerance was investigated. Ultra-lean operation (up to  $\lambda$ ~2) was also demonstrated while a correlation between the nozzle orifice diameters and overall burn duration was suggested. Tolou et al. [68] developed a physics-based GT-POWER model of the Prototype II DM-TJI system and predicted the ancillary work requirement to operate the additional components of the DM-TJI system. Vedula et al. [69] reported the net indicated thermal efficiency of the Prototype I DM-TJI engine

for both lean and 30% nitrogen-diluted near-stochiometric operation. Vedula et al. [70] also studied the effect of pre-chamber fuel injection timing including pre-chamber air injection and different injection pressures on iso-octane/air combustion in a DM-TJI system equipped rapid compression machine for a global lambda of 3.0. Song et al. [71] worked on control oriented combustion and state-space models based on the prototype I DM-TJI engine. The study conducted by Atis et al. [67] on the Prototype II DM-TJI optical engine demonstrated that the DM-TJI system has the potential to offer very high EGR dilution tolerance but no investigation has been conducted so far on assessing how much of an efficiency benefit does DM-TJI/Jetfire system offer compared to other pre-chamber systems with active fuel scavenging only or no active scavenging (passive) at all. Since the pre-chamber scavenging during the compression stroke (and hence the EGR tolerance) depends heavily on pre-chamber design and nozzle configuration it is difficult to determine EGR tolerance with different scavenging schemes if the pre-chamber design details are not identical. To that end, the interchangeable Jetfire 'cartridge' design becomes very useful. The cam actuated air valve can be deactivated easily to operate the system in active fuel injection only mode or without any pre-chamber fuel injection. This enables comparison of different scavenging techniques with the same pre-chamber design and assessment of the effectiveness of additional air introduction to the pre-chamber. Additionally, the Jetfire cartridge was also replaced with a spark plug cartridge that did not contain any pre-chamber and gave the chance to test the same loadspeed condition with conventional SI configuration. The change in compression ratio due to the removal of the pre-chamber was addressed with addition of shims between the head and the bottom end of the engine. This enabled further assessment of the benefits provided by the DM-TJI/Jetfire system against a conventional SI combustion design within the same engine geometry. While several studies compared actively fueled [113] and passive [114] pre-chamber jet ignition systems

against conventional SI configuration at elevated compression ratio and stoichiometric conditions, there has not been any published study that investigates separate auxiliary air delivery to the prechamber that enables high EGR dilution tolerance. Typically, with pre-chamber ignition systems lean (excess air diluted) combustion has been the focus of research so far. The poor EGR dilution tolerance has always been one of the shortcomings of the pre-chamber ignition systems without any active purging. The only published studies that have shown to deal with high EGR dilution rate (up to 32%) with the pre-chamber utilized a specially developed injection system that injected a premixed air fuel mixture to the pre-chamber [115,116] and showed a comparison between the active and passive pre-chamber system with the conventional spark plug design. While the studies conducted by Sens et al.[115,116] clearly showed the potential of high rate of EGR dilution at elevated compression ratio in regard to the thermal efficiency benefits the actual experimental EGR rate was limited to a maximum of 32% as well as the scavenging scheme differed from the Jetfire system where the pre-chamber was purged with premixed air fuel mixture instead of separate pre-chamber fuel and air introduction.

## **5.3 Experimental Setup and Procedure**

Engine tests were performed on a single-cylinder Prototype III DM-TJI metal engine equipped with interchangeable Jetfire 'cartridge'. Most features of the experimental setup have been described in Chapter 4. The experimental setup and the methodology had two major exceptions from the discussion provided in Section 4.3. As demonstrated in figure 5.1, the boost-cart in the upper left-hand corner of the test bench schematic was deactivated in the study reported in the previous chapter; for the current study, the boost-cart was utilized to provide enough boost and dilution at 7 bar and higher IMEPs. For tests at higher rpm and loads of 16 to 21 bar IMEPg, a larger second-stage supercharger (EATON TVS R900) was added to ensure that enough boost and

EGR rate could be maintained. A photograph of the actual engine test bench at the Michigan State University Energy and Automotive Research Lab is shown in figure 5.2, depicting the single-cylinder engine equipped with all test cell instrumentation.

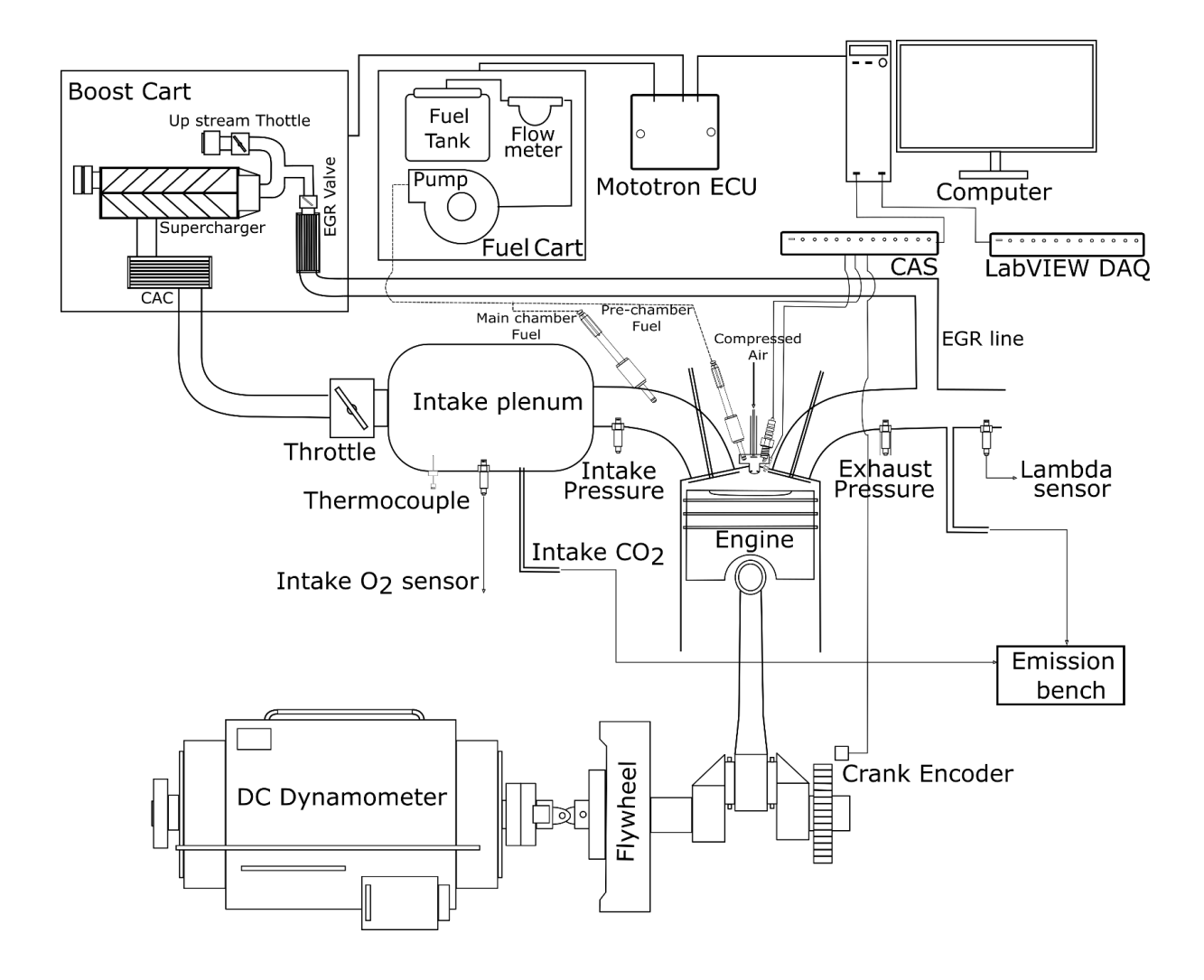


Figure 5.1 Schematic of the experimental test bench (boost-cart active)

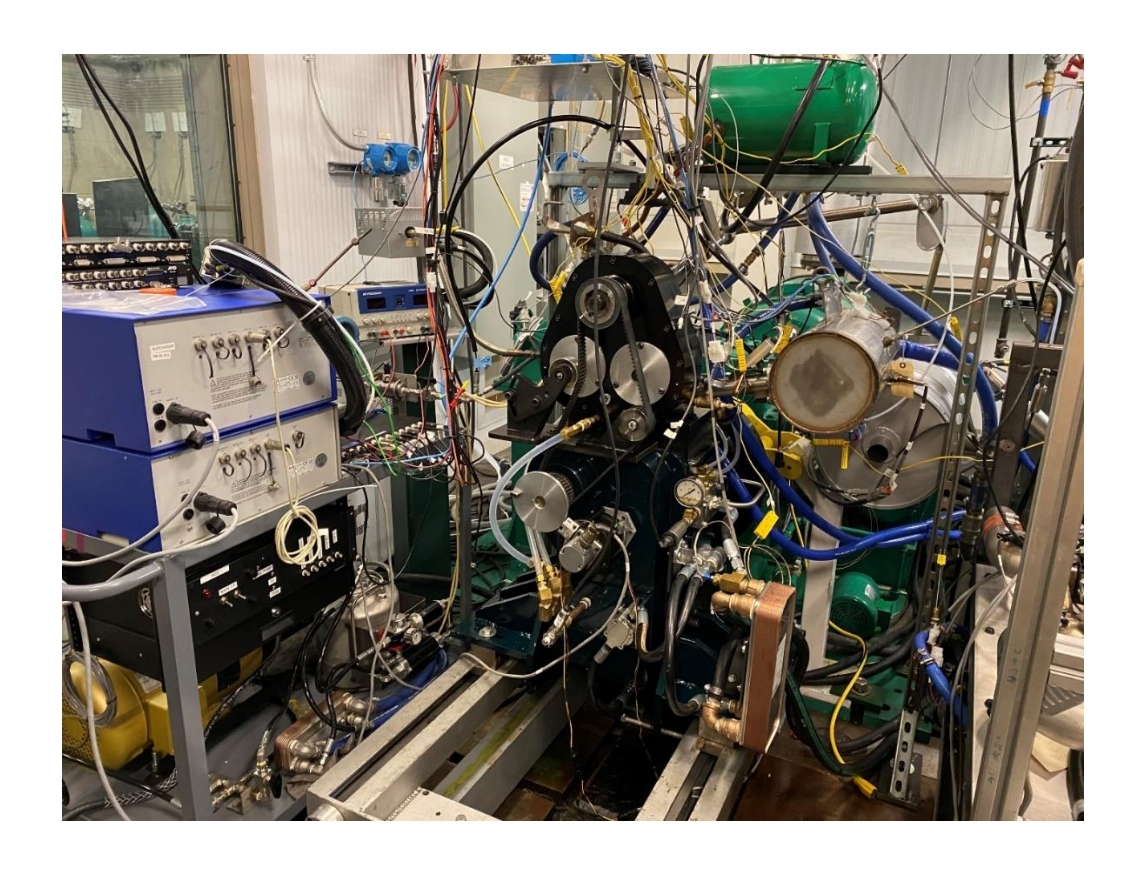


Figure 5.2 Prototype III DM-TJI engine at MSU EARL test cell



Figure 5.3 Jetfire cartridge design details



Figure 5.4 Interchangeable Jetfire cartridges

Another major change in the engine for the current study was the modification of the Jetfire cartridge design to test different ignition and pre-chamber scavenging schemes. To operate the pre-chamber in 'fuel injection mode only' or the 'TJI active' mode, the pre-chamber air valve was deactivated by removing the rocker arm and plugging off the lifter (shown in figure 5.3). This deactivated the pre-chamber air valve and the air supply to to pre-chamber. Also, a cartridge block without any pre-chamber cavity and with only a spark plug was built so that conventional spark ignition (SI) configuration could be tested on the same engine. Figure 5.4 shows the Jetfire cartridge with air valve, spark plug and the pre-chamber fuel injector inserted as well as the spark plug cartridge with only a 8 mm spark plug protruding from the cartridge instead of the pre-chamber nozzle. The change in compression ratio due to the removal of pre-chamber volume was adjusted using metal shims between the head and the bottom end of the engine. The tests were carried out with the Jetfire cartridge first. Then the air valve was deactivated to test the TJI active and passive mode. Finally, the Jetfire cartridge was replaced with the spark plug cartridge to test the same operating conditions with SI.

Since the current study does not required comparison between  $\lambda$  and EGR rate, the volumetric

EGR rate has not been converted to mass basis. Thus, in the current chapter, the EGR rate reported in subsequent sections are all based on 'wet' and 'volume' basis. The EGR rate calculation procedure has been reported in detail in section 4.3 of the previous chapter.

#### **5.4 Results and Discussion**

Maximum EGR tolerance limit for each configuration was identified based on two criteria-combustion stability limit set as 3% COV of IMEP and a knock limit set as more than 10% cycle crossing a 1.0 bar POD (Pressure Oscillation Difference). An operating condition was deemed to be a stable knock free operating point if it satisfied both the combustion stability and knock limit criteria.

## 5.4.1 Jetfire: 6 bar IMEPg at 1500 rpm, different pre-chamber air pressure

This part of results and discussion sections deals with identifying the maximum EGR dilution tolerance of the Jetfire system at 1500 rpm 6 bar. At 6 bar IMEPg load three levels (15, 30 and 45 psig) of pre-chamber supply air pressure were investigated. Figure 5.5, 5.6 and 5.7 show the gross indicated efficiency and COV of IMEP plotted against CA50 with different EGR amounts (ranging from 0% to about 42-43%) for pre-chamber air upstream pressure of 45, 30 and 15 psig, respectively. These figures also include the vertical dotted 'knock limit' lines in the top gross indicated efficiency plots to identify the operating point beyond which the aforementioned knock limit is exceeded. From figure 5.5 it is clear that with 45 psig air pressure the Jetfire system was able to maintain stable operation (with <3% COV<sub>IMEP</sub>) for up to 43% (v/v) external EGR. It is also observed that indicated efficiency increases with the addition of more EGR dilution until the COV<sub>IMEP</sub> limit is reached. This observation is more apparent in figure 5.6 and 5.7 where the highest EGR amount tested did not translate into the highest indicated efficiency due to increase in combustion variability and subsequent loss in combustion efficiency. Thus, addition of EGR helps

in increasing the efficiency until the combustion stability limit is reached. In this study, this EGR tolerance limit has been identified as the highest amount of EGR that could still maintain COV of IMEP limit of less than 3%.

With addition of EGR the combustion temperature drops which reduces both the heat transfer and exhaust heat loss and results in higher efficiency. Addition of EGR also reduces knocking tendency and the resulting knock-limited CA50 moves closer toward the MBT timing yielding even further increase in efficiency. In fact, with the elevated 13.3:1 compression ratio it was found that beyond 35% EGR rate the operation is not knock limited at all.

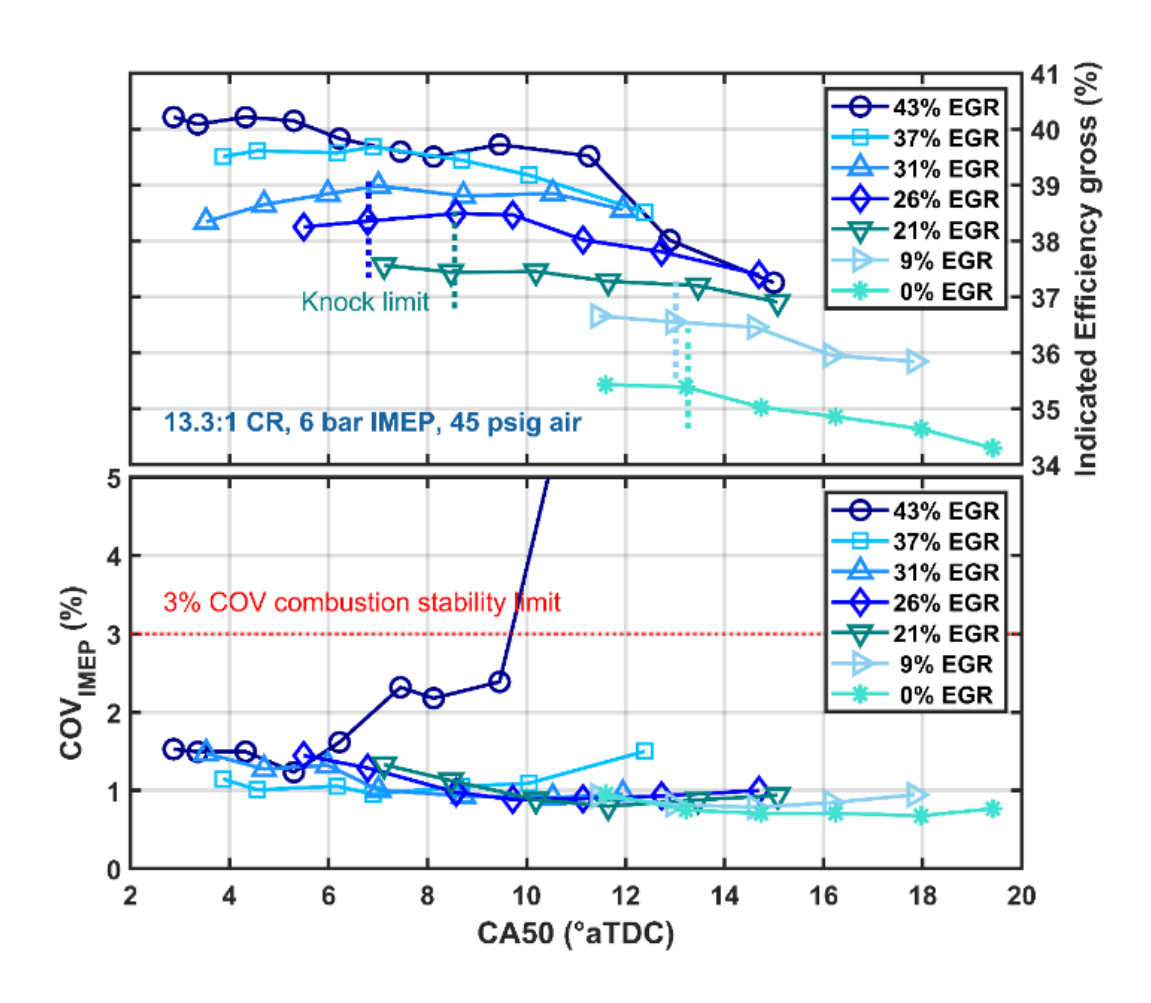


Figure 5.5 Gross indicated efficiency and COV of IMEP versus CA50 with different EGR rate at 1500 rpm and 6 bar IMEPg obtained with 45 psig pre-chamber air pressure Jetfire configuration

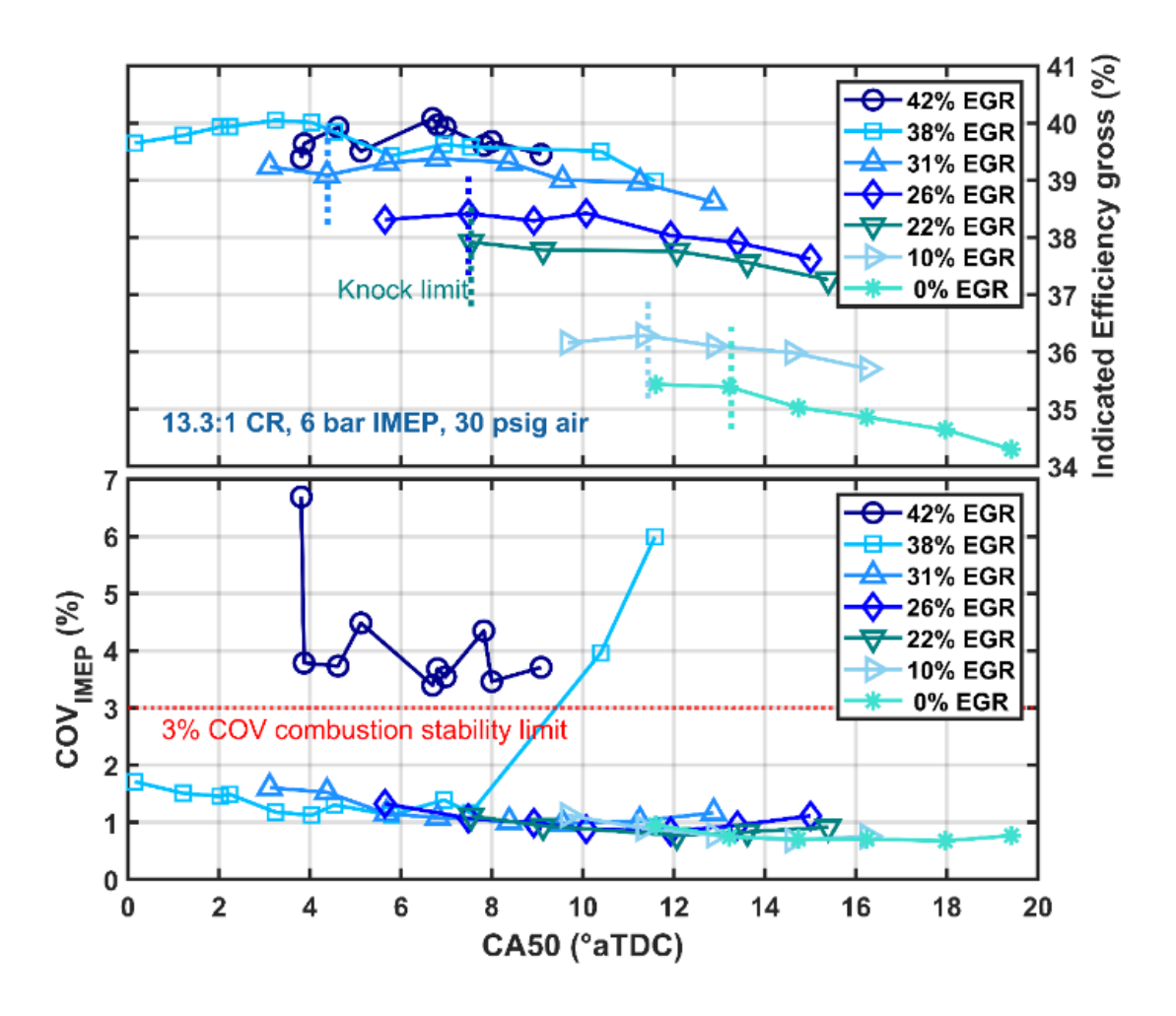


Figure 5.6 Gross indicated efficiency and COV of IMEP versus CA50 with different EGR rate at 1500 rpm and 6 bar IMEPg obtained with 30 psig pre-chamber air pressure Jetfire configuration

Figure 5.6 shows that with 30 psig pre-chamber air pressure, 42% EGR rate results in COV<sub>IMEP</sub> of more than 3% but when the EGR was decreased to 38% the COV<sub>IMEP</sub> improved. Since only discrete EGR rates with about 5% step size were used, the maximum EGR tolerance for the 30 psig air pressure is identified as 38%. It is difficult to conclude that this configuration would not work for 40% EGR rate without testing. Possibly a 1% increment at these limiting EGR values would better serve as the absolute EGR tolerance limit at corresponding EGR level. To avoid an overly large test matrix, a larger 5% step size was chosen. In fact, in figure 5.7 results it is shown that with 15

psig air pressure the highest gross indicated efficiency was obtained with an EGR rate 2% lower than the tolerance limit. As seen in the top graph of figure 5.7, with 38% EGR the COV<sub>IMEP</sub> goes beyond the 3% combustion stability limit and the efficiencies are comparable with 32% EGR values. This is due to the increase in combustion variability and a resulting decrease in combustion stability at the limiting cases. Similar trends are discussed in later part of this article. However, when the EGR was decreased to 36% COV<sub>IMEP</sub> went down within the 3% range and about 1 percentage point improvement was seen in gross indicated efficiency.

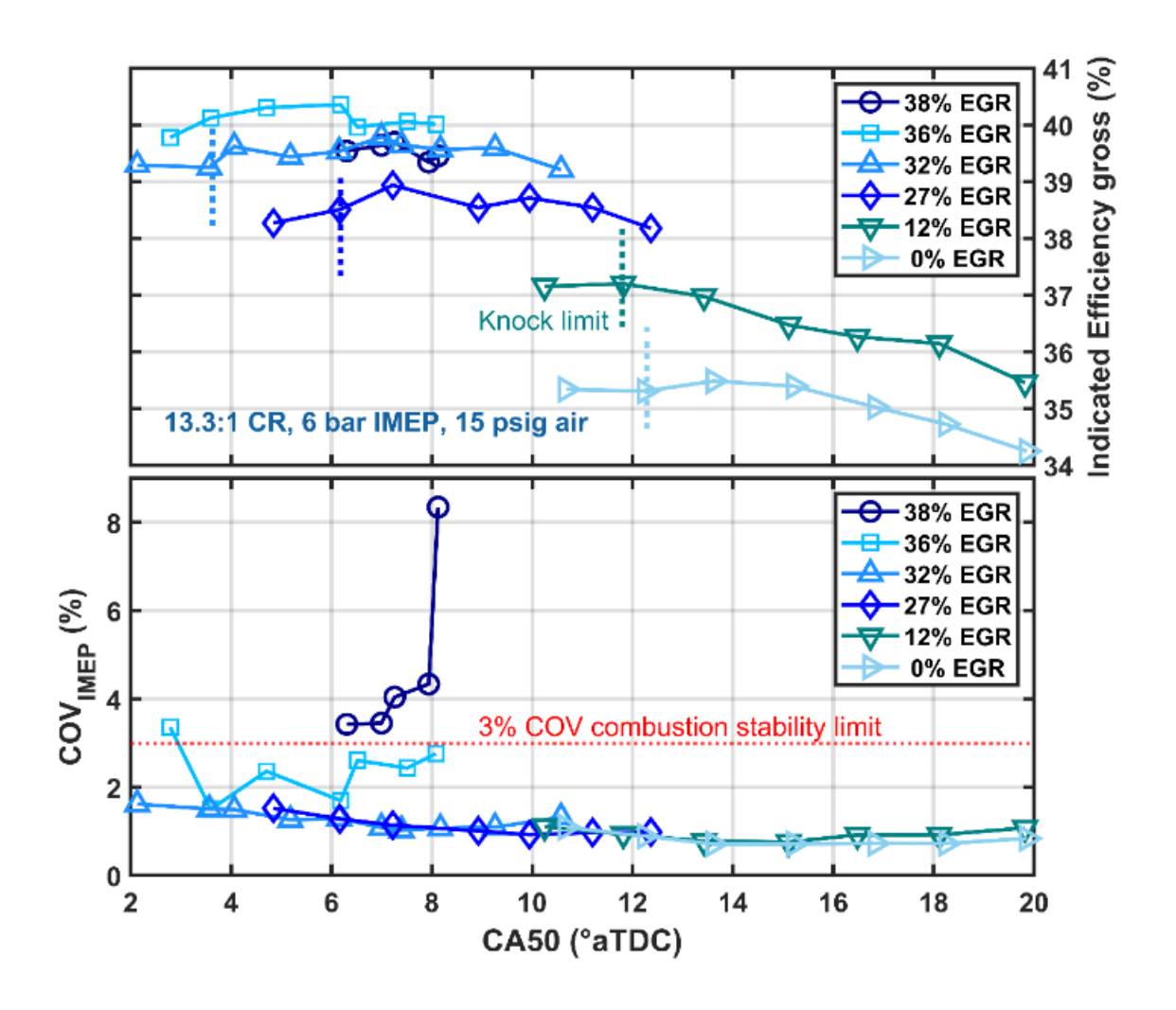


Figure 5.7 Gross indicated efficiency and COV of IMEP versus CA50 with different EGR rate at 1500 rpm and 6 bar IMEPg obtained with 15 psig pre-chamber air pressure Jetfire configuration

An interesting observation from figure 5.5, 5.6 and 5.7 is that while at 15 psig air pressure the maximum EGR tolerance was lower than both 30 psig and 45 psig cases, under similar EGR dilution level the 15 psig case consistently showed marginally better gross indicated efficiency than the rest. Though the maximum EGR tolerance was the lowest for the 15 psig case, it actually demonstrated the highest gross indicated efficiency at the maximum dilution limit. This suggests that the air flowing through the pre-chamber and nozzle during the pre-chamber purging might contribute to cooling down the pre-chamber cartridge and cause even more heat loss in addition to the heat loss incurred by the increased surface area of the pre-chamber. The higher the air flow rate is (proportional to the air pressure), the higher the heat loss will be, leading to lower indicated efficiency. Pre-chamber air flow rates for different air pressures are given in figure 5.8.

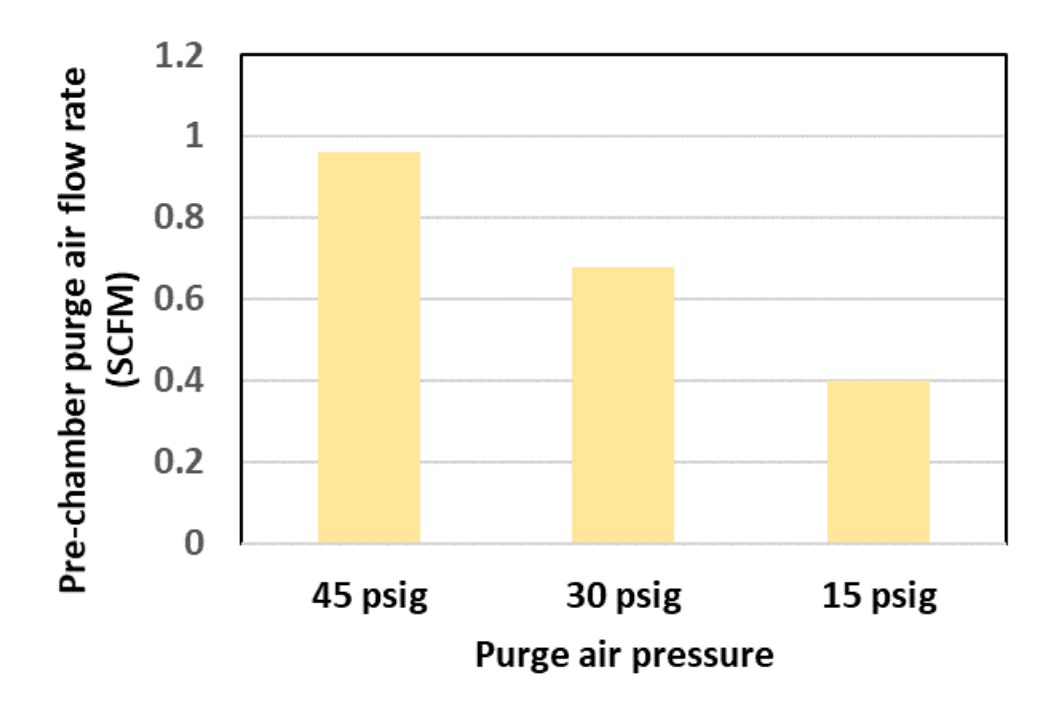


Figure 5.8 Pre-chamber air flow rate measured by LFE for different compressed air pressures at 1500 rpm and 6 bar IMEPg

Another possible explanation could be that with the 15 psig case 17% smaller fuel injection pulse width was used in the pre-chamber compared to 30 psig and 45 psig cases. Excess pre-chamber

fueling reduces thermal efficiency [117]. Thus, with more fuel being injected with the 30 psig and 45 psig cases, the thermal efficiency might have suffered because it was more than what was needed to maintain required stoichiometry and the extra fuel adds to the losses. Lesser fuel being injected should have lesser cooling effect as well. In fact, a first law loss analysis for the 30% EGR case under similar CA50 (~7 °aTDC) with different pre-chamber air valve pressure shows that the 15 psig case does indeed have lower heat loss compared to the 45 and 30 psig cases. Figure 5.9 shows the split of losses for different pre-chamber purge air pressures under identical EGR rate and combustion phasing.

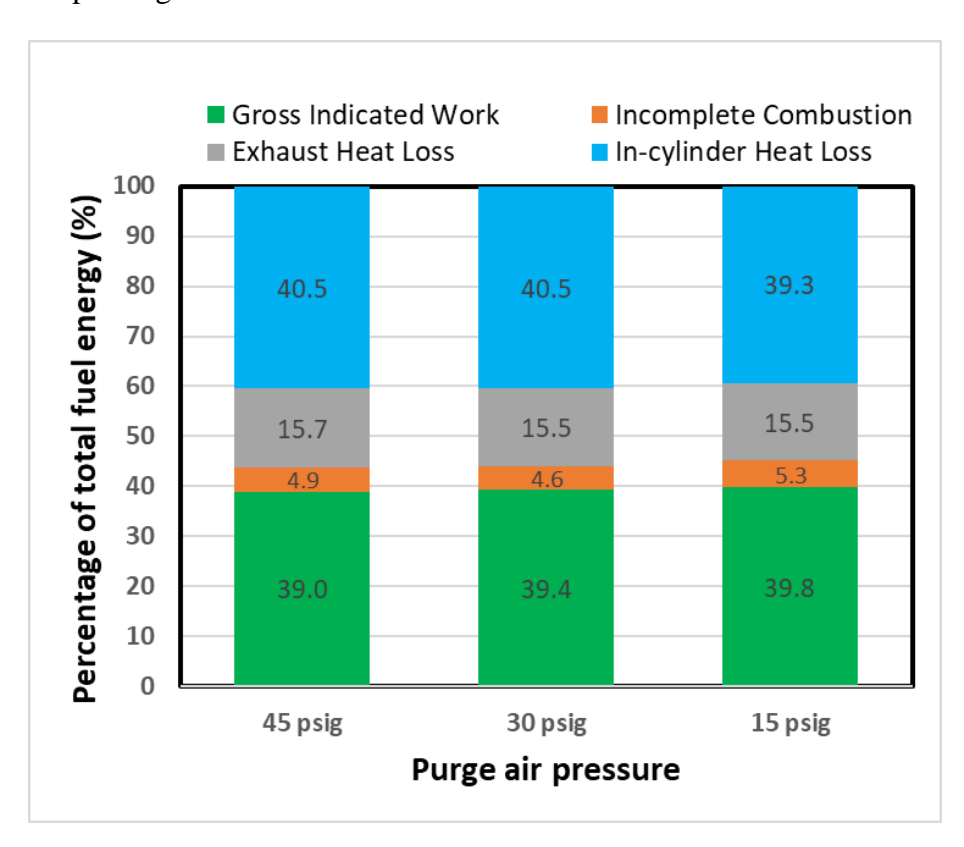


Figure 5.9 Split of losses with different purge air pressure for the Jetfire system operating at 30% EGR rate at 1500 rpm 6 bar IMEPg for CA50 of 7  $^{\circ}$ aTDC

Thus, at 1500 rpm 6 bar IMEPg load higher pre-chamber pressure resulted in higher external EGR tolerance but the highest gross indicated efficiency was found at the lowest 15 psig air pressure

setting. The slightly higher maximum EGR tolerance enabled by higher pre-chamber air flow cannot offset the heat loss and purge work disadvantage caused by the increased air and possibly fuel flow. This is especially true for load conditions that are not limited by knock. Without being knock limited, slightly better maximum EGR tolerance does not contribute much in terms of gross indicated thermal efficiency. A comparison of the net efficiency between the different air pressure settings is given in a later section.

## 5.4.2 TJI passive: 6 bar IMEPg at 1500 rpm

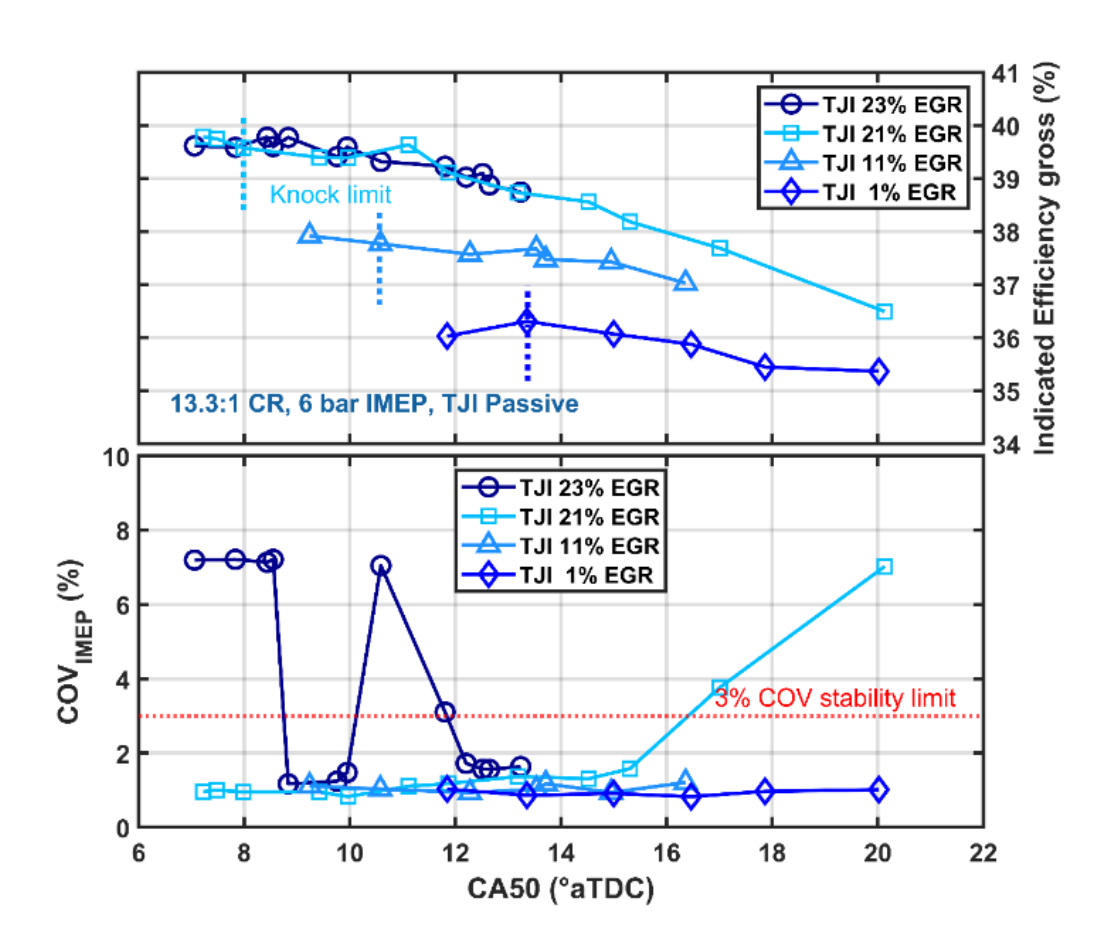


Figure 5.10 Gross indicated efficiency and COV of IMEP versus CA50 with different EGR rate at 1500 rpm and 6 bar IMEPg obtained with TJI passive configuration

Figure 5.10 shows the gross indicated efficiency and COV of IMEP at a CA50 sweep with

increasing EGR rate for TJI passive system i.e., TJI with no pre-chamber fuel injection. Up to 25% EGR rate was tried with this configuration but the combustion variability was too high to include those results in this figure. As evident from figure 5.10, even at 23% EGR, the passive TJI configuration had difficulties maintaining the 3% COV<sub>IMEP</sub> stability limit. A similar trend with knock limited CA50 moving towards MBT timing with addition of higher EGR rate was observed here as well.

## 5.4.3 TJI active: 6 bar IMEPg at 1500 rpm

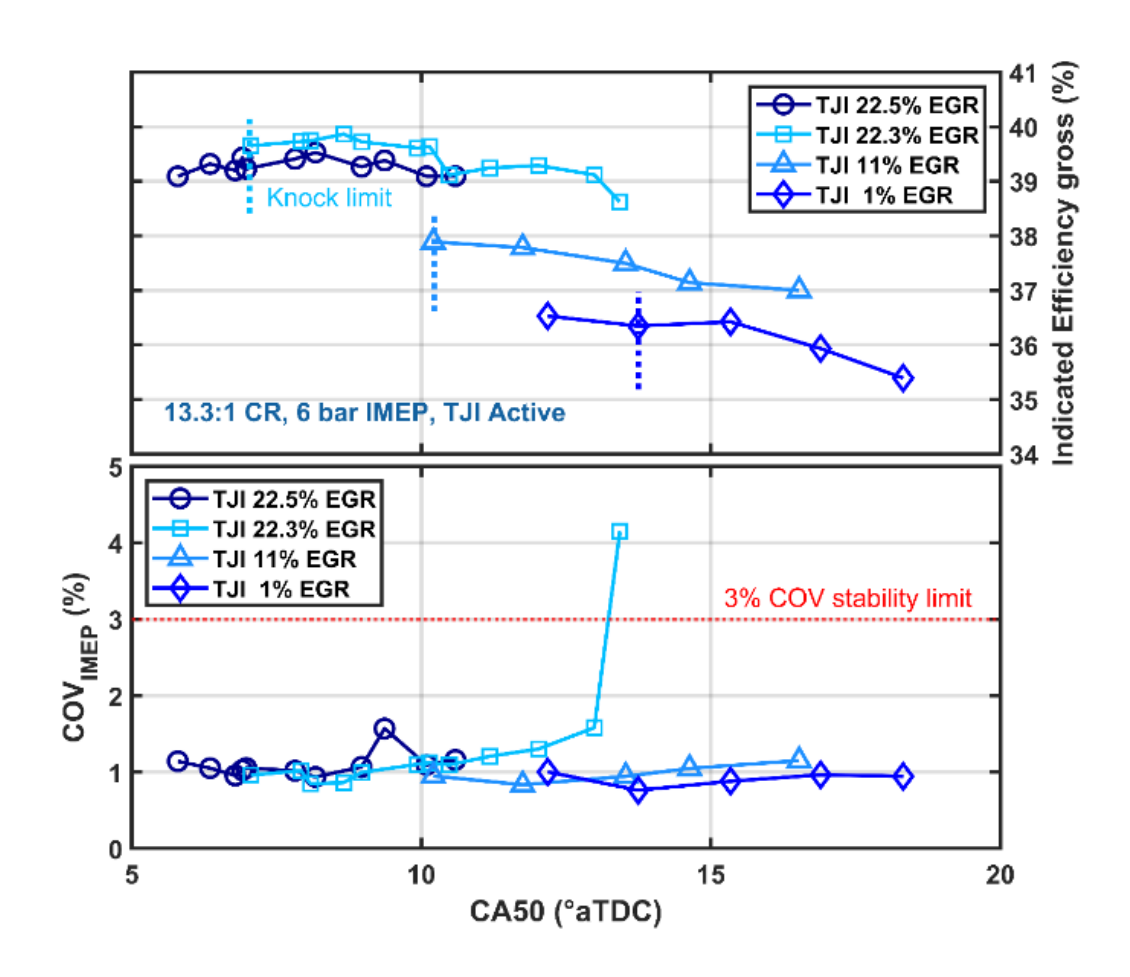


Figure 5.11 Gross indicated efficiency and COV of IMEP versus CA50 with different EGR rate at 1500 rpm and 6 bar IMEPg obtained with TJI active configuration

Gross indicated efficiency and COV of IMEP with increasing EGR dilution rates are plotted in

figure 5.11 for active TJI configuration i.e., TJI with additional fuel injection inside the prechamber. At 22.5% EGR rate the combustion stability was better with active TJI compared to passive configuration but when the EGR rate was increased to 25% combustion variability again increased too much ( $COV_{IMEP}$  around 15-20%) to be included within the same set of graphs. Similar to the passive TJI an EGR tolerance limit of up 23% was observed with active TJI configuration at 1500 rpm 6 bar load. Thus, TJI with additional fuel injection inside the prechamber did not help much on extending the EGR dilution tolerance limit. Accordingly, the gross indicated efficiency found for the two TJI configurations were comparable to each other and one did not show any particular advantage over the other. The absolute value of the gross indicated efficiency was 0.6 to 0.9 percentage point lower than the previously shown Jetfire results at 6 bar IMEPg.

## **5.4.4** SI: 6 bar IMEPg at 1500 rpm

Figure 5.12 shows the gross indicated efficiency and COV of IMEP with increasing EGR rate for the conventional SI configuration without any pre-chamber. Beyond 24% EGR rate the combustion stability went beyond the value of 8% and was not included in figure 5.12. Even at 23 to 24% EGR rate it was difficult to achieve the 3% COV combustion stability limit without being knock limited. At 20% EGR rate several points were found to have acceptable combustion stability without reaching the knock limit. One other general observation was that with SI the combustion stability, even at lower EGR rate, was not as good as the Jetfire or TJI cases. They were still within the acceptable limit but both Jetfire and TJI showed better combustion stability under similar level of EGR dilution.

However, SI configuration showed a clear advantage on gross indicated thermal efficiency over

the pre-chamber configurations. Without any EGR, SI demonstrated a gross indicated efficiency of about 38.6% (more than 2 percentage points higher than the nearest pre-chamber values with no EGR). At the EGR tolerance limit SI showed a maximum of 40.7% gross indicated efficiency which is 0.3 percentage point better than the best Jetfire efficiency case with more than 50% more EGR tolerance limit. This advantage for SI in terms of gross thermal efficiency resulted from the lack of additional heat loss due to the pre-chamber configurations. Pre-chamber systems with their increased surface area for the combustion chamber incorporate an inherent increase in heat loss that decreases the thermal efficiency compared to a conventional SI system.

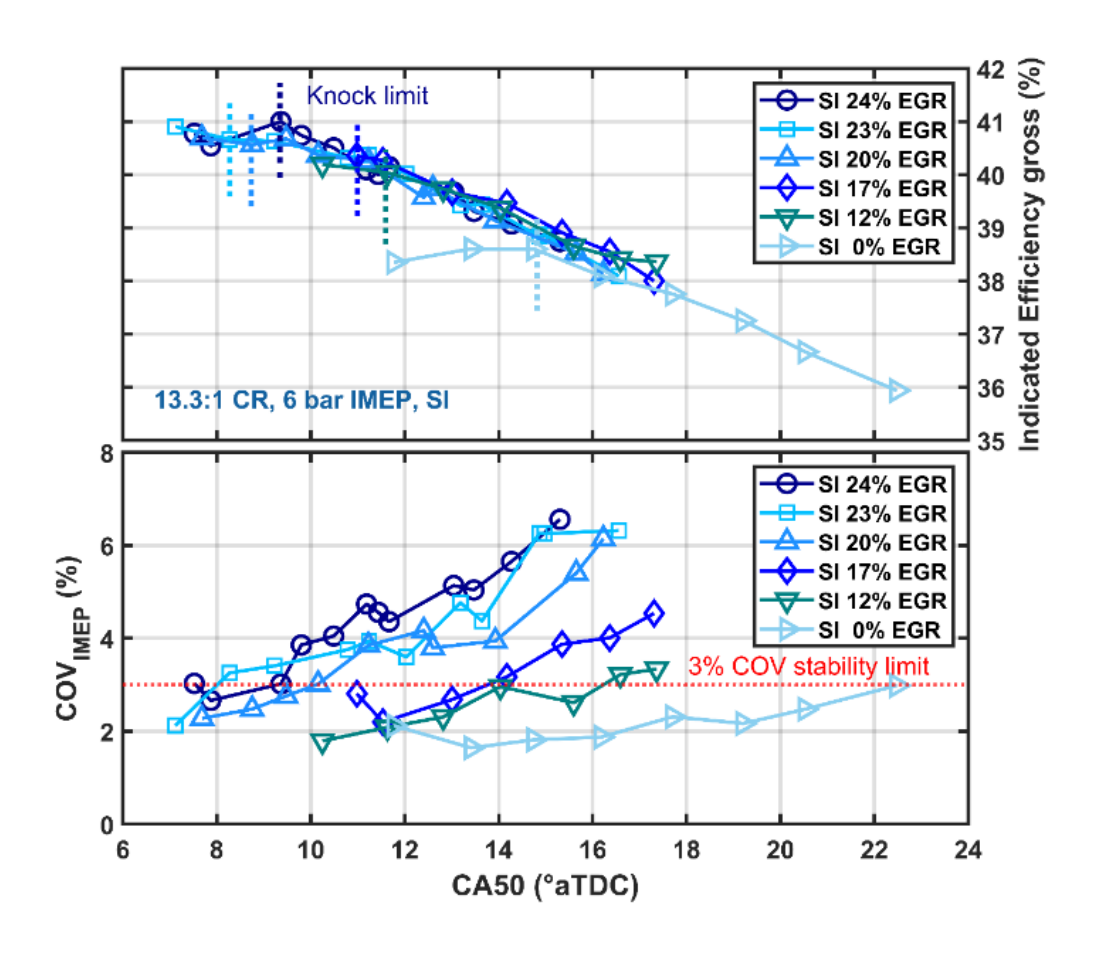


Figure 5.12 Gross indicated efficiency and COV of IMEP versus CA50 with different EGR rate at 1500 rpm and 6 bar IMEPg obtained with SI configuration

5.4.5 Comparison: Jetfire vs TJI active vs TJI passive vs SI at 6 bar IMEPg 1500 rpm

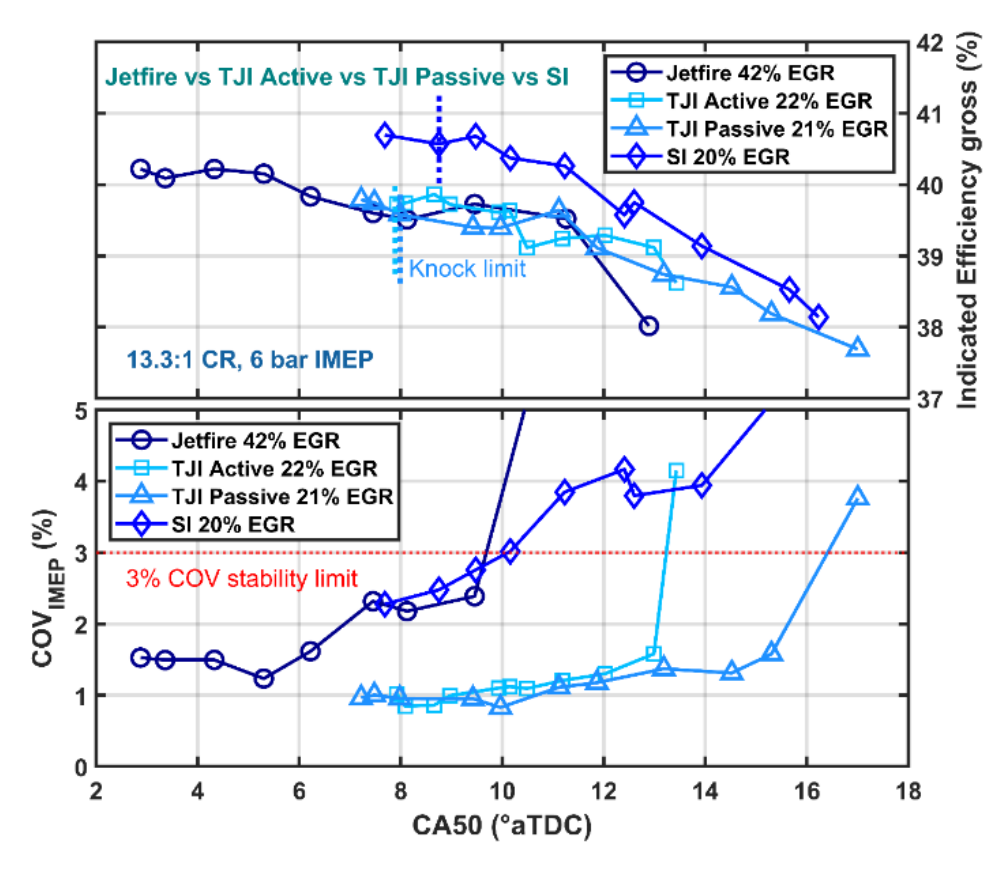


Figure 5.13 Comparison of gross indicated efficiency and COV of IMEP versus CA50 at 1500 rpm and 6 bar IMEPg with highest EGR rate between Jetfire, TJI active, TJI passive and SI

Figure 5.13 compares the gross indicated efficiency and COV of IMEP found with the highest stable EGR diluted limit for Jetfire, TJI active, TJI passive and SI configuration. Jetfire with 45 psig pre-chamber air pressure was selected for this comparison instead of the 15 psig case to demonstrate the maximum stable EGR tolerance limit for the Jetfire even though it was found that the lower pre-chamber pressure/flow rate would lead to slightly better efficiency. The advantage of SI over the pre-chamber configurations is clear from figure 5.13. This advantage in gross thermal efficiency of SI system mainly results from a reduced heat loss for the conventional SI compared to pre-chamber configurations. Among the pre-chamber cases Jetfire still showed an advantage over the TJI cases. In case of Jetfire though there is an additional work required for the

supply of pre-chamber purge air which decreases the net indicated work. As well as enabling decrease in heat transfer loss and substantial knock relief by lowering the combustion temperature, higher EGR tolerance limit helps with the de-throttling and lowers the pumping loss as well. Thus, higher EGR rate helps improve the net indicated efficiency considerably.

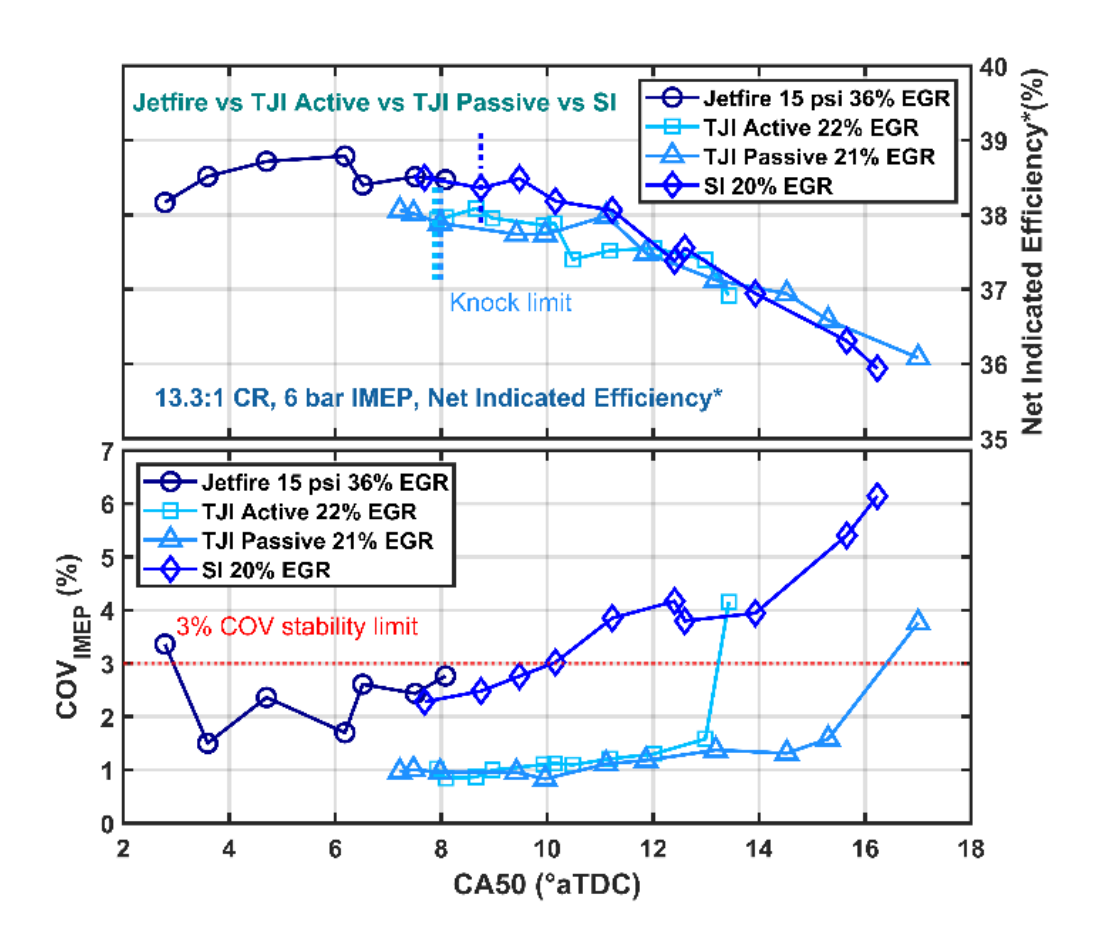


Figure 5.14 Comparison of net indicated efficiency and COV of IMEP versus CA50 at 1500 rpm and 6 bar IMEPg with highest stable EGR rate between Jetfire, TJI active, TJI passive and SI; Jetfire includes the work loss due to purge air supply

Figure 5.14 plots the net indicated efficiency and COV of IMEP between the best efficiency cases obtained with Jetfire, TJI active, TJI passive and SI at 6 bar IMEPg and 1500 rpm. It should be noted that the net indicated efficiency shown with the Jetfire includes the work loss due to supply of the compressed purge air to the pre-chamber. It is clear from figure 5.14 that Jetfire provides

the highest net indicated thermal efficiency compared to TJI configurations as well as the SI configuration. Thus, at load conditions where knocking is not a major constraint Jetfire can still be very effective in lowering the pumping loss and offset the increased heat loss disadvantage of prechamber combustion systems. Additionally, the higher EGR rate lowers the main chamber combustion temperature as well and reduces heat loss.

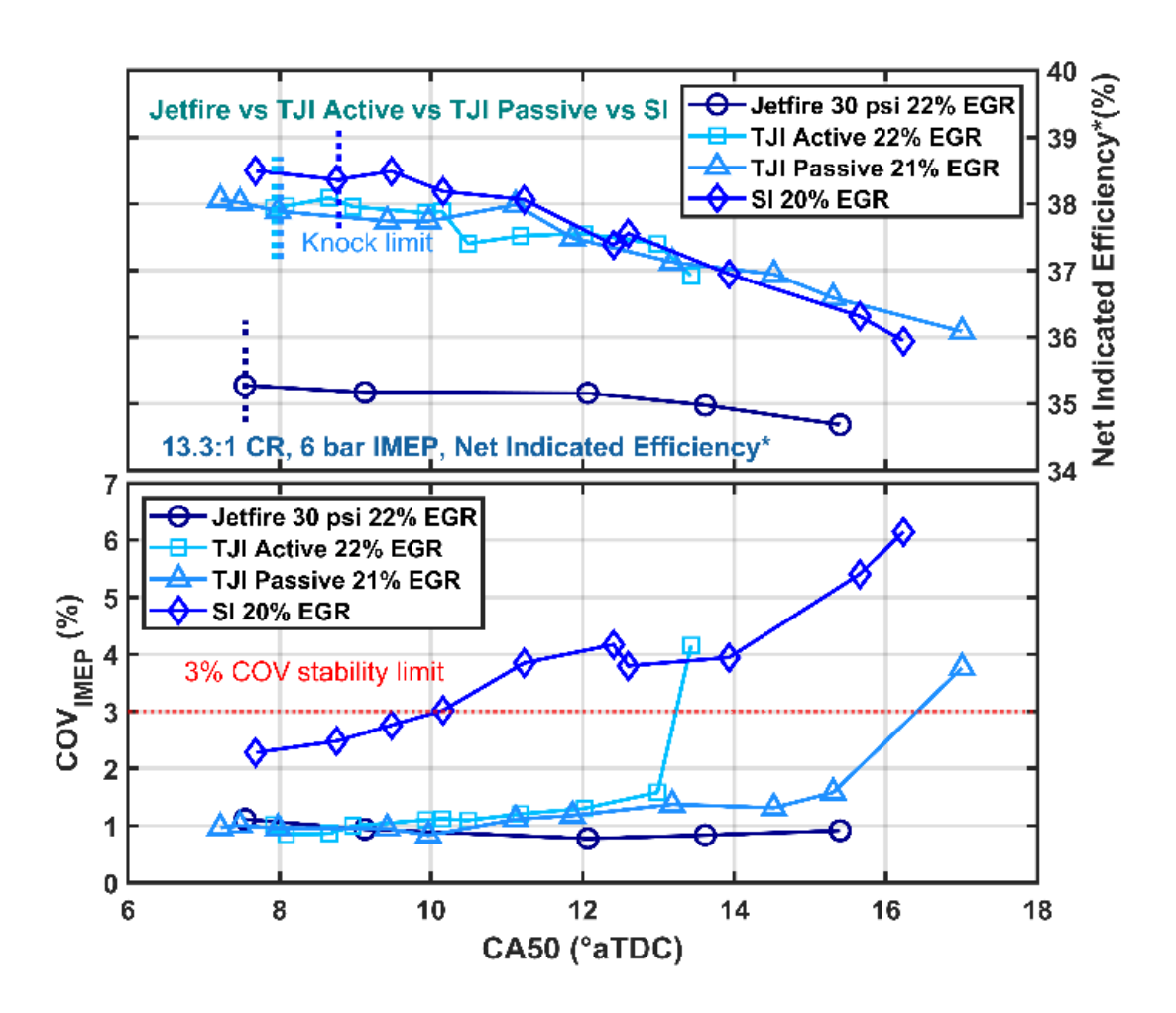


Figure 5.15 Comparison of net indicated efficiency and COV of IMEP versus CA50 at 1500 rpm and 6 bar IMEPg at approximately 20-22% EGR rate between Jetfire, TJI active, TJI passive and SI; Jetfire includes the work loss due to purge air supply

As it was shown in figure 5.14, at 6 bar IMEPg and 1500 rpm, Jetfire ignition delivered comparable net indicated thermal efficiency to the SI and TJI cases while operating with almost twice as much

EGR dilution compared to the others. Thus, at low load situations, Jetfire requires considerably higher dilution in order to achieve parity with the other pre-chamber configurations. The results shown in figure 5.15 confirm this. In figure 5.15, results obtained for net indicated thermal efficiency and COV of IMEP at 6 bar IMEPg and 1500 rpm have been compared between Jetfire 30 psi, TJI active, TJI passive and SI; all operating with approximately 20-22% EGR rate. It is seen that at a similar EGR rate Jetfire offers substantially lower (about 2.8-3 percentage point) net indicated thermal efficiency compared to TJI or SI. The additional work loss due to purge work supply as well as additional heat loss from the pre-chamber due to purge air flow lowers the indicated work. Since all of the configurations were operated with similar EGR rate, Jetfire did not get additional benefits of lowering the main chamber heat loss or the pumping work. This comparison was shown to demonstrate the additional heat loss aspect of the Jetfire system due to the purge air delivery and should not be treated as a way of determining which ignition system offered the best thermal efficiency. In figure 5.15, the Jetfire with half the tolerance limit was compared with the TJI and SI systems with their maximum tolerance limit, hence the lower efficiency shown by Jetfire. Jetfire system can actually maintain stable combustion with almost twice as much dilution compared to TJI or SI systems at 6 bar load. Figure 5.14 showed that at maximum EGR tolerance limits, Jetfire provided the best results in terms of net indicated thermal efficiency.

Figure 5.16 gives a first law energy breakdown of the work and loss terms between the ignition systems already compared in figure 5.15, as a verification to confirm that it is indeed the increased heat loss that contributed to the lower net indicated efficiency from Jetfire at around 20% EGR compared to other systems. Since Jetfire can operate with almost twice as much dilution, it offsets this disadvantage and delivers the best results among the tested ignition schemes.

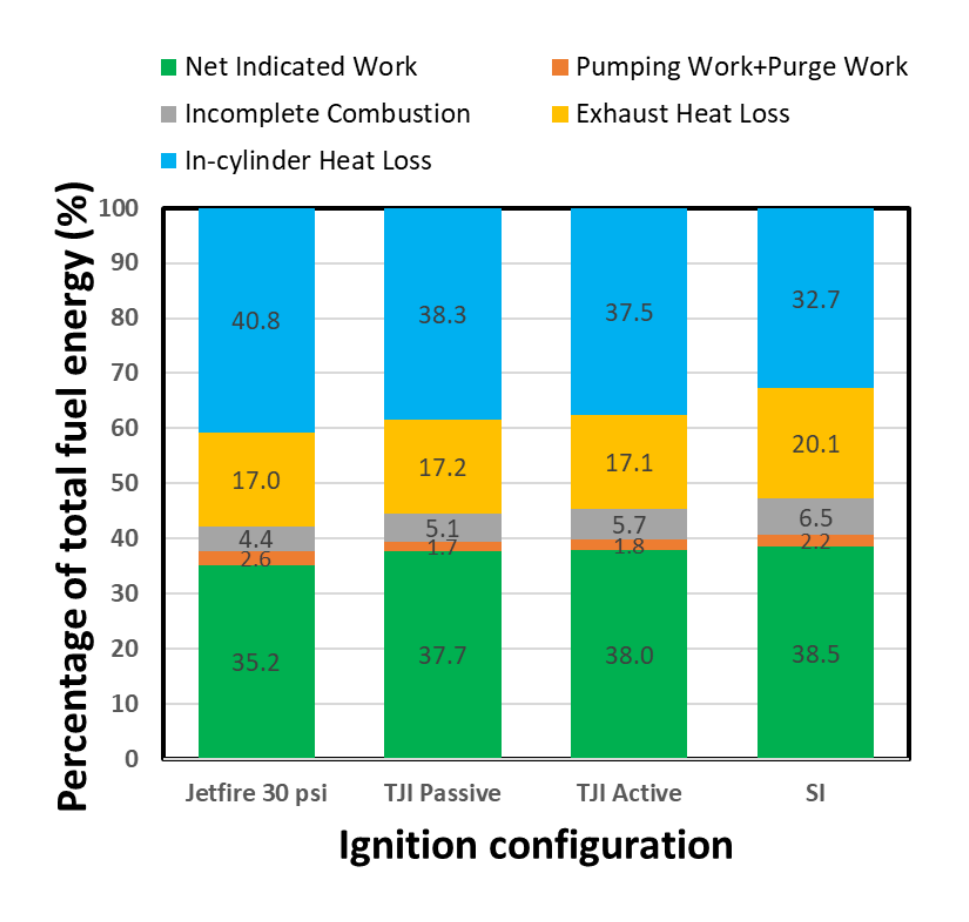


Figure 5.16 Comparison of split of losses between Jetfire, TJI passive, TJI active and SI operating at 1500 rpm and 6 bar IMEPg, at their maximum individual thermal efficiency points

Figure 5.17 compares the gross indicated efficiency, combustion efficiency, manifold absolute pressure and finally, the net indicated efficiency between the Jetfire cases with different prechamber air pressures along with the two TJI and SI configurations at varying EGR rates. Figure 5.17(a) displays gross indicated efficiency against varying EGR rates. It is clear that for all the cases the indicated efficiency increases with increasing dilution level. With increased dilution the combustion temperature decreases, which results in decreased in-cylinder heat loss and exhaust heat loss. These, along with lower pumping loss at higher EGR, increase the indicated work considerably. Figure 5.18 shows a first law energy break up of different losses for the Jetfire 15 psi case at increasing dilution level and confirms the above explanations.

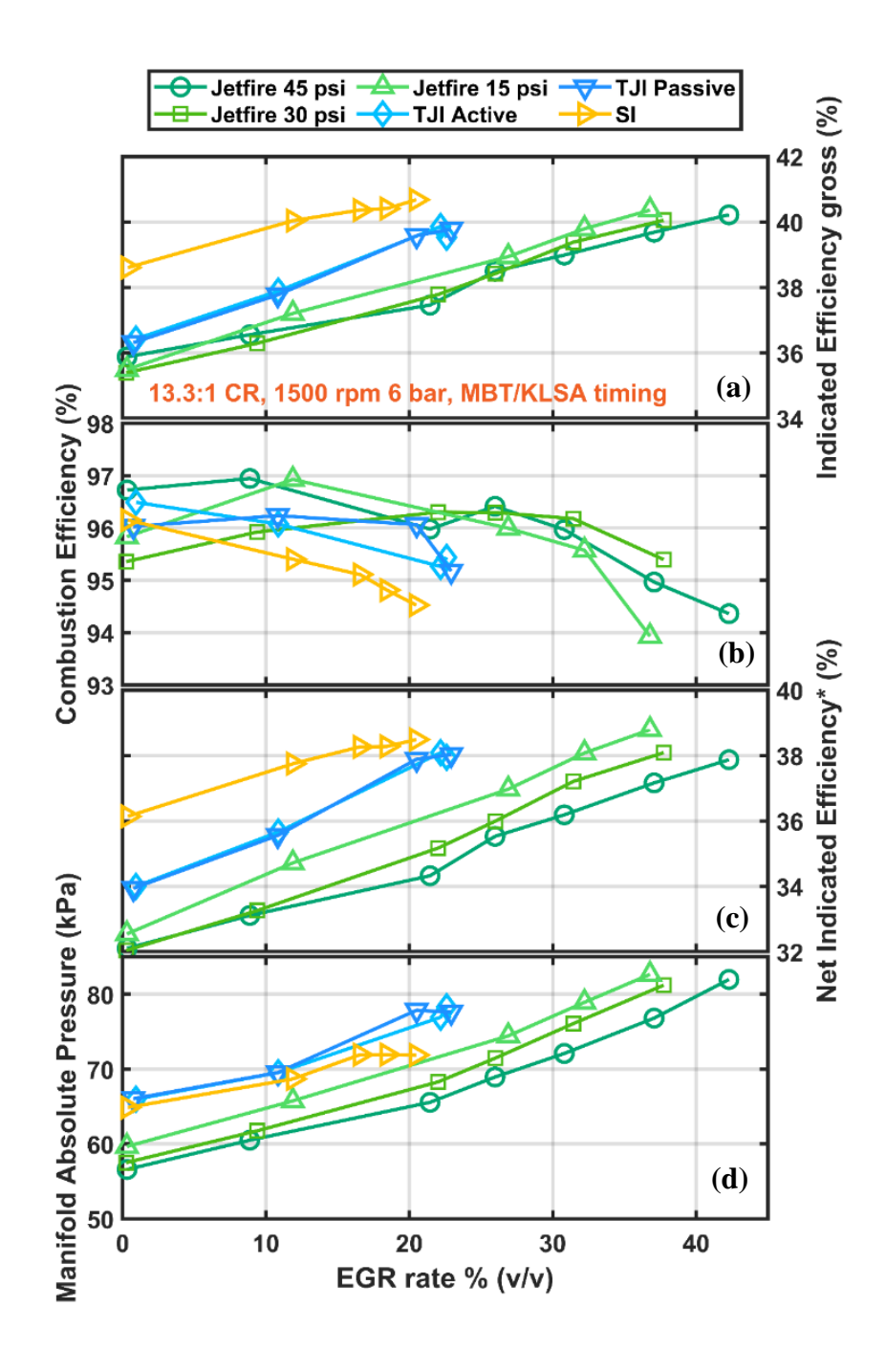


Figure 5.17 Gross indicated efficiency, combustion efficiency, net indicated efficiency\* and manifold absolute pressure at 1500 rpm and 6 bar IMEPg condition with varying EGR rate for Jetfire, TJI active, TJI passive and SI. The net indicated efficiency for Jetfire subtracts the work required to deliver the pre-chamber purge air (referred using an asterisk)

Figure 5.17(a) also shows a clear advantage of the SI configuration compared to the pre-chamber

cases. Even at more than twice the EGR rate Jetfire with 45 psig air pressure showed slightly lower gross indicated efficiency than the SI. Both the TJI active and passive configuration showed a similar level of EGR tolerance and comparable gross indicated efficiency figures. Jetfire with 15 psig showed the best gross indicated efficiency even though the maximum EGR tolerance was almost 7 percerntage points lower than the 45 psig air pressure case. Another interesting observation was that under identical EGR dilution rate (up to 21-22%) SI performed the best followed by the two TJI cases and the three Jetfire cases consistentlylagged behind the TJI cases. This could be due to the additional heat loss resulting from the pre-chamber air purge or the considerably higher pre-chamber fuel injection (up to 4.5% of the total fuel) used with the Jetfire cases.

Figure 5.17(b) shows the calculated combustion efficiency from the logged emission measurements with the different combustion systems at varying EGR rate. It is clear that the Jetfire cases could maintain comparable combustion efficiency with almost twice as much external EGR rate compared to TJI or SI cases.

Figure 5.17 (c) compares the net indicated efficiency of Jetfire cases against the TJI and SI configurations. The net indicated efficiencies for the Jetfire cases have been determined after subtracting the work required to compress and deliver the pre-chamber purge work. Even after subtracting the parasitic losses due to the purge air supply Jetfire with 15 psig air configuration showed a clear advantage over the other pre-chamber configurations and also over the SI. This happens due to a combination of lowest purge work demand with the least amount of air supply to the pre-chamber as well as the least amount of pumping loss resulting from the highest manifold absolute pressure. Both of these factors contribute towards offsetting the additional heat loss with the pre-chamber, and help to surpass the SI efficiency. This shows that Jetfire with its ability to

operate with very high EGR dilution can actually be on par or even better than the traditional SI configuration at low-to-mid load throttled conditions.

Additionally, figure 17(c) also shows that, without any EGR, SI demonstrates more than 2 percentage points advantage over the TJI cases and almost 4 percentage points advantage over the Jetifire cases. Only around the EGR tolerance limit the advantage of SI diminishes due to a considerable decrease in combustion efficiency. At around 21-22% EGR dilution rate Jetfire cases show 2 to 4 percentage points decrease in net indicated efficiency. Thus, it should be noted that at these low- to mid-load non-knock limited conditions Jetfire can only be effective in terms of thermal efficiency when run with higher EGR dilution to offset the additional heat loss and purge work requirement accrued by the pre-chamber air supply.

Figure 5.14(d) compares the manifold absolute pressure with different combustion configurations at increasing EGR dilution rate. The three Jetfire cases show a considerably higher (more than 10 kPa) manifold pressure than the SI due to the utilization of almost twice as much EGR. Interestingly, Jetfire with 15 psig demonstrated the highest manifold pressure (hence the least pumping loss) amoung the Jetfire cases. Since additional air is delivered to the engine through the pre-chamber air valve, to maintain the same lambda 1 operation at constat load, the requirement to deliver air though the intake valves drops slightly with increase in pre-chamber air flow. Hence the manifold pressure was the lowest (under similar dilution level) with the highest pre-chamber pressure case i.e., at 45 psig.

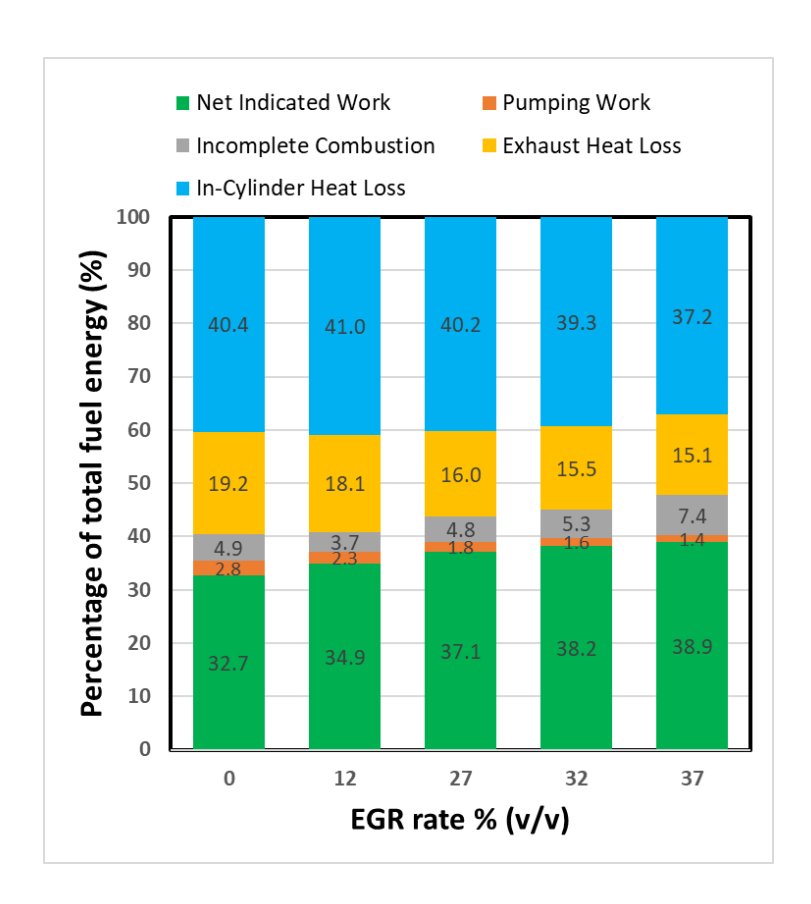


Figure 5.18 Split of losses for Jetfire at 1500 rpm and 6 bar IMEPg condition with varying EGR rate and 15 psig pre-chamber air. Numbers on the bar chart correspond to the percentages of total fuel energy

Figure 5.19 presents the MBT or knock limited CA50, 0-10 mass fraction burn duration, 10-90% mass fraction duration and COV of IMEP of the main chamber pressure with varying dilution rate for Jetfire, TJI and SI cases. It is clear from figure 5.19(a) that with the addition of EGR the CA50 timing can be more advanced and moved closer to the MBT timing for all the cases. The higher EGR tolerance of the Jetfire system enables the earliest CA50 phasings.

The 0-10% mass fraction burn duration or sometimes referred as the flame development angle plots given in figure 5.19(b) show that SI consistently showed a higher flame development angle compared to the rest of the cases signifying its single point flame initiation process. The cases with varied pre-chamber configurations all showed considerably smaller 0-10% burn duration than SI. This is due to the multiple jets starting main chamber ignition at multiple locations around the

main chamber, simultaneously resulting in rapid burning of main chamber mixture.

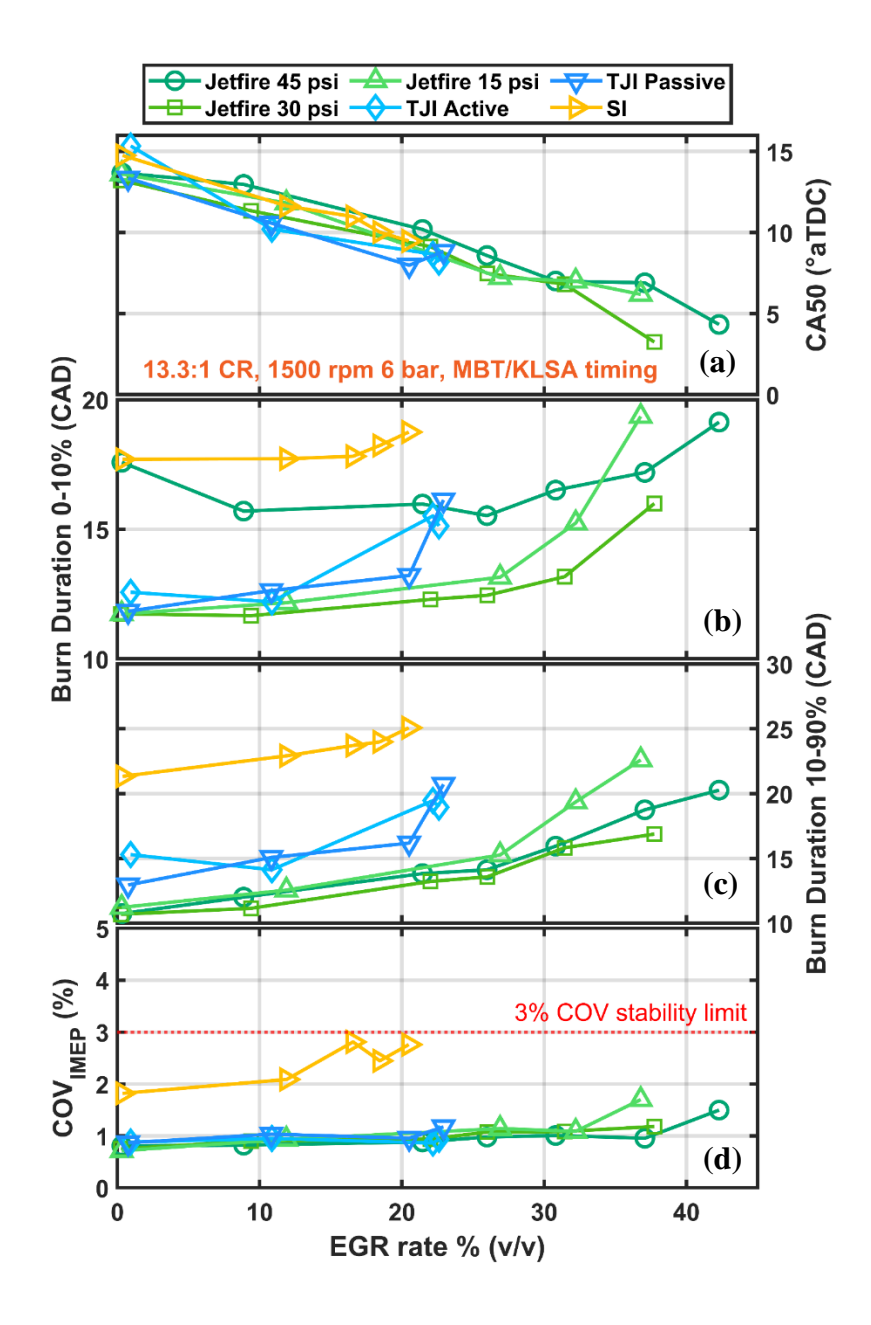


Figure 5.19 CA50, 0-10% burn duration, 10-90% burn duration and COV of IMEP at 1500 rpm and 6 bar IMEPg condition with varying EGR rate for Jetfire, TJI active, TJI passive and SI

For all the cases the 0-10% burn duration increased with increasing dilution rate. This is expected since with increased EGR dilution the mixture becomes increasingly difficult to ignite.

Interestingly with Jetfire 45 psig pre-chamber air case the 0-10% burn duration is much higher than the rest of the pre-chamber cases. This suggests that the fueling strategy in the pre-chamber for the 45 psig pre-chamber air pressure was not as good as for the rest, especially at lower EGR levels. In fact, the pre-chamber fueling strategy was similar to the 30 psig case but the 15 psig had slightly different fueling strategy. This suggests how critical the pre-chamber air/fuel scavenging strategy is for active pre-chamber systems.

Figure 5.19(c) plots the 10-90% mass fraction burn duration, sometimes referred to as the rapid burning angle at different EGR dilution rate for different ignition configurations. As expected, the 10-90% burn duration increased with increase in EGR rate for all the configurations. SI consistently showed higher burn duration than the pre-chamber cases which is understandable given the single point versus the multipoint flame initiation between the single spar plug and the pre-chamber turbulent jets. Also, the 10-90% burn duration is directly related to the 0-10% burn duration. Quicker 0-10% burn duration resulted in quicker 10-90% duration. The pre-chamber mixture ignitability and the resulting jet characteristics determine the 0-10% burn duration and in turn the 10-90% burn duration. Another interesting observation was that the Jetfire consistently demonstrated smaller 10-90% burn duration under similar level of dilution (up to 22-23%) at similar CA50 phasing. This suggests that the jets emerging from the pre-chamber nozzle with the Jetifre system might have induced more turbulence to the main chamber mixture to burn the main chamber mixture more quickly than the TJI cases. Thus, the additional air purge along with the fuel injection in the pre-chamber not only ensures high EGR mixture ignitability inside the prechamber but also results in stronger pre-chamber jets inducing higher turbulence in the main chamber.

Figure 5.19(d) shows the COV of IMEP at increasing dilution level with different ignition

configurations. It is clear that all the pre-chamber ignition systems provide a marked improvement in combustion stability compared to the conventional SI configuration. It should also be noted that the Jetfire system could maintain very good combustion stability (<1.5% COV<sub>IMEP</sub>) up to 43% external EGR rate which is almost twice as much as the SI or TJI.

#### 5.4.6 Jetfire: 10 bar IMEPg at 1500 rpm, different pre-chamber air pressure

Figures 5.20, 5.21 and 5.22 show the gross indicated efficiency and COV of IMEP with the Jetfire system operating at 1500 rpm and 10 bar IMEPg with different EGR rate and with 75, 60 and 45 psig pre-chamber air pressure, respectively. EGR rates of 33% and above were tested for the 10 bar IMEPg load conditions. In initial set of test runs up to 45% external EGR rate was investigated. With higher EGR rate the pre-chamber ignitability becomes critical. Pre-chamber mixture ignitability for the Jetfire system is heavily determined by the pre-chamber air timing and flow rate, along with the correct metering strategy of the pre-chamber fuel. The initial pre-chamber fuel injection strategy could only successfully tolerate up to 44 to 45% external EGR rate. Later, the pre-chamber fuel injection strategy was modified to operate with up to 50% external EGR dilution. These higher EGR rates (up to 50%) were tested with only the 75 psig pre-chamber air pressure conditions. Figure 5.20 shows the gross indicated efficiency and COV of IMEP at 10 bar IMEPg and 1500 rpm with 75 psig pre-chamber air pressure. It is demonstrated from this figure that the Jetfire system could maintain stable operation while maintaining the knock limit with up to 50% EGR rate. As for the initial set of tests with previous calibration up to 44% EGR tolerance was exhibited. With increasing EGR the knock limited CA50 moved closer to the MBT timing. It is observed that only the 49-50% EGR cases were able to achieve CA50 phasing of 6-10 CAD aTDC. Accordingly, higher EGR percentage was associated with better gross indicated efficiency. It is also seen that the highest gross indicated efficiency of about 42.2% was found with the 49% EGR

rate not the 50% EGR rate. This is because at limiting values the combustion variability increases and the combustion efficiency goes down which results in a decrease in gross indicated efficiency. This trend of decreasing combustion efficiency at high EGR will be discussed in detail in later sections.

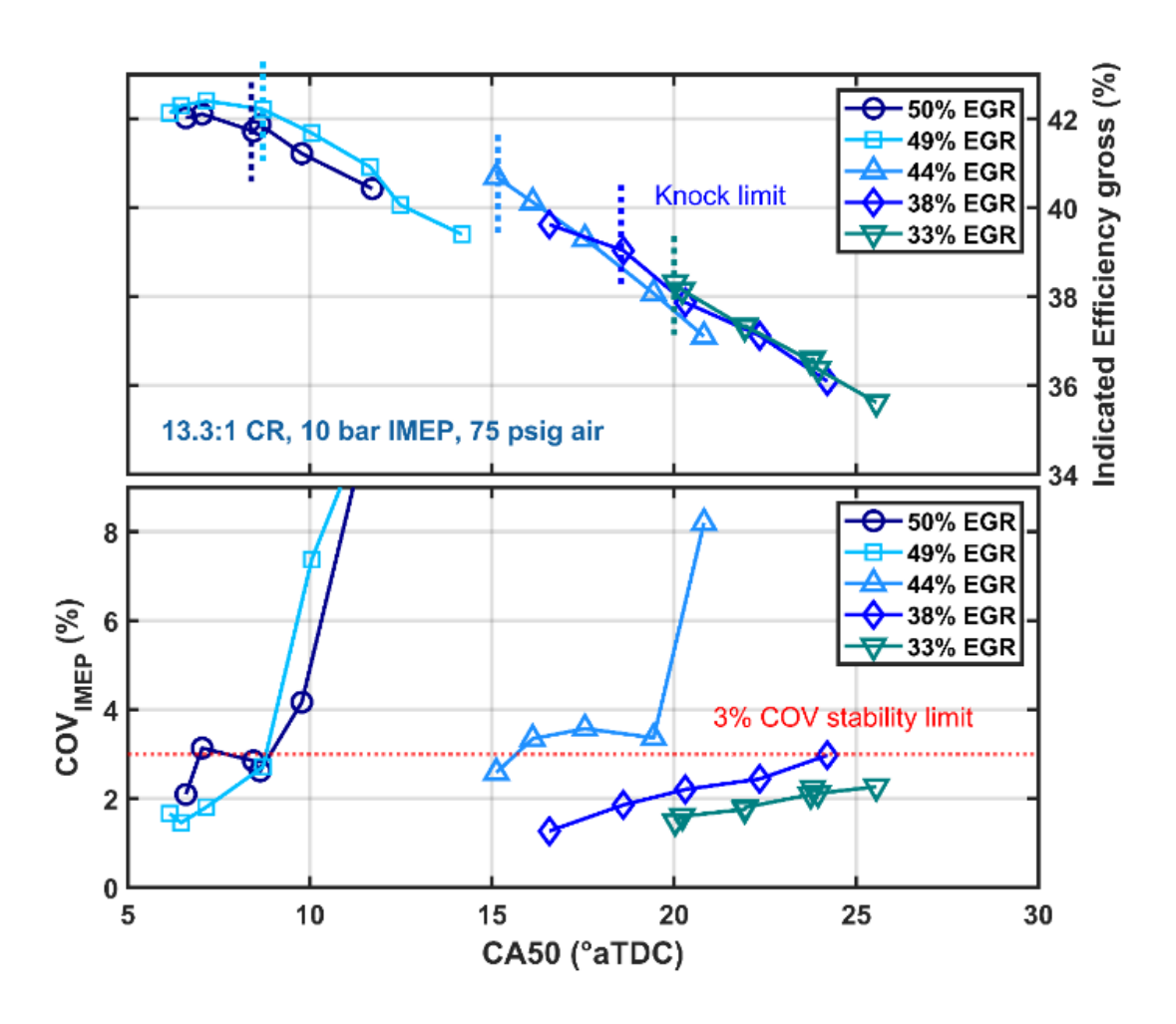


Figure 5.20 Gross indicated efficiency and COV of IMEP versus CA50 with different EGR rate at 1500 rpm and 10 bar IMEPg with 75 psig pre-chamber air pressure; Jetfire

Figure 5.21 shows the same gross indicated efficiency and COV of IMEP at different EGR rate for the 60 psig pre-chamber air pressure. It is seen that stable operation could be maintained up to 42% EGR rate. Beyond that it was difficult to get stable, knock-free operation with good

combustion stability. This is expected since it was tested with the previous pre-chamber fuel calibration and at lower 60 psig pre-chamber air. With less pre-chamber air, lower dilution tolerance is expected. Similar behavior was observed with the 6 bar IMEPg load condition as well. Additionally, it is seen that at 10 bar IMEPg condition the COV<sub>IMEP</sub> changes steadily with increase in EGR level. While COV<sub>IMEP</sub> improves with earlier combustion phasing at the same EGR level, with increasing EGR rates the each individual trend line moves toward higher COV ranges. Thus, with addition of EGR the change in combustion stability was more noticeable. This is unlike the 6 bar IMEPg operating conditions where the COV<sub>IMEP</sub> traces at different EGR level were grouped very closely together for the pre-chamber cases.

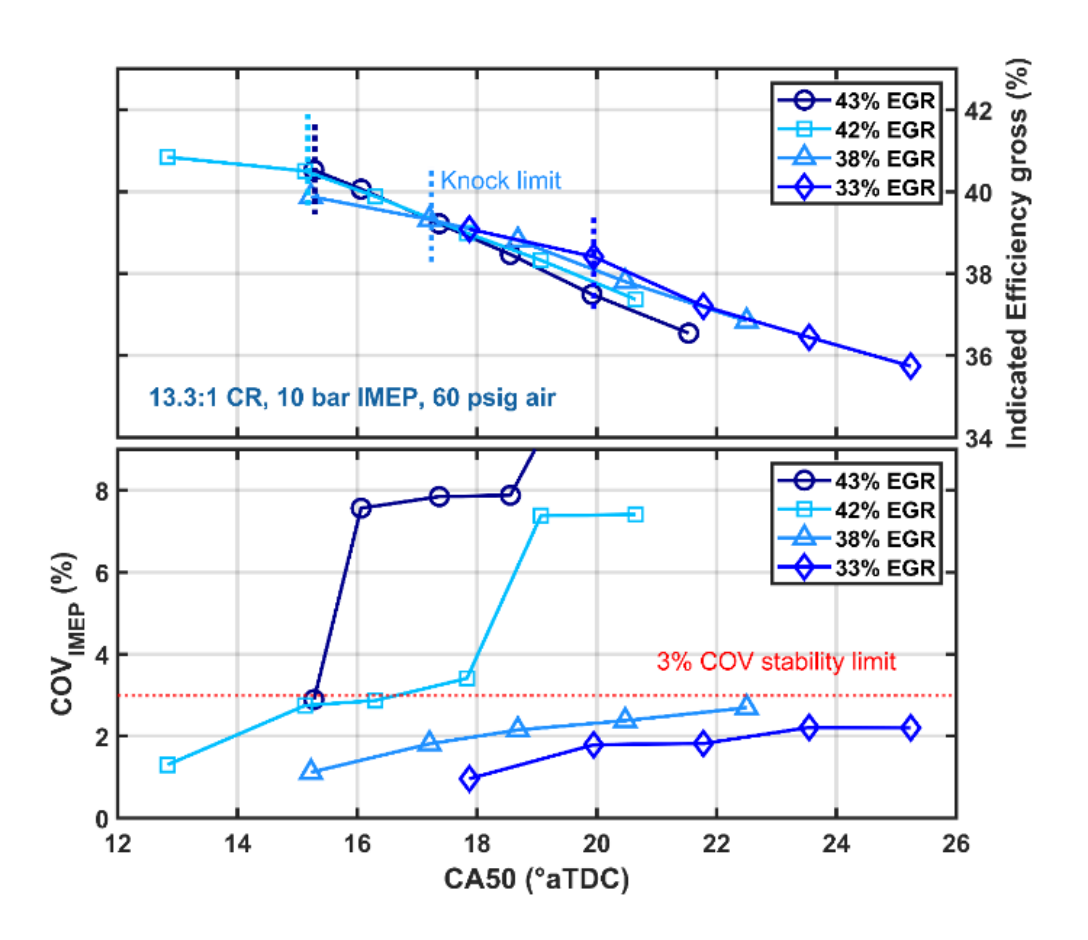


Figure 5.21 Gross indicated efficiency and COV of IMEP versus CA50 with different EGR rate at 1500 rpm and 10 bar IMEPg with 60 psig pre-chamber air pressure; Jetfire

With 45 psig pre-chamber air pressure up to 41% EGR tolerance was observed at 10 bar IMEPg and 1500 rpm conditions (shown in figure 5.22). Similar to the earlier observation knock limited CA50 improved with addition of higher EGR as expected.

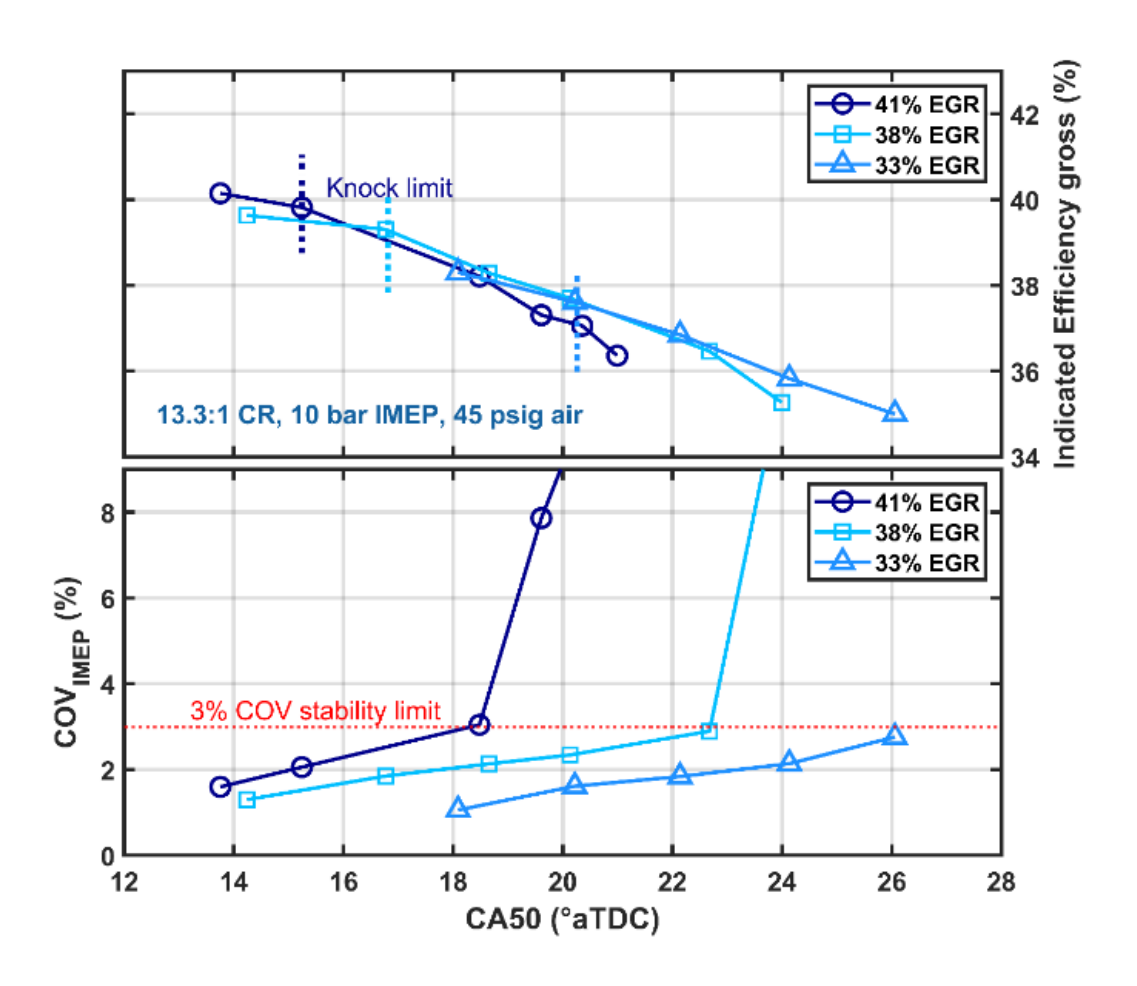


Figure 5.22 Gross indicated efficiency and COV of IMEP versus CA50 with different EGR rate at 1500 rpm and 10 bar IMEPg with 45 psig pre-chamber air pressure; Jetfire

In general, it was seen that higher pre-chamber air pressure led to slightly higher EGR tolerance. In fact, compared to the 45 psig pre-chamber air pressure case, the 75 psig case showed about 3 percentage points higher EGR tolerance (under the initial pre-chamber fuel calibration) with almost twice as much purge work requirement for the pre-chamber air delivery (as shown in figure 5.23). 75 psig and 60 psig pre-chamber air pressure resulted in very comparable gross indicated

efficiency figures while the 45 psig efficiency was found to be slightly lower. Interestingly, the CA50 phasing for all three cases were around 15 CAD aTDC. Thus, 1 to 3% higher EGR tolerance did not necessarily translate into better combustion phasing but did increase the indicated efficiency slightly. Higher air pressure becomes worthwhile only when the EGR tolerance limit extension is high enough to ensure considerably better combustion phasing and hence considerably higher indicated efficiency.

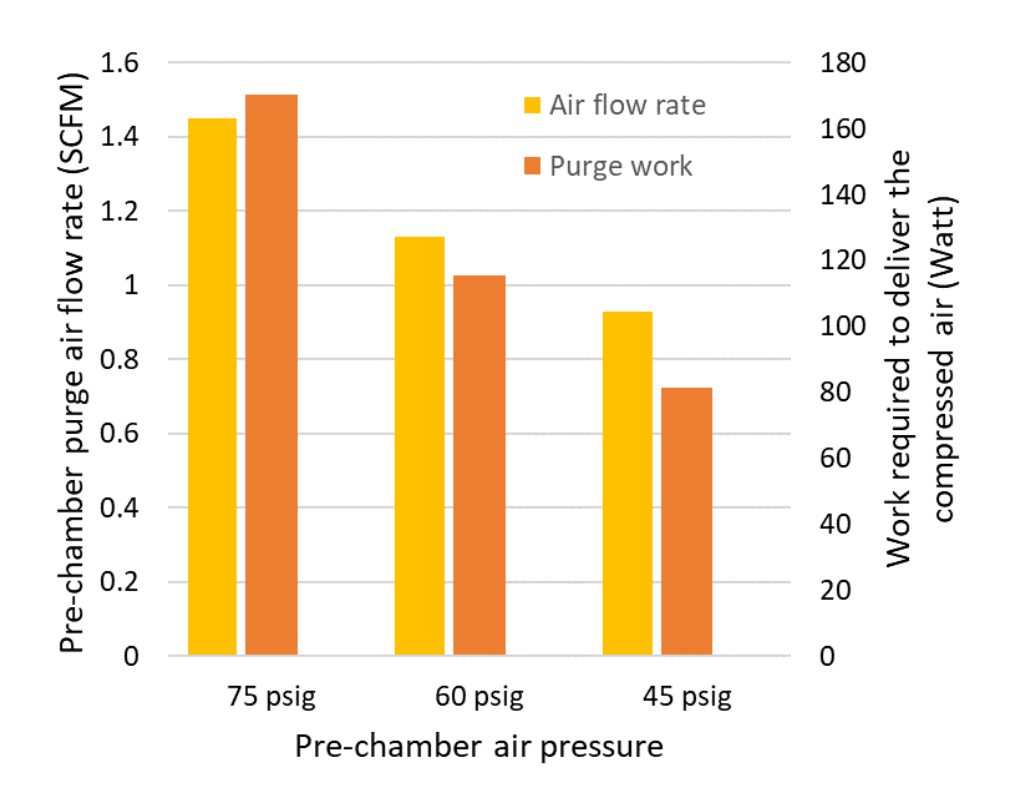


Figure 5.23 Pre-chamber air flow rate measured by LFE and the corresponding purge work requirement calculated using Womack fluid power design data sheet for varying compressed air pressure at 1500 rpm and 10 bar IMEPg

Figure 5.23 demonstrates the pre-chamber air flow rate for different pre-chamber upstream air pressures and their corresponding work losses for the supply of that compressed air to the pre-chamber at 10 bar IMEPg and 1500 rpm. The pre-chamber air flow rate was measured in SCFM by a LFE installed upstream of the pre-chamber air valve. As expected, higher flow rate was

measured at higher air pressure and the corresponding work required to deliver that air was also higher. The work requirement was estimated based on the LFE measurement and the values obtained from the Womack fluid power design data sheet with an assumed 85% isentropic efficiency of the compressor [86].

# 5.4.7 TJI active: 10 bar IMEPg at 1500 rpm

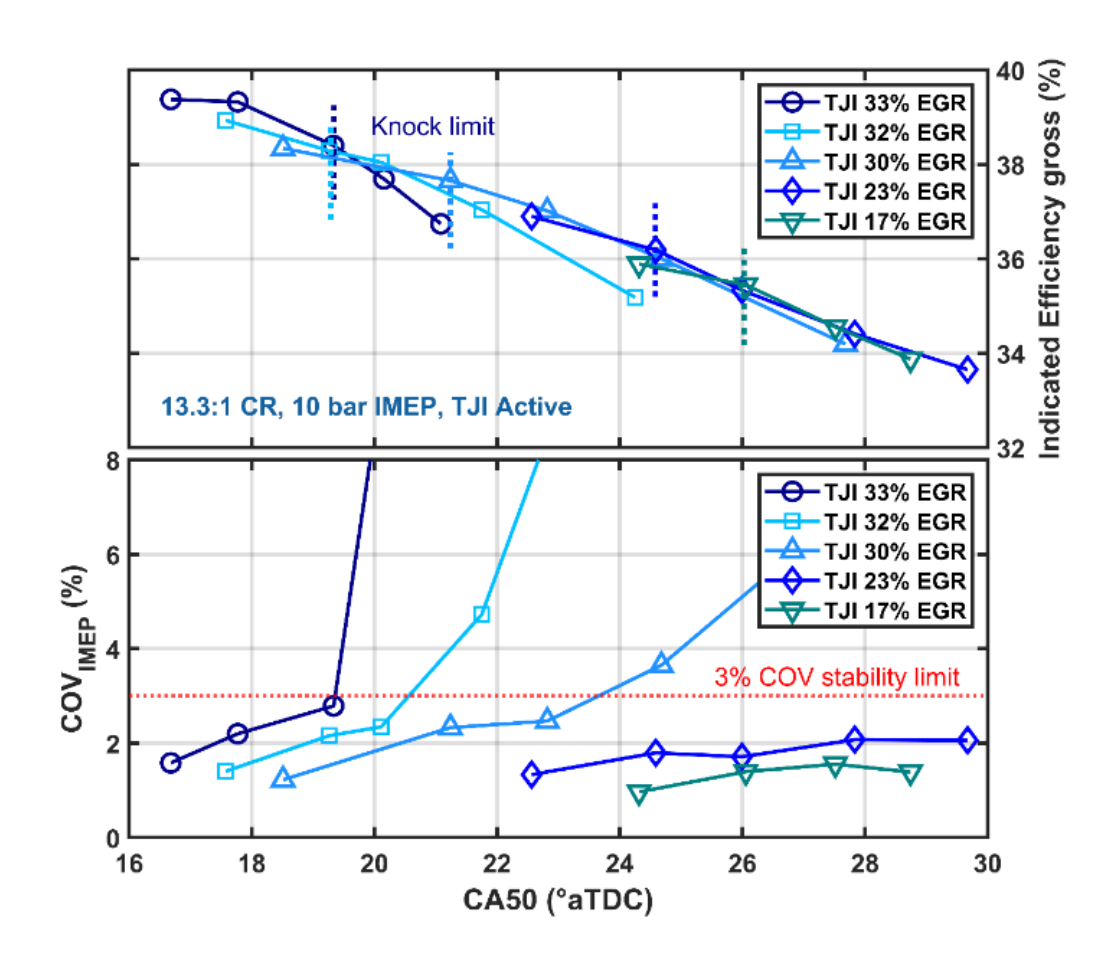


Figure 5.24 Gross indicated efficiency and COV of IMEP versus CA50 with different EGR rate at 1500 rpm and 10 bar IMEPg; TJI active

Figure 5.24 plots the gross indicated efficiency and COV of IMEP at different EGR dilution level with the TJI active configuration i.e., TJI with auxiliary fuel injection to the pre-chamber. Similar

trends with the EGR rate and knock-limited CA50 and gross indicated efficiency were observed as before. As shown in figure 5.24 the highest external EGR tolerance with the TJI active configuration was found to be 33%. This is more than 50% lower than the Jetfire EGR tolerance limit and results in almost 4 CAD later combustion phasing and about 3.8 percentage points drop in gross indicated efficiency compared to Jetfire at the same load condition.

# 5.4.8 TJI passive: 10 bar IMEPg at 1500 rpm

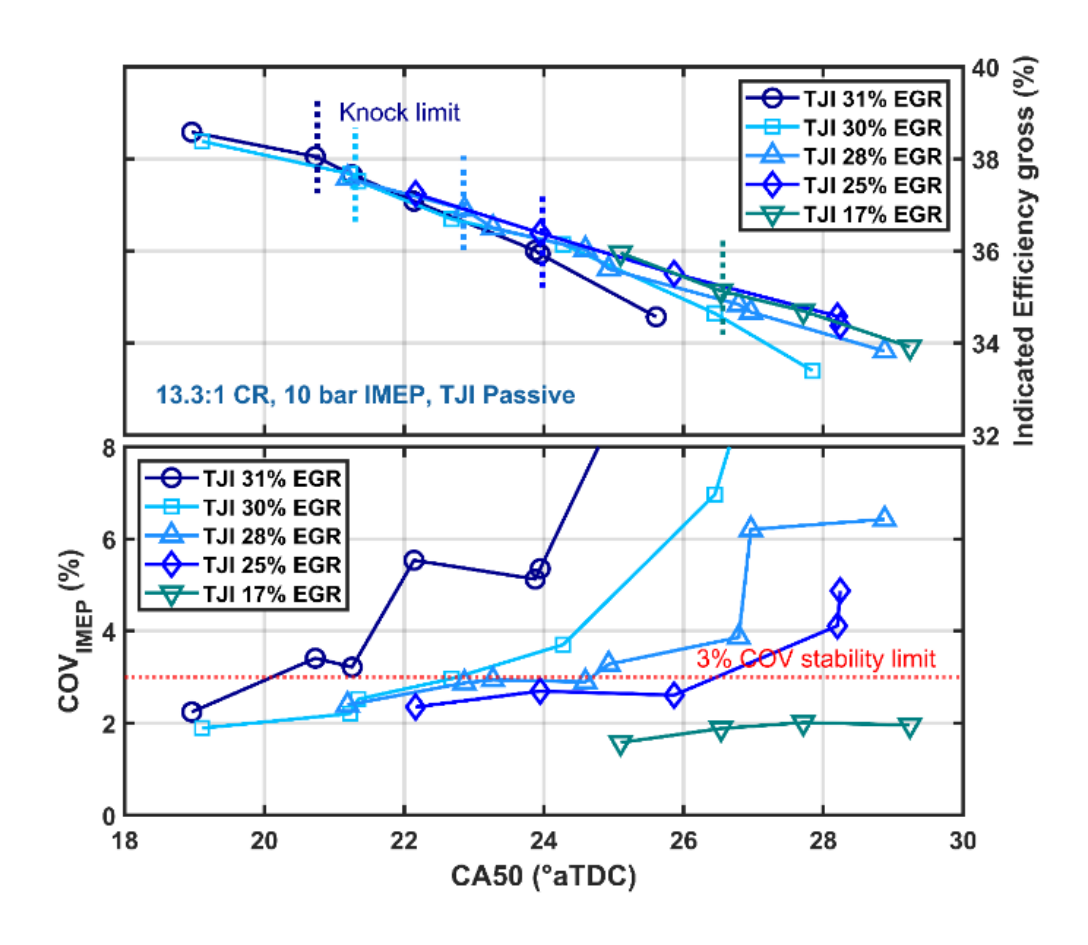


Figure 5.25 Gross indicated efficiency and COV of IMEP versus CA50 with different EGR rate at 1500 rpm and 10 bar IMEPg; TJI passive

Gross indicated efficiency and COV of IMEP results with varying EGR rate for the TJI passive cases i.e., TJI without any pre-chamber fuel injection are plotted in figure 5.25. Passive TJI

configuration results show a maximum EGR tolerance of 31% and indicated efficiencies slightly lower than the active configuration. The slight advantage in indicated efficiency shown by the active TJI is due to a 2% point higher maximum EGR tolerance that resulted in to CA50 advance of about 2 CAD.

# 5.4.9 SI: 10 bar IMEPg at 1500 rpm

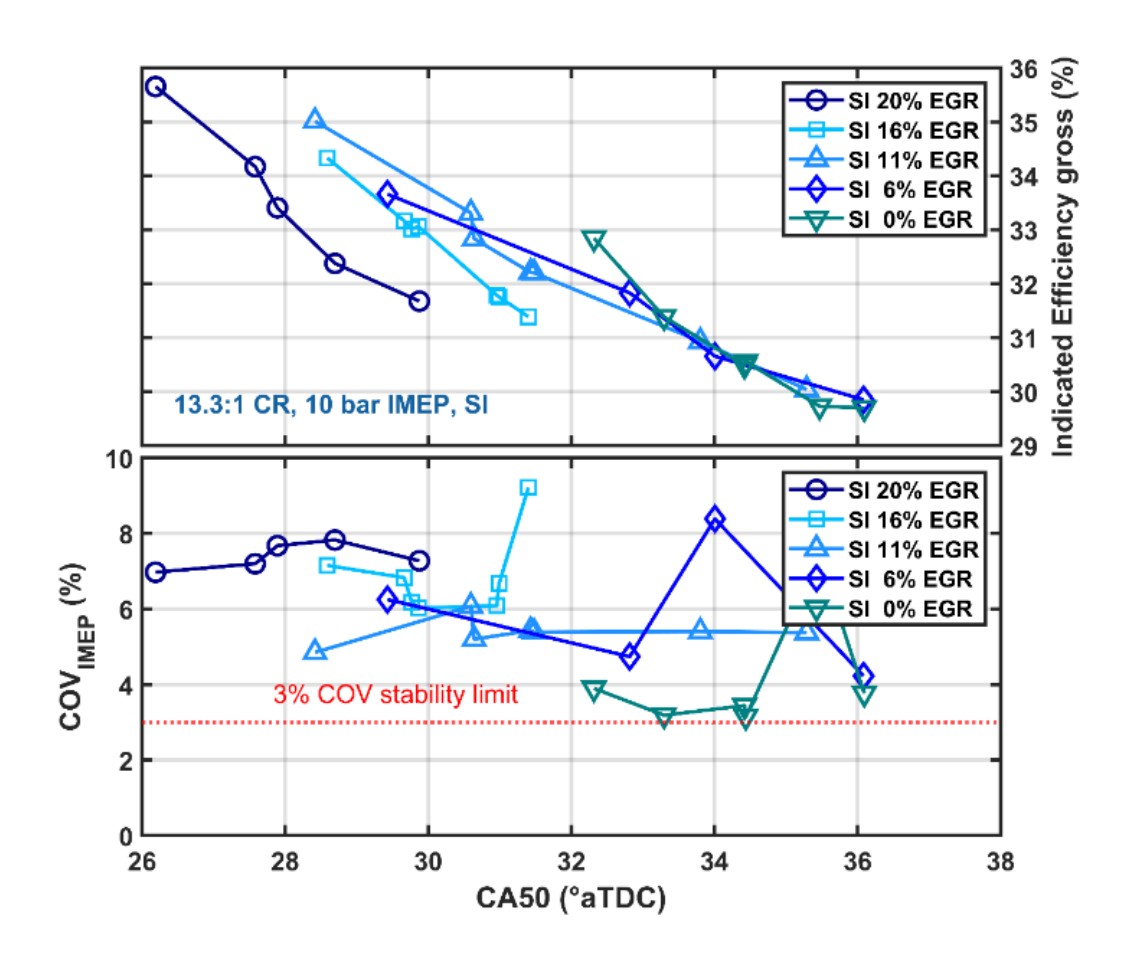


Figure 5.26 Gross indicated efficiency and COV of IMEP versus CA50 with different EGR rate at 1500 rpm and 10 bar IMEPg; SI

Figure 5.26 shows the gross indicated efficiency and COV of IMEPg at 10 bar 1500 rpm condition with varying EGR level for the conventional SI configuration at 13.3:1 compression ratio. Unlike

the pre-chamber systems discussed before SI operation was not possible at 10 bar IMEPg load at this elevated compression ratio. As shown by the bottom plot in figure 5.23 none of the data points are within the 3% COV stability limit. At 13.3:1 CR SI configuration is so knock prone that to avoid knocking the combustion phasing needs to be retarded aggressively which results into poor combustion stability. Even with such retarded phasing, more than half of each CA50 sweeps shown in figure 5.26 were knocking heavily. Since none of the operating points could meet the 3% COV stability limit knock limit lines were not displayed in this figure. This result shows the inability of the conventional SI configuration to operate at high geometric compression ratio without decreasing the effective compression ratio through EIVC or LIVC timing. On the other hand, all the pre-chamber systems could maintain knock free stable operation under the same compression ratio. The unique characteristics of the pre-chamber systems to prevent 'end gas autoignition' by preventing longer residence time for the end gas through faster burn rate and distributed ignition points spread throughout the combustion chamber, makes them suitable to operate at higher geometric compression ratios without decreasing the effective compression ratio. On the other hand, with conventional SI system, operation at high load becomes problematic due to high knocking tendency.

# 5.4.10 Comparison: Jetfire vs TJI active vs TJI passive vs SI at 10 bar IMEPg 1500 rpm

Figure 5.27 compares the gross indicated efficiency and COV of IMEP between Jetfire, TJI and SI configuration at knock limited stable 1500 rpm and 10 bar IMEPg operating condition with the highest corresponding EGR dilution limits. For Jetfire both 75 psig and 60 psig pre-chamber air pressures were compared to show what sort of benefit a small optimization in air/fuel timing could provide for the Jetfire system. SI 0% EGR case was included as well, even though SI was unable to meet the 3% COV stability limit, to show what sort of efficiency benefits can be expected

compared to stoichiometric no EGR SI configuration. The highest EGR tolerance for the corresponding ignition technologies was determined based on the knock limited stable operating points with less than 3% COV<sub>IMEP</sub>.

Figure 5.27 shows that the Jetfire system had a maximum EGR tolerance limit of 49% and a corresponding gross indicated efficiency of slightly above 42%. This was found with the prechamber air pressure set at 75 psig and a slightly different pre-chamber fueling strategy compared to the initial test runs. At 60 psig pre-chamber air pressure up to 42% EGR tolerance limit was established with the initial set of pre-chamber fuel calibrations. The gross indicated efficiency at this condition dropped to about 40.5%. TJI active demonstrated a maximum EGR tolerance of 32% with a gross indicated efficiency of around 38.4%. TJI passive showed slightly lower EGR tolerance than the active system with the highest EGR limit of 30% and a gross efficiency value around 37.8%.

At 13.3:1 compression ratio SI, could not operate in a stable manner and showed 0 EGR tolerance and unacceptable combustion stability with a highest gross indicated efficiency of about 31.8%. Thus, Jetfire shows a considerable advantage in maximum EGR tolerance limit and a corresponding increase in gross indicated thermal efficiency. Additional air supply to the prechamber allows the Jetfire system to purge the trapped residuals out of the pre-chamber and maintain combustible mixture inside the pre-chamber even with high rate of EGR dilution. Higher EGR rate not only decreases the heat transfer and exhaust heat loss by decreasing the in-cylinder temperature but also provides substantial knock relief and provides better combustion phasing and higher thermal efficiency.

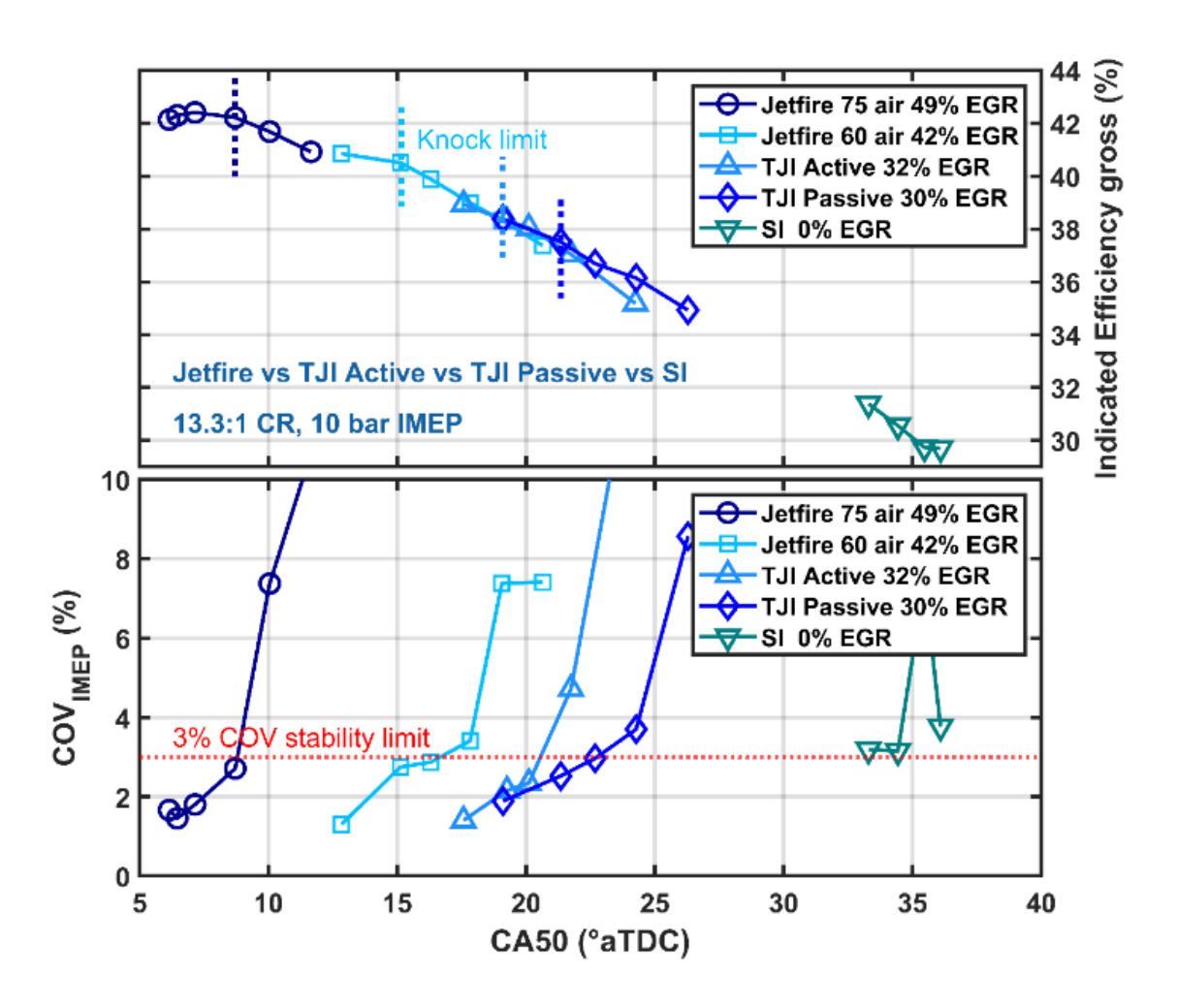


Figure 5.27 Comparison of gross indicated efficiency and COV of IMEP versus CA50 at 1500 rpm and 10 bar IMEPg with highest EGR rate between Jetfire, TJI active, TJI passive and SI

While Jetfire provides a clear advantage in terms of gross indicated efficiency, additional work is required to compress and deliver the pre-chamber purge air. This in turn will decrease the net work output. In figure 5.28 the gross indicated efficiency along with the purge work subtracted gross indicated efficiency, combustion efficiency and manifold absolute pressure are plotted with increasing dilution level for different pre-chamber air pressure Jetfire configuration along with the TJI active and passive configurations for 1500 rpm and 10 bar IMEPg load condition. Since SI could not maintain stable operation at this load condition and compression ratio it was omitted

from this set of plots.

Figure 5.28(a) plots gross indicated efficiency against increasing EGR dilution rate. The higher the EGR tolerance limit was the higher the gross indicated efficiency was. But as discussed previously additional work is required to compress and deliver the pre-chamber purge air. An estimation of the pre-chamber purge work required at different pre-chamber air pressure settings is given in figure 5.23. In figure 5.28(b) the purge work subtracted gross indicated efficiencies are plotted against increasing EGR dilution. Instead of the gross indicated efficiency, this 'purge work subtracted gross indicated efficiency' provides an actual idea of what real world efficiency benefit Jetfire can provide compared to passive or active TJI configurations. Based on the purge work loss estimations shown in figure 5.23 about 0.5-1 percentage point drop off in efficiency has been calculated. In figure 5.28(b) it is apparent that compared to the TJI cases the Jetfire cases dropped slightly due to this purge work being subtracted from the gross efficiency values. Despite this drop in gross indicated efficiency, figure 5.28(b) demonstrates that Jetfire at its highest tolerable EGR dilution limit provides a 2.8 percentage point higher efficiency that the TJI active configuration with maximum EGR rate. And compared to TJI passive the Jetfire system provided a 3.5 percentage point increase in gross indicated efficiency. This increase in indicated efficiency is considerably greater than the close to 1 percentage point increase shown at 6 bar IMEPg load. As the knock propensity increases with higher load the higher EGR tolerance and the corresponding advantage with combustion phasing makes the Jetfire system even more effective.

Figure 5.28(c) compares the combustion efficiency of the Jetfire system with the TJI systems. It is apparent that the Jetfire system could maintain comparable combustion efficiency if not slightly better than the TJI configuration even with more than 50% higher EGR dilution rate.

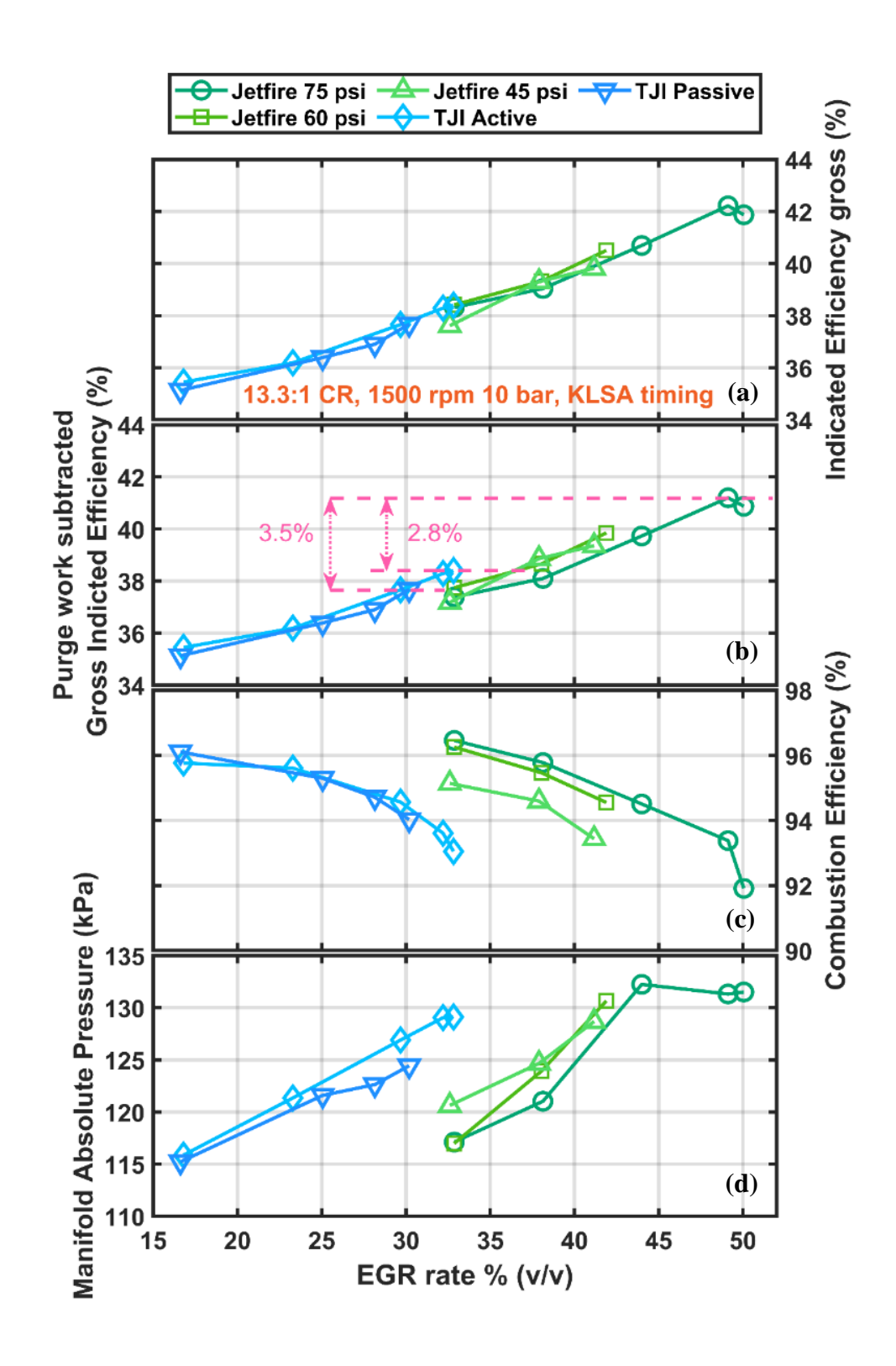


Figure 5.28 Gross indicated efficiency, purge work subtracted gross indicated efficiency, combustion efficiency and manifold absolute pressure at 1500 rpm and 10 bar IMEPg condition with varying EGR rate for Jetfire, TJI active, TJI passive and SI

Figure 5.28(d) compares the manifold absolute pressure (MAP) at increasing dilution rate between Jetfire and TJI systems. It was interesting that at a similar dilution level of around 30-33% EGR Jetfire required lower manifold pressure than the TJIs. This is because of the additional air introduction through the pre-chamber air valve. Since some portion of the charge air is provided during the pre-chamber purging through the air valve the intake manifold absolute pressure requirement is lowered to maintain the same lambda 1 operation at similar loads. Another observation was that even with an increase in EGR level up to 50% EGR with the new pre-chamber calibration compared to the upper limit of 44% EGR with the initial pre-chamber fueling strategy the manifold pressure did not increase, in fact it was slightly lower. This happens due to the superior knock limited combustion phasing provided by the higher EGR rate. With a CA50 phasing close to MBT timing IMEPg increased and to maintain the same nominal 10 bar IMEPg the fuel injection requirement decreased. Accordingly, the fresh air requirement also dropped to maintain lambda 1 operation. Thus, a higher EGR rate can be maintained without any further increase in manifold pressure. Increased manifold pressure typically results in higher knocking tendency and this actually helped to make the higher EGR dilution even more effective.

Figure 5.29 compares the knock limited CA50, 0-10% mass fraction burn duration, 10-90% burn duration and COV of IMEP with increasing EGR dilution rate for the Jetfire and TJI systems. In figure 5.29(a) it is apparent that the higher the EGR tolerance limit was the closer the knock limited CA50 moved towards the MBT timing of 7-8 CAD aTDC. In fact, only the 49-50% EGR points, with the 75 psig pre-chamber air pressure Jetfire system, were able to reach the MBT phasing while maintaining the good combustion stability within acceptable knock limits. Hence it exhibited the highest indicated efficiency among the tested pre-chamber configurations.

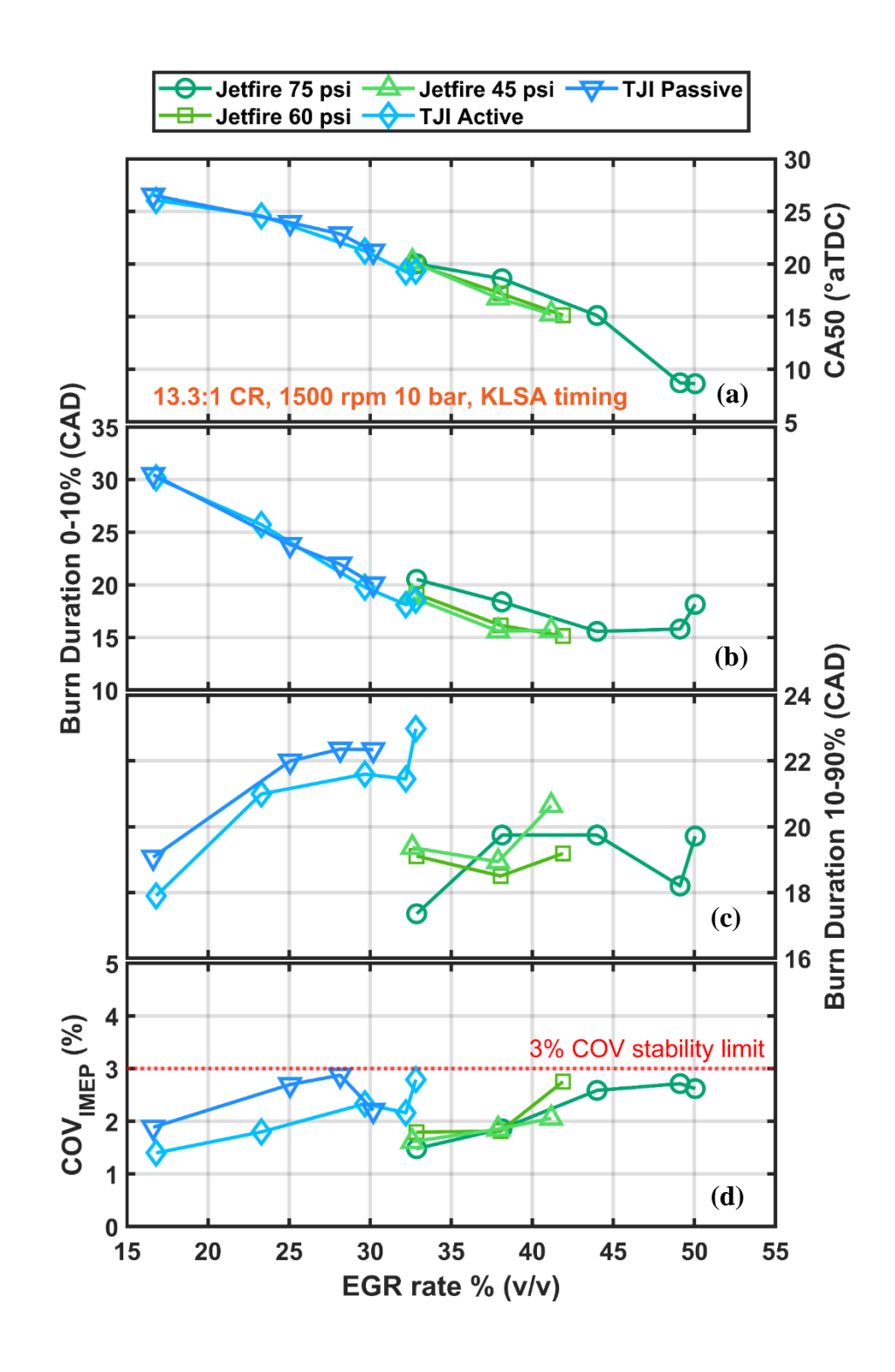


Figure 5.29 CA50, 0-10% burn duration, 10-90% burn duration and COV of IMEP at 1500 rpm and 10 bar IMEPg condition with varying EGR rate for Jetfire, TJI active, and TJI passive. SI inoperable without knock at high CR 10 bar load

Figure 5.29(b) compares the 0-10% burn duration between Jetfire and TJI variants. It is interesting that with lower dilution 0-10% burn durations were actually longer. This is due to the combustion phasing disadvantage at lower EGR rate. At lower EGR rate the pre-chamber spark timing had to be retarded to avoid knock and this made the ignition in the main chamber difficult even with lower dilution.

Figure 5.29(c) compares the 10-90% burn duration between Jetfire and TJI configurations. Within the two TJI systems, TJI active showed slightly faster 10-90 burn duration even though the 0-10% burn durations were almost identical. Moreover, the 10-90% burn duration showed an increasing trend with addition of EGR. On the other hand, it was difficult to identify any clear trends with Jetfire. It was not clear how different pre-chamber air affected either 0-10% or 10-90% burn duration parameters. However, it is apparent from figure 5.29(c) that all the Jetfire configurations provided substantially faster 10-90% burn durations compared to TJIs even at substantially higher EGR rates. While the 10-90% burn duration is heavily dependent on the combustion phasing (CA50), even with similar EGR rate and identical CA50 figure 5.29(c) clearly demonstrates that Jetfire offered faster burn duration than the TJI configuration. This suggests that the jet induced turbulence and entrainment must be higher with the Jetfire ignition system compared to the TJI systems. These are primarily functions of the pre-chamber combustion. The additional air supply to the pre-chamber ensures that with the Jetfire cases the pre-chamber mixture stoichiometry can be maintained within a range that results in stronger jets.

Figure 5.29(d) serves as a reminder of how much benefit Jetfire provides in terms of maintaining superior combustion stability at higher dilution rate. The COV<sub>IMEP</sub> values plotted in figure 5.29(d) show that Jetfire system could maintain acceptable combustion stability (<3% COV<sub>IMEP</sub>) up to 50% external EGR rate whereas the TJI active system could only tolerate up to 33% EGR.

## 5.4.11 Comparison: Jetfire vs SI at 8 bar IEMPg

Since SI was inoperable at 10 bar IMEPg with the elevated 13.3:1 compression ratio, additional test runs with both Jetfire and SI operating at 8 bar IMEPg at 1500 rpm were conducted. This provided the opportunity to compare the Jetfire and SI at a knock-limited environment.

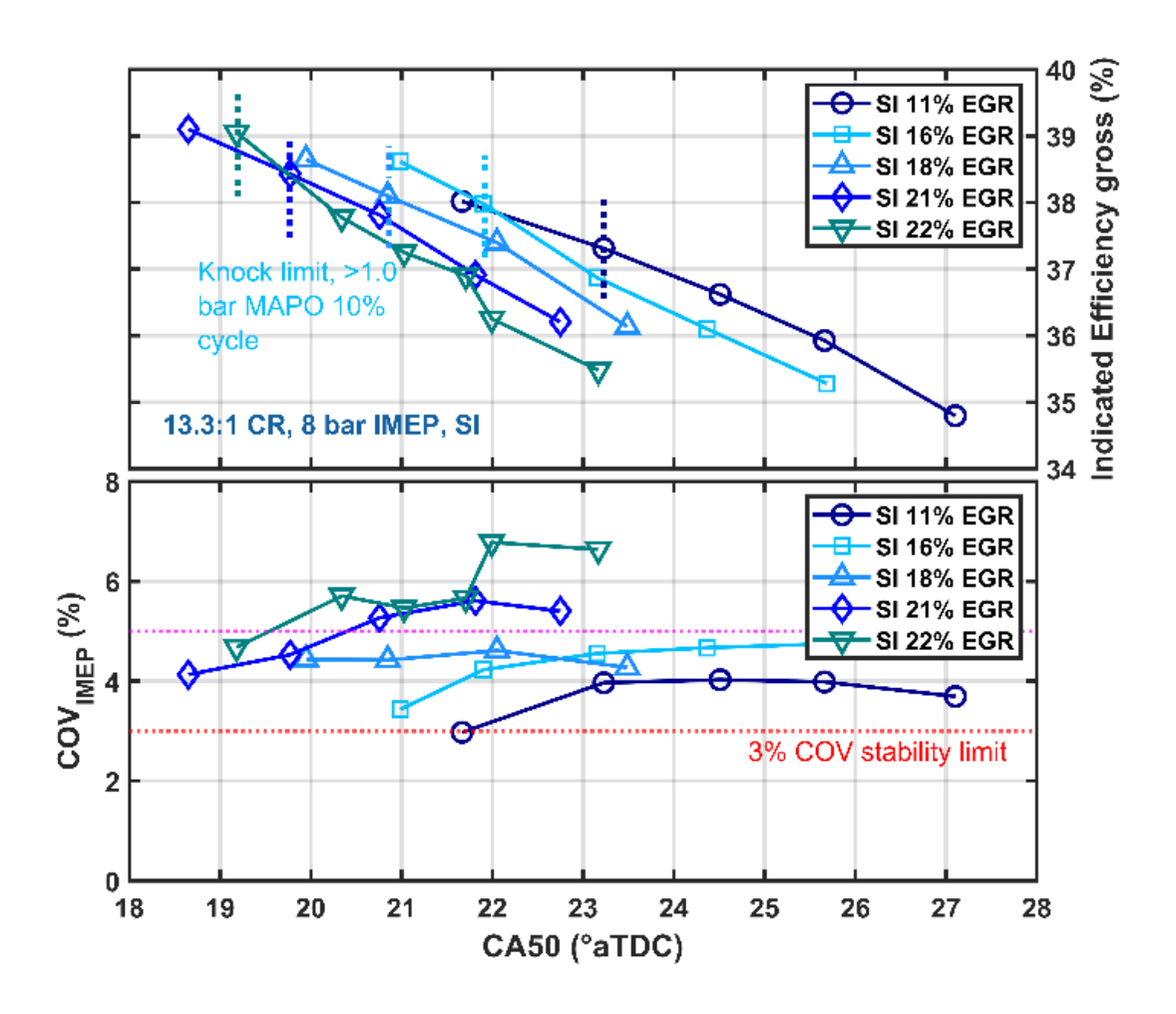


Figure 5.30 Gross indicated efficiency and COV of IMEP versus CA50 with different EGR rate at 1500 rpm and 8 bar IMEPg; SI

Figure 5.30 shows gross indicated efficiency and COV of IMEP with different EGR rates obtained with SI configuration operating at 8 bar IMEPg and 1500 rpm. As is evident from figure 5.30, with SI at this high 13.3:1 compression ratio it was difficult to maintain operation within the 3% COV

combustion stability limit and acceptable knock limit even at 10% EGR. With a higher EGR rate combustion phasing was better and the efficiency increased, but combustion stability suffered even further. To have some level of comparison with Jetfire at similar loads, a less conservative combustion stability threshold of 5% COV of IMEP limit was chosen. Close observation of figure 5.30 shows that SI with up to 18% EGR could maintain operation within the 5% COV limit without crossing the knock threshold.

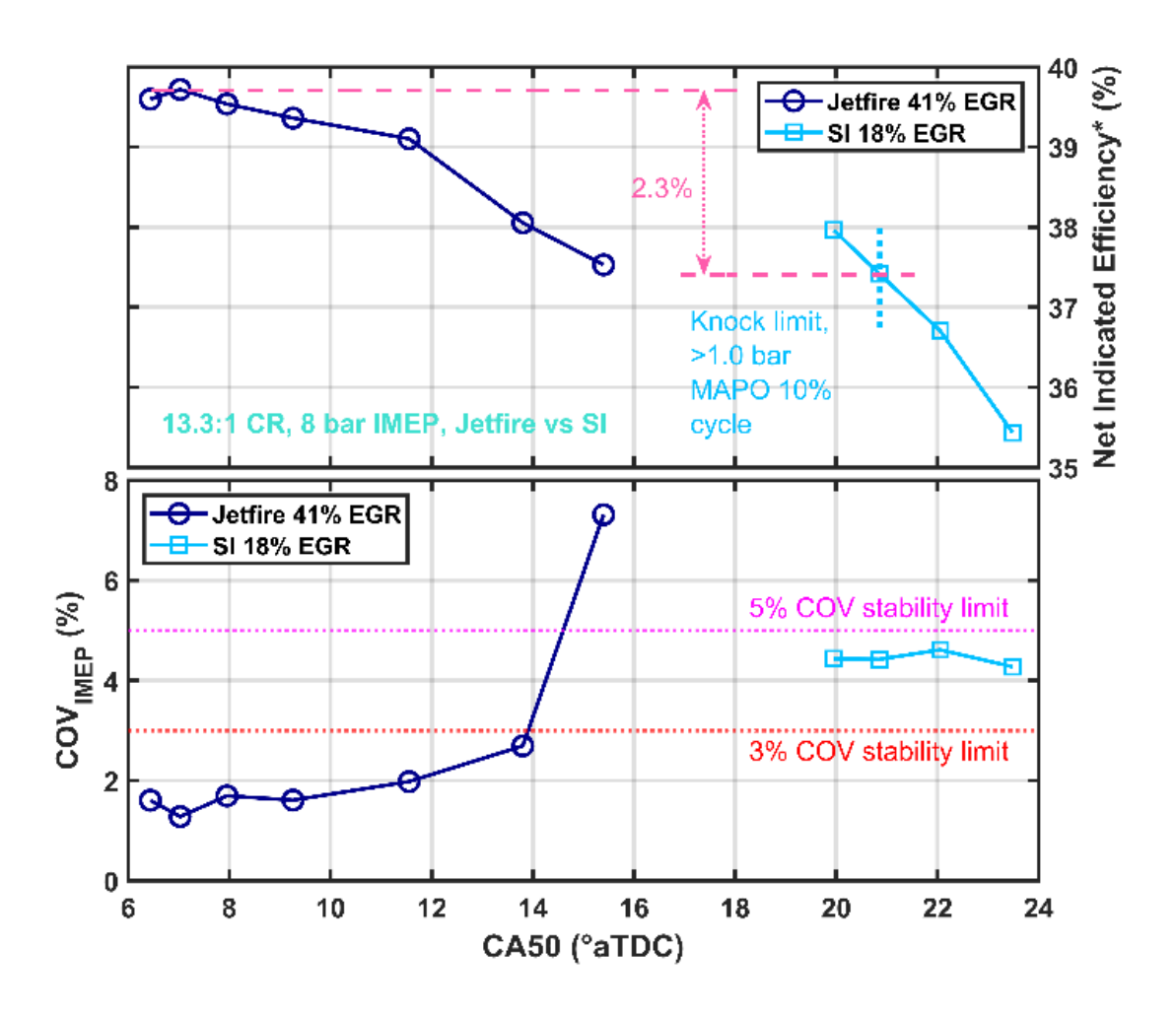


Figure 5.31 Comparison of gross indicated efficiency and COV of IMEP versus CA50 between Jetfire and SI at 1500 rpm and 8 bar IMEPg with highest EGR rate within stable combustion limit, Jetfire pre-chamber air pressure 60 psig

Figure 5.31 compares the net indicated efficiency and COV of IMEP between SI operating with

18% EGR and 5% COV limit against the results obtained with Jetfire operating with 41% EGR and 3% COV combustion stability limit. Net indicated efficiency values for the Jetfire take in to account the work loss to supply the purge air to the pre-chamber. It is clear from figure 5.31 that Jetfire offers considerable advantage in terms of thermal efficiency and combustion stability compared to SI. In fact, an increase of 2.3 percentage points in net indicated efficiency was obtained with Jetfire compared to SI while delivering far better combustion stability. Considerably higher EGR dilution tolerance limit of Jetfire permits more advanced combustion phasing, which subsequently results in better thermal efficiency. Even with the increased heat loss characteristics of the Jetfire, in knock-limited operating conditions such as the one that was tested here, combustion phasing benefits far outweigh the additional heat losses. Thus, while at 6 bar load Jetfire only delivered marginally better net indicated thermal efficiency, at higher loads the efficiency advantage increases. The more knock limited the conditions are, the more favorable Jetfire becomes compared to the other ignition systems tested.

#### 5.4.12 Jetfire high EGR load sweep: 2 to 10 bar IMEPg at 1500 rpm

A load sweep was conducted from 2 bar IMEPg up to 10 bar IMEPg at a speed of 1500 rpm to determine the highest EGR tolerance at each load condition. The upper range of the load sweep was limited by the lack of any variable valve timing techniques such as EIVC or LIVC to reduce the effective compression ratio.

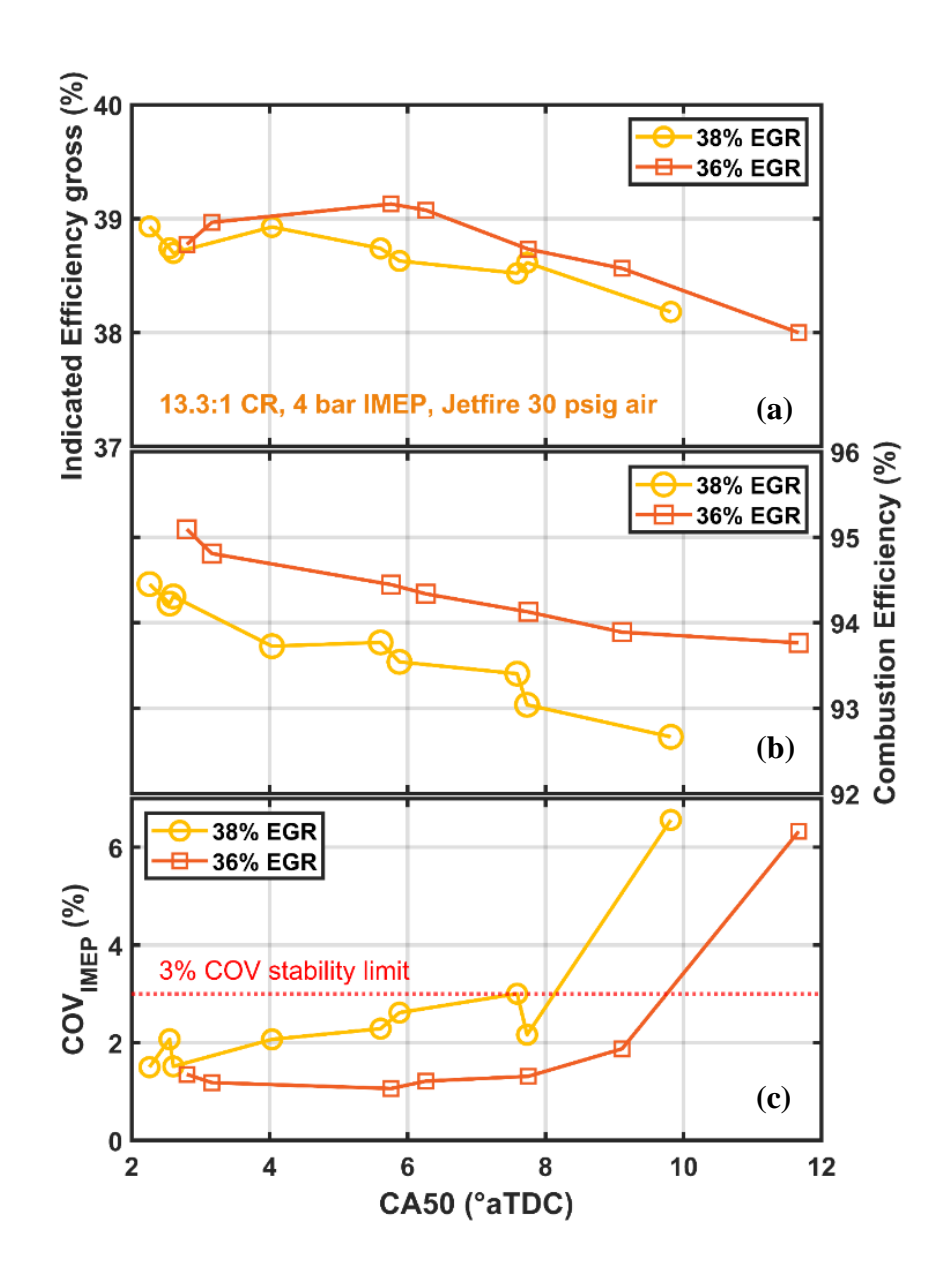


Figure 5.32 Gross indicated efficiency, combustion efficiency and COV of IMEP at 1500 rpm and 4 bar IMEPg with different EGR rates close to dilution limit

Figure 5.32 shows the gross indicated efficiency, combustion efficiency and COV of IMEP at 4 bar nominal IMEPg and 1500 rpm with two different EGR rates. A pre-chamber air pressure of 30 psig was used for this test. While it was possible to maintain stable combustion with COVIMEP less than 3% with up to 38% EGR, due to decreased combustion efficiency (figure 32(b) the higher

gross indicated efficiency was actually found with a slightly lower 36% EGR rate. Highest gross indicated efficiency of slightly above 39% was achieved at the 4 bar IMEPg condition.

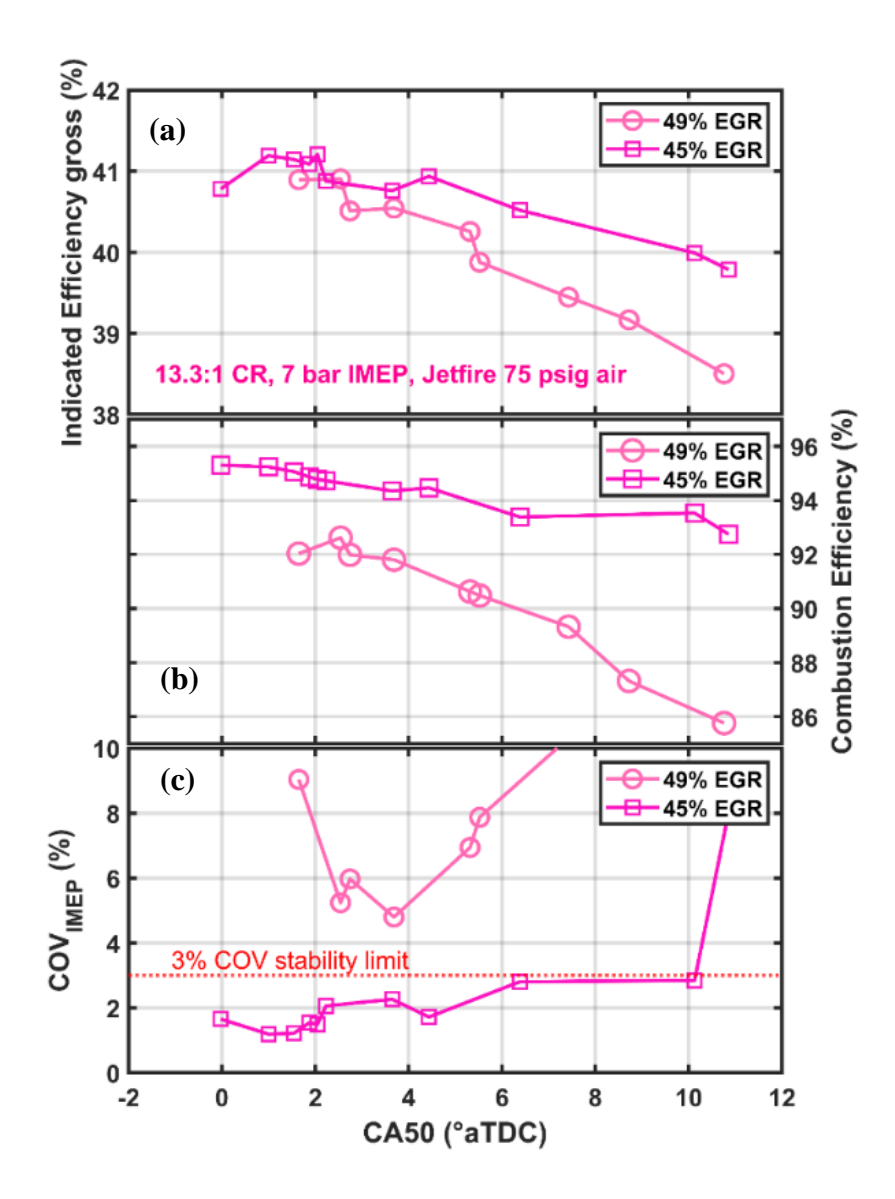


Figure 5.33 Gross indicated efficiency, combustion efficiency and COV of IMEP at 1500 rpm and 7 bar IMEPg with different EGR rates close to dilution limit

Figures 5.33 and 5.34 show the gross indicated efficiency, combustion efficiency and COV of IMEP at 1500 rpm and 7 bar IMEPg and 8 bar IEMPg, respectively. EGR rate of up to 49% was used in both cases. No knocking was encountered in these conditions. While 7 bar IMEPg

struggled with 49% EGR to maintain good combustion stability 8 bar IMEPg exhibited better stability at the same 49% EGR rate. Due to considerable decrease in combustion efficiency, the highest gross indicated efficiencies were obtained with lower 45% and 44% EGR, respectively.

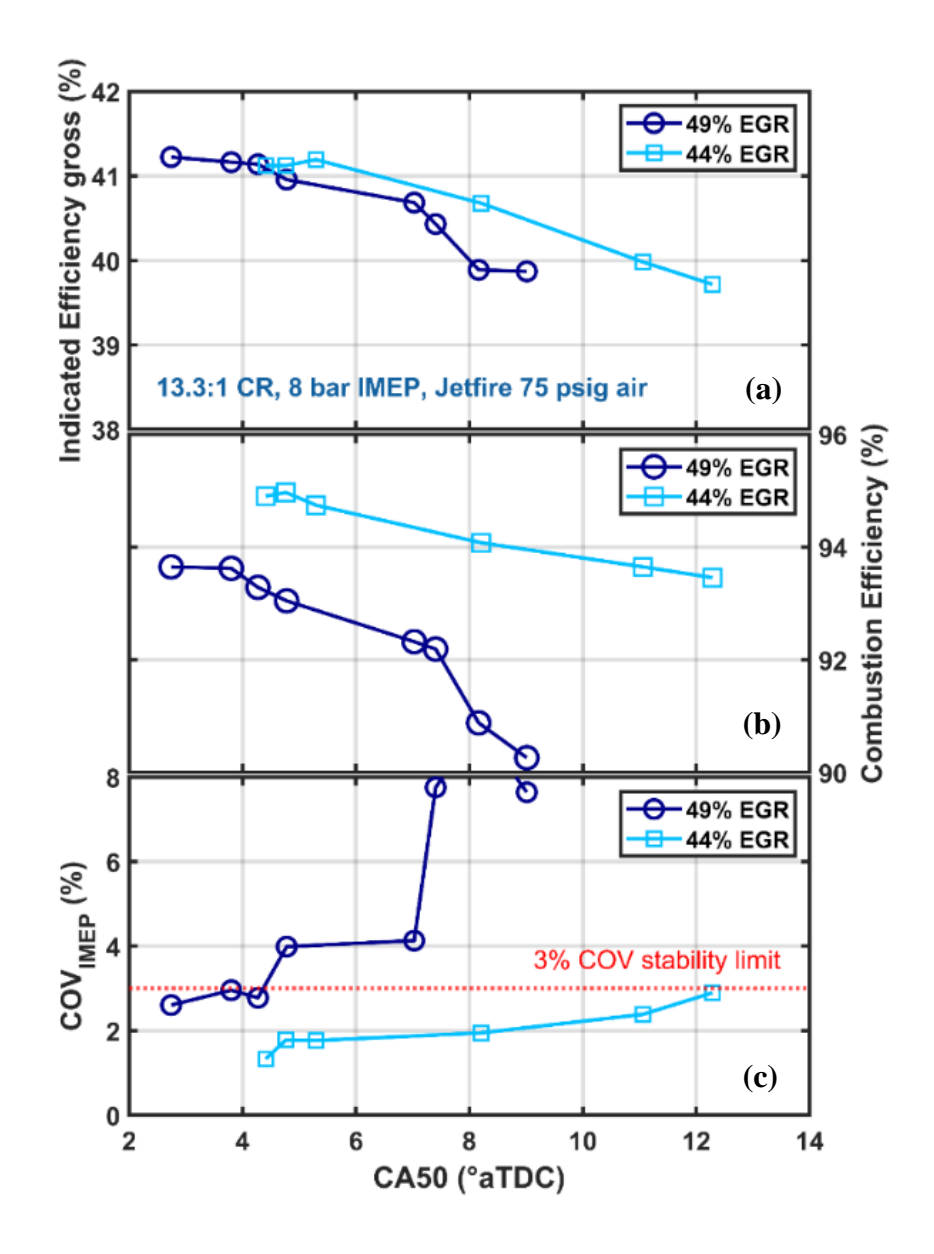


Figure 5.34 Gross indicated efficiency, combustion efficiency and COV of IMEP at 1500 rpm and 8 bar IMEPg with different EGR rates close to dilution limit

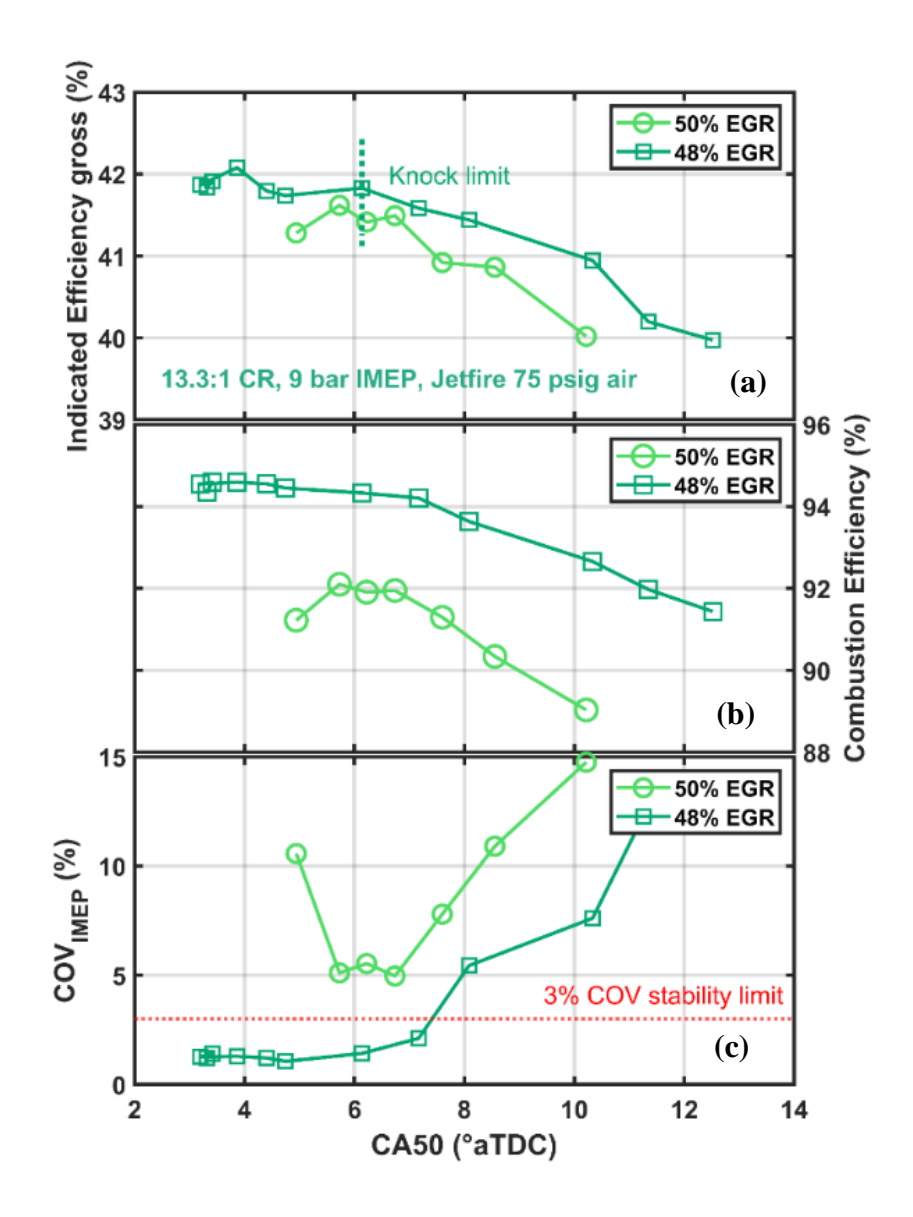


Figure 5.35 Gross indicated efficiency, combustion efficiency and COV of IMEP at 1500 rpm and 9 bar IMEPg with different EGR rate close to dilution limit

Figures 5.35 and 5.36 show the gross indicated efficiency, combustion efficiency and COV of IMEP obtained at 1500 rpm and 9 bar IMEPg and 10 bar IMEPg. At these load conditions the operation was knock limited. Vertical lines in the indicated efficiency graph denote the knock limited CA50 beyond which the conditions cross the knock threshold. As demonstrated by figure

5.35(a) it was difficult to maintain less than 3% COV stability limit with 50% EGR rate at 9 bar IMEPg. But at slightly lower 48% EGR the combustion stability was significantly better which resulted in a higher combustion efficiency as well. Knock limited gross indicated efficiency of 41.8% was obtained at a CA50 of around 6 CAD aTDC.

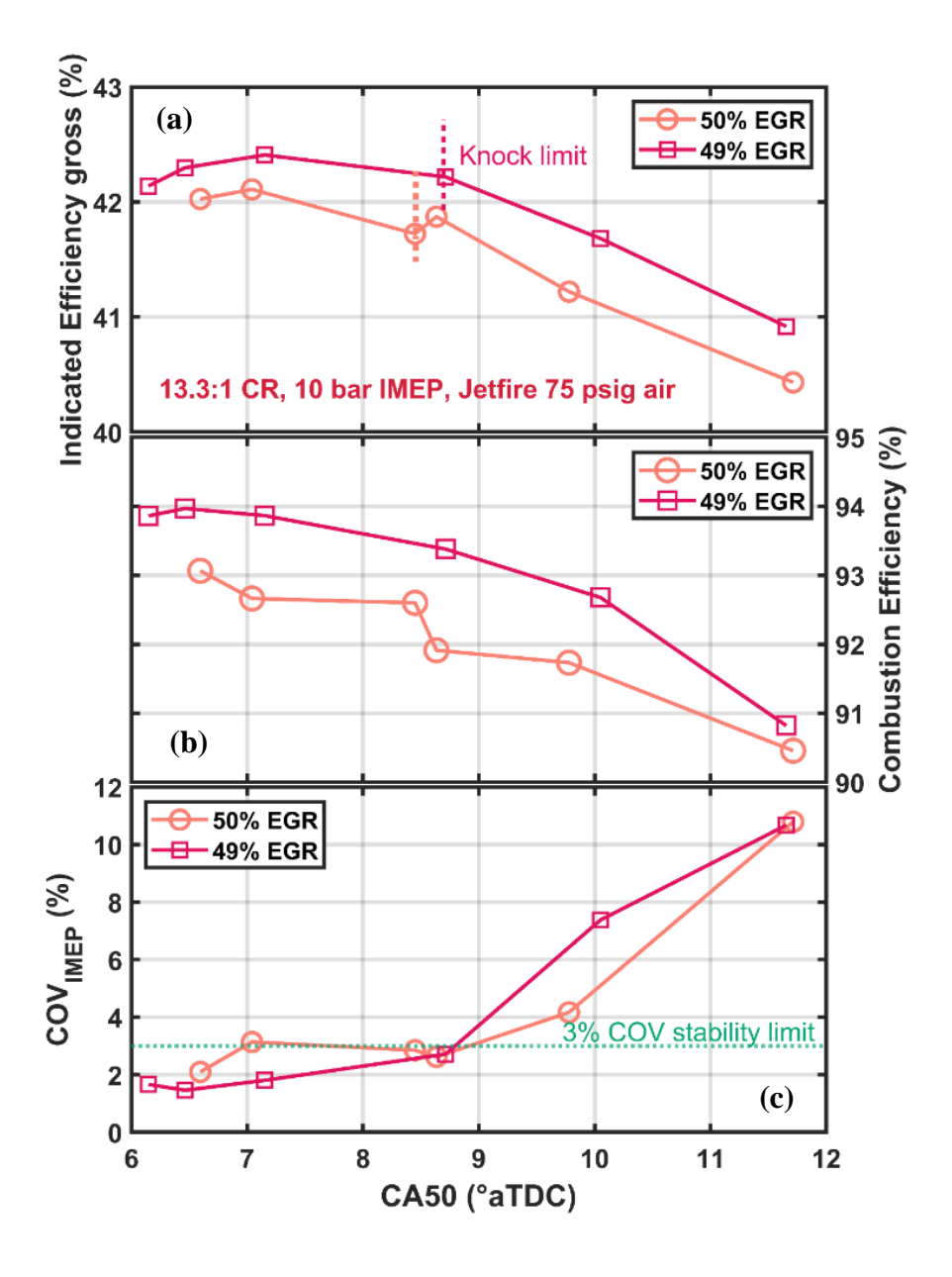


Figure 5.36 Gross indicated efficiency, combustion efficiency and COV of IMEP at 1500 rpm and 10 bar IMEPg with different EGR rate close to dilution limit

Figure 5.36 with 10 bar IMEPg shows similar trends as well. At 10 bar IMEPg less than 3% combustion stability could be maintained up to 50% EGR rate but due to decrease in combustion stability and less variability, the lower 49% EGR yielded the highest gross indicated efficiencies throughout the entire CA50 sweep. With a knock limited CA50 of close to 8.5 CAD aTDC a maximum of about 42.2% gross indicated efficiency was obtained at 10 bar IMEPg with 49% external EGR dilution rate.

At the limiting EGR rates a common observation throughout the entire load range was that the highest gross efficiency was typically obtained with a slightly lower EGR rate than the maximum tolerable limit due to decrease in combustion efficiency. Determination of EGR tolerance limit should be based on both the indicated efficiency and COV of IMEP.

Figure 5.37 plots gross indicated efficiency, combustion efficiency, NOx emission measurements and COV of IMEP at different loads ranging from 2 bar to 10 bar IMEPg with their respective maximum tolerable EGR limits. Figure 5.37(a) shows that 2 bar IMEPg with 15% EGR demonstrated the lowest gross indicated efficiency of about 35.2%. This is markedly lower than rest because of the significantly higher percentage of heat loss at such low load. 2 bar IMEPg demonstrates a lower EGR tolerance as well. At lower loads it is difficult to maintain high EGR rate because of the significantly decreased combustion temperatures inside the pre-chamber and the main chamber.

At 4 bar IMEPg with 36% EGR, gross indicated efficiency of about 39% was achieved. The maximum gross indicated efficiency of 42.2% was obtained at 10 bar IMEPg. Generally, it is seen that the gross indicated efficiency increased with increasing load. This happens due to the lower percentage of heat loss at higher IMEPs. Most importantly, it is observed that the Jetfire system

could maintain a significantly higher percentage of external EGR rate for a broader load range compared to the reported data from ignition systems. Accordingly, higher indicated efficiency in the vicinity of 40% could be maintained throughout a broader load range as well.

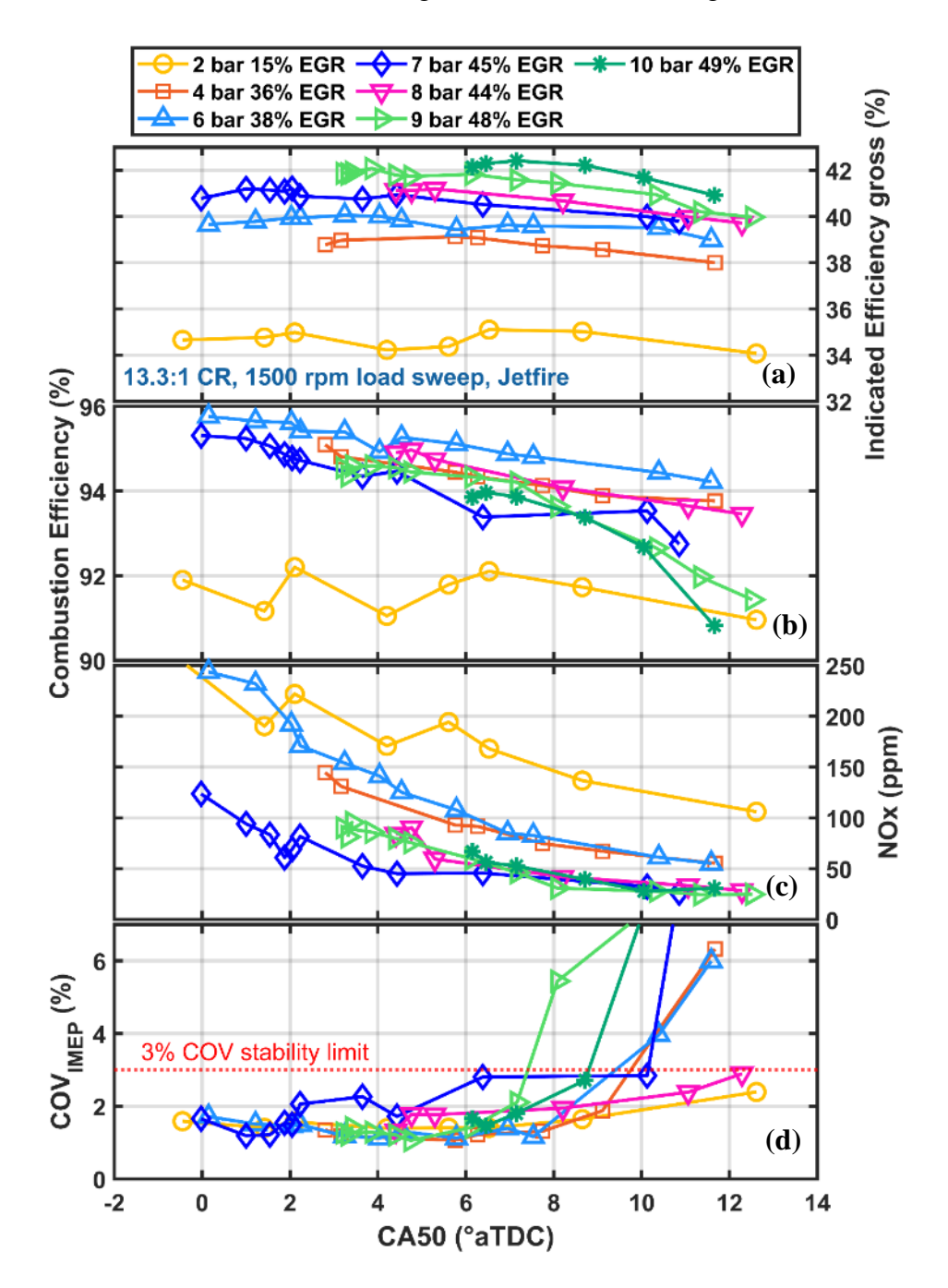


Figure 5.37 Gross indicated efficiency, combustion efficiency, NOx emission and COV of IMEP at 1500 rpm and 2 bar to 10 bar IMEPg load sweep at maximum tolerable EGR limits

Figure 5.37(b) plots the combustion efficiency obtained with different loads. Other than the 2 bar case rest maintained very good combustion efficiency at considerably high level of EGR dilution rate. As expected, combustion efficiency generally increased with advance CA50 phasing for all the loads. Advancing the CA50 meant that a higher percentage of cylinder charge was consumed before the rapid expansion takes place and results into bulk flame quenching.

Figure 5.37(c) shows the NOx emission results at different load conditions. Due to higher than 40% EGR rate involved in loads of 7 bar and higher, most of the resulting NOx emission was lower than 100 ppm at high loads. Depending on combustion phasing, NOx emission in the range of 15 to 20 ppm was observed with 7 to 10 bar loads. In general, it is seen that higher EGR rate resulted in lower NOx emission which is expected since NOx formation is largely dependent on combustion temperature and with higher EGR rate combustion temperature drops significantly which results in a marked decrease in NOx emission.

Figure 5.37(d) shows the effectiveness of the Jetfire system to maintain very good combustion stability throughout the entire 2 to 10 bar IMEPg load range at considerably higher EGR dilution rate than other pre-chamber or SI systems. Overall, substantially higher rate of EGR dilution tolerance throughout the entire 2 to 10 bar load range means that Jetfire system has the potential to deliver a substantial fuel economy benefit if it can be utilized in an adaptive manner.

## 5.4.13 Jetfire: lower compression ratio 10 bar IMEPg at 1500 rpm

While Jetfire system was able to maintain knock free stable operation with up to 50% EGR dilution at a maximum load of 10 bar IMEPg, the highest achievable load condition at the high compression ratio (13.3:1) configuration was limited by knocking. It was difficult to increase the load beyond 10 bar IMEPg without running in to higher knock. Due to tendency of knocking at higher loads the compression ratio was decreased from 13.3:1 to 8.9:1. This enabled testing of higher loads up to 21 bar IMEPg. Although due to the decrease in compression ratio the gross indicated efficiency also decreases.

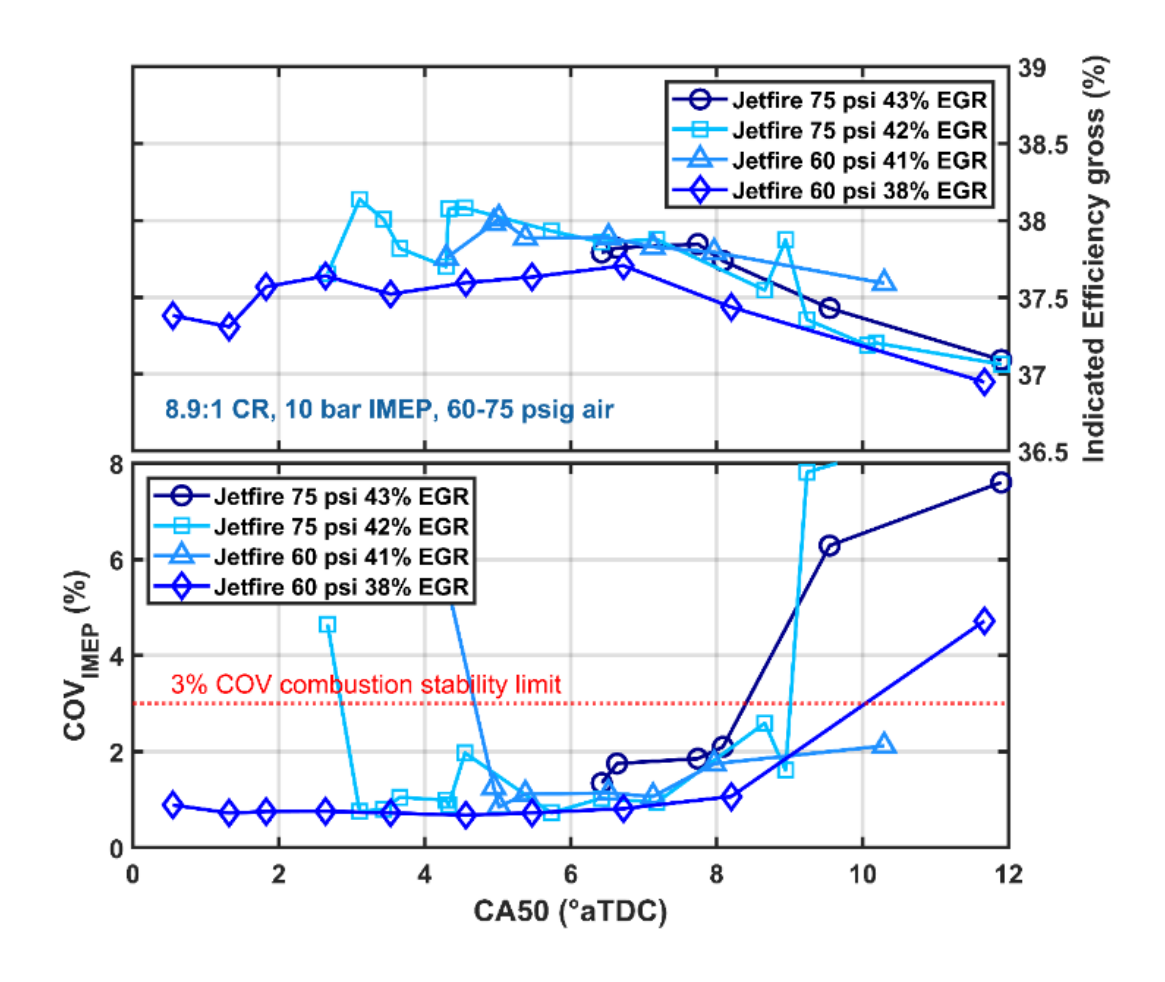


Figure 5.38 Comparison of gross indicated efficiency and COV of IMEP versus CA50 at 1500 rpm and 10 bar IMEPg with about 40% EGR rate at lower 8.9:1 compression ratio

As shown in figure 5.38 at about 42 to 43% EGR rate up to 38% gross indicated efficiency was obtained at similar operating condition of 1500 rpm and 10 bar IMEPg. This is about 2.5 percentage point lower than the gross indicated efficiency obtained with 13.3:1 compression ratio at similar speed-load condition and EGR rate (shown in figure 5.39). With 75 psig and 60 psig the maximum EGR tolerance rate of 43% and 41% was obtained, respectively. This is 1 percentage point lower than the highest EGR tolerance limit obtained with the higher compression ratio. This behavior is expected since higher compression will result in higher charge temperature at the time of ignition inside the pre-chamber.

#### 5.4.14 Jetfire: effect of compression ratio

Figure 5.39 compares the gross indicated efficiency and COV of IMEP due to change in compression ratio under similar EGR dilution rate at 1500 rpm 10 bar IMEPg load condition. It is clear that higher compression ratio offers substantial efficiency benefit over the lower compression ratio with similar dilution level. Higher compression ratio enables the combustion gas to expand through a higher temperature difference, thus increasing the indicated work. Although at 13.3:1 compression ratio the operation is still knock limited, the resulting knock limited efficiency is still better than the low compression results. In fact, the effect of combustion phasing is more prominent at higher compression than the lower compression from the indicated efficiency standpoint.

In figure 5.39 the indicated efficiencies for the higher compression ratio plotted against CA50 are much steeper than the plots at lower compression ratio. This suggests that high EGR dilution rate can be more effective at high compression ratio than the low compression ratio. Higher the EGR rate better the combustion phasing will become, and the combustion phasing has a much greater effect at high compression. In fact, figure 5.39 suggests that at low compression ratio a degree of spark advance around MBT results in negligible efficiency gain, whereas at high compression ratio

a degree of spark advance before the knock limit, increases the gross indicated efficiency by almost 1 percentage point.

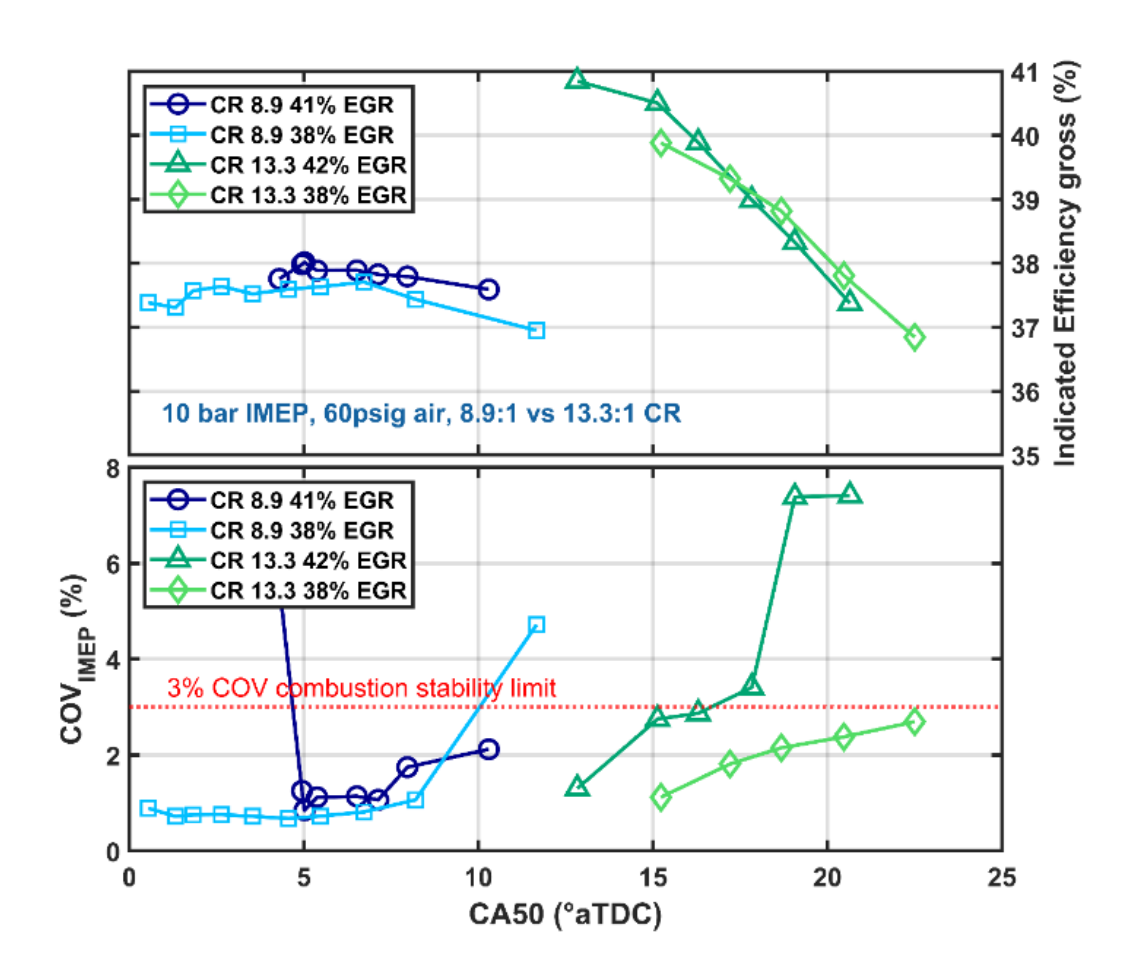


Figure 5.39 Comparison of gross indicated efficiency and COV of IMEP between 13.3:1 and 8.9:1 compression ratio at 1500 rpm and 10 bar IMEPg with similar EGR dilution rate and 60 psig prechamber air pressure

A similar trend was observed with the EGR limit as well, at low compression ratio 3 percentage points increase in EGR resulted in about 0.2 percentage point change in maximum gross indicated efficiency. In contrast, at higher compression ratio, a 4 percentage points increase in EGR rate resulted in about 1.5 percentage point increase in gross indicated efficiency. This suggests that Jetfire ignition system with its high EGR tolerance limit can be more effective at high compression

ratio knock limited situations though at high compression ratio more than 10 bar IMEPg loads can be difficult to achieve due to knocking. Miller valve timing could be used to mitigate this issue. At 38% EGR lowering the compression ratio resulted into a drop of 1.6 percentage point in efficiency and at 41-42% EGR the drop in efficiency due to lower compression was about 2.5 percentage points.

#### 5.4.15 Jetfire: high loads at low compression ratio

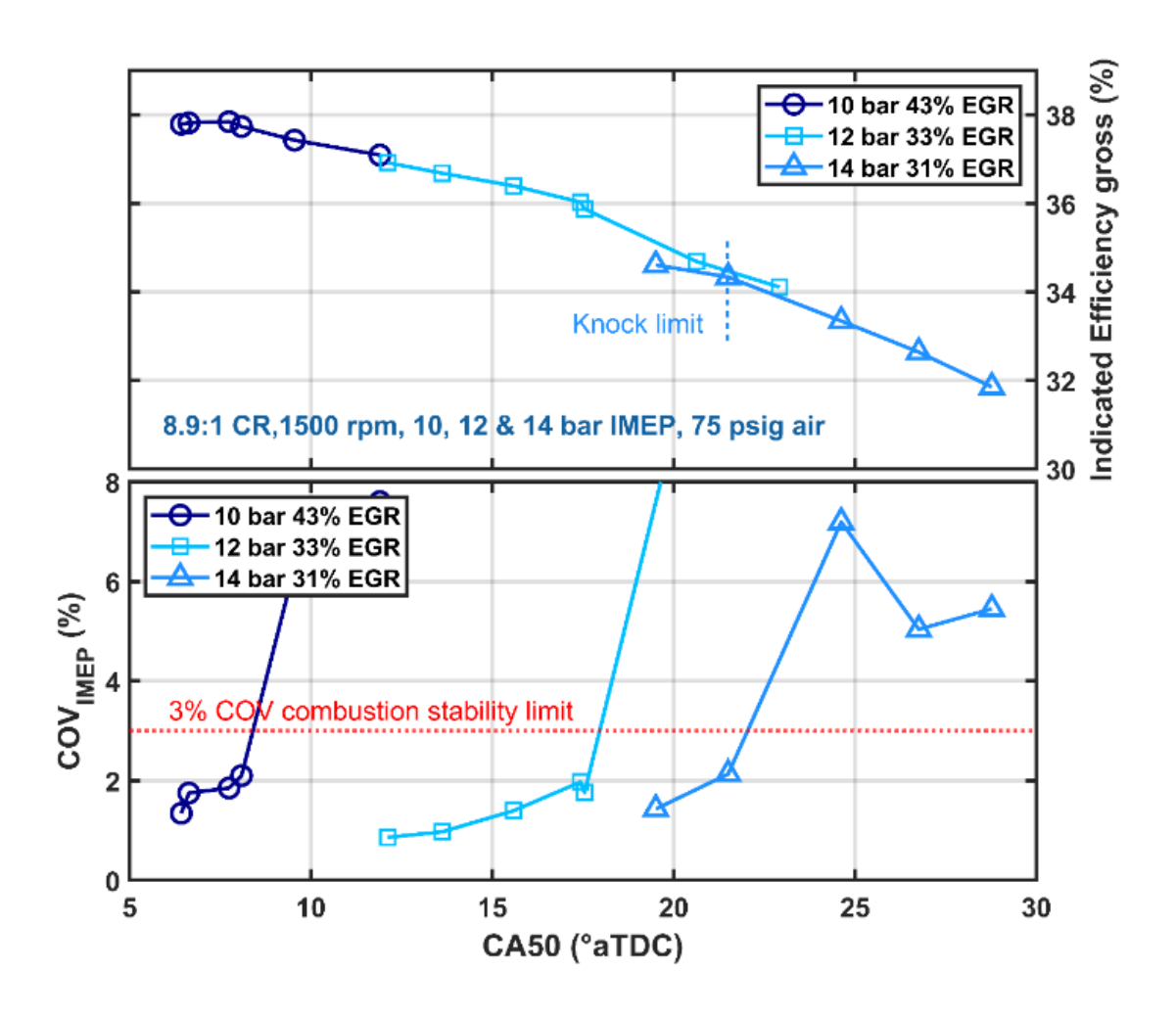


Figure 5.40 Comparison of gross indicated efficiency and COV of IMEP at 10, 12 and 14 bar IMEPg and 1500 rpm at 8.9:1 compression ratio and pre-chamber air valve pressure of 75 psig

Figure 5.40 compares the gross indicated efficiency and COV of IMEP at increasing load condition

tested at 1500 rpm with low compression ratio. It was found that with increase in load the gross indicated efficiency dropped significantly. This happens mainly due to the knock-limited combustion phasing effect. As seen in figure 5.40, at 10 bar IMEPg not only was the load lower but also the EGR rate was 10 percentage points more than the 12 bar IMEPg case. This enables better combustion phasing at 10 bar, resulting in an increase in gross indicated efficiency. Between 12 bar IMEPg and 14 bar IMEPg cases, higher load meant higher knocking tendency and required significant spark retard to maintain knock within the set limit. The 14 bar IMEPg case had the most retarded combustion phasing resulting in the lowest obtained efficiency values within the group.

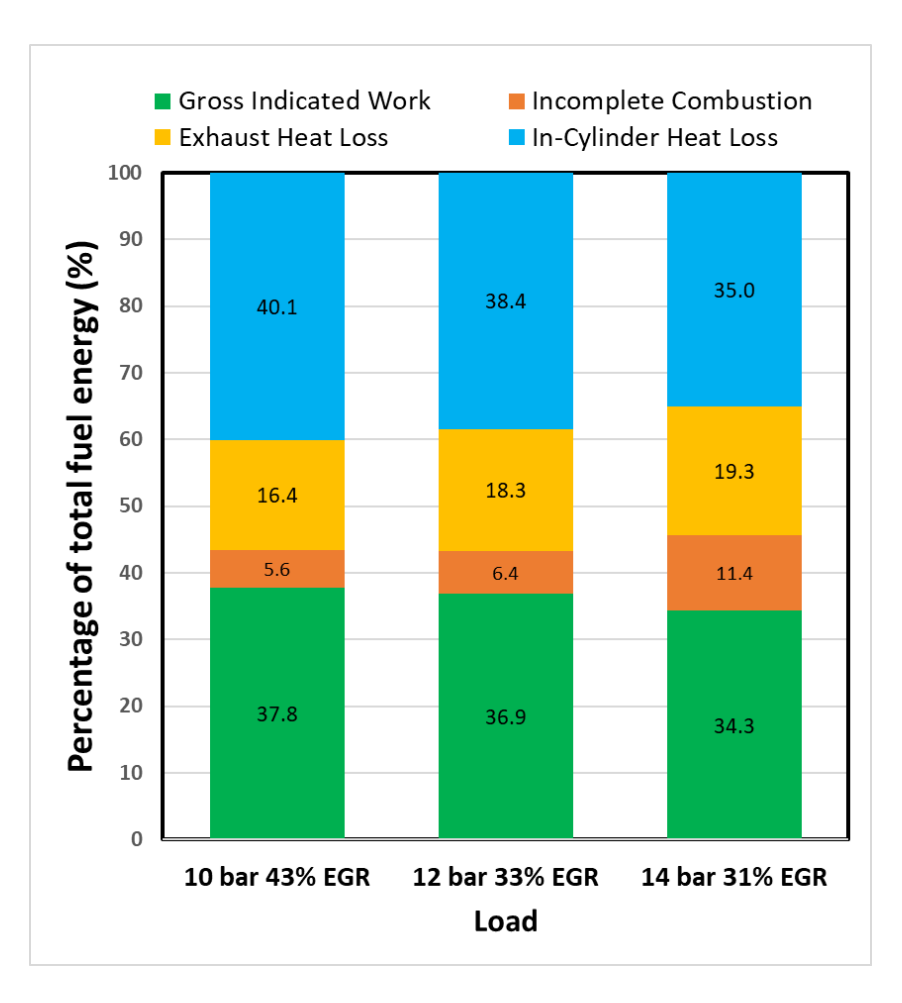


Figure 5.41 Comparison of gross indicated efficiency and COV of IMEP at 10, 12 and 14 bar IMEPg and 1500 rpm at 8.9:1 compression ratio and MBT/KLSA timing

Figure 5.41 compares the different loss percentages determined from first law analysis at different load conditions and 1500 rpm at their highest indicated efficiency points. The benefit of combustion phasing is apparent from the 10 bar IMEP energy split where highest indicated work was obtained. While better combustion phasing results in the lowest exhaust loss, the in-cylinder heat loss was found to be the highest. However, the decrease in exhaust loss and incomplete combustion loss offset the increase in heat loss. With higher loads the system becomes more knock prone and greater spark retard is required to maintain stable operation within the knock limit. This retarded combustion phasing results in substantially higher exhaust enthalpy loss and decreased combustion efficiency as well. Even if the in-cylinder heat loss is lower due to retarded spark timing, incomplete combustion loss and a much greater exhaust enthalpy loss far outweigh the decreased heat loss and results into overall reduction in gross indicated efficiency. Another interesting observation from figure 5.41 was that at the 14 bar IMEPg the incomplete combustion loss was almost doubled compared to that in the 10 and 12 bar cases. This suggests that at a given engine speed there is a load limit characterized by knock limited operation beyond which the combustion phasing and the in-cylinder turbulence limit the combustion efficiency and incurs efficiency losses.

# 5.4.16 Jetfire: effect of engine speed at high dilution

Figure 5.42 compares the gross indicated efficiency and COV of IMEP obtained at 12 bar and 14 bar IMEPg with similar EGR rate but at different engine speeds. It is clear from the plots shown in figure 5.42 that at both load conditions higher engine speeds led to increased gross indicated efficiency. At 12 bar IMEPg load increasing the engine speed from 1500 rpm to 2000 rpm resulted in an increase of about 2.7 percentage points increase in maximum gross indicated efficiency. On the other hand, at 14 bar IMEPg load increasing the engine speed from 1500 rpm to 2000 rpm led

to an increase of 3.6 percentage points in knock limited gross indicated efficiency. Since similar dilution levels were used for all these cases it can be concluded that higher engine speed results in better knocking characteristic as evidenced by the advanced CA50 phasing at higher speeds. With higher engine speed the in-cylinder turbulence increases which increases the burn rate of the incylinder air fuel charge and prevents knocking. This reduced knocking tendency at higher engine speed enables the CA50 to be advanced further. This advanced CA50 phasing contributes to the the increase in gross indicated efficiency at higher engine speeds. A first law energy breakdown at these different speeds provides more detail about the gain in gross indicated work with higher engine speeds.

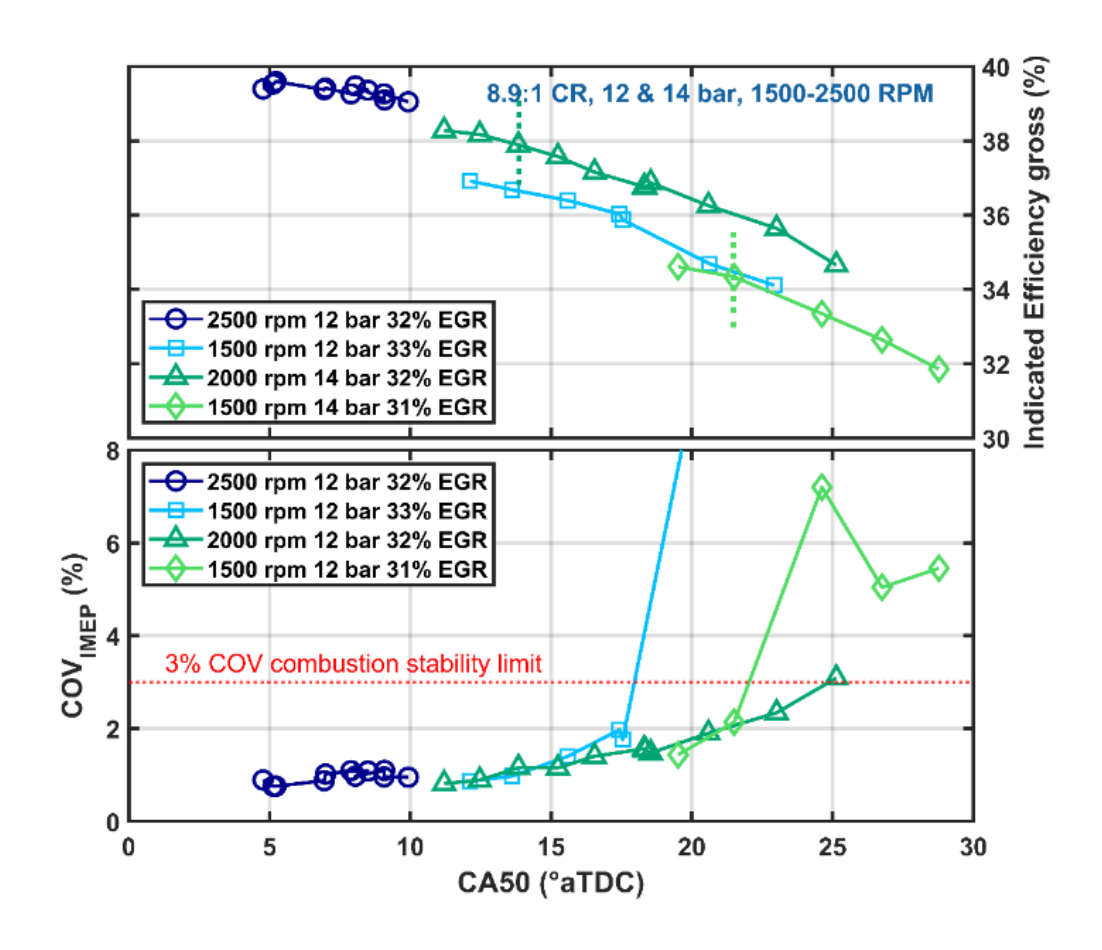


Figure 5.42 Comparison of gross indicated efficiency and COV of IMEP at 12 and 14 bar IMEPg with different rpm

Figure 5.43 shows the split of losses at 12 and 14 bar IMEPg at different engine speeds and calculated at their respective MBT or KLSA operating points. It is apparent from figure 5.43 that the increase in gross indicated work at higher engine speed primarily results from a considerable decrease in in-cylinder heat losses at elevated speed. At higher engine speed the cycle time is decreased which in turn reduces the available time duration for the heat transfer to take place. This reduces the heat transfer loss considerably and increases the indicated work. Another observation is that at 14 bar load 2000 rpm case results in a considerable decrease in incomplete combustion loss compared to the 1500 rpm. This happens due to the increased turbulence and a subsequent increase in burn rate at higher engine speeds.

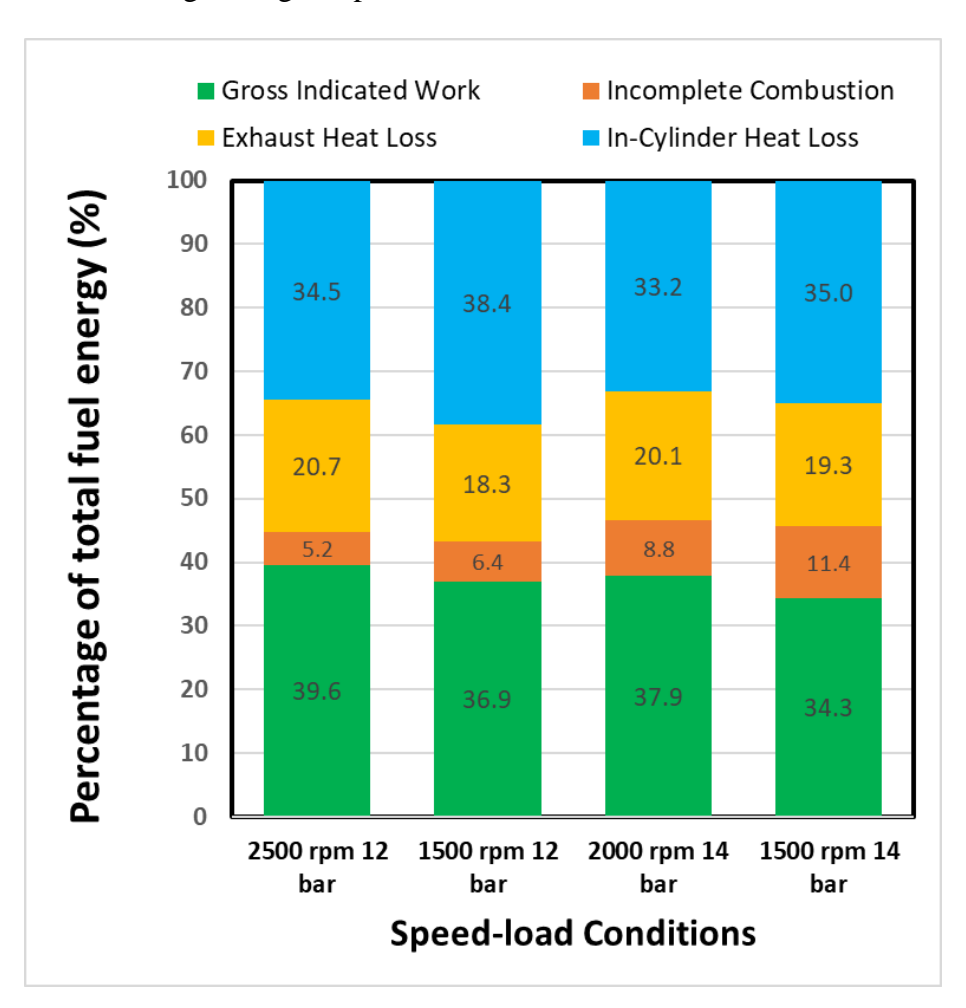


Figure 5.43 Split of losses at 12 and 14 bar IMEPg with different engine speed at MBT/KLSA timing

These results suggest that the gross/net indicated efficiencies reported earlier at 1500 rpm and high EGR load sweep points have the potential to yield even higher efficiency figures at higher engine speeds. Further experiments at higher engine speed are needed to confirm that.

## 5.4.17 Jetfire: high loads (up to 21 bar IMEP) diluted operation at 2000 rpm

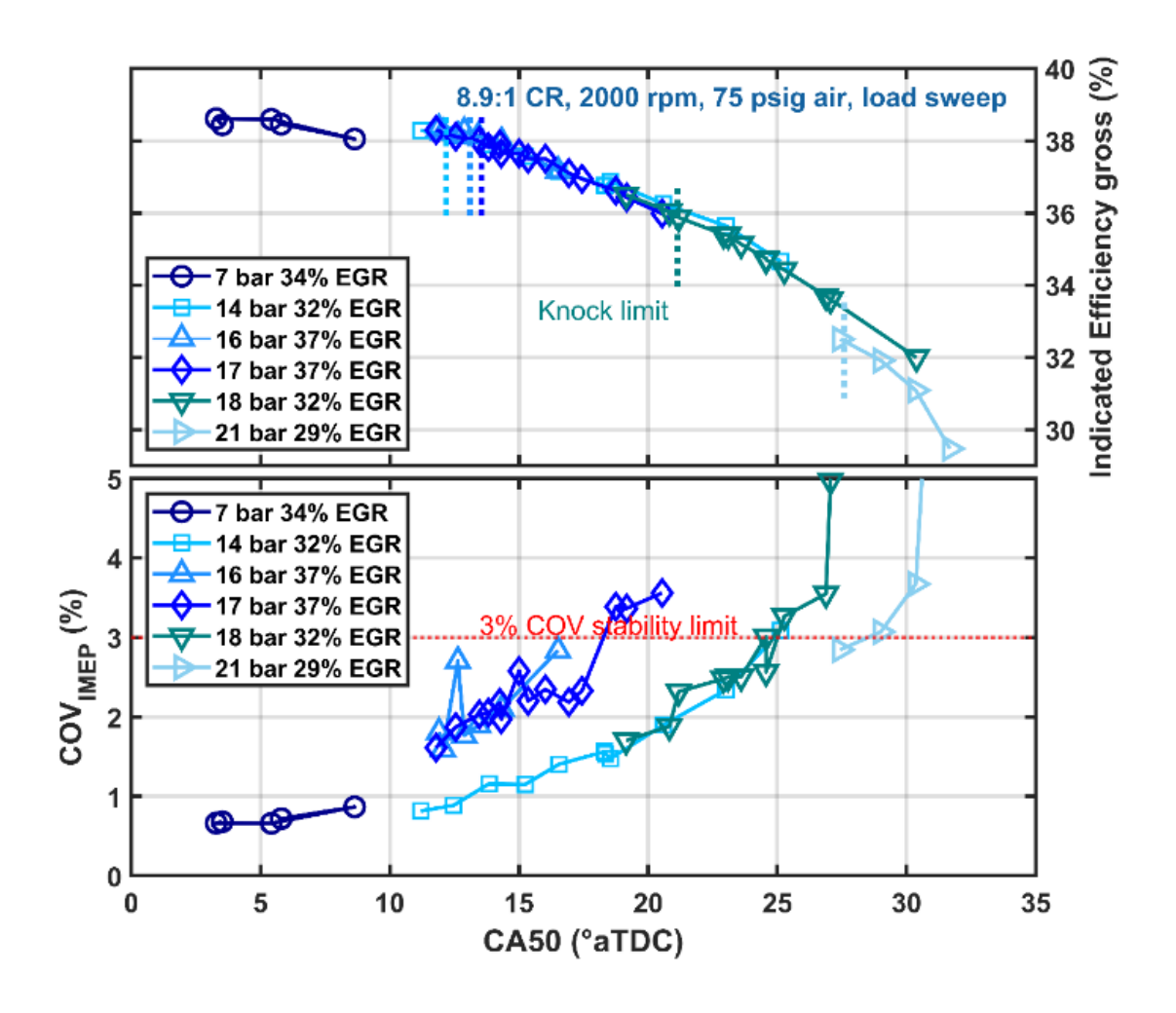


Figure 5.44 Gross indicated efficiency and COV of IMEP at 2000 rpm and different loads ranging from 7 to 21 bar IMEPg, 75 psig pre-chamber air pressure

Figure 5.44 shows that the Jetfire system could maintain acceptable combustion stability with considerably higher EGR percentage up to a maximum load of 21 bar IMEPg at 2000 rpm. While the gross indicated efficiency was the lowest at slightly above 32% at 21 bar operating point, for

rest of the load points considerably higher efficiency values were obtained. In fact, up to 17 bar IMEPg the Jetfire system could maintain knock limited gross indicated efficiency of around 38% which is comparable to the efficiency obtained at 7 bar IMEPg. At 18 bar IMEPg the gross indicated efficiency was still about 36%. This shows that the Jetfire system could maintain comparable efficiency through a broader load range while maintaining high EGR tolerance. These results were obtained during a preliminary test run and high EGR rates were not tested. Jetfire system has already been shown to work with much higher EGR rate than what was used in this set of test runs and further tests should improve upon the results shown in figure 5.44.

## 5.4.18 Comparison: Jetfire vs SI at low compression ratio

While lowering the compression ratio of the Jetfire system from 13.3:1 to 8.9:1 enabled testing loads higher than 10 bar IMEPg, the indicated efficiency suffers considerably (up to about 6% drop as previously shown in figure 5.39). Jetfire system becomes more effective at knock-limited high-compression-ratio environment where the faster combustion and high EGR tolerance enabled by the air/fuel purged pre-chamber allows considerable advantage in maintaining stable operation within the knock limit. To emphasize this point, additional tests were conducted with conventional SI system at the same 8.9:1 and 1500 rpm 10 bar IMEPg load with maximum allowable EGR rate. Figure 5.45 shows the results from this set of tests in terms of gross indicated efficiency and COV of IMEP obtained at different EGR dilution rates. It is seen from figure 5.45 that at 23% EGR rate it was difficult for SI to maintain less than 3% COV combustion stability limit. Decreasing the EGR rate to 20% kept the combustion stability within the acceptable limit. Since this was at a lower compression ratio, a more conservative knock limit of 10% of the cycles crossing 0.5 bar MAPO was chosen for the knock limited CA50 determination. A maximum of slightly above 37% gross indicated efficiency was obtained at SI configuration with a maximum EGR dilution

tolerance of 20%.

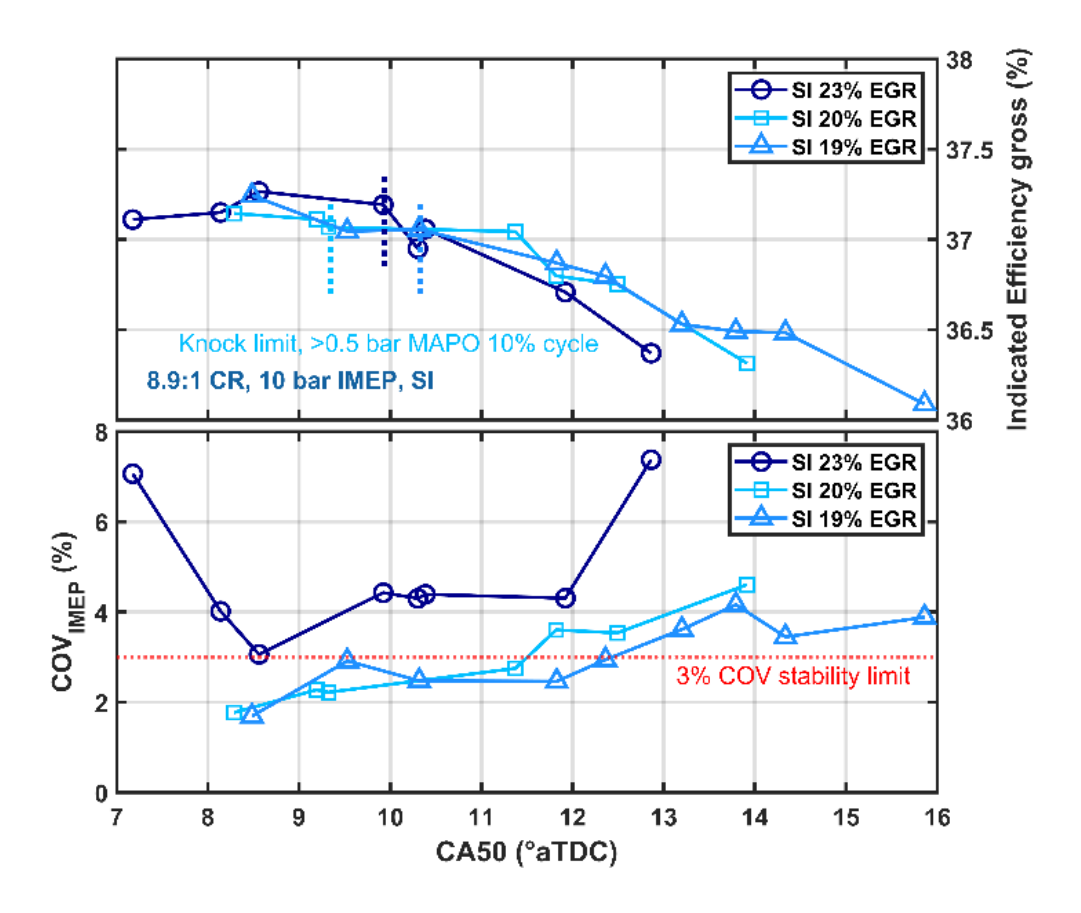


Figure 5.45 Gross indicated efficiency and COV of IMEP with different EGR rate at 1500 rpm and 10 bar IMEPg at 8.9:1 compression ratio obtained with conventional SI system

Figure 5.46 compares the results obtained at 1500 rpm 10 bar IMEPg between Jetfire and conventional SI with their highest EGR dilution limits at 8.9:1 compression ratio. Figure 5.46(a) compares the gross indicated efficiency obtained with the Jetfire with 42% EGR against the SI with 20% EGR. While Jetfire clearly shows twice as much dilution tolerance compared to SI, only 1 percentage point increase in gross indicated efficiency was observed. Besides, additional work is required for the Jetfire to compress and supply the pre-chamber purge air which will lower the indicated efficiency as well. This data with the Jetfire at lower compression ratio were obtained with 60 psig pre-chamber air pressure. This additional purge air delivery work results into 0.6

percentage point decrease in indicated efficiency. Ultimately, Jetfire could only provide a modest 0.4 percentage point improvement in indicated efficiency over the conventional SI at lower compression ratio non knocking environment. Even with more than 40% EGR dilution, higher heat transfer loss due to increased surface area from the pre-chamber prevented the Jetfire system to provide considerable improvement over SI.

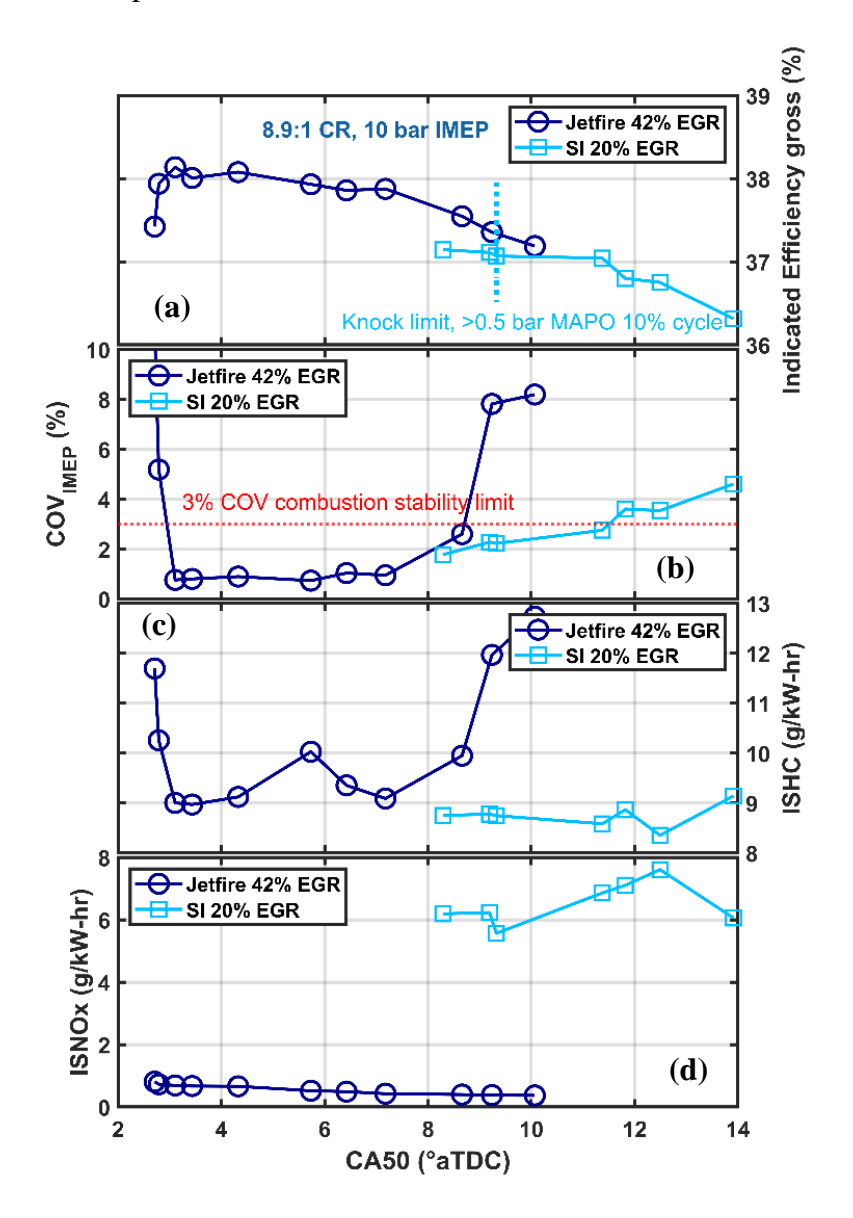


Figure 5.46 Comparison of (a) gross indicated efficiency, (b) COV of IMEP, (c) indicated specific hydrocarbon emission and (d) indicated specific NOx emission between the Jetfire and conventional SI systems at highest respective EGR dilution limit

As mentioned previously, a more conservative 0.5 bar MAPO threshold was set for knock limit for this comparison to indicate the advantage with knocking with Jetfire. While under this conservative knock threshold SI operation was found to be knock limited, even with a CA50 of approximately 2.5 CAD Jetfire did not show any indication of knocking. Thus, with Jetfire even though the indicated efficiency does not show a marked improvement over SI, higher EGR tolerance still provides substantial benefit in lowering knock tendency. This could be even more prominent with the knock threshold set to lower limits. From figure 5.46(b) it is seen that the Jetfire system could maintain better combustion stability even with twice as much EGR dilution compared to SI. This shows the effectiveness of the Jetfire system to deal with very high EGR dilution rate.

Figure 5.46(c) compares the indicated specific hydrocarbon emission between Jetfire and SI. It is seen from this figure that Jetfire demonstrated marginally higher (but still very much comparable) hydrocarbon emission compared to SI. This is expected since Jetfire was operating with more than twice as much EGR dilution rate compared to SI and high EGR dilution almost always results in slightly elevated hydrocarbon (HC) emission.

Figure 5.46(d) on the other hand shows another substantial advantage of utilizing high EGR rate in engines and that is significant decrease in NOx emission. It is seen from figure 5.46(d) that with Jetfire around 0.5-0.6 g/kW-hr indicated specific NOx emission was obtained; whereas with SI the indicated specific NOx emission was around 6-7 g/kW-hr. Thus, Jetfire provides more than 90% decrease in NOx emission compared to SI. In spite of such advantage with NOx emission, a moderate increase in indicated efficiency compared to SI makes the Jetfire system less effective at non-knocking conditions. This is similar to the findings at 6 bar IMEPg at elevated compression ratio presented before where it was seen that Jetfire could provide only modest improvement over

SI. Nonetheless, Jetfire still provides a slight improvement over SI in all these non-knocking situations. Traditionally, TJI and similar pre-chamber systems operating at stoichiometric conditions (lambda 1) suffer significantly to compete with SI in terms of thermal efficiency because of the significant increase in heat loss inherent to the pre-chamber-initiated ignition systems. Jetfire on the other hand, with its high EGR tolerance limit offsets this higher pre-chamber heat loss and makes the system on par or even marginally better than SI in terms of thermal efficiency.

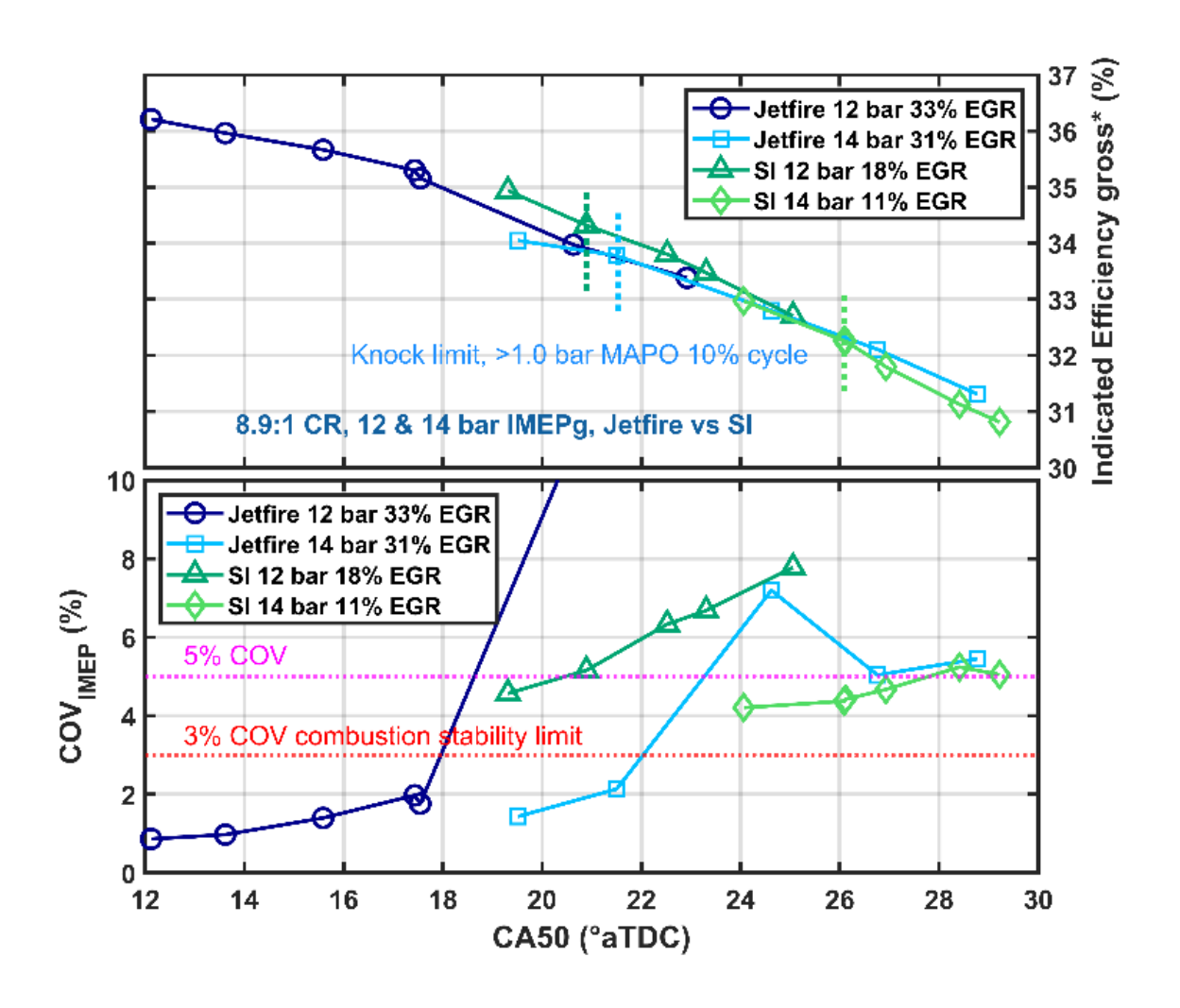


Figure 5.47. Comparison of gross indicated efficiency and COV of IMEP between Jetfire and SI operating at 12 and 14 bar IMEPg and 1500 rpm at 8.9:1 compression ratio. For Jetfire the gross indicated efficiency includes the purge work loss

To demonstrate the effectiveness of Jetfire compared to traditional SI a test run was conducted with SI operating at higher knock limited 12 and 14 bar IMEPg loads and 1500 rpm. A separate CFD analysis conducted at 1500 rpm with the current engine head and intake port geometry showed significantly lower turbulence compared to modern intake ports. From the initial test runs it was evident that higher load operation (12-14 bar IMEPg) especially with EGR was difficult to maintain with a COV<sub>IMEP</sub> limit of 3% and a knock threshold of 10% cycles exceeding 1 bar MAPO. Thus, for the spark sweep with SI at 12 and 14 bar IMEPg loads a less conservative COV<sub>IMEP</sub> limit of 5% was targeted. Figure 5.47 compares the results obtained from these higher load spark sweeps against the results obtained previously with the Jetfire system at the same loads and compression ratio. Jetfire was capable of maintaining very good combustion stability (<3% COV<sub>IMEP</sub>) at both 12 and 14 bar IMEPg loads with a maximum EGR rate of 33 and 32%, respectively. In contrast, SI barely maintained 5% COV at 12 bar IMEPg with 18% EGR and 14 bar IMEPg with 10% EGR. Figure 5.47 clearly demonstrates that at knock limited operating conditions Jetfire offers substantial advantage in combustion phasing compared to SI. Substantially higher EGR tolerance with the Jetfire system allowed it to lower the knocking tendency and advance the combustion phasing considerably. Advanced combustion phasing enabled by the Jetfire system resulted into considerable increase in gross indicated efficiency compared to SI. As shown in figure 5.47, at 12 bar IMEPg load Jetfire delivers about 1.9 percentage points higher indicated efficiency compared to SI. At 14 bar IMEPg, with Jetfire a 1.5 percentage points higher indicated efficiency was obtained compared to traditional EGR. The Jetfire gross efficiency figures include the loss incurred due to purge air delivery. If the SI combustion stability limit were set to the same scale as that of Jetfire, these numbers would have been even higher. For pre-chamber systems the jets emerging from the main chamber not only initiate combustion at multiple sites distributed around the main

chamber but also introduce additional turbulence to ensure fast flame speed. Thus, intake flow and geometry induced turbulence or lack thereof might not have the same effect on the pre-chamber systems as it has on the SI system. Further investigation is required to confirm that. In any case, it is evident from this set of experiments that even with lower compression ratio at knock limited high load operating conditions Jetfire system offers substantial benefits over conventional SI system in terms of EGR tolerance, combustion stability and thermal efficiency.

## 5.4.19 Jetfire: aluminum vs stainless steel cartridge design

The original Jetfire cartridge made from stainless steel did not have any active cooling arrangement other than the pre-chamber purge air cooling flowing through it. This arrangement resulted in Jetfire cartridge temperature rising beyond 250 °C under continuous operation for extended periods of time. In response to this overheating concern, the Jetfire cartridge material was changed to aluminum and the head was re-machined to make provision for coolant flow around the Jetfire cartridge to keep the temperature under control. All the previous test results with the Jetfire cartridge presented before had been obtained with the aluminum cartridge. It was found that the modified head and cartridge material offered significant increase in cooling. In fact, during testing the aluminum cartridge temperature did not exceed 120 °C limit. While this aggressive cooling design served its purpose at demonstrating the relative effectiveness of Jetfire through the results presented here, excess cooling can actually be counterproductive to the combustibility of the prechamber mixture with high percentage of EGR dilution. Due to the higher quenching tendency of the EGR diluted combustion any additional cooling of the pre-chamber can lead to even further deterioration of ignitability of the pre-chamber mixture. There was also an additional disadvantage of increased heat loss from the cooler pre-chamber as well. Based on the Jetfire cartridge average temperature (around 110-115 °C for majority of the time) measured during the testing with the

aluminum cartridge, a decision was made to run some preliminary tests with a stainless-steel cartridge that maintains a comparatively higher pre-chamber cartridge temperature. This stainless-steel cartridge did have additional coolant flowing around it due to the re-machined head, but the annular flow passage was smaller compared to the aluminum design.

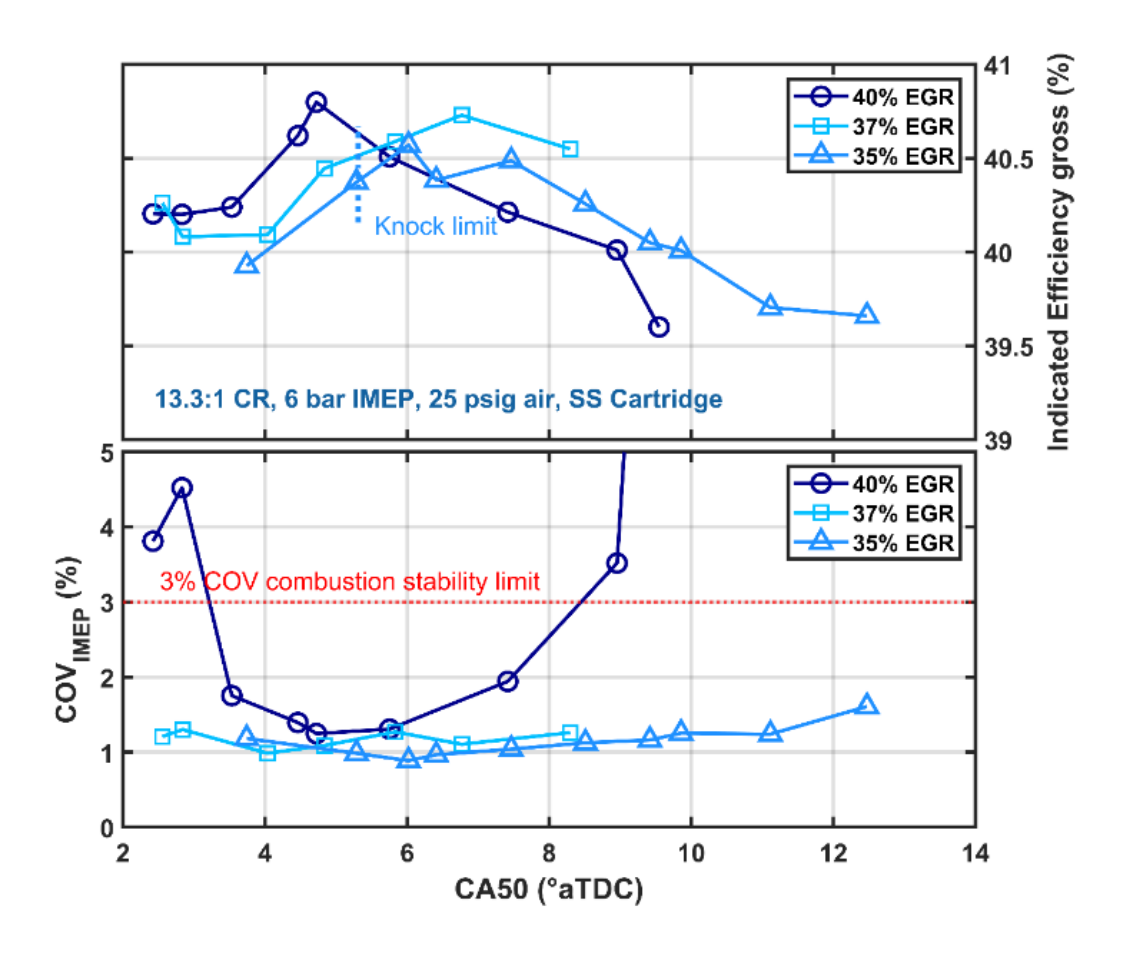


Figure 5.48 Gross indicated efficiency and COV of IMEP versus CA50 at varying EGR rate at 1500 rpm and 6 bar IMEPg with 25 psig pre-chamber air pressure; Jetfire with stainless steel cartridge

Figure 5.48 shows some preliminary results obtained with the stainless-steel cartridge at 6 bar IEMPg and 1500 rpm with 25 psig pre-chamber air pressure and different EGR dilution rate. 25 psig pre-chamber air pressure was chosen based on a maximum air flow rate of 0.5 SCFM. As it demonstrated in figure 5.48, Jetfire with stainless-steel cartridge could maintain stable operation

with up to 40% EGR dilution rate with 25 psig pre-chamber air pressure. This maximum EGR tolerance is 4 percentage point higher than the maximum EGR tolerance with 15 psig pre-chamber air pressure and 2 percentage point higher than the 30 psig air pressure, both obtained with aluminum cartridge. The maximum cartridge temperatures during this set of tests were found to be around 190 °C, about 80 °C higher than those found with aluminum cartridge. According to the results shown in figure 5.48, this elevated cartridge temperature improves the maximum EGR tolerance of the system. If the stainless-steel case is compared to the 30 psig aluminum case, it is observed that with almost 25% lower air flow rate in the pre-chamber stainless-steel cartridge could offer about 5% higher EGR tolerance limit.

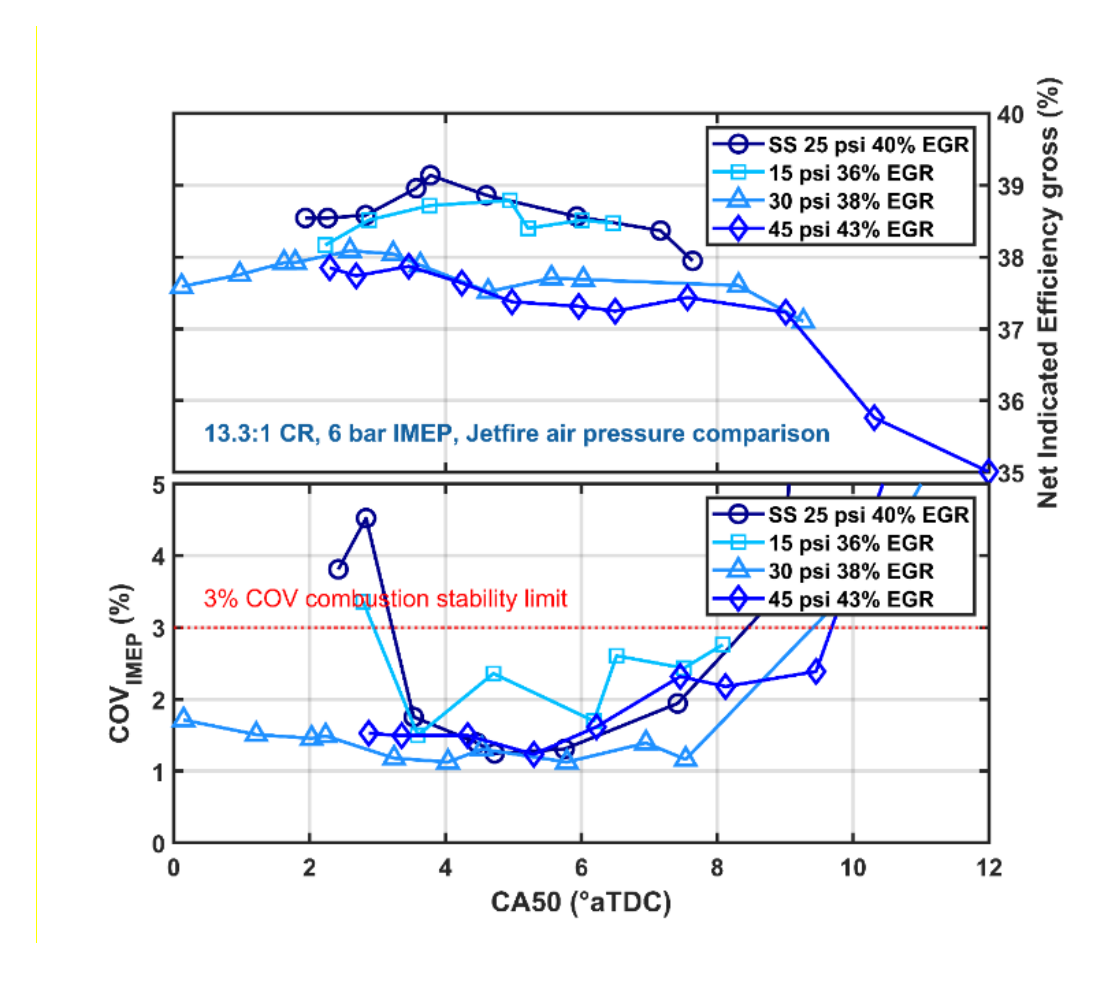


Figure 5.49 Net indicated efficiency and COV of IMEP versus CA50 at 1500 rpm and 6 bar IMEPg with the highest EGR rate at different pre-chamber air pressure; Jetfire aluminum versus stainless steel cartridge

Figure 5.49 compares the net indicated efficiency obtained with the aluminum and stainless-steel cartridge with different pre-chamber air pressures. With the aluminum cartridge it is observed that the lower pre-chamber air pressure showed higher net indicated efficiency. This is due to the higher purge air work loss associated with supply of increased amount of air to the pre-chamber at higher upstream pressure. The stainless-steel cartridge clearly shows an advantage over the aluminum results (as shown in figure 5.49) in terms of net indicated thermal efficiency. Note that this net indicated efficiency includes the work loss due to the purge air delivery to the pre-chamber. While the stainless-steel cartridge with 25 psig pre-chamber air pressure showed only a moderate 0.3 percentage point improvement in net indicated efficiency over the aluminum cartridge with 15 psig pre-chamber air pressure when combustion stability is concerned figure 5.49 shows that stainless steel cartridge provided lesser combustion variability compared to the aluminum cartridge even with more than 10% higher EGR.

Figure 5.50 shows a first law energy breakdown that compares the losses in efficiency for different Jetfire and TJI cases against the conventional SI at their respective highest efficiency points. It is clear that SI has an advantage in terms of in-cylinder heat loss over the pre-chamber systems. This disadvantage in increased heat loss can be offset by the pre-chamber systems by reducing the exhaust enthalpy losses and lowering the pumping work while maintaining acceptable combustion efficiency. It is clear that both TJI systems with their similar dilution limits to the SI cannot provide enough advantage to offset the losses. Jetfire cases with lower pre-chamber air pressure settings, on the other hand, provide enough advantage to offset the increased heat loss and enable a moderate improvement in net indicated efficiency over SI. The fact that the preliminary tests with stainless-steel cartridge provided the highest efficiency cases shows that there is definitely room for further improvement in Jetfire cartridge system design and operation. Similar conclusion was

obtained at 10 bar IMEPg and load sweep conditions where improved pre-chamber operating strategy helped to deliver even greater advantage over TJI systems.

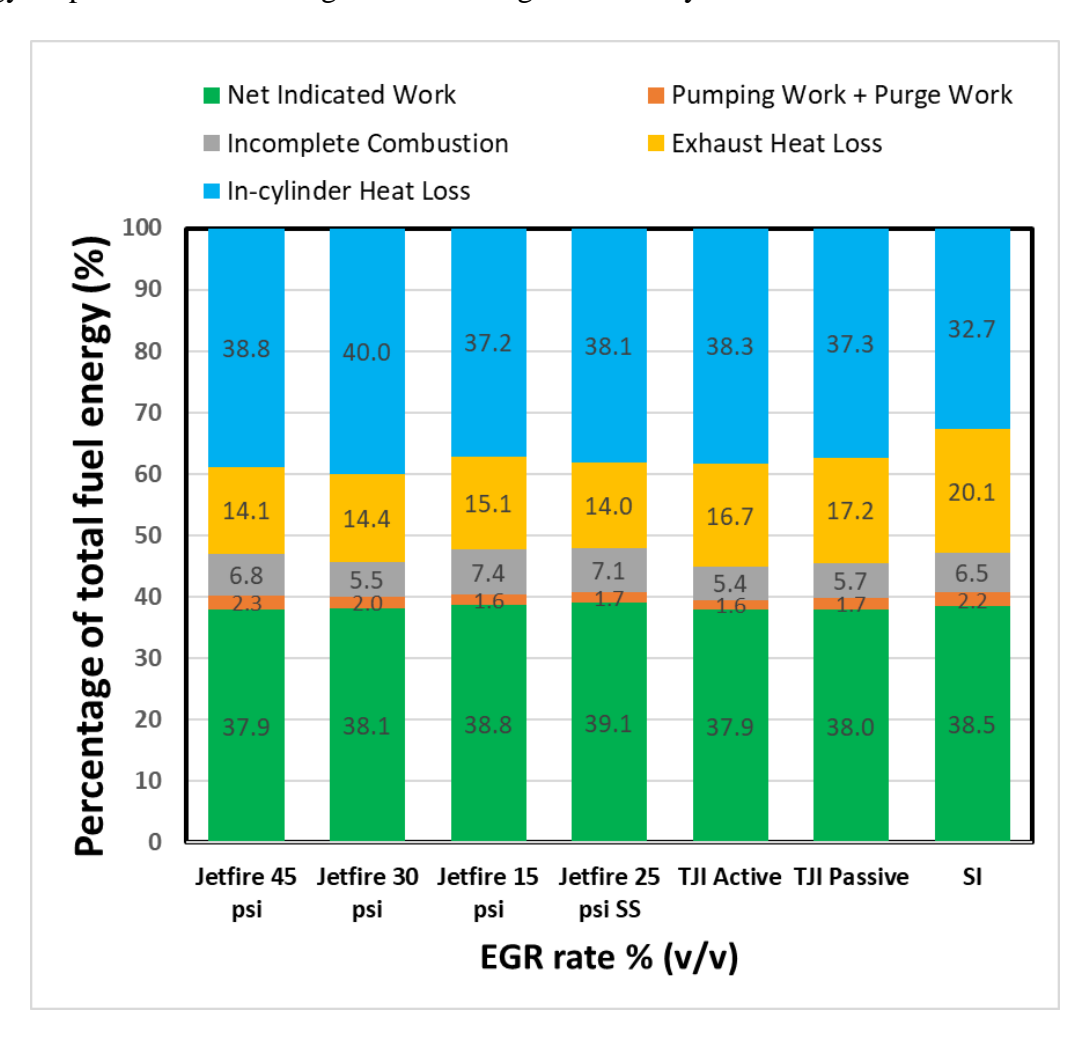


Figure 5.50 Split of losses at 1500 rpm and 6 bar IMEPg condition between Jetfire, TJI active, TJI passive and SI with the highest dilution limits. Numbers on the bar chart correspond to the percentages of total fuel energy

# **5.5 Summary and Conclusions**

In this study a single cylinder metal engine equipped with interchangeable Jetfire (DM-TJI), Turbulent Jet Ignition (TJI, active and passive) and Spark Ignition (SI) cartridges was tested at 6 bar and 10 bar loads at 1500 rpm and with varying external EGR rate to investigate the relative effectiveness of each ignition system at an elevated compression ratio of 13.3:1. With Jetfire three

levels of pre-chamber purge air pressure were investigated at both load conditions. Maximum EGR tolerance limit and indicated efficiency have been identified with each ignition system. The results are summarized as follows-

- At 6 bar IMEP, Jetfire was found to be slightly more favorable pre-chamber solution compared to active and passive TJI systems and was on par with conventional SI in terms of net indicated thermal efficiency.
- At 6 bar IMEP, TJI active, TJI passive and SI all offered somewhat similar maximum external EGR tolerance of 21% to 23%. Jetfire on the other hand, maintained a maximum EGR tolerance of 43%, around twice as much compared to the others.
- Since the mid load 6 bar IMEP operation was not as knock limited as higher load conditions
  would be with high compression ratio, despite almost 100% improvement in EGR tolerance
  limit, Jetfire provided only a moderate improvement at best in thermal efficiency compared
  to others.
- At 6 bar IMEP, Jetfire becomes comparable to TJI or SI in terms of thermal efficiency only when operated with very high rate of EGR dilution (35% and above) to order to offset the additional heat loss and purge work requirement accrued by the pre-chamber air supply. At lower EGR rates Jetfire delivered substantially lower thermal efficiency compared to rest of the ignition systems. Thus, pre-chamber air purge becomes worthwhile only when operated at higher EGR rate.
- For the Jetfire system tested at 6 bar IMEP, higher pre-chamber air pressure/flow rate resulted in about 13 to 20% higher external EGR tolerance limits (depending on the air

pressure used). At 6 bar IMEP, Jetfire system with the lowest 15 psig pre-chamber air pressure seemed to be the most favorable configuration in terms of thermal efficiency. Due to the comparatively lower importance of knock at this mid-load condition, higher EGR tolerance beyond a certain limit does not necessarily become more effective especially given the additional heat loss and the parasitic work loss incurred due to the pre-chamber air purge.

- SI system was found to be inoperable without knock and within 3% COV<sub>IMEP</sub> limit at 10 bar IMEP load at a high 13.3:1 compression ratio.
- At 10 bar, TJI passive achieved a maximum of 37.7% gross indicated efficiency with maximum EGR tolerance of 30%. On the other hand, active TJI configuration was able to extend the maximum EGR tolerance limit to 33% with a slight increase in gross indicated thermal efficiency to 38.4%.
- At 10 bar IMEP load Jetfire system provided substantial efficiency benefits over TJI active and passive configurations. Jetfire could maintain stable combustion (<3% COV<sub>IMEP</sub>) with a maximum EGR dilution rate of 50%. With Jetfire, highest knock-limited gross indicated efficiency of 42.2% was obtained at 10 bar IMEPg with an EGR dilution rate of 49% at 75 psig pre-chamber air pressure. After accounting for the parasitic loss of approximately 1 percentage point to deliver the compressed air to the pre-chamber, the gross indicated thermal efficiency was found to be 41.2 %, which is 3.5 percentage points higher than TJI passive and 2.8 percentage points higher than TJI active. Thus, at knock-limited 10 bar IMEP condition, Jetfire provided more than 7% and 9% higher indicated thermal efficiency than TJI active and TJI passive, respectively.

- Load sweep from 2 bar to 10 bar IMEPg at 1500 rpm and 13.3:1 compression ratio revealed that the Jetfire system maintained close to 40% or greater gross indicated thermal efficiency for all other loads except at 2 bar. At 2 bar 35.1% gross indicated efficiency was obtained with 15% EGR. At 4 bar load 39.1% gross indicated efficiency was observed with up to 38% EGR. At 6 bar the EGR tolerance went up to 43% with maximum gross indicated efficiency of 40.2%. Between 7 bar and 10 bar IMEPg, EGR dilution tolerance ranging from 44% up to 50% was observed with gross indicated efficiency of 41% and greater. In general, it was observed that increasing load helped in improving the EGR tolerance limit as well as the gross indicated efficiency.
- Due to the inability of SI to match the pre-chamber operating ranges at higher 10 bar load the compression ratio was lowered to 8.9:1 and an additional comparison was done between Jetfire (DM-TJI) and SI at 8.9:1 compression ratio. It was observed that even with a lower compression ratio, at higher loads knock-limited environment Jetfire system offered substantial benefits in terms of combustion stability, knock mitigation and thermal efficiency.
- Limited experiments at higher engine speed showed that the advantage of high EGR
  dilution in terms of lowering the in-cylinder heat loss becomes more effective at higher
  speeds. Operations with Jetfire at higher engine speed could potentially offer even higher
  efficiency gains compared to other ignition systems with considerably lower EGR
  tolerance limit.
- Preliminary tests at 6 bar IMEPg and 1500 rpm with stainless steel cartridge instead of aluminum cartridge revealed that higher cartridge temperature delivered better EGR

tolerance under similar pre-chamber air flow. The indicated efficiency was also found to be improved slightly. This suggests that there are potential benefits of maintaining higher pre-chamber cartridge temperature. More work is required to comment on the implications of higher pre-chamber temperature at higher speed-load situations.

- It was generally observed that higher pre-chamber air flow rate led to higher external EGR tolerance. However, the gain in EGR tolerance limit is not always justified at low- to midload conditions because of the lesser concern with knocking. This is because of the higher purge work loss associated with higher pre-chamber air flow. On the other hand, at high loads where the operation is primarily knock-limited, gain in EGR rate yields substantial knock mitigation and subsequent advantage in combustion phasing and efficiency. In that situation, higher pre-chamber air flow rate and hence higher purge work loss can still be of considerable advantage.
- The results obtained with this investigative comparison demonstrate a definite advantage of the Jetfire system over TJI active and passive configurations as well as conventional SI. The advantages became more prominent in high-load, knock-limited situations. Despite the clear advantage demonstrated by the Jetfire system it should be mentioned that the Jetfire system is largely unoptimized. Clearly, more work it required to realize the full benefits from this system.
- Additionally, it should be noted that high rate of EGR dilution at boosted condition has significant implications in terms of engine power density, boost device sizing, EGR availability and handling, etc. The Jetfire ignition clearly has potential, but further developmental effort is required to fully assess its practical viability.

#### **CHAPTER 6**

#### CONCLUSIONS AND FUTURE WORK

## **6.1 Concluding Remarks**

Dilution with EGR instead of excess air can be considerably advantageous from the point of view of compatibility with widely used three-way catalytic converter to reduce the engine-out emissions. The Dual Mode, Turbulent Jet Ignition (DM-TJI) or the Jetfire® ignition system with additional purge air supply to the pre-chamber enables the pre-chamber equipped engines to maintain very high EGR dilution tolerance compared to pre-chamber ignition technologies that either have no active fuel injection inside the pre-chamber or have only the auxiliary fuel injection. While previous investigations on DM-TJI systems have shown the possibility of high dilution tolerance with the additional pre-chamber air supply by maintaining better control to the pre-chamber mixture stoichiometry, actual EGR dilution was still in 'concept' stage.

In this dissertation, actual engine test results demonstrating up to 50% external EGR (v/v) dilution rate with the Prototype III DM-TJI or the Jetfire(® cartridge equipped metal engine have been presented for the first time. It has been shown that EGR dilution can offer similar benefits to the excess air dilution in terms of thermal efficiency especially at knock limited situation while maintaining stoichiometric operation and be compatible with the three-way catalyst. This suggests that the DMTJI/Jetfire® ignition could offer a viable technology pathway to realize the benefits of diluted low temperature combustion without incurring additional cost for the aftertreatment system.

In this work, a comparative analysis between Jetfire, TJI active, TJI passive and conventional SI has been presented. Results showed that Jetfire ignition with its considerably higher (more than 50

to 100%) EGR dilution tolerance compared to the others provided a maximum of 7 to 9% improvement in thermal efficiency compared to TJI configurations and greater than 11% improvement over SI. The analysis revealed that Jetfire becomes more effective at higher load knock limited situation. Jetfire and the other pre-chamber systems maintained stable, knock-free operation at higher loads where conventional SI failed to operate. Because of the high EGR dilution tolerance Jetfire provided substantial advantage in knock mitigation and hence thermal efficiency at high load knock limited operation. As the push towards downsized turbocharged engines with high power density becomes even more prominent, Jetfire ignition technology could be a very effective approach especially when coupled with split power hybrid applications.

#### **6.2 Recommendations for Future Work**

While the current analysis showed that Jetfire ignition system can be of considerable benefit at high load knock limited situation, it should be noted that the investigation was conducted on a limited number of speed-load situations. A broader test matrix with higher speeds and loads will be able to deliver a better estimation on the real-world fuel economy benefits with more validating data to support these claims.

The current study showed comparable results between Jetfire, TJI and SI at a nominal load 6 bar IMEPg and 1500 rpm. While it has been identified that Jetfire can successfully maintain high EGR dilution rate at lower loads, further comparison is necessary to evaluate the relative effectiveness of the Jetfire system compared to TJI or SI at low load operations.

While the results obtained with the current Prototype III have clearly demonstrated its benefits over others, the system is mostly unoptimized in terms of critical jet ignition specific parameters such as the pre-chamber shape and volume, nozzle orifice orientation, distribution and diameter,

orifice l/d ratio, pre-chamber volume to nozzle area ratio. Further research efforts are required to achieve optimal performance from the DM-TJI system.

The focus of the current work was to demonstrate the capability of the DM-TJI/Jetfire system at dealing with high EGR dilution and no substantial effort was made at optimizing the system starting from its design to the way the system was calibrated to obtain high EGR tolerance. While it is encouraging to observe such potential from an unoptimized system, a substantial numerical and experimental effort will be required to realize the full benefits of the DM-TJI/Jetfire system. The current Jetfire system has several limitations such as the pre-chamber purge air timing control or the pre-chamber fuel metering. More developmental works are necessary to address these issues.

The current air delivery mechanism not only is limited in terms of fixed timing, the air flow rate to the pre-chamber is also estimated to be considerably higher than what is required to maintain a high dilution rate. This increases the parasitic losses for the purge air delivery. Future work should concentrate on optimizing these to deliver optimal efficiency from the system.

The high-load knock-limited operation has been identified to be the most effective scenario for the Jetfire ignition system to demonstrate its high thermal efficiency potential. However, the actual knocking mechanism with respect to the jet ignition is yet to be fully understood. The additional pressure oscillations due to either the local fast burning rate of the hot jets or the gas dynamic effect of pre-chamber jets creating pressure waves (jet shocks) has been not investigated in detail. This creates an additional challenge at knock quantification. This phenomenon regarding pre-chamber ignition related pressure oscillations needs to be further investigated to obtain clear ideas on knock limited operations.

Boosted high load operation with Jetfire ignition has been demonstrated in this study but long-

term implications in terms of durability and pre-chamber deposits have not been addressed. Along with the further optimization and better packaging of the cartridge components, durability of the pre-chamber and related components should be addressed.

High EGR diluted boosted application has several implications such as engine power density, boost device sizing, EGR handling and availability, etc. The DM-TJI/Jetfire system provides the solution to address the central issue of igniting a highly EGR diluted mixture but more work is required towards increasing the technology readiness level of the Jetfire® ignition and its successful implementation.

**BIBLIOGRAPHY** 

### **BIBLIOGRAPHY**

- 1. United States Environmental Protection Agency, "Inventory of U.S. Greenhouse Gas Emissions and Sinks Fast Facts and Data Highlights," (April), 2020.
- 2. U.S. Energy Information Administration, "Annual Energy Outlook 2020 with projections to 2050," 2020.
- 3. Attard, W.P., Fraser, N., Parsons, P., and Toulson, E., "A turbulent jet ignition pre-chamber combustion system for large fuel economy improvements in a modern vehicle powertrain," *SAE Int. J. Engines* 3(2):20–37, 2010, doi:10.4271/2010-01-1457.
- 4. Toulson, E., Schock, H.J., and Attard, W.P., "A review of pre-chamber initiated jet ignition combustion systems," *SAE Tech. Pap.*, 2010, doi:10.4271/2010-01-2263.
- 5. Ricardo, H.R., "Internal Combustion Engine," US Patent 1,271,942, 1918.
- 6. Turkish, M.C., "3 Valve stratified charge engines: Evolvement, analysis and progression," *SAE Tech. Pap.*, 1974, doi:10.4271/741163.
- 7. Ricardo, H.R., "RECENT RESEARCH WORK ON THE INTERNAL-COMBUSTION ENGINE," *SAE Tech. Pap.* (220001), 1922, doi:https://doi.org/10.4271/220001.
- 8. Summers, C.E., "Internal Combustion Engine," US Patent 2,314,175, 1943.
- 9. Mallory, M., "Internal Combustion Engine," US Patent 2,121,920, 1937.
- 10. Bagnulo, A., "Engine with Stratified Mixture," US Patent 2,422,610, 1947.
- 11. Heintz, R.M., "Internal Combustion Engine," US Patent 2,884,913, 1959.
- 12. Turkish, M.C., "Prechamber and valve gear design for 3-valve stratified charge engines," *SAE Tech. Pap.*, 1975, doi:10.4271/751004.
- 13. Gussak, L.A., Karpov, V.P., and Tikhonov, Y. V., "The application of lag-process in prechamber engines," *SAE Tech. Pap.*, 1979, doi:10.4271/790692.
- 14. Noguchi, M., Sanda, S., and Nakamura, N., "Development of toyota lean burn engine," *SAE Tech. Pap.*, 1976, doi:10.4271/760757.
- 15. Brandstetter, W., "The Volkwagen Lean Burn PC-Engine Concept," SAE Tech. Pap., 1980, doi:10.4271/800456.
- 16. Adams, T., "Torch Ignition for Combustion Control of Lean Mixtures," *SAE Tech. Pap.* (790440), 1979, doi:10.4271/790440.
- 17. Date, T. and Nomura, T., "Research and development of the carburetor for the CVCC

- engine," SAE Tech. Pap., 1980, doi:10.4271/800507.
- 18. Introducing the CVCC/1972, https://global.honda/heritage/episodes/1972introducing thecvcc.html.
- 19. Dale, J.D. and Oppenheim, A.K., "Enhanced ignition for I. C. Engines with premixed gases," *SAE Tech. Pap.*, 1981, doi:10.4271/810146.
- 20. Yamaguchi, S., Ohiwa, N., and Hasegawa, T., "Ignition and burning process in a divided chamber bomb," *Combust. Flame* 59(2):177–187, 1985, doi:10.1016/0010-2180(85)90023-9.
- 21. Allison, P.M., Oliveira, M. de, Giusti, A., and Mastorakos, E., "Pre-chamber ignition mechanism: Experiments and simulations on turbulent jet flame structure," *Fuel* 230(December 2017):274–281, 2018, doi:10.1016/j.fuel.2018.05.005.
- 22. Oppenheim, A.K., "Combustion in Piston Engines: Technology, Evolution, Diagnosis and Control," Springer, New York, 2004.
- 23. Gussak, L.A., "High chemical activity of incomplete combustion products and a method of prechamber torch ignition for avalanche activation of combustion in internal combustion engines," *SAE Tech. Pap.*, 1975, doi:10.4271/750890.
- 24. Gussak, L.A., "The role of chemical activity and turbulence intensity in prechamber-torch organization of combustion of a stationary flow of a fuel-air mixture," *SAE Tech. Pap.*, 1983, doi:10.4271/830592.
- 25. Goosak, L.A., "Method of Prechamber-torch Ignition in Internal Combustion Engines," US Patent 3,230,939, 1966.
- 26. Oppenheim, A.K. and Kuhl, A.L., "Paving the way to Controlled Combustion Engines (CCE)," *SAE Tech. Pap.*, 1995, doi:10.4271/951961.
- 27. Oppenheim, A.K., Beltramo, J., Faris, D., Maxson, J.A., Horn, K., and Stewart, H.E., "Combustion by Pulsed Jet Plumes-Key to Controlled Combustion Engines," *SAE Tech. Pap.*, 1989, doi:10.4271/890153.
- 28. Lezanski, T., Kesler, M., Rychter, T., Teodorczyk, A., and Wolanski, P., "Performance of Pulsed Jet Combustion (PJC) System in a research engine," *SAE Tech. Pap.* (412), 1993, doi:10.4271/932709.
- 29. Hensinger, D.M., Maxson, J.A., Hom, K., and Oppenheim, A.K., "Jet plume injection and combustion," *SAE Tech. Pap.*, 1992, doi:10.4271/920414.
- 30. Latsch, R., "The Swirl-Chamber Spark Plug: A Means of Faster, More Uniform Energy Conversion in the Spark-Ignition Engine," 1984, doi:10.4271/840455.
- 31. Weng, V., Gindele, J., Töpfer, G., Spicher, U., Latsch, R., and Kuhnert, D., "Investigation

- of the bowl-prechamber-ignition (BPI) concept in a direct injection gasoline engine at part load," *SAE Tech. Pap.*, 1999, doi:10.4271/1999-01-3658.
- 32. Watson, H.C., "Internal Combustion Engine Ignition Device," US Patent 5,611,307, 1997.
- 33. Lumsden, G. and Watson, H.C., "Optimum control of an S.I. engine with a  $\lambda$ =5 capability," *SAE Tech. Pap.*, 1995, doi:10.4271/950689.
- 34. Attard, W.P., Toulson, E., Hamori, F., and Watson, H.C., "Combustion system development and analysis of a carbureted and PFI normally aspirated small engine," *SAE Int. J. Engines* 3(2):511–528, 2010, doi:10.4271/2010-32-0095.
- 35. Wakai, K., Kito, S., and Sumida, I., "Effect of small hydrogen jet flame on augmentation of lean combustion," *SAE Tech. Pap.*, 1993, doi:10.4271/931943.
- 36. Kito, S., Wakai, K., Takahashi, S., Fukaya, N., and Takada, Y., "Ignition limit of lean mixture by hydrogen flame jet ignition," *JSAE Rev.* 21(3):373–378, 2000, doi:https://doi.org/10.1016/S0389-4304(00)00057-6.
- 37. Couet, S., Higelin, P., and Moreau, B., "APIR: A new firing concept for the internal combustion engines-sensitivity to knock and in-cylinder aerodynamics," *SAE Tech. Pap.*, 2001, doi:10.4271/2001-01-1954.
- 38. Robinet, C., Higelin, P., Moreau, B., Pajot, O., and Andrzejewski, J., "A new firing concept for internal combustion engines: 'i'APIR,'" *SAE Tech. Pap.*, 1999, doi:10.4271/1999-01-0621.
- 39. Najt, P., Rask, R., and Reuss, D., "Dual Mode Engine Combustion Process," US Patent 6,595,181, 2003.
- 40. Kojic, A., Hathout, J., Cook, D., and Ahmed, J., "Control of Auto-Ignition Timing for Homogeneous Combustion Jet Ignition Engines," US Patent 7,107,964, 2006.
- 41. Getzlaff, J., Pape, J., Gruenig, C., Kuhnert, D., and Latsch, R., "Investigations on prechamber spark plug with pilot injection," *SAE Tech. Pap.*, 2007, doi:10.4271/2007-01-0479.
- 42. Attard, W.P., Kohn, J., and Parsons, P., "Ignition energy development for a spark initiated combustion system capable of high load, high efficiency and near zero NOx emissions," *SAE Int. J. Engines* 3(2):481–496, 2010, doi:10.4271/2010-32-0088.
- 43. Attard, W.P. and Parsons, P., "Flame kernel development for a spark initiated pre-chamber combustion system capable of high load, high efficiency and near zero NOx emissions," *SAE Int. J. Engines* 3(2):408–427, 2010, doi:10.4271/2010-01-2260.
- 44. Attard, W.P. and Parsons, P., "A normally aspirated spark initiated combustion system capable of high load, high efficiency and near zero NOx emissions in a modern vehicle powertrain," *SAE Int. J. Engines* 3(2):269–287, 2010, doi:10.4271/2010-01-2196.

- 45. Glasson, N., Lumsden, G., Dingli, R., and Watson, H., "Development of the HAJI system for a multi-cylinder spark ignition engine," *SAE Tech. Pap.*, 1996, doi:10.4271/961104.
- 46. Toulson, E., Watson, H.C., and Attard, W.P., "The Lean Limit and Emissions at Near-Idle for a Gasoline HAJI System with Alternative Pre-Chamber Fuels," *SAE Tech. Pap.*, 2007, doi:10.4271/2007-24-0120.
- 47. Boretti, A.A., Brear, M.J., and Watson, H.C., "Experimental and numerical study of a hydrogen fuelled I.C. engine fitted with the Hydrogen Assisted Jet Ignition system," *Proceedings of the 16th Australasian Fluid Mechanics Conference, 16AFMC*, 1142–1147, 2007.
- 48. Attard, W.P., Toulson, E., Hamori, F., and Watson, H.C., "Combustion system development and analysis of a carbureted and PFI normally aspirated small engine," *SAE Tech. Pap.* 3(2), 2010, doi:10.4271/2010-32-0095.
- 49. Toulson, E., Watson, H.C., and Attard, W.P., "Modeling alternative prechamber fuels in jet assisted ignition of gasoline and LPG," *SAE Tech. Pap.*, 2009, doi:10.4271/2009-01-0721.
- 50. Boretti, A., Watson, H., and Tempia, A., "Computational analysis of the lean-burn directinjection jet ignition hydrogen engine," *Proc. Inst. Mech. Eng. Part D J. Automob. Eng.* 224(2):261–269, 2010, doi:10.1243/09544070JAUTO1278.
- 51. Watson, H.C. and Mehrani, P., "The performance and emissions of the turbocharged always lean burn spark ignition (TC-ALSI) engine," *SAE Tech. Pap.*, 2010, doi:10.4271/2010-01-1235.
- 52. Attard, W., "Turbulent jet ignition pre-chamber combustion system for spark ignition engines," US 2012/0103302 A1, United States Patent Application Publication, United States, 2012.
- 53. Attard, W., "Turbulent Jet Ignition Pre-Chamber Combustion System for Spark Ignition Engines," US Patent 8,857,405, 2014.
- 54. Attard, W.P., Toulson, E., Huisjen, A., Chen, X., Zhu, G., and Schock, H., "Spark ignition and pre-chamber turbulent jet ignition combustion visualization," *SAE Tech. Pap.*, 2012, doi:10.4271/2012-01-0823.
- 55. Attard, W.P. and Blaxill, H., "A Gasoline Fueled Pre-Chamber Jet Ignition Combustion System at Unthrottled Conditions," *SAE Int. J. Engines* 5(2):315–329, 2012, doi:10.4271/2012-01-0386.
- 56. Attard, W.P. and Blaxill, H., "A lean burn gasoline fueled pre-chamber jet ignition combustion system achieving high efficiency and low NOx at part load," *SAE Tech. Pap.*, 2012, doi:10.4271/2012-01-1146.
- 57. Attard, W.P. and Blaxill, H., "A single fuel pre-chamber jet ignition powertrain achieving high load, high efficiency and near zero NOx emissions," *SAE Int. J. Engines* 5(3):734–

- 746, 2012.
- 58. Attard, W.P., Toulson, E., Huisjen, A., Chen, X., Zhu, G., and Schock, H., "Spark ignition and pre-chamber turbulent jet ignition combustion visualization," *SAE Tech. Pap.*, 2012, doi:10.4271/2012-01-0823.
- 59. Bunce, M. and Blaxill, H., "Methodology for Combustion Analysis of a Spark Ignition Engine Incorporating a Pre-Chamber Combustor," *SAE Tech. Pap.*, 2014, doi:10.4271/2014-01-2603.
- 60. Bunce, M., Blaxill, H., Kulatilaka, W., and Jiang, N., "The effects of turbulent jet characteristics on engine performance using a pre-chamber combustor," *SAE Tech. Pap.*, 2014, doi:10.4271/2014-01-1195.
- 61. Bunce, M. and Blaxill, H., "Sub-200 g/kWh BSFC on a Light Duty Gasoline Engine," *SAE Tech. Pap.*, 2016, doi:10.4271/2016-01-0709.
- 62. Peters, N., Krishna Pothuraju Subramanyam, S., Bunce, M., Blaxill, H., and Cooper, A., "Optimization of Lambda across the Engine Map for the Purpose of Maximizing Thermal Efficiency of a Jet Ignition Engine," *SAE Tech. Pap.*, 2020, doi:10.4271/2020-01-0278.
- 63. Peters, N., Bunce, M., and Blaxill, H., "The impact of engine displacement on efficiency loss pathways in a highly dilute jet ignition engine," *SAE Tech. Pap.*, 2019, doi:10.4271/2019-01-0330.
- 64. Peters, N., Krishna, S., Subramanyam, P., Bunce, M., Blaxill, H., Pihl, J., Moses-debusk, M., Hamilton, B.A., and Tew, D., "Design and Development of a High-Efficiency Single Cylinder Natural Gas-Fueled Jet Ignition Engine," *SAE Tech. Pap. 2019-32-0565*, 2020.
- 65. Peters, N., Krishna, S., Subramanyam, P., Bunce, M., and Blaxill, H., "Optimization of the Mechanical and Thermodynamic Efficiency Loss," *Proceedings of the ASME 2019 Internal Combustion Engine Division Fall Technical Conference*, 2019, doi:10.1115/ICEF2019-7213.
- 66. Schock, H., Zhu, G., Toulson, E., and Stuecken, T., "Internal Combstion Engine," US Patent 10,161,296 B2, 2018.
- 67. Atis, C., Chowdhury, S.S., Ayele, Y., Stuecken, T., Schock, H., and Voice, A.K., "Ultra-Lean and High EGR Operation of Dual Mode, Turbulent Jet Ignition (DM-TJI) Engine with Active Pre-chamber Scavenging," *SAE Tech. Pap.*, 2020, doi:10.4271/2020-01-1117.
- 68. Tolou, S. and Schock, H., "Experiments and modeling of a dual-mode, turbulent jet ignition engine," *Int. J. Engine Res.* 21(6):966–986, 2019, doi:10.1177/1468087419875880.
- 69. Vedula, R.T., Song, R., Stuecken, T., Zhu, G.G., and Schock, H., "Thermal efficiency of a dual-mode turbulent jet ignition engine under lean and near-stoichiometric operation," *Int. J. Engine Res.* 18(10):1055–1066, 2017, doi:10.1177/1468087417699979.

- 70. Vedula, R.T., Gentz, G., Stuecken, T., Toulson, E., and Schock, H., "Lean Burn Combustion of Iso-Octane in a Rapid Compression Machine Using Dual Mode Turbulent Jet Ignition System," *SAE Int. J. Engines* 11(1):3–11, 2018, doi:10.4271/03-11-01-0007.
- 71. Song, R., Vedula, R.T., Zhu, G., and Schock, H., "A control-oriented combustion model for a turbulent jet ignition engine using liquid fuel," *Int. J. Engine Res.* 19(8):813–826, 2018, doi:10.1177/1468087417731698.
- 72. CO2 EMISSION STANDARDS FOR PASSENGER CARS AND LIGHT-COMMERCIAL VEHICLES IN THE EUROPEAN UNION, https://theicct.org/sites/default/files/publications/EU-LCV-CO2-2030\_ICCTupdate\_201901.pdf, 2019.
- 73. Joshi, A., "Review of Vehicle Engine Efficiency and Emissions," *SAE Int. J. Adv. Curr. Pr. Mobil.* 11(6):734–761, 2019, doi:10.4271/2018-01-0329.
- 74. Chinnathambi, P., Bunce, M., and Cruff, L., "RANS Based Multidimensional Modeling of an Ultra-Lean Burn Pre-Chamber Combustion System with Auxiliary Liquid Gasoline Injection," *SAE Tech. Pap.*, 2015, doi:10.4271/2015-01-0386.
- 75. Gentz, G., Thelen, B., Toulson, E., Litke, P., and Hoke, J., "Combustion Visualization, Performance, and CFD Modeling of a Pre-Chamber Turbulent Jet Ignition System in a Rapid Compression Machine," *SAE Int. J. Engines* 8(2):538–546, 2015, doi:10.4271/2015-01-0779.
- 76. Attard, W.P., Kohn, J., and Parsons, P., "Ignition Energy Development for a Spark Initiated Combustion System Capable of High Load, High Efficiency and Near Zero NOx Emissions," *SAE Int. J. Engines* 3(2):481–496, 2010, doi:10.4271/2010-32-0088.
- 77. Attard, W.P., Bassett, M., Parsons, P., and Blaxill, H., "A new combustion system achieving high drive cycle fuel economy improvements in a modern vehicle powertrain," *SAE Tech. Pap.*, 2011, doi:10.4271/2011-01-0664.
- 78. Yoshida, T., Sato, A., Suzuki, H., Tanabe, T., and Takahashi, N., "Development of High Performance Three-Way-Catalyst," *SAE Tech. Pap.*, 2006, doi:10.1299/jsmemag.101.954\_390.
- 79. Heywood, J.B., "Internal Combustion Engine Fundamentals," Second Ed, McGraw-Hill Education, New York, 2018.
- 80. Yorobiev Ya., I., Zharnov, V.M., and Naumenko, V.D., "Internal combustion engine.," US Patent 10,161,296 B2, 1985.
- 81. Song, R., Vedula, R.T., Zhu, G., and Schock, H., "Optimal Combustion Phasing Control of a Turbulent Jet Ignition Engine," *Proc. Am. Control Conf.* 23(4):1811–1822, 2018, doi:10.23919/ACC.2018.8431841.
- 82. Vedula, R.T., "OPTICAL INVESTIGATIONS AND EFFICIENCY MEASUREMENTS

- OF A DUAL-MODE TURBULENT JET IGNITION ENGINE UNDER LEAN AND HIGH-EGR NEAR-STOICHIOMETRIC CONDITIONS," Michigan State University, 2016, doi:https://doi.org/doi:10.25335/M5RX1K.
- 83. Tolou, S., "EXPERIMENTS AND MODEL DEVELOPMENT OF A DUAL MODE, TURBULENT JET IGNITION ENGINE," Michigan State University, 2019, doi:https://doi.org/10.25335/2yhx-9e25.
- 84. Friedman, R. and Johnston, W.C., "The wall-quenching of laminar propane flames as a function of pressure, temperature, and air-fuel ratio," *J. Appl. Phys.* 21(8):791–795, 1950, doi:10.1063/1.1699760.
- 85. Rassweiler, G.M. and Withrow, L., "Motion pictures of engine flames correlated with pressure cards," *SAE Tech. Pap.*, 1938, doi:10.4271/380139.
- 86. Womack Machine Supply Co., "Horsepower Required for Compressing Air," https://www.womackmachine.com/engineering-toolbox/data-sheets/horsepower-required-for-compressing-air/, Sep. 2020.
- 87. Lavoie, G.A., Ortiz-Soto, E., Babajimopoulos, A., Martz, J.B., and Assanis, D.N., "Thermodynamic sweet spot for highefficiency, dilute, boosted gasoline engines," *Int. J. Engine Res.* 14(3):260–278, 2013, doi:10.1177/1468087412455372.
- 88. Tully, E.J. and Heywood, J.B., "Lean-burn characteristics of a gasoline engine enriched with hydrogen plasmatron fuel reformer," *SAE Tech. Pap.*, 2003, doi:10.4271/2003-01-0630.
- 89. Ivanič, Ž., Ayala, F., Goldwitz, J., and Heywood, J.B., "Effects of hydrogen enhancement on efficiency and NOx emissions of lean and EGR-diluted mixtures in a SI engine," *SAE Tech. Pap.*, 2005, doi:10.4271/2005-01-0253.
- 90. Maiboom, A., Tauzia, X., and Hétet, J.F., "Experimental study of various effects of exhaust gas recirculation (EGR) on combustion and emissions of an automotive direct injection diesel engine," *Energy* 33(1):22–34, 2008, doi:10.1016/j.energy.2007.08.010.
- 91. Ladommatos, N., Abdelhalim, S.M., Zhao, H., and Hu, Z., "The Dilution, Chemical, and Thermal Effects of Exhaust Gas Recirculation on Diesel Engine Emissions Part 1: Effect of Reducing Inlet Charge Oxygen," *SAE Tech. Pap.*, 1996, doi:10.4271/961165.
- 92. Ladommatos, N., Abdelhalim, S.M., Zhao, H., and Hu, Z., "The Dilution, Chemical, and Thermal Effects of Exhaust Gas Recirculation on Diesel Engine Emissions Part 4: Effects of Carbon Dioxide and Water Vapour," *SAE Tech. Pap.*, 1997, doi:10.4271/971660.
- 93. Duva, B.C., Wang, Y.C., Chance, L., and Toulson, E., "The Effect of Exhaust Gas Recirculation (EGR) on Fundamental Characteristics of Premixed Methane/Air Flames," *SAE Tech. Pap.*, 2020, doi:10.4271/2020-01-0339.
- 94. Hu, E., Jiang, X., Huang, Z., and Iida, N., "Numerical study on the effects of diluents on

- the laminar burning velocity of methane-air mixtures," *Energy and Fuels* 26(7):4242–4252, 2012, doi:10.1021/ef300535s.
- 95. Maiboom, A., Tauzia, X., and Hétet, J.F., "Influence of high rates of supplemental cooled EGR on NOx and PM emissions of an automotive HSDI diesel engine using an LP EGR loop," *Int. J. Energy Res.* 32:1383–1398, 2008, doi:10.1002/er.1455.
- 96. Caton, J.A., "A comparison of lean operation and exhaust gas recirculation: Thermodynamic reasons for the increases of efficiency," *SAE Tech. Pap.* 2013-01–0266, 2013, doi:10.4271/2013-01-0266.
- 97. Lee, S., Park, S., Kim, C., Kim, Y.M., Kim, Y., and Park, C., "Comparative study on EGR and lean burn strategies employed in an SI engine fueled by low calorific gas," *Appl. Energy* 129:10–16, 2014, doi:10.1016/j.apenergy.2014.04.082.
- 98. Ibrahim, A. and Bari, S., "A comparison between EGR and lean-burn strategies employed in a natural gas SI engine using a two-zone combustion model," *Energy Convers. Manag.* 50(12):3129–3139, 2009, doi:10.1016/j.enconman.2009.08.012.
- 99. Saanum, I., Bysveen, M., Tunestål, P., and Johansson, B., "Lean burn versus stoichiometric operation with EGR and 3-way catalyst of an engine fueled with natural gas and hydrogen enriched natural gas," *SAE Tech. Pap.* 116:35–45, 2007, doi:10.4271/2007-01-0015.
- 100. Benajes, J., Novella, R., Gomez-Soriano, J., Martinez-Hernandiz, P.J., Libert, C., and Dabiri, M., "Evaluation of the passive pre-chamber ignition concept for future high compression ratio turbocharged spark-ignition engines," *Appl. Energy* 248(April):576–588, 2019, doi:10.1016/j.apenergy.2019.04.131.
- 101. Kargul, J., Stuhldreher, M., Barba, D., Schenk, C., Bohac, S., McDonald, J., Dekraker, P., and Alden, J., "Benchmarking a 2018 Toyota Camry 2.5-liter atkinson cycle engine with cooled-EGR," *SAE Tech. Pap.* 2019-April(April):601–638, 2019, doi:10.4271/2019-01-0249.
- 102. GRI-Mech Thermodynamic Data, http://combustion.berkeley.edu/gri-mech/data/thermo table.html, Jun. 2020.
- 103. Hoepke, B., Jannsen, S., Kasseris, E., and Cheng, W.K., "EGR Effects on Boosted SI Engine Operation and Knock Integral Correlation," *SAE Int. J. Engines* 5(2):547–559, 2012, doi:10.4271/2012-01-0707.
- 104. Chaos, M., Kazakov, A., Zhao, Z., and Dryer, F.L., "A High-Temperature Chemical Kinetic Model for Primary Reference Fuels," *Int. J. Chem. Kinet.* (39):399–414, 2007, doi:10.1002/kin.
- 105. Mehl, M., Curran, H.J., Pitz, W.J., and Westbrook, C.K., "Chemical kinetic modeling of component mixtures relevant to gasoline," *European Combustion Meeting*, Vienna, Austria, 2009.

- 106. Duva, B.C., Chance, L., and Toulson, E., "Laminar flame speeds of premixed iso-octane/air flames at high temperatures with CO2 dilution," *SAE Int. J. Adv. Curr. Pr. Mobil.* 1(3):1148–1157, 2019, doi:10.4271/2019-01-0572.
- 107. Einewall, P., Tunestal, P., and Johansson, B., "Lean burn natural gas operation vs. stoichiometric operation with EGR and a three way catalyst," *SAE Tech. Pap.*, 2005, doi:10.4271/2005-01-0250.
- 108. General Motors Automotive Engine Test Code for Spark Ignition Engines, 1994.
- 109. Mueller, M., "General Air Fuel Ratio and EGR Definitions and their Calculation from Emissions," *SAE Tech. Pap.*, 2010, doi:10.4271/2010-01-1285.
- 110. Surnilla, G., Soltis, R., Hilditch, J., House, C., Clark, T., and Gerhart, M., "Intake Oxygen Sensor for EGR Measurement," *SAE Tech. Pap.*, 2016, doi:10.4271/2016-01-1070.
- 111. Ayala, F.A., Gerty, M.D., and Heywood, J.B., "Effects of combustion phasing, relative airfuel ratio, compression ratio, and load on SI engine efficiency," *SAE Tech. Pap.*, 2006, doi:10.4271/2006-01-0229.
- 112. Quader, A.A., "Lean combustion and the misfire limit in spark ignition engines," *SAE Tech. Pap.*, 1974, doi:10.4271/741055.
- 113. Stadler, A., Sauerland, H., Härtl, M., and Wachtmeister, G., "The Potential of Gasoline Fueled Pre Chamber Ignition Combined with Elevated Compression Ratio," *SAE Tech. Pap.*, 2020, doi:10.4271/2020-01-0279.
- 114. Yu, X., Zhang, A., Baur, A., Voice, A., and Engineer, N., "Statistical Quantification of Knock with Spark Ignition and Pre-Chamber Jet Ignition in a Light Duty Gasoline Engine," *Proceedings of the ASME 2020 Internal Combustion Engine Division Fall Technical Conference*. ASME 2020 Internal Combustion Engine Division Fall Technical Conference, 1–21, 2020, doi:https://doi.org/10.1115/ICEF2020-2941.
- 115. Sens, M. and Binder, E., "Pre-Chamber Ignition as a Key Technology for Future Powertrain Fleets," *MTZ Worldw.* 80(2):44–51, 2019, doi:10.1007/s38313-018-0150-1.
- 116. Sens, M., Günther, M., Medicke, M., and Walther, U., "Developing a Spark-Ignition Engine with 45 % Efficiency," *MTZ Worldw*. 81(4):46–51, 2020, doi:10.1007/s38313-020-0194-x.
- 117. Chinnathambi, P., Thelen, B., Cook, D., and Toulson, E., "Performance metrics for fueled and unfueled turbulent jet igniters in a rapid compression machine," *Appl. Therm. Eng.* 182:115893, 2021, doi:10.1016/j.applthermaleng.2020.115893.